NUREG/CR-6739, Vol. 1
PNNL-13576

FRAPTRAN: A Computer Code for the Transient Analysis of Oxide Fuel Rods

Pacific Northwest National Laboratory

U.S. Nuclear Regulatory Commission
Office of Nuclear Regulatory Research
Washington, DC 20555-0001

AVAILABILITY OF REFERENCE MATERIALS IN NRC PUBLICATIONS

NRC Reference Material

As of November 1999, you may electronically access NUREG-series publications and other NRC records at NRC's Public Electronic Reading Room at www.nrc.gov/NRC/ADAMS/index.html. Publicly released records include, to name a few, NUREG-series publications; *Federal Register* notices; applicant, licensee, and vendor documents and correspondence; NRC correspondence and internal memoranda; bulletins and information notices; inspection and investigative reports; licensee event reports; and Commission papers and their attachments.

NRC publications in the NUREG series, NRC regulations, and *Title 10, Energy*, in the Code of *Federal Regulations* may also be purchased from one of these two sources.

1. The Superintendent of Documents
   U.S. Government Printing Office
   Mail Stop SSOP
   Washington, DC 20402–0001
   Internet: bookstore.gpo.gov
   Telephone: 202-512-1800
   Fax: 202-512-2250
2. The National Technical Information Service
   Springfield, VA 22161–0002
   www.ntis.gov
   1–800–553–6847 or, locally, 703–605–6000

A single copy of each NRC draft report for comment is available free, to the extent of supply, upon written request as follows:

Address: Office of the Chief Information Officer,
Reproduction and Distribution
Services Section
U.S. Nuclear Regulatory Commission
Washington, DC 20555-0001
E-mail: DISTRIBUTION@nrc.gov
Facsimile: 301–415–2289

Some publications in the NUREG series that are posted at NRC's Web site address www.nrc.gov/NRC/NUREGS/indexnum.html are updated periodically and may differ from the last printed version. Although references to material found on a Web site bear the date the material was accessed, the material available on the date cited may subsequently be removed from the site.

Non-NRC Reference Material

Documents available from public and special technical libraries include all open literature items, such as books, journal articles, and transactions, *Federal Register* notices, Federal and State legislation, and congressional reports. Such documents as theses, dissertations, foreign reports and translations, and non-NRC conference proceedings may be purchased from their sponsoring organization.

Copies of industry codes and standards used in a substantive manner in the NRC regulatory process are maintained at—

The NRC Technical Library
Two White Flint North
11545 Rockville Pike
Rockville, MD 20852–2738

These standards are available in the library for reference use by the public. Codes and standards are usually copyrighted and may be purchased from the originating organization or, if they are American National Standards, from—

American National Standards Institute
11 West 42nd Street
New York, NY 10036–8002
www.ansi.org
212–642–4900

Legally binding regulatory requirements are stated only in laws; NRC regulations; licenses, including technical specifications; or orders, not in NUREG-series publications. The views expressed in contractor-prepared publications in this series are not necessarily those of the NRC.

The NUREG series comprises (1) technical and administrative reports and books prepared by the staff (NUREG–XXXX) or agency contractors (NUREG/CR–XXXX), (2) proceedings of conferences (NUREG/CP–XXXX), (3) reports resulting from international agreements (NUREG/IA–XXXX), (4) brochures (NUREG/BR–XXXX), and (5) compilations of legal decisions and orders of the Commission and Atomic and Safety Licensing Boards and of Directors' decisions under Section 2.206 of NRC's regulations (NUREG–0750).

DISCLAIMER: This report was prepared as an account of work sponsored by an agency of the U.S. Government. Neither the U.S. Government nor any agency thereof, nor any employee, makes any warranty, expressed or implied, or assumes any legal liability or responsibility for any third party's use, or the results of such use, of any information, apparatus, product, or process disclosed in this publication, or represents that its use by such third party would not infringe privately owned rights.

NUREG/CR-6739, Vol. 1
PNNL-13576

FRAPTRAN: A Computer Code for the Transient Analysis of Oxide Fuel Rods

Manuscript Completed: August 2001
Date Published: August 2001

Prepared by
M.E. Cunningham, C.E. Beyer, P.G. Medvedev, PNNL
G.A. Berna, GABC

Pacific Northwest National Laboratory
Richland, WA 99352

Subcontractor:
G.A. Berna Consulting
2060 Sequoia Drive
Idaho Falls, ID 83404

H. Scott, NRC Project Manager

Prepared for
Division of Systems Analysis and Regulatory Effectiveness
Office of Nuclear Regulatory Research
U.S. Nuclear Regulatory Commission
Washington, DC 20555-0001
NRC Job Code W6200

ABSTRACT

The Fuel Rod Analysis Program Transient (FRAPTRAN) is a FORTRAN language computer code that calculates the transient performance of light-water reactor fuel rods during reactor power and coolant transients for hypothetical accidents such as loss-of-coolant accidents, anticipated transients without scram, and reactivity-initiated accidents. FRAPTRAN calculates the temperature and deformation history of a fuel rod as function of time-dependent fuel rod power and coolant boundary conditions. FRAPTRAN is intended to be used as a "stand alone" code. The phenomena modeled by FRAPTRAN include: a) heat conduction, b) heat transfer from cladding to coolant, c) elastic-plastic fuel and cladding deformation, d) cladding oxidation, and e) fuel rod gas pressure. FRAPTRAN was developed from the FRAP-T6 code and incorporates burnup-dependent parameters and corrects errors. Burnup dependent parameters may be initialized from the FRAPCON-3 steady-state single rod fuel performance code.

CONTENTS

Abstract iii

Executive Summary xi

Acknowledgments xiii

1 Introduction 1.1

1.1 Objectives and Scope of the FRAPTRAN Code 1.1
1.2 Relation to Other NRC Codes 1.3
1.3 Significant Changes From FRAP-T6 ..... 1.5
1.4 Report Outline 1.6

2 General Modeling Description 2.1

2.1 Order and Interaction of Models 2.1
2.2 Fuel and Cladding Temperature Model 2.3

2.2.1 Local Coolant Conditions 2.5
2.2.2 Heat Generation 2.5
2.2.3 Gap Conductance 2.6
2.2.4 Fuel Thermal Conductivity 2.8
2.2.5 Fuel Rod Cooling 2.9
2.2.6 Heat Conduction and Temperature Solution 2.11

2.3 Plenum Gas Temperature Model 2.15

2.3.1 Plenum Temperature Equations 2.15
2.3.2 Heat Conduction Coefficients 2.19
2.3.3 Gamma Heating of the Spring and Cladding 2.23

2.4 Fuel Rod Mechanical Response Model 2.24

2.4.1 General Considerations in Elastic-Plastic Analysis 2.25
2.4.2 Extension to Creep and Hot Pressing 2.29
2.4.3 Rigid Pellet Model 2.31
2.4.4 Cladding Ballooning Model 2.48

2.5 Fuel Rod Internal Gas Pressure Response Model 2.49

2.5.1 Static Fuel Rod Internal Gas Pressure 2.50
2.5.2 Transient Internal Gas Flow 2.51
2.5.3 Fission Gas Production and Release 2.52

3 User Information 3.1

3.1 Code Structure and Computation 3.1
3.2 Input Information 3.3
3.3 Output Information 3.6
3.4 Nodalization, Accuracy, and Computation Time Considerations 3.6
3.5 Comments and Guidance on Operating FRAPTRAN 3.9

4 References 4.1

Appendix A - Input Instructions for FRAPTRAN A.1
Appendix B - Example Problem B.1
Appendix C - Calculation of Cladding Surface Temperature C.1
Appendix D - Heat Transfer Correlations and Coolant Models D.1
Appendix E - Numerical Solution of the Plenum Energy Equations E.1
Appendix F - Description of Subroutines F.1
Appendix G - Input Option for Data File With Transient Coolant Conditions G.1

FIGURES

1.1 Schematic of Typical LWR Fuel Rod 1.2

1.2 Locations at Which Fuel Rod Variables are Evaluated 1.4

2.1 Order of General Models 2.2

2.2 Flow Chart of Fuel and Cladding Temperature Model 2.4

2.3 Relation of Surface Heat Flux to Surface Temperature 2.10

2.4 Description of Geometry Terms in Finite Difference Equation for Heat Conduction 2.13

2.5 Flow Chart of Plenum Temperature Calculation 2.16

2.6 Energy Flow in Plenum Model 2.16

2.7 Spring Noding 2.16

2.8 Cladding Noding 2.17

2.9 Geometrical Relationship Between the Cladding and Spring 2.21

2.10 Typical Isothermal Stress-Strain Curve 2.25

2.11 Schematic of the Method of Successive Elastic Solutions 2.29

2.12 Fuel Rod Geometry and Coordinates 2.34

2.13 Calculations of Effective Stress σ_e from $d\varepsilon^p$ 2.36

2.14 Stress-Strain Curve and Unloading Path 2.41

2.15 Calculation of Effective Stress for a Given Increment of Plastic Strain 2.42

2.16 Axial Thermal Expansion Using FRACAS-I 2.46

2.17 Description of the BALON2 Model 2.49

2.18 Internal Pressure Distribution With the Gas Flow Model 2.52

2.19 Hagen Number Versus Width of Fuel-Cladding Gap 2.53

3.1 Flow Chart of FRAPTRAN (Part 1) 3.2

3.2 Flow Chart of FRAPTRAN (Part 2) 3.2

3.3 Flow Chart of FRAPTRAN (Part 3) 3.2

3.4 Example of Fuel Rod Nodalization 3.8

TABLES

2.1 Heat Transfer Mode Selection and Correlations 2.10

2.2 Nomenclature for Plenum Thermal Model 2.18

2.3 Elastic-Plastic Governing Equations 2.28

3.1 Name and Function of Principal FRAPTRAN Subcodes 3.1

3.2 Input Information 3.4

3.3 Variables Read from FRAPCON-3 File for Burnup Initialization of FRAPTRAN 3.5

3.4 FRAPTRAN Output Information 3.7

EXECUTIVE SUMMARY

FRAPTRAN (Fuel Rod Analysis Program Transient) is a FORTRAN language computer code developed for the U.S. Nuclear Regulatory Commission to calculate the transient thermal and mechanical behavior of light-water reactor fuel rods. FRAPTRAN will be applied for the evaluation of fuel behavior during reactor power and coolant transients such as reactivity accidents, boiling-water reactor power oscillations without scram, and loss-of-coolant-accidents up to burnup levels of 65 GWd/MTU.

FRAPTRAN uses a finite difference heat conduction model for the transient thermal solution, the FRACAS-I mechanical model, and the MATPRO material properties package. To account for the effects of high burnup, FRAPTRAN uses a new model for UO_2 thermal conductivity that incorporates the degradation effects of burnup and a revised model for Zircaloy mechanical properties that accounts for the effect of oxidation and hydrides in addition to irradiation damaage. Burnup-dependent fuel rod initial conditions can be obtained from the companion FRAPCON-3 steady-state fuel rod performance code.

FRAPTRAN was developed from the FRAP-T6 transient code and is intended to replace the FRAP-T6 code. The development approach for FRAPTRAN was to implement applicable existing high-burnup models rather than developing new models, to not substantially change the code structure, to remove no longer needed or used coding, to correct known or found problems in FRAP-T6, and to improve ease of use. To meet these objectives, in addition to changing fuel and cladding models, other changes include deleting dynamic dimensioning and options such as uncertainty analysis, failure analysis, and licensing evaluation models.

Provided in this report (Volume 1) is a description of the code structure and limitations, a summary of the fuel performance models, and the code input instructions. Provided in Volume 2 is the code assessment based on comparisons of code predictions to fuel rod integral performance data up to high burnup (65 GWd/MTU).

ACKNOWLEDGEMENTS

The authors acknowledge Dr. Ralph Meyer and Mr. Harold Scott of the U.S. Nuclear Regulatory Commission for their technical guidance on the development of FRAPTRAN.

1 INTRODUCTION

The ability to accurately calculate the performance of light-water reactor (LWR) fuel during irradiation, and during both long-term steady-state and various operational transients and hypothetical accidents, is an objective of the reactor safety research program being conducted by the U.S. Nuclear Regulatory Commission (NRC). To achieve this objective, the NRC has sponsored an extensive program of analytical computer code development and both in-reactor and out-of-reactor experiments to generate the data necessary for development and verification of the computer codes. Provided in this report is a description of the FRAPTRAN (Fuel Rod Analysis Program Transient) code developed to calculate the response of single fuel rods to operational transients and hypothetical accidents at burnup levels up to 65 GWd/MTU. The FRAPTRAN code is the successor to the FRAP-T (Fuel Rod Analysis Program-Transient) code series developed in the 1970s and 1980s. FRAPTRAN is also a companion code to the FRAPCON-3 code (Berna et al. 1997) developed to calculate the steady-state high burnup response of a single fuel rod.

A major driver for FRAPTRAN was to incorporate new burnup-dependent models and understanding and develop a code that could predict cladding strain resulting from transients. The FRAP-T computer code series was developed in the 1970s and 1980s for predicting the performance of LWR fuel rods during operational transients and hypothetical accidents. However, since FRAP-T6 (Siefken et al. 1981; Siefken et al. 1983) was completed, additional experimental data and knowledge of fuel performance have been obtained, thus necessitating an update to the code. Provided in this report (Volume 1) is a description of the code structure and limitations, a summary of the fuel performance models, and the code input instructions. Provided in Volume 2 is the code assessment based on comparisons of code predictions to fuel rod integral performance data up to high burnup (65 GWd/MTU).

1.1 Objectives and Scope of the FRAPTRAN Code

FRAPTRAN is an analytical tool that calculates LWR fuel rod behavior when power and/or coolant boundary conditions are rapidly changing. This is in contrast to the FRAPCON-3 code that calculates the time (burnup) dependent behavior when power and coolant boundary condition changes are sufficiently slow for the term "steady-state" to apply. FRAPTRAN calculates the variation with time, power, and coolant conditions of fuel rod variables such as fuel and cladding temperatures, cladding elastic and plastic stress and strain, and fuel rod gas pressure. Variables that are slowly varying with time (burnup) such as fuel rod densification and swelling, cladding creep and irradiation growth, and fission gas release, are not calculated by FRAPTRAN. However, the state of the fuel rod at the time of a transient, which is dependent on those variables not calculated by FRAPTRAN, may be read from a file generated by FRAPCON-3 or manually entered by the user.

FRAPTRAN will serve as a research tool for analysis of fuel response to postulated design-basis accidents such as reactivity accidents, boiling-water reactor (BWR) power and coolant oscillations without scram, and loss-of-coolant-accidents (LOCAs); understanding and interpreting experimental results; and guiding of planned experimental work. Examples of planned applications for FRAPTRAN include defining transient performance limits, identifying data or models needed for understanding transient fuel performance, and in assessing the effect of fuel design changes such as new cladding alloys and mixed-oxide fuel. FRAPTRAN will be used to perform sensitivity analyses of the effects of parameters such as fuel-cladding gap size, rod internal gas pressure, and cladding ductility and strength

on the response of a fuel rod to a postulated transient. Fuel rod responses of interest include cladding strain, location of ballooning, cladding oxidation, etc.

An LWR fuel rod typically consists of UO_2 fuel pellets enclosed in Zircaloy cladding, as shown in Figure 1.1. The primary function of the cladding is to contain the fuel column and the radioactive fission products. If the cladding does not crack, rupture, or melt during a reactor transient, the radioactive fission products are contained within the fuel rod. During some reactor transients and hypothetical accidents, however, the cladding may be weakened by a temperature increase, embrittled by oxidation, or over stressed by mechanical interaction with the fuel. These events alone or in combination can cause cracking or rupture of the cladding and release of the radioactive products to the coolant. Furthermore, the rupture or melting of the cladding of one fuel rod can alter the flow of reactor coolant and reduce the cooling of neighboring fuel rods. This event can lead to the loss of a "coolable" reactor core geometry.

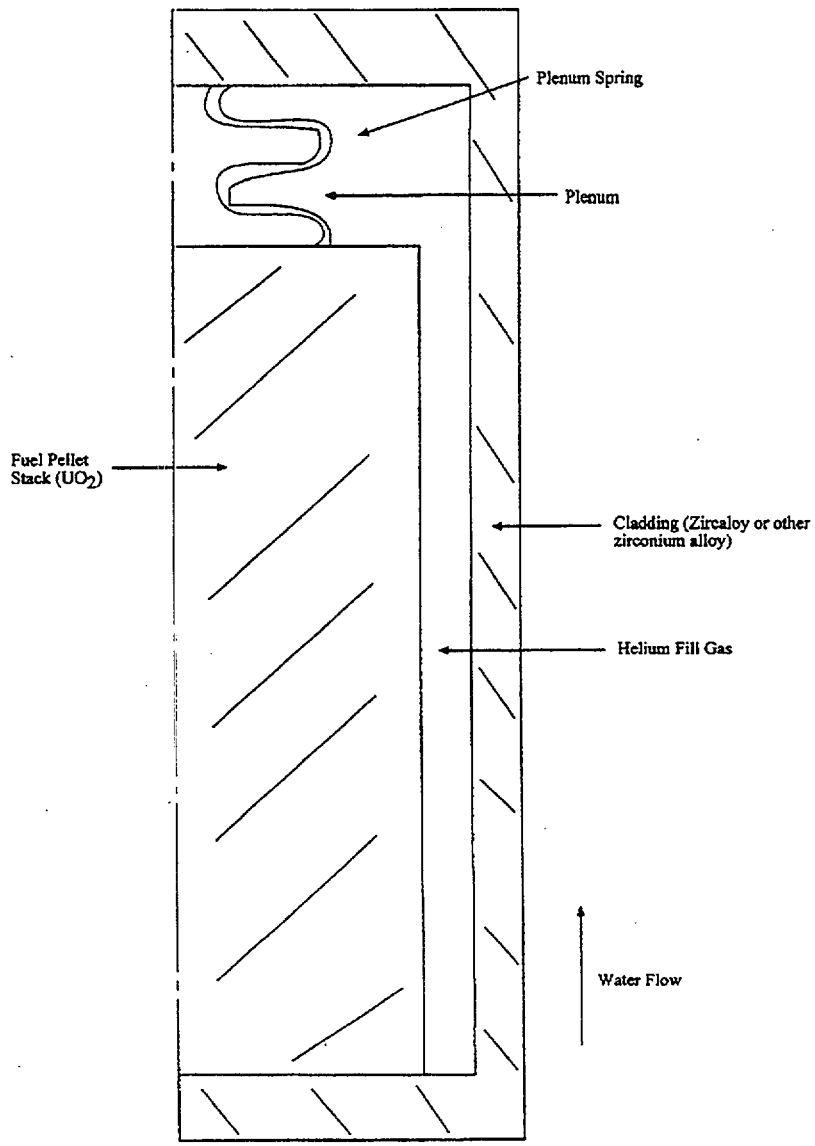

Figure 1.1 Schematic of Typical LWR Fuel Rod

Most reactor operational transients and hypothetical accidents will adversely influence the performance of the fuel rod cladding. During an operational transient such as a turbine trip without bypass (for boiling-water reactors), the reactor power may temporarily increase and cause an increase in the thermal expansion of the fuel, which can lead to the mechanical interaction of the fuel and cladding and over stress the cladding. During an operational transient such as a loss-of-flow event, the coolant flow decreases, which may lead to film boiling on the cladding surface and an increase in the cladding temperature. During a loss-of-coolant-accident (LOCA), the heat generated by the radioactive decay of fission products is not completely removed by the coolant and the cladding temperature increases. The temperature increase weakens the cladding and may also lead to cladding oxidation, which embrittles the cladding.

The FRAPTRAN code has the capability of modeling the phenomena which influence the performance of fuel rods in general and the temperature, embrittlement, and stress of the cladding in particular. The code has a heat conduction model to calculate the transfer of heat from the fuel to the cladding, and a cooling model to calculate the transfer of heat from the cladding to the coolant. The code has an oxidation model to calculate the extent of cladding embrittlement and the amount of heat generated by cladding oxidation. A mechanical response model is included to calculate the stress applied to the cladding by the mechanical interaction of the fuel and cladding, by the pressure of the gases inside the rod, and by the pressure of the external coolant.

The models in FRAPTRAN use finite difference techniques to calculate the variables which influence fuel rod performance. The variables are calculated at user-specified slices of the fuel rod, as shown in Figure 1.2. Each slice is at a different axial elevation and is defined to be an axial node. At each axial node, the variables are calculated at user specified radial locations. Each location is at a different radius and is defined to be a radial node. The variables at any given axial node are assumed to be independent of the variables at all other axial nodes (stacked one-dimensional solution, also known as a 1-D1/2 solution).

1.2 Relation to Other NRC Codes

FRAPTRAN is the successor to FRAP-T6 and is based on FRAP-T6.[a] Major changes incorporated in FRAPTRAN include burnup-dependent material properties and models, simplification of the code, and correction of errors identified since FRAP-T6 was issued. The two principal model changes are incorporation of a burnup-dependent fuel thermal conductivity and cladding mechanical properties dependent on fast fluence and precipitated hydrogen, which vary with burnup. Simplifications have included removing dynamic dimensioning,[b] the uncertainty analysis option, and a failure analysis option. The uncertainty and failure analysis options were removed because they were not being used by the NRC and rod failure predictions were not considered to be accurate. The code has also been made Fortran-90 compatible. Because of the addition of burnup-dependent material properties and models, the user has increased options for specifying the initial conditions of a fuel rod for a transient.

---

[a]PNNL began development work with FRAP-T6, Version 21. Modifications were made to FRAP-T6 by INEL between 1981 (Siefken et al. 1981) and 1983 (Siefken et al. 1983) and when PNNL began work on FRAPTRAN in 1997. However, PNNL a) was not been able to uncover documentation on all the modifications, and b) discovered some discrepancies between INEL's 1981 document, it's references, and the coding of FRAP-T6, Version 21.

[b]Dynamic dimensioning was used in FRAP-T6 because of the computer limitations at the time the code was developed. Current computers no longer have the memory restrictions present in the 1980s so dynamic dimensioning is no longer needed and the coding can be simplified.

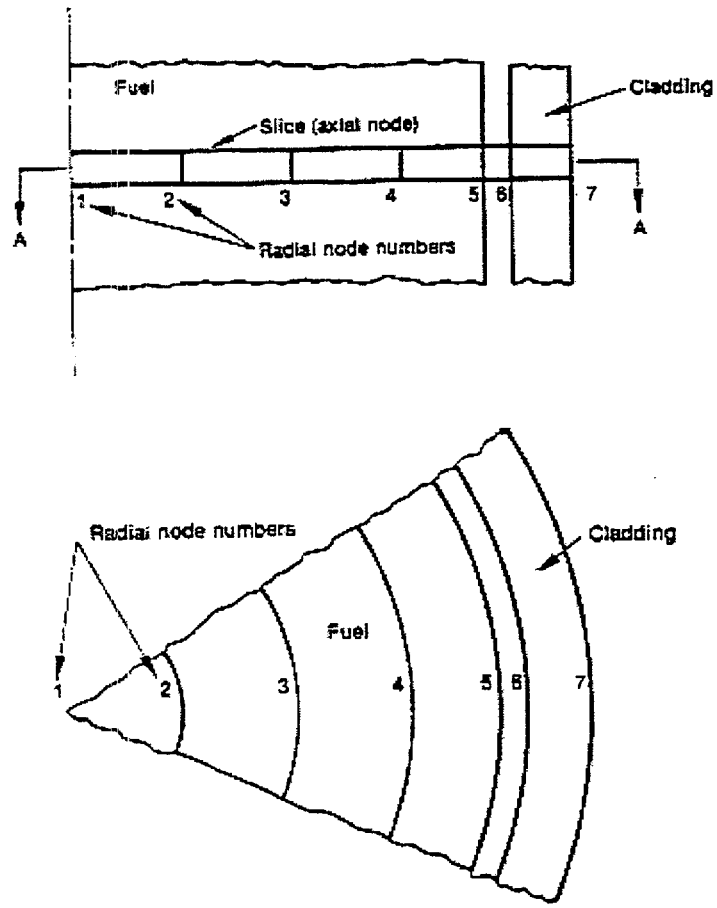

Figure 1.2 Locations at Which Fuel Rod Variables are Evaluated

For transient analyses at other than beginning-of-life conditions, FRAPTRAN needs to be provided with input parameters that account for the effect of burnup; e.g., radial dimensions that account for fuel swelling and cladding creepdown. These values may be obtained from a steady-state fuel performance code such as FRAPCON-3 which predicts fuel rod performance during long-term normal reactor operation to burnup levels of 65 GWd/MTU. Codes such as FRAPCON-3 calculate the change with time (burnup) of fission gas inventory, fuel densification and swelling, cladding permanent strain, fuel radial power and burnup profiles, and other time/burnup dependent parameters. For use with FRAPTRAN, FRAPCON-3 writes the values of these time/burnup dependent parameters to a data file which may be read by FRAPTRAN.

FRAPTRAN uses the MATPRO-11, Revision 2 (Hagrman, Reymann, and Mason 1981), materials properties package to define the thermal and mechanical properties of the UO_2 fuel and Zircaloy cladding at temperatures ranging from room temperature to melting. The package also calculates the conductivity and viscosity of helium and fission gases. The applicable ranges and uncertainties of the property models are also described in the MATPRO documentation. The package is embedded within FRAPTRAN so that code user does not have to supply any material properties. Some of the MATPRO routines have been modified for burnup dependency as was done for FRAPCON-3. These modified models are described in this document and the development of the models is described in Lanning, Beyer, and Painter (1997).

1.3 Significant Changes from FRAP-T6

A number of changes in both models and code structure have been made in the process of making FRAPTRAN from FRAP-T6; these are briefly summarized below.

Model Changes

- incorporate a burnup and gadolinia dependent fuel thermal conductivity
- incorporate Zircaloy mechanical properties dependent on fast neutron fluence and hydrogen content
- addition of thermal effect of outer surface Zircaloy oxide layer
- addition of options to specify time-dependent transient fission gas release and gaseous fuel swelling histories (adjustable input parameters for selected phenomena); FRAPTRAN does NOT include models to calculate transient fission gas release or fuel swelling
- modifications to gap conductance coding to match FRAPCON-3

Code Structure Changes

- removal of dynamic dimensioning and implementation of fixed array sizes to simplify the coding
- making the coding Fortran-90 compatible
- implementation of NAMELIST input to simplify input
- removal of uncertainty sensitivity analysis option
- removal of licensing evaluation models (LACE) option
- removal of failure analysis (FRAIL) option
- implementation of FRAPCON-3/FRAPTRAN initialization option for burnup dependent variables
- implementation of default equal-area ring node structure instead of equal-width ring node structure to put more emphasis on the pellet periphery
- implementation of radial profiles of power and burnup as a function of axial position to support burnup dependent models; option to specify multiple, time-dependent axial power profiles; axial profiles of cladding hydrogen concentration to support the burnup-dependent cladding mechanical properties; and axial profiles of cladding oxidation thickness

The FRAP-T6 code had several options that are not being made available to the user of FRAPTRAN. Those options are described below:

- FRAP-T6 has two options to calculate mechanical response: the rigid-pellet FRACAS-I model and the deformable-pellet FRACAS-II model. FRACAS-II has not been assessed and a deformable-pellet model may be unnecessary in most applications. Therefore, this option is not being made available to the FRAPTRAN user and no discussion of the FRACAS-II model is included in this document although the coding is still embedded in FRAPTRAN.[a]

- FRAP-T6 had the option of using the FASTGRASS fission gas release model to calculate fission gas release during transients, but the FASTGRASS model does not accurately predict transient fission gas release; i.e., it significantly underpredicts transient fission gas release. Therefore, this option is not being made available to the FRAPTRAN user and no discussion of the FASTGRASS model is included in this document although the coding is still embedded in FRAPTRAN. However, an option for the user to specify the transient time-dependent fission gas release is provided.

- FRAP-T6 had the option to read an output file from the RELAP-4 thermal-hydraulics code to define coolant conditions. This link has not been maintained during the development of either the RELAP or FRAP-T6/FRAPTRAN code series; therefore, this option is not being made available to the FRAPTRAN user. The option to read a formatted file of coolant conditions is still available to the user; see the input instructions in Appendix A.

- FRAP-T6 had options to a) perform an automated sensitivity analysis by varying input parameters; b) perform failure assessments (FRAIL package); and c) perform calculations using licensing analysis models (LACE package). These options were seldom used, they had not been maintained or verified, and they added complexity to the coding; therefore, the coding for these options has been deleted and is not present in FRAPTRAN.

- FRAP-T6 had the option for the user to specify considerable variations in azimuthal power and temperature profiles. No immediate use was seen for these options in FRAPTRAN, so these options are not being made available to the FRAPTRAN user at this time and no further discussion of these options is provided although the coding is still embedded in FRAPTRAN.

1.4 Report Outline

This report serves as both the model description document and the user input manual. A description of the analytical models is provided in Section 2. The overall structure of the code, the input and output information, and the user's means of controlling computational accuracy and run time are summarized in Section 3 along with some guidance on using the code. A description of the required control and input data is provided in Appendix A. A sample problem solution which illustrates the code input and output is provided in Appendix B. Provided in Appendices C and D are additional details on the heat transfer models and correlations. A description of the numerical scheme for calculating plenum temperatures is provided in Appendix E. The subroutines that compose each subcode in FRAPTRAN are provided in Appendix F. An option for providing transient coolant conditions directly from a file is provided in Appendix G.

This document provides a description of the first version of FRAPTRAN. Additional work is planned for the code and will be released in future versions along with revised documentation. Examples of planned

[a]FRAPCON-3 also uses only FRACAS-I for cladding stress and strain predictions.

future development for FRAPTRAN include updating the high-burnup cladding mechanical properties based on data currently being generated, developing and implementing transient fission gas release and transient fuel swelling models, updating the ANS decay heat model, and incorporating a revised fuel thermal conductivity model to improve high burnup and burnable poison calculations.

2 GENERAL MODELING DESCRIPTION

Several phenomenological models are required to calculate the transient performance of fuel rods. Models are included in FRAPTRAN to calculate a) heat conduction, b) cladding stress and strain, and c) rod internal gas pressure. Each of these general models are comprised of several specific models. For example, the heat conduction model includes models of a) the conduction of heat across the fuel-cladding gap, b) the transfer of heat from the cladding to the coolant, and c) the conduction of heat in a composite cylinder.

This section of the report first describes the order and interaction of the various models. Then the details of each model are discussed. This discussion includes a) a list of the assumptions upon which the model is based, b) the dependent and independent variables in each model, and c) the equations used to solve for the values of the dependent variables.

2.1 Order and Interaction of Models

The order of the general models in FRAPTRAN are shown in Figure 2.1. The solution for the fuel rod variables begins with the calculation of the temperatures of the fuel and cladding. The temperature of the gases in the fuel rod is then calculated. Next, the stresses and strains in the fuel and cladding are calculated. The pressure of the gas inside the fuel rod is then calculated. This sequence of calculations is cycled until essentially the same temperature distribution (i.e., within specified convergence criteria) is calculated for two successive cycles. Finally, the cladding oxidation and fission gas release (if specified by the user) are calculated. Time is then incrementally advanced, and the complete sequence of calculations is then repeated to obtain the values of the fuel rod variables at the advanced time.

The models interact with each other in several ways. The temperature of the fuel, which is calculated by the thermal model, is dependent upon the width of the fuel-cladding gap and fuel-cladding interfacial pressure, which is calculated by the deformation model. The diameter of the fuel pellet is dependent upon the temperature distribution in the fuel pellet. The mechanical properties of the cladding vary significantly with temperature. The internal gas pressure varies with the temperature of the fuel rod gases and the strains of the fuel and cladding. The stresses and strains in the cladding are dependent upon the internal gas pressure. In addition, there is a burnup dependence to the initial value of numerous variables necessary for calculating the transient response of a fuel rod.

The model interactions are taken into account by iterative calculations. The variables calculated in one model are treated as independent variables by the other models. For example, the fuel-cladding gap size, which is calculated by the deformation model, is treated as an independent variable by the thermal model. On the first iteration of a new time step, the thermal model assumes the fuel-cladding gap size is equal to the value calculated by the deformation model on the last iteration of the previous time step. On the i-th iteration, the thermal model assumes the fuel-cladding gap size is equal to the value calculated by the deformation model in the (i-1)-th iteration.

The sequence of the iterative computations is shown in Figure 2.1. Two nested loops of calculations are repeatedly cycled until convergence occurs. In the inside loop, the deformation and gas pressure models are repeatedly cycled until two successive cycles calculate gas pressure within the convergence criteria. If cladding ballooning is not occurring, convergence usually occurs within two cycles. In the outside

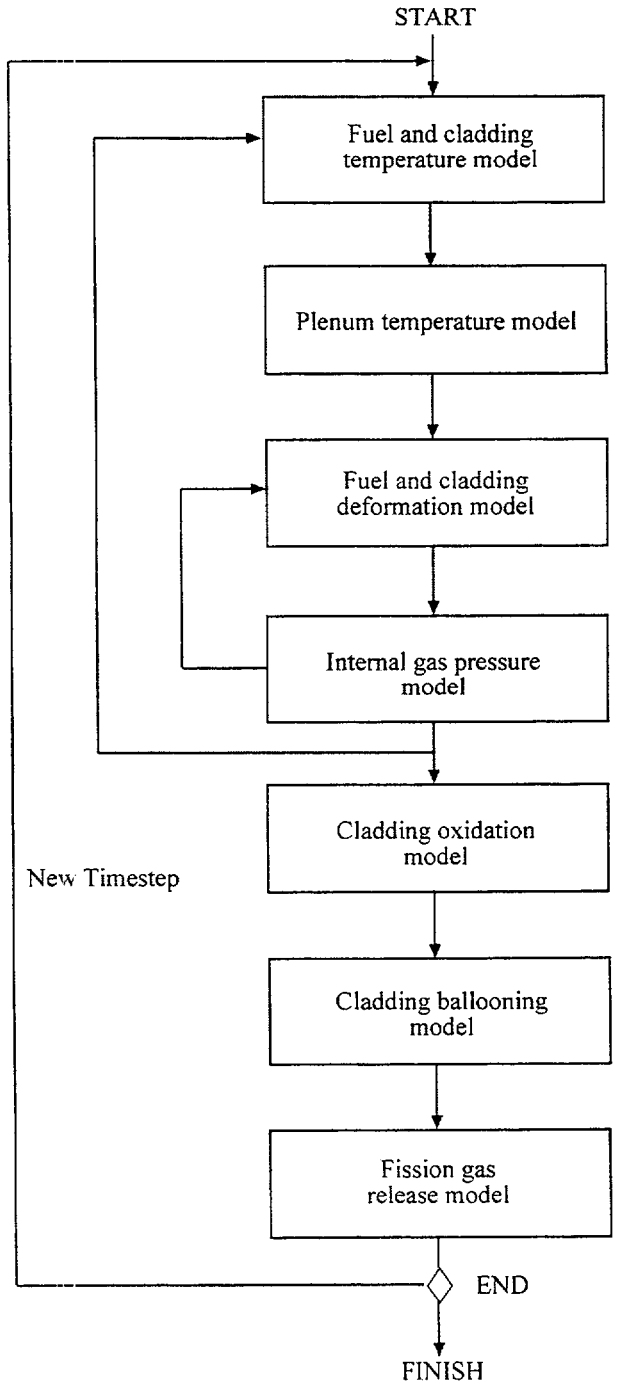

Figure 2.1 Order of General Models

loop, the fuel and cladding thermal model, plenum gas thermal model, and the inner loop are repeatedly cycled until the fuel rod temperature distribution is calculated within the convergence criteria. Convergence usually occurs within two or three cycles. After the computations of the outer loop have converged, the cladding oxidation and fission gas release are calculated, and a new time step is taken.

The convergences of both the inner and outer calculational loops are accelerated by use of the method of Newton. In the inner loop, the deformation model for the (i+1)-th iteration is given the predicted gas pressure for the (i+1)-th iteration. The gas pressure is predicted by the method of Newton and is based on the gas pressures calculated in the (i-1)-th and (i)-th iterations. The gas pressure is predicted by:

$$P_p^{i+1} = \left(P_c^{i-1} - \frac{P_c^i - P_c^{i-1}}{P_p^i - P_p^{i-1}} P_p^{i-1} \right) \Bigg/ \left(1 - \frac{P_c^i - P_c^{i-1}}{P_p^i - P_p^{i-1}} \right)$$

where: P_p^{i+1} = gas pressure predicted for the (i+1)-th iteration
P_p^i = gas pressure predicted for the i-th iteration
P_c^i = gas pressure calculated by the i-th iteration.

The convergence of the outer loop is accelerated in a manner similar to that of the inner loop, but with the fuel-cladding gap conductance as the predicted variable instead of the gas pressure.

NOTE: The following descriptions of the models used in FRAPTRAN present the models and equations in SI units. This provides a consistency with the FRAP-T6 description (Siefken et al. 1981) and the FRAPCON-3 description (Berna et al. 1997). However, the user should be aware that the coding itself, because of its vintage and multiple developers over the years, has been done in a mixture of SI, English, and some unusual units. This results in frequent units conversion in the code and the coding looking different than the written description. Therefore, to help the user compare this description with the actual coding, some constants and/or equations will also be provided in this document as they actually appear in the coding.

2.2 Fuel and Cladding Temperature Model

The fuel and cladding temperature model applies the laws of heat transfer and thermodynamics to calculate the temperature distribution throughout the fuel rod. The solution is performed in several steps by division of the dependent variables into smaller groups and then solving each group of variables in sequence.

A flow chart of the fuel and cladding temperature model is provided in Figure 2.2. First, the local coolant conditions (pressure, quality, and mass flux) are determined, either by a one-dimensional transient fluid flow model or from an input coolant boundary condition file. Then the heat generation in the fuel is found by interpolation in the user-input tables of fuel rod power distribution and power history. Through use of the most recently calculated fuel-cladding gap size, the value of the fuel-cladding gap conductance is calculated. This calculation obtains the gas properties from the MATPRO materials properties package. In addition, values of the fuel thermal conductivity are obtained from a modified MATPRO routine (see Section 2.2.4). Next the surface temperature of the cladding is calculated. This calculation includes a determination of the mode of convective or boiling heat transfer

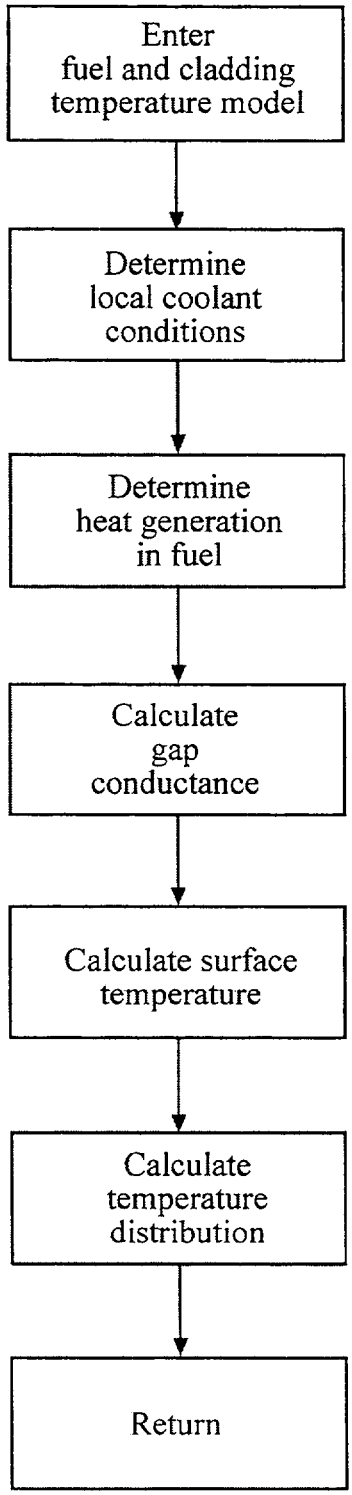

Figure 2.2 Flow Chart of Fuel and Cladding Temperature Model

and an evaluation of the surface heat transfer coefficient. Finally, the temperature distribution throughout the fuel and cladding is determined by the solution of a set of simultaneous equations.

The models used in the temperature calculations involve a number of assumptions and limitations, the most important of which are:

1. No heat conduction in the longitudinal direction.

2. Steady-state critical heat flux correlations are assumed to be valid during transient conditions.

3. Steady-state cladding surface heat transfer correlations are assumed to be valid during transient conditions.

4. Coolant is water.

2.2.1 Local Coolant Conditions

The pressure, mass flux, and inlet enthalpy of the coolant are needed to calculate fuel rod cooling. The coolant pressure is also needed to calculate the cladding deformation. In general, the coolant conditions should be calculated by a thermal-hydraulic code and then be input to FRAPTRAN. The coolant pressure and mass flux must always be specified by user input. Depending on the option selected by the user, the coolant enthalpy can be specified by either user input or calculated by the fluid flow model in FRAPTRAN, as described in Appendix D. The format for inputting coolant conditions via a file is provided in Appendix G.

2.2.2 Heat Generation

Heat is generated in the fuel by fissioning of uranium or plutonium atoms and by radioactive decay of fission products. The heat generation must be determined by a reactor physics analysis and be input to FRAPTRAN. Alternatively, only the heat generation due to fissioning is prescribed by input, and that due to radioactive decay is calculated by the ANS decay heat model (Scatena and Upham 1973). If the reactor is scrammed at initiation of an accident, so that no heat is generated by fissioning during the accident, the last option may be used.

The heat generation input consists of three sets of tables:

1. linearly-averaged rod power as a function of time,

2. normalized power as a function of axial position (normalized to average of 1.0), and

3. normalized power as a function of radial position (normalized to average of 1.0) at each axial position.

The normalized radial power profiles are assumed not to change during the short time period of the calculations. The normalized axial power profiles may change with time during the transient as defined by the user.

Heat is generated in the cladding during oxidation of the Zircaloy. The amount of oxidation and heat generation is negligible for cladding at a temperature less than 1000K, but is significant for cladding at temperatures greater than 1300K. The amount of heat generation is calculated by the cladding oxidation model(s).

2.2.3 Gap Conductance

FRAPTRAN uses a modified version of the gap conductance model used in FRAPCON-3 (Lanning, Beyer, and Painter 1997).

The fuel-cladding gap conductance model consists of three terms:

$$h_{gap} = h_{gas} + h_r + h_{solid} \tag{2.1}$$

where: h_{gap} = total gap conductance (W/m^2-K)
h_{gas} = conductance through gas in the gas gap (W/m^2-K)
h_r = conductance by radiation from fuel outer surface to cladding inner surface (W/m^2-K)
h_{solid} = conductance by fuel-cladding solid-solid contact (W/m^2-K)

2.2.3.1 Gas Conductance

The conductance through the gas in the fuel-cladding gap is defined as:

$$h_{gas} = K_{gas} / \left(x_{gap} + x_{jump} \right) \tag{2.2}$$

where: K_{gas} = gas thermal conductivity (W/m-k) from MATPRO routine GTHCON
x_{gap} = the width of the gas gap (m)
where a minimum gas gap is defined as the maximum of the combined fuel and cladding roughness ($R_f + R_c$) or 1.27×10^{-7} m (0.5×10^{-5} inch in the coding)
R_f = fuel surface roughness (m)
R_c = cladding surface roughness (m)
x_{jump} = combined fuel and cladding temperature jump distance (m)

The combined temperature jump distance term accounts for the temperature discontinuity caused by incomplete thermal accommodation of gas molecules to surface temperature. The terms also account for the inability of gas molecules leaving the fuel and cladding surfaces to completely exchange their energy with neighboring gas molecules, which produces a nonlinear temperature gradient near the fuel and cladding surfaces. The terms are calculated by the equation:

$$x_{jump} = a \bullet [K_{gas} \bullet T_{gas}^{0.5} / P_{gas}] / [\Sigma (f_j \bullet a_j / M_j^{0.5})] \tag{2.3}$$

where: a = 0.024688 (=2.23 in the coding)
T_{gas} = temperature of the gas in the fuel-cladding gap (K)
P_{gas} = pressure of the gas in the fuel-cladding gap (N/m^2)
f_j = mole fraction of j-th gas component
a_j = accommodation coefficient of the j-th gas component
M_j = molecular weight of j-th gas component (g-moles)

The accommodation coefficients for helium and xenon are calculated by the equations

$$a_{He} = 0.425 - 2.3\text{x}10^{-4} \bullet T_{gas} \qquad (2.4)$$
$$a_{Xe} = 0.749 - 2.5\text{x}10^{-4} \bullet T_{gas}$$

If T_{gas} is greater than 1000K, then T_{gas} is set equal to 1000K.

The accommodation coefficients for gases of other molecular weights, such as argon and krypton, are determined by interpolation using the equation:

$$a_j = a_{He} + [M_j - M_{He}][a_{Xe} - a_{He}]/[M_{Xe} - M_{He}] \qquad (2.5)$$

2.2.3.2 Radiation Heat Conductance

The radiation heat conductance term in Equation (2.1), h_r, is usually only significant when cladding ballooning has occurred. Then the gas conductance term is small because of the large fuel-cladding gap width. The radiation term is calculated by the expression:

$$h_r = \sigma F_e F_a (T_f^2 + T_c^2)(T_f + T_c) \qquad (2.6)$$

where: σ = Stefan-Boltzmann constant = $5.6697\text{x}10^{-8}$ W/m^2-K^4 (= $0.4806\text{x}10^{-12}$ in the coding)
F_e = emissivity factor determined by MATPRO routine EMSSF2
F_a = configuration factor = 1.0
T_f = temperature of fuel outer surface (K)
T_c = temperature of cladding inner surface (K)

2.2.3.3 Solid-Solid Conductance

The heat conductance from fuel-cladding solid-solid contact is defined as follows:

$$h_{solid} = 0.4166 \bullet k_m \bullet P_{rel} \bullet R_{mult} / (R \bullet E), \text{ if } P_{rel} > 0.003 \qquad (2.7)$$

$$\begin{aligned} R_{mult} &= 333.3 \bullet P_{rel}, \text{ if } P_{rel} \le 0.0087 \\ &= 2.9, \text{ if } P_{rel} > 0.0087 \\ &= 0.00125 \bullet k_m / (R \bullet E), \text{ if } 0.003 > P_{rel} > 9.0\text{x}10^{-6} \\ &= 0.4166 \bullet k_m \bullet P_{rel}^{0.5} / (R \bullet E), \text{ if } P_{rel} < 9.0\text{x}10^{-6} \end{aligned}$$

where: h_{solid} = solid-solid gap conductance (W/m^2-K)
P_{rel} = ratio of interfacial pressure to cladding Meyer hardness (Meyer hardness determined from MATPRO routine CMHARD)
k_m = mean thermal conductivity of fuel and cladding (W/m-K)
= $2K_fK_c/(K_f+K_c)$ where K_f and K_c are the fuel and cladding thermal conductivities, respectively, evaluated at their respective surface temperatures
R = $(R_f^2 + R_c^2)^{1/2}$ where R_f and R_c are the fuel and cladding surface roughness, respectively (m)
E = $\exp[5.738 - 0.528 \bullet \ln(R_f \bullet a)]$ where $a = 3.937\text{x}10^7$ µm (=$1.0\text{x}10^6$ µin in the coding)

The interfacial pressure is limited to a maximum value of 4000 psia when calculating h_{solid}.

2.2.4 Fuel Thermal Conductivity

The fuel thermal conductivity model used in FRAPTRAN incorporates dependencies on local burnup, gadolinia (Gd_2O_3) concentration, and initial plutonium concentration, and is the same model as used in FRAPCON-3 (Lanning, Beyer, and Painter 1997).

The conductivity for irradiated fuel is defined as the unirradiated conductivity modified by a series of factors to account for burnup, porosity, and radiation effects, as follows:

$$K_{fuel} = K_{base} \bullet FD \bullet FP \bullet FM \bullet FR \tag{2.8}$$

where: K_{fuel} = corrected fuel thermal conductivity (W/m-K)
K_{base} = non-irradiated thermal conductivity assuming 100% theoretical density
FD = burnup correction accounting for the effect of dissolved fission products
FP = burnup correction accounting for the effect of precipitated fission products
FM = Maxwell porosity correction factor
FR = radiation effects correction factor

K_{base}, FD, FP, FM, and FR are further defined as follows:

2.2.4.1 Base Fuel Thermal Conductivity (K_{base})

Lucuta, Matzke, and Hastings (1996) recommended a fuel thermal conductivity model for UO_2 that was accepted for FRAPCON-3 (Lanning, Beyer, and Painter 1997). This model correlates data from SIMFUEL plus data from fuel over a range of burnup levels. The Lucuta model has been modified to incorporate the effect of gadolinia (by adding a term to the denominator of the phonon term) and using the rule of mixtures, based on specific heats, to account for PuO_2 additions. The resulting equation as used in FRAPTRAN (and FRAPCON-3) is:

$$K_{base} = mix \bullet [1./(0.0375 + 2.165\text{x}10^{-4} \bullet T + 1.5 \bullet Gd) + (4.75\text{x}10^{9}/T^{2})\exp(-16361/T)] \tag{2.9}$$

where: T = temperature (K)
Gd = weight fraction of gadolinia (Gd_2O_3)
mix = effect of initial plutonium concentration on fuel thermal conductivity
= 1.0 for UO_2 (no PuO_2)
= $c_v(UO_2) \bullet (1\text{-}Pu) + c_v(PuO_2)$
$c_v(UO_2)$ = volume specific heat of UO_2
$c_v(PuO_2)$ = volume specific heat of PuO_2
Pu = initial plutonium fraction in fuel

2.2.4.2 Dissolved Fission Products Factor (FD)

The effect of dissolved fission products in the fuel matrix is reflected by the following burnup and temperature-dependent factor.

$$FD = (a + b) \bullet \arctan[1/(a+b)] \tag{2.10}$$

where: $a = 1.09/B^{3.265}$
$b = 0.0643 \cdot (T)^{1/2}/B^{1/2}$
B = local burnup in atom% (1 atom% = 9.383 GWd/MTU at 200 MeV/fission)

2.2.4.3 Precipitated Fission Products Factor (FP)

The effect of precipitated fission products in the fuel matrix is reflected by the following burnup and temperature-dependent factor:

$$FP = 1.0 + [0.019 \cdot B/(3.0 - 0.019 \cdot B] \cdot [1.0/(1.0 + \exp((1200 - T)/100)] \quad (2.11)$$

2.2.4.4 Porosity Factor (FM)

The effect of porosity is accounted for by the Maxwell factor, as follows:

$$FM = (1 - p) / [1 + (s-1) \cdot p] \quad (2.12)$$

where: p = porosity fraction
= 1- fractional theoretical density
s = shape factor
= 1.5 for spherical pores (as used in the coding)

2.2.4.5 Radiation Effects Factor (FR)

The effect of radiation is accounted for by the following equation:

$$FR = 1.0 - [0.2 / (1 + \exp((T-900)/80)] \quad (2.13)$$

2.2.5 Fuel Rod Cooling

The fuel rod cooling model calculates the amount of heat transfer from the fuel rod to the surrounding coolant. In particular, the model calculates the heat transfer coefficient, heat flux, and temperature at the cladding surface. These variables are determined by the simultaneous solution of two independent equations for cladding surface heat flux and surface temperature.

One of the equations is the appropriate correlation for convective heat transfer from the fuel rod surface. This correlation relates surface heat flux to surface temperature and coolant conditions. Different correlations are required for different heat transfer modes, such as nucleate or film boiling. The relation of the surface heat flux to the surface temperature for the various heat transfer modes is shown in Figure 2.3. Logic for selecting the appropriate mode and the correlations available for each mode are shown in Table 2.1. The correlations are described in Appendix D.

The second independent equation containing surface temperature and surface heat flux as the only unknown variables is derived from the finite difference equation for heat conduction at the mesh bordering the fuel rod surface. A typical plot of this equation during the nucleate boiling mode of heat transfer is also shown in Figure 2.3. The intersection of the plot of this equation and that of the heat transfer correlations determines the surface heat flux and temperature. The derivation of this equation

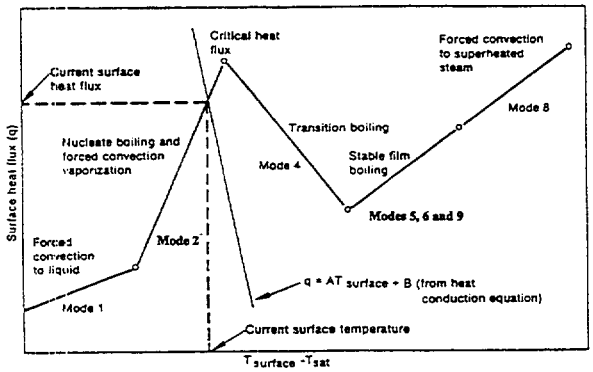

Figure 2.3 Relation of Surface Heat Flux to Surface Temperature

Table 2.1 Heat Transfer Mode Selection and Correlations

Heat Transfer Mode	Range[a]	Heat Transfer Correlation[b]
1. Forced convection to liquid	$T_w<T_{sat}$ or $Q_2<Q_1<Q_{crit}$	Dittus-Boelter (Dittus and Boelter 1930)
2. Nucleate boiling	$Q_1<Q_2<Q_{crit}$; $T_w>T_{sat}$	Chen (Behling et al. 1981)
4. High flow transition boiling	$Q_2>Q_{crit}$; $Q_4>Q_5$; G>200,000	McDonough, Milich, and King (McDonough, Milich, and King 1958)
5. High flow film boiling	$Q_2>Q_{crit}$; $Q_5>Q_4$; G>200,000 or $Q_5>Q_6$	Groeneveld (Groeneveld 1969) Dougall-Rohsenow (Dougall and Rohsenow 1963) Condie-Bengston (McDonough, Milich, and King 1958)
6. Low flow boiling and free convection	$Q_2>Q_{crit}$; $Q_6>Q_5$; G<200,000	modified Hsu and Bromley-Pomeranz (Behling et al. 1981)
8. Forced convection to superheated steam	X>1	Dittus-Boelter (Dittus and Boelter 1930)
9. Low pressure film boiling[c]	P<500 and range of mode 5	Dougall-Rohsenow (Dougall and Rohsenow 1963)

[a]The symbols used are:
Q_i = surface heat flux for I-th heat transfer mode
Q_{crit} = critical heat flux
T_w = cladding surface temperature
T_{sat} = saturation temperature of coolant
X = coolant quality
G = mass flux (lb_m/hr-ft^2)
P = coolant pressure (psia)
[b]For each heat transfer mode shown, only one of the listed correlations next to the parameter limits describing the range of the heat transfer mode is used. The correlation to be used is specified in the input.
[c]If a film boiling correlation other than Groenveld is specified, mode 9 is not considered.

and the simultaneous solution for surface temperature and surface heat flux are described in Appendix C. Neither of the two equations solved simultaneously contains past iteration values so that numerical instabilities at the onset of nucleate boiling are avoided. A separate set of heat transfer correlations is used to calculate fuel rod cooling during the reflooding portion of a LOCA. During this period, liquid cooling water is injected into the lower plenum and the liquid level gradually rises over a period of time to cover the fuel rods. This complex heat transfer process is modeled by a set of empirical relations derived from experiments performed in the FLECHT facility (Cadek et al. 1972). A description of these models is presented in Appendix D.

2.2.5.1 Thermal Effect of Cladding Outer Surface Oxide Layer

An addition for FRAPTRAN relative to FRAP-T6 is to account for the thermal barrier effect of the cladding outer surface oxide layer.[a] This thermal effect is accounted for by calculating the temperature change across the oxide layer. The temperature at the oxide outer surface is defined by the coolant heat transfer equations described above. After the temperature change across the oxide layer is calculated, the temperature change is added to the fuel rod surface temperature calculated from the coolant conditions. This revised temperature is then used to define the cladding surface temperature used in the temperature solution defined in Section 2.2.6. In effect, the oxide layer temperature calculation redefines the cladding surface temperature from that derived from the coolant heat transfer equations.

The temperature change across the oxide layer is defined in terms of a steady-state solution:

$$\Delta T_{oxide} = q'' \, \Delta r_{oxide} / k_{oxide}$$

where: ΔT_{oxide} = the temperature change across the oxide (K)
q'' = the surface heat flux (W/m^2)
Δr_{oxide} = the thickness of the oxide layer (m)
k_{oxide} = the thermal conductivity of the oxide (W/m-K)

The oxide thermal conductivity is evaluated at the fuel rod surface temperature defined from the coolant heat transfer and is calculated using the ZOTCON routine from MATPRO-11. The steady-state solution is conservative for the fuel rod temperature solution.

2.2.6 Heat Conduction and Temperature Solution

Once values for the heat generation, gap conductance, and cladding surface temperature have been obtained, the complete temperature distribution in the fuel and cladding is obtained by applying the law for heat conduction in solids, in either one or two dimensions as specified by the code user.

2.2.6.1 One-Dimensional Radial Heat Conduction

Heat conduction in the radial direction in both the fuel and cladding is described by the equation:

$$\int_v \rho \, C_p \frac{\partial T}{\partial t} \, dv = \int_s k \bar{\nabla} T \cdot d\bar{s} + \int_v q \, dV \qquad (2.14)$$

where: T = temperature, K
t = time, s
q = volumetric heat generation rate, W/m^3
C_p = specific heat, J/kg-K
ρ = density, kg/m^3
k = thermal conductivity, W/m-K-s

[a]FRAP-T6 and FRAPTRAN calculate the oxide surface layer thickness, but FRAP-T6 assumed that the oxide layer had no thermal effect on the temperature calculations. This assumption is acceptable for thin oxide layers, but significant temperature increases are possible for thick oxide layers.

The first integral calculates the enthalpy change of an arbitrary infinitesimal volume of material, the second the heat transfer through the surface of the volume, and the third the heat generation within the volume. The parameters C_p and k are temperature dependent. The fuel thermal conductivity is also burnup dependent. The following boundary conditions are used with Equation 2.14:

$$\left.\frac{\partial T}{\partial r}\right|_{r=0} = 0$$

$$\left. T \right|_{r=r_o} = T_s$$

where: r = radial position, m

r_o = outer radius of fuel, m

T_s = fuel rod outer surface temperature, K (see Section 2.2.5 and Appendix C for solution for T_s)

Equation 2.14 is numerically solved by using an implicit finite difference approximation. The solution method is taken from the HEAT-1 code (Wagner 1963). The solution method accounts for temperature and time dependent thermal properties; transient spatially varying heat generation; and melting and freezing of the fuel and cladding.

With Figure 2.4 as a reference for geometry terms, the finite difference approximation for heat conduction is:

$$\frac{(T_n^{m+1} - T_n^m)\,(c_{ln}\,h_{ln}^v + c_{rn}\,h_{rn}^v)}{\Delta t} = -\,(T_n^{m+1/2} - T_{n-1}^{m+1/2})\,k_{ln}\,h_{ln}^s + (T_{n+1}^{m+1/2} - T_n^{m+1/2})\,k_{rn}\,h_{rn}^s + Q_{ln}\,h_{ln}^v + Q_{rn}\,h_{rn}^v \tag{2.15}$$

where:

T_n^{m+1} = temperature at radial node n and time point m+1 (K)

$T_n^{m+1/2}$ = $0.5\,(T_n^m + T_n^{m+1})$

Δt = time step (s)

c_{ln} = volumetric heat capacity on left side of node n ($J/m^3 \cdot k$)

c_{rn} = volumetric heat capacity on right side of node n ($J/m^3 \cdot k$)

k_{rn} = thermal conductivity at right side of node n ($W/m \cdot k$)

k_{ln} = thermal conductivity at left side of node n ($W/m \cdot k$)

h_{ln}^v = volume weight of mesh spacing on left side of radial node n (m^2)

$$= \pi \Delta r_{ln}\left(r_n - \frac{\Delta r_{ln}}{4}\right)$$

h_{rn}^v = volume weight on right side of node n (m^2)

$$= \pi \Delta r_{rn}\left(r_n + \frac{\Delta r_{rn}}{4}\right)$$

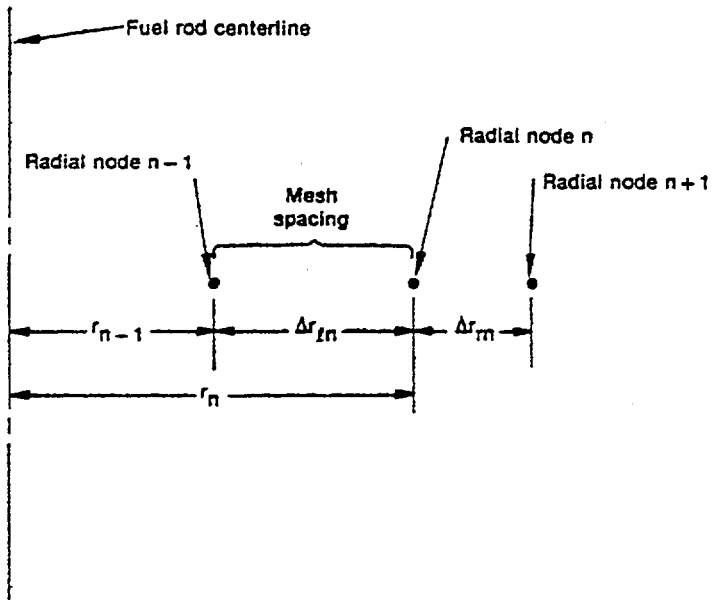

Figure 2.4 Description of Geometry Terms in Finite Difference Equation for Heat Conduction

$h_{\ell n}^{s}$ = surface weight on right side of node n

$$= \frac{2\pi}{\Delta r_{\ell n}}\left(r_n - \frac{\Delta r_{rn}}{2}\right)$$

h_{rn}^{s} = surface weight on right side of node n

$$= \frac{2\pi}{\Delta r_{rn}}\left(r_n + \frac{\Delta r_{rn}}{2}\right)$$

$Q_{\ell n}$ = heat generation per unit volume for mesh spacing on left side of radial node n (W/m^3).

If a phase change from solid to liquid, or liquid to solid, occurs at radial node n, Equation 2.15 is modified to account for the storage or release of the heat of fusion while the temperature remains equal to the melting temperature. The modified equation is:

$$\rho H\,(h_{\ell n}^{v} + h_{rn}^{v})\,\frac{d\alpha_n^{m+1/2}}{dt} = -\,(T_L - T_{n-1}^{m+1/2})\,k_{\ell n}\,h_{\ell n}^{s} + (T_{n+1}^{m+1/2} - T_L)\,k_{rn}\,h_{rn}^{s} + Q_{\ell n}^{m+1/2}\,h_{\ell n}^{v} + Q_{rn}^{m+1/2}\,h_{rn}^{v} \tag{2.16}$$

where: $\frac{d\,\alpha_n^{m+1/2}}{dt}$ = rate of change of volume fraction of material melted in the two half mesh spacings on either side of radial node n during the midpoint of the time step (s^{-1})

H = heat of fusion of the material (J/kg)

T_L = melting temperature of the material (K)

The phase change from solid to liquid is complete when:

$$\sum_{m=M_1}^{m=M_2} \frac{d\alpha_n^{m+1/2}}{dt} \Delta t^m = 1$$

where: M_1 = number of time step at which melting started
M_2 = number of time step at which melting ends
Δt^m = size of m-th time step, s

The finite difference approximations at each radial node are combined together to form one tri-diagonal matrix equation. The equation has the form:

$$\begin{vmatrix} b_1 & c_1 & 0 & 0 & \\ a_2 & b_2 & c_2 & 0 & 0's \\ 0 & a_3 & b_3 & c_3 & \\ & \cdot & \cdot & \cdot & \\ & & \cdot & \cdot & \\ & & \cdot & \cdot & \cdot \\ & 0's & a_{N-1} & b_{N-1} & c_{N-1} \\ & & 0 & a_N & b_N \end{vmatrix} \begin{vmatrix} T_1^{m+1} \\ T_2^{m+1} \\ T_3^{m+1} \\ \cdot \\ \cdot \\ \cdot \\ T_{N-1}^{m+1} \\ T_N^{m+1} \end{vmatrix} = \begin{vmatrix} d_1 \\ d_2 \\ d_3 \\ \cdot \\ \cdot \\ \cdot \\ d_{N-1} \\ d_N \end{vmatrix} \tag{2.17}$$

Equation 2.17 is solved by Gaussian elimination for the radial node temperatures. Because the off-diagonal elements are negative and the sum of the diagonal elements is greater than the sum of the off-diagonal elements, little roundoff error occurs as a result of using Gaussian elimination.

When the forward reduction step of Gaussian elimination has been applied to Equation 2.17, the last equation in the transformed equation is:

$$A\ T_N^{m+1} + B = q_N^{m+1} \tag{2.18}$$

where: T_N^{m+1} = cladding surface temperature (K)
q_N^{m+1} = cladding surface heat flux (W/m^2)
A, B = coefficients that are defined in Appendix C.

Equation 2.18 is combined with the correlation for convective heat transfer to solve for the cladding surface temperature, as previously shown in Figure 2.3.

The description of the calculations for the temperature distribution in the fuel and cladding is complete at this point. The calculation of the temperature of the gas in the fuel rod plenum is then needed to complete the solution for the fuel rod temperature distribution. This calculation is performed by a separate model and is described in the following section.

2.3 Plenum Gas Temperature Model

To calculate the internal fuel rod pressure, the temperature for all gas volumes in the fuel rod must be calculated. Under steady-state and transient reactor conditions, approximately 40 to 50% of the gas in a fuel rod is located in the fuel rod plenum provided at the top, and sometimes the bottom, of the fuel rod. Two options are available to define the temperatures of the gas in the plenum. The default is to assume the gas temperature to 10K higher than the local coolant temperature. A more detailed model to calculate the temperature is available as a user option, the model includes all thermal interactions between the plenum gas and the top pellet surface, hold-down spring, and cladding wall.

The transient plenum temperature model is based on three assumptions.

1. The temperature of the top surface of the fuel stack is independent of the plenum gas temperature.

2. The plenum gas is well mixed by natural convection.

3. Axial temperature gradients in the spring and cladding are small.

The first assumption allows the end-pellet temperature to be treated as an independent variable. The second assumption permits the gas to be modeled as one lumped mass with average properties. The third assumption allows the temperature response of the cladding and spring to be represented by a small number of lumped masses.

The plenum temperature model consists of a set of six simultaneous first order differential equations that model the heat transfer between the plenum gas and the structural components of the plenum. These equations involve heat transfer coefficients between the various components. The heat transfer equations for the plenum temperature are described in Section 2.3.1. The required heat transfer coefficients are described in Section 2.3.2. Finally, the calculation of the gamma heating of the plenum hold-down spring and cladding is described in Section 2.3.3. A flow chart of the calculation is shown in Figure 2.5.

2.3.1 Plenum Temperature Equations

The plenum thermal model calculates the energy exchange between the plenum gas and structural components. The structural components consist of the hold-down spring, end pellet, and cladding. Energy exchange between the gas and structural components occurs by natural convection, conduction, and radiation. A schematic of these energy exchange mechanisms is shown in Figure 2.6. The spring is modeled by two nodes of equal mass (a center node and a surface node) as shown in Figure 2.7. The cladding is modeled by three nodes (two surface nodes and one center node) as shown in Figure 2.8. The center node has twice the mass of the surface nodes. This nodalization scheme results in a set of six energy equations from which the plenum thermal response can be calculated. The transient energy equations for the gas, spring, and cladding are as follows (the nomenclature used in the equations is defined in Table 2.2):

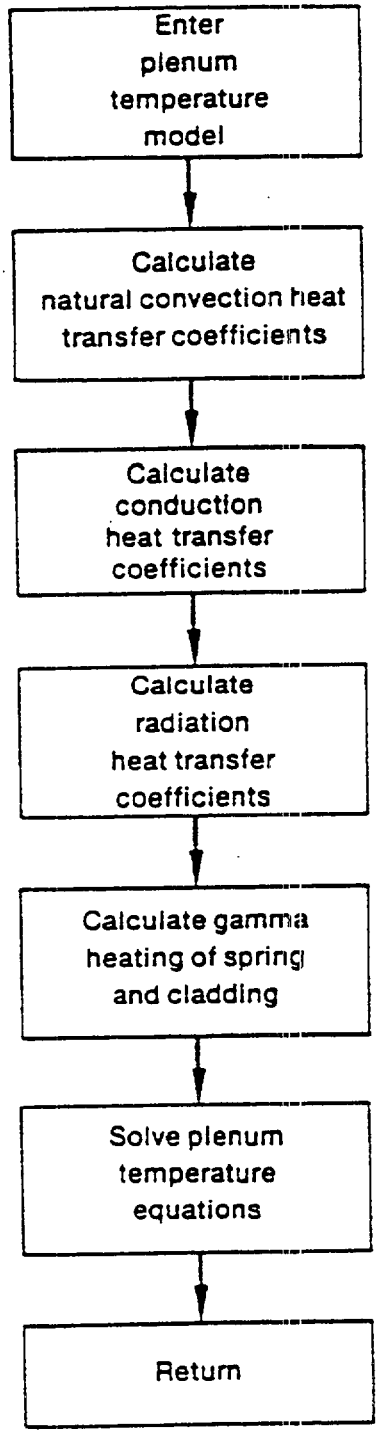

Figure 2.5 Flow Chart of Plenum Temperature Calculation

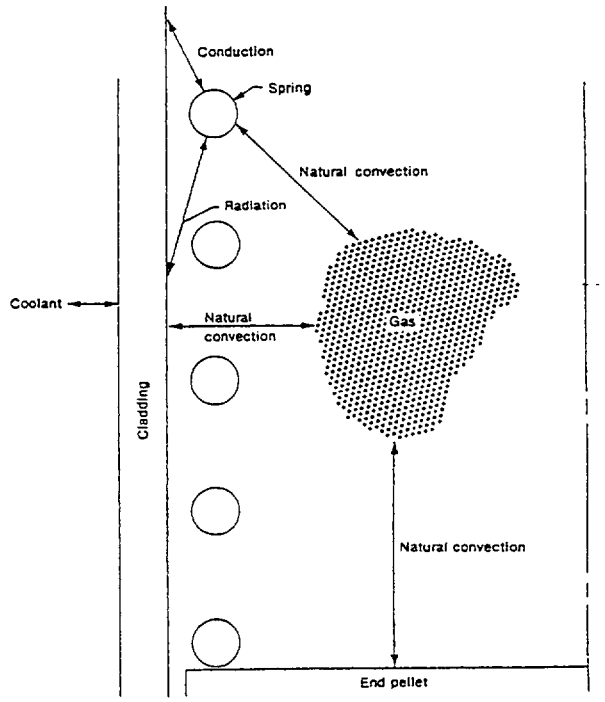

Figure 2.6 Energy Flow in Plenum Model

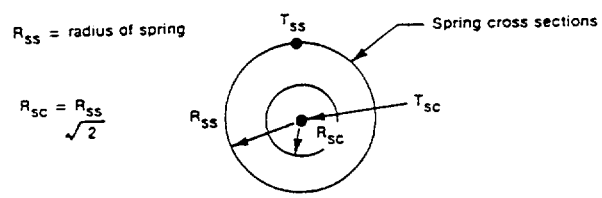

Figure 2.7 Spring Noding

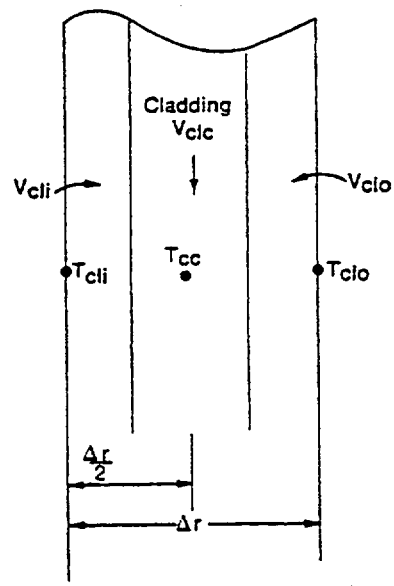

Figure 2.8 Cladding Noding

1. Plenum gas

$$\rho_g V_g C_g \frac{\partial T_g}{\partial t} = A_{ep} h_{ep} (T_{ep} - T_g) + A_{cl} h_{cl} (T_{cli} - T_g) + A_{ss} h_s (T_{ss} - T_g) \tag{2.19}$$

2. Spring center node

$$V_{sc} C_s \rho_s \frac{\partial T_{sc}}{\partial t} = \bar{q} V_{sc} + \frac{A_{sc} K_s (T_{ss} - T_{sc})}{R_{ss}} \tag{2.20}$$

3. Spring surface node

$$V_{ss} C_s \rho_s \frac{\partial T_{ss}}{\partial t} = \bar{q} V_{ss} + A_{sc} K_s (T_{sc} - T_{ss}) + A_{ss} h_{rads} (T_{cli} - T_{ss}) + A_{ss} h_s (T_g - T_{ss}) + A_{ss} h_{cons} (T_{cli} - T_{ss}) \tag{2.21}$$

where: h_{cons} = conductance between the spring and cladding

The conductance, h_{cons}, is used only when a stagnant gas condition exists; that is, when the natural convection heat transfer coefficient for the spring (h_s) is zero.

Table 2.2 Nomenclature for Plenum Thermal Model	
Quantities	**Subscripts**
A = surface area	cl = cladding
C = heat capacitance	clc = cladding center node
DIAC = diameter of the spring coil	cli = cladding interior node
DIAS = diameter of the spring wire	clo = cladding outside node
$\bar{F}_{1-2}$ = gray-body shape factor from body 1 to body 2	cool = coolant
F_{1-2} = view factor from body 1 to body 2	conc, cons = conduction between the spring and cladding
Gr = Grashof number	conv = convective heat transfer to coolant
h = surface heat transfer coefficient	ep = end pellet
I = gamma flux	g = gas
ID = inside diameter of the cladding	p = plenum
K = thermal conductivity	sc = spring center node
L = length	ss = spring surface node
OD = outside diameter of the cladding	s = spring
Pr = Prandtl number	rads, radc = radiation heat transfer between the spring and cladding
q = energy	m, m+1 = old and new time step
q'' = surface heat flux	
q''' = volumetric heat generation	
R = radius	
Δr = thickness of the cladding: (OD-ID)/2	
T = temperature	
V = volume	
σ = Stefan-Boltzmann constant	
C_g = heat capacitance of gas, set equal to the value of 5.188×10^3 J/kg-K, which is the heat capacitance of helium	
ρ = density	
$\sum\gamma$ = absorption coefficient	
ε = emissivity	
δ = spring to cladding spacing: (ID-DIAC)/2	
t = time	

4. Cladding interior node

$$\rho_{cl}\, C_{cl}\, V_{cli} \frac{\partial T_{cli}}{\partial t} = A_{cl}\, h_{radc}\, (T_{ss} - T_{cli}) + A_{cl}\, h_{cl}\, (T_g - T_{cli}) + A_{cl}\, h_{conc}\, (T_{ss} - T_{cli}) + \frac{A_{cl}\, K_{cl}}{\Delta r/2} (T_{clc} - T_{cli}) + \bar{q}\, V_{cli} \tag{2.22}$$

5. Cladding central node

$$\rho_{cl}\, C_{cl}\, V_{clc} \frac{\partial T_{clc}}{\partial t} = \bar{q}\, V_{clc} + \frac{A_{cl}\, K_{cl}}{\Delta r/2} (T_{cli} - T_{clc}) + \frac{A_{cl}\, K_{cl}}{\Delta r/2} (T_{clo} - T_{clc}) \tag{2.23}$$

6. Cladding exterior node

$$T_{clo} = T_{cool} \tag{2.24}$$

For steady-state analysis, the time derivatives of temperature on the left side of Equations 2.19 through 2.23 are set equal to zero, and the temperature distribution in the spring and cladding is assumed to be uniform.

To obtain a set of algebraic equations, Equations 2.19 through 2.24 are written in the Crank-Nicolson (Crank and Nicolson 1974) implicit finite difference form. This formulation results in a set of six equations and six unknowns.

The details of the finite difference formulation of Equations 2.19 through 2.24 and the logic of the plenum temperature model are given in Appendix E.

2.3.2 Heat Conduction Coefficients

Heat transfer between the plenum gas and the structural components occurs by natural convection, conduction, and radiation. The required heat transfer coefficients for these three modes are described in the following.

2.3.2.1 Natural Convection Heat Transfer Coefficients

Energy exchange by natural convection occurs between the plenum gas and the top of the fuel pellet stack, the spring, and the cladding. Heat transfer coefficients h_{ep}, h_s, and h_{cl}, in the equations above, model this energy exchange. To calculate these heat transfer coefficients, the top of the fuel stack is

assumed to be a flat plate, the spring is assumed to be a horizontal cylinder, and the cladding is assumed to be a vertical surface. Both laminar and turbulent natural convection are assumed to occur. Correlations for the heat transfer coefficients for these types of heat transfer are obtained from Kreith (1964) and McAdams (1954).

The flat plate natural convection coefficients used for the end pellet surface heat transfer are given below.

1. For laminar conditions on a heated surface

$$h_{ep} = 0.54\ K_g\ (Gr \times Pr)^{0.25} / ID \tag{2.25}$$

2. For turbulent conditions (Grashof Number (Gr) greater than 2.0×10^7) on a heated surface

$$h_{ep} = 0.14\ K_g\ (Gr \times Pr)^{0.33} / ID \tag{2.26}$$

3. For laminar conditions on a cooled surface

$$h_{ep} = 0.27\ K_g\ (Gr \times Pr)^{0.25} / ID \tag{2.27}$$

The following natural convection coefficients for horizontal cylinders are used for the film coefficient for the spring.

1. For laminar conditions

$$h_s = 0.53\ K_g\ (Gr \times Pr)^{0.25} / DIAS \tag{2.28}$$

2. For turbulent conditions (Gr from 1×10^9 to 1×10^{12})

$$h_s = 0.18\ (T_g - T_{ss})^{0.33} \tag{2.29}$$

The vertical surface natural convection coefficients used for the cladding interior surface are given below.

1. For laminar conditions

$$h_{cl} = 0.55\ K_g\ (Gr \times Pr)^{0.25} / L_p \tag{2.30}$$

2. For turbulent conditions (Gr greater than 1×10^9)

$$h_{cl} = 0.021\ K_g\ (Gr \times Pr)^{0.4} / L_p \tag{2.31}$$

These natural convection correlations were derived for flat plates, horizontal cylinders, and vertical surfaces in an infinite gas volume. Heat transfer coefficients calculated using these correlations are expected to be higher than those actually existing within the confined space of the plenum. However, until plenum temperature experimental data are available, these coefficients are believed to provide an acceptable estimate of the true values.

2.3.2.2 Conduction Heat Transfer Coefficients

Conduction of energy between the spring and cladding is represented by the heat transfer coefficients h_{cons} and h_{conc} in Equations 2.21 and 2.22. These coefficients are both calculated when stagnant gas conditions exist. The conduction coefficients are calculated on the basis of the spring and cladding geometries shown in Figure 2.9, and the following assumptions:

1. The cladding and spring surface temperatures are uniform.

2. Energy is conducted only in the direction perpendicular to the cladding wall (heat flow is one-dimensional).

On the basis of these assumptions, and the geometry given in Figure 2.9, the energy (q) conducted from an elemental surface area of the spring ($L_s R_s d\theta$) to the cladding is:

$$dq = \frac{K_g(T_{ss} - T_{cli})\,(L_s\, R_s \sin(\theta)\, d\theta)}{(d + R_s - R_s \sin\theta)} \tag{2.32}$$

where: θ = the azimuthal coordinate.

By integration of Equation 2.32 over the surface area of the spring facing the cladding, the total flow of energy is given by:

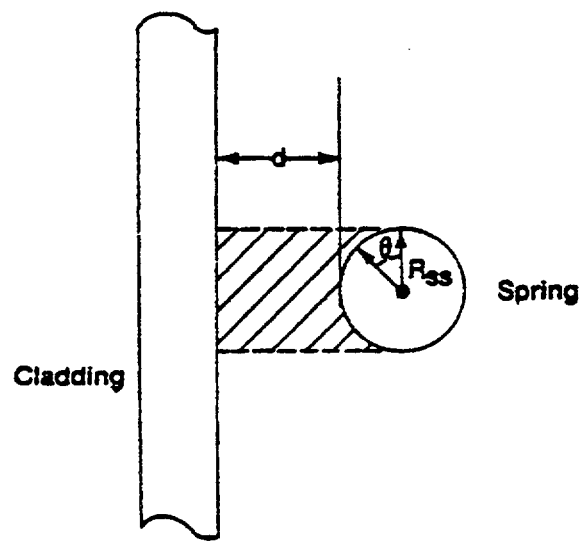

Figure 2.9 Geometrical Relationship Between the Cladding and Spring

$$q = \frac{k_g A_{ss}}{\pi} (T_{ss} - T_{cli}) \left[- \frac{\pi}{2R_s} \right.$$

$$\left. + \frac{2}{R_s} \left\{ \frac{\frac{1}{1-R_s^2}}{(\delta+2R_s)^2} + \mathrm{Tan}^{-1} \left[\left(\mathrm{Tan}\left(\frac{\theta}{2}\right) - \frac{R_s}{(\delta+2R_s)} \right) \Big/ \left(1 - \frac{R_s^2}{(\delta+2R_s)^2} \right) \right] \right\} \right]_{\theta=0}^{\theta=\frac{\pi}{2}} \tag{2.33}$$

The two conduction heat transfer coefficients are given by:

$$h_{cons} = q/A_{ss} (T_{ss} - T_{cli})$$

and

$$h_{conc} = hc_{ons} A_{ss}/A_{cl}$$

When natural convection heat transfer exists (h_{cl} or h_s greater than 0.0), energy is assumed to flow to the gas from the spring and then from the gas to the cladding wall, or vice versa. Under these conditions, h_{cons} and h_{conc} are set equal to zero. Therefore, h_{cons} and h_{conc} are used only when the temperature is uniform throughout the plenum. Future plenum data or analytical analysis may indicate that natural convection flow between the spring and cladding does not exist, in which case non-zero conduction coefficients will be used at all times.

2.3.2.3 Radiation Heat Transfer Coefficients

Transport of energy by radiation between the spring and cladding is included in the plenum model by use of the heat transfer coefficients h_{rads} and h_{radc}, in Equations 2.21 and 2.22. These coefficients are derived from the radiant energy exchange equation for two gray bodies in thermal equilibrium (Kreith 1964) as follows:

$$q_{1-2} = A_1 \bar{F}_{1-2} \sigma (T_1^4 - T_2^4) \tag{2.34}$$

where q_{1-2} is the net rate of heat flow by radiation between bodies 1 and 2.

The gray body factor ($\bar{F}_{1-2}$) is related to the geometrical view factor (F_{1-2}) from body 1 to body 2 by:

$$A_1 \bar{F}_{1-2} = \frac{1}{(1-\varepsilon_1)/A_1 \varepsilon_1 + 1/A_1 F_{1-2} + (1-\varepsilon_2)/A_{22}} \tag{2.35}$$

Using Equations 2.34 and 2.35 and approximating the geometric view factor from the cladding to the spring (F_{cl-s}) by:

$$F_{cl-s} = \frac{A_{ss}}{2\ A_{cl}} + \frac{(2A_{cl} - A_{ss})\ A_{ss}}{4A_{cl}^{\ 2}} \tag{2.36}$$

the net radiation energy exchange between the cladding and spring may be written as:

$$q_{cl-s} = A_{cl}\ \bar{F}_{cl-s}\ (T_{cli}^4 - T_{ss}^4) \tag{2.37}$$

The radiation heat transfer coefficients, h_{rads} and h_{radc}, are calculated by:

$$h_{radc} = \left(q_{cl-s} / A_{cl}\right) (T_{cli} - T_{ss}) \tag{2.38}$$

and

$$h_{rads} = (h_{radc} A_{cl}) / A_{ss} \quad . \tag{2.39}$$

2.3.3 Gamma Heating of the Spring and Cladding

The volumetric power generation term, q, used in Equations 2.20 through 2.23 represents the gamma radiation heating of the spring and cladding. A simple relationship is used to calculate q. The relationship used is derived from the gamma flux attenuation equation:

$$-dI(x) = \Sigma_\gamma\ I(x)\ dx \tag{2.40}$$

where $I(x)$ = gamma flux
$\Sigma\gamma$ = gamma ray absorption coefficient
x = spatial dimension of solid on which the gamma radiation is incident.

Because the cladding and spring are thin in cross-section, the gamma ray flux can be assumed constant throughout the volume. Of the gamma flux, I, incident on the spring and cladding, the portion absorbed, ΔI, can be described by:

$$-\Delta I = \Sigma_\gamma\ I\bar{x} \tag{2.41}$$

where $\bar{x}$ is the thickness of the spring or cladding. Therefore, the volumetric gamma ray absorption rate is given by:

$$-\frac{\Delta I}{\bar{x}} = \Sigma_\gamma\ I\ . \tag{2.42}$$

Equation 2.42 can also represent gamma volumetric energy deposition by letting I represent the energy flux associated with the gamma radiation. Approximately 10% of the energy released in the fissioning of uranium is in the form of high energy gamma radiation. Therefore, the gamma energy flux leaving the fuel rod would be approximately equal to 10% of the thermal flux. The gamma energy flux throughout the reactor can then be estimated by

$$I = 0.10\bar{q}_{rod} \tag{2.43}$$

where $\bar{q}_{rod}$ is the average fuel rod power (kW/m). For zirconium, $\Sigma\gamma$ is approximately 36.1 m^{-1}. Therefore, the gamma energy deposition rate is given by:

$$-\frac{\Delta I}{\bar{x}} = \bar{q} = 3.61\ \bar{q}_{rod} \tag{2.44}$$

Equation 2.44 is an estimate of the gamma heating rate for the spring and cladding.

2.4 Fuel Rod Mechanical Response Model

An accurate analysis of the fuel and cladding mechanical response is necessary in any fuel rod response analysis because the heat transfer across the fuel-cladding gap is a strong function of the gap size. In addition, an accurate calculation of stresses in the cladding is needed so that an accurate prediction of the extent of cladding ballooning and failure (and subsequent release of fission products) can be made.

In analyzing the mechanical response of fuel rods, two physical situations are encountered. The first situation occurs when the fuel pellets and cladding are not in contact. Here, the problem of a cylindrical shell (the cladding) with specified internal and external pressures and a specified cladding temperature distribution must be solved. This situation is called the "open gap" regime.

The second situation encountered is when the fuel pellets come into contact with the cladding. This will occur as a combination of differential thermal expansion between the fuel and cladding, fission-product induced swelling of the fuel, and creep-down of the cladding. This situation is called the "closed gap" regime and results in fuel pellet-cladding mechanical interaction (PCMI).

The mechanical model used in FRAPTRAN for calculating the mechanical response of the fuel and cladding is the FRACAS-I model; this model is also used in FRAPCON-3. This model does not account for stress-induced deformation of the fuel and is, therefore, called the rigid pellet model. This model includes the effects of thermal expansion of the fuel pellet, rod internal gas pressure, and thermal expansion, plasticity, and high temperature creep of the cladding.

After the cladding strain has been calculated by either mechanical model, the strain is compared with the value of an instability strain obtained from MATPRO. If the instability strain has been exceeded at any point along the rod, then the cladding cannot maintain a cylindrical shape and local ballooning occurs. For the local region at which instability is predicted, a large deformation ballooning analysis is performed. This analysis allows for non-axisymmetric large deformation of the cladding and can take into account local axial and circumferential temperature variations. Modification of local heat transfer coefficients is calculated as the cladding ballooning progresses and additional surface area is presented to the coolant.

In Section 2.4.1, the general theory of plastic analysis is outlined. In Section 2.4.2, the theory is extended to include creep and hot pressing. In Section 2.4.3, the equations for the FRACAS-I model are described. In Section 2.4.4, the model for local cladding ballooning is summarized.

2.4.1 General Considerations in Elastic-Plastic Analysis

Problems involving elastic-plastic deformation and multiaxial states of stress involve a number of aspects that do not require consideration in a uniaxial problem. In the following discussion, an attempt is made to briefly outline the structure of incremental plasticity and to outline the Method of Successive Substitutions (also called Method of Successive Elastic Solutions) which has been used successfully in treating multiaxial elastic-plastic problems (Mendelson 1968). The method can be used for any problem for which a solution based on elasticity can be obtained. This method is used in both the rigid pellet and deformable pellet models.

In a problem involving only uniaxial stress, σ_1, the strain, ε_1, is related to the stress by an experimentally determined stress-strain curve, as shown in Figure 2-11, and Hooke's Law which is taken as:

$$\varepsilon_1 = \frac{\sigma_1}{E} + \varepsilon_1^P + \int \alpha \, dT \tag{2.45}$$

where ε_1^p is the plastic strain and E is the modulus of elasticity. The onset of yielding in the code is calculated to occur at the true yield stress, which can be determined directly from Figure 2.10. Given a load (stress) history, the resulting deformation can be determined in a simple fashion. Increase of the yield stress with work-hardening is easily calculated directly from Figure 2.10.

In a problem involving multiaxial states of stress, however, the situation is not so clear. In such a problem, a method of relating the onset of plastic deformation to the results of a uniaxial test is required. Furthermore, when plastic deformation occurs, some means is needed for determining how much plastic deformation has occurred and how that deformation is distributed among the individual components of strain. These two complications are taken into account by use of the so-called "yield function" and "flow rule," respectively.

A substantial quantity of experimental evidence exists on the onset of yielding in a multiaxial stress state. The bulk of this evidence supports the von Mises yield criterion (Murphy 1946), which asserts that yielding occurs when the stress state is such that:

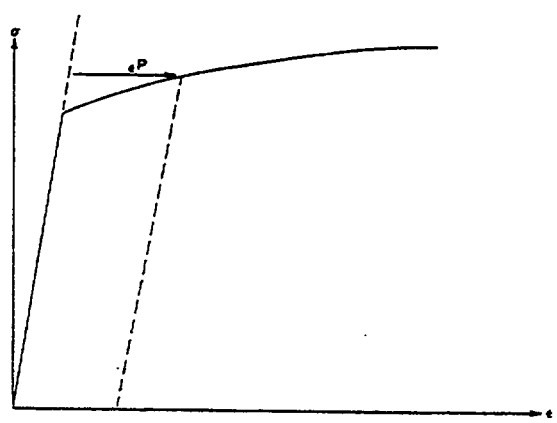

Figure 2.10 Typical Isothermal True Stress-Strain Curve

$$0.5\ [(\sigma_1 - \sigma_2)^2 + (\sigma_2 - \sigma_3)^2 + (\sigma_3 - \sigma_1)^2] = \sigma_y^{\ 2} \tag{2.46}$$

where the σ_i values are the principal stresses and σ_y is the yield stress as determined in a uniaxial stress-strain test. The square root of the left side of Equation 2.46 is referred to as the "effective stress," σ_e, and this effective stress is one commonly used type of yield function.

To determine how the yield stress changes with permanent deformation, the yield stress is hypothesized to be a function of the equivalent plastic strain, ε^P. An increment of equivalent plastic strain is determined at each load step, and ε^P is defined as the sum of all increments incurred, as follows:

$$\varepsilon^P \underset{=}{\Delta} \sum d\varepsilon^P \ . \tag{2.47}$$

Each increment of effective plastic strain is related to the individual plastic strain components by:

$$d\varepsilon^P = \frac{\sqrt{2}}{3}\left[\left(d\varepsilon_1^P - d\varepsilon_2^P\right)^2 + \left(d\varepsilon_2^P - d\varepsilon_3^P\right)^2 + \left(d\varepsilon_3^P - d\varepsilon_1^P\right)^2\right]^{1/2} \tag{2.48}$$

where $d\varepsilon_1^p$, $d\varepsilon_2^p$, and $d\varepsilon_3^p$ are the plastic strain components in principal coordinates. Well known experimental results indicate that at pressures on the order of the yield stress, plastic deformation occurs with no change in volume. This implies that:

$$d\varepsilon_1^P + d\varepsilon_2^P + d\varepsilon_3^P = 0 \tag{2.49}$$

In a uniaxial test with $\sigma_1=\sigma$ and $\sigma_2=\sigma_3=0$, the plastic strain increments are:

$$d\varepsilon_2^P = d\varepsilon_3^P = -1/2\ d\varepsilon_1^P \ . \tag{2.50}$$

Hence, in a uniaxial test, Equations 2.46 and 2.48 reduce to

$$\begin{aligned} \sigma_e &= \sigma_1 \\ d\varepsilon^P &= d\varepsilon_1^P \end{aligned} \tag{2.51}$$

Thus, when the assumption is made that the yield stress is a function of the total effective plastic strain (called the Strain Hardening Hypothesis [Mendelson 1968]), the functional relationship between yield stress and plastic strain can be taken directly from a uniaxial stress-strain curve by virtue of Equation 2.51.

The relationship between the magnitudes of the plastic strain increments and the effective plastic strain increment is provided by the Prandtl-Reuss Flow Rule (Prandtl 1924):

$$d\varepsilon_i^P = \frac{3\ d\varepsilon^P}{2\ \sigma_e} S_i \qquad i = 1, 2, 3 \tag{2.52}$$

where the S_i values are the deviatoric stress components (in principal coordinates) defined by:

$$S_i = \sigma_i - \frac{1}{3}(\sigma_1 + \sigma_2 + \sigma_3) \qquad i = 1, 2, 3 \tag{2.53}$$

Equation 2.52 embodies the fundamental observation of plastic deformation; that is, plastic strain increments are proportional to the deviatoric stresses. The constant of proportionality is determined by the choice of the yield function (Mendelson 1968). Direct substitution shows that Equations 2.46, 2.47, 2.48, 2.52, and 2.53 are consistent with one another.

Once the plastic strain increments have been determined for a given load step, the total strains are determined from a generalized form of Hooke's Law given by:

$$\begin{aligned}
\varepsilon_1 &= \frac{1}{E}\{\sigma_1 - \upsilon(\sigma_2 + \sigma_3)\} + \varepsilon_1^P + d\varepsilon_1^P + \int \alpha dT \\
\varepsilon_2 &= \frac{1}{E}\{\sigma_2 - \upsilon(\sigma_1 + \sigma_3)\} + \varepsilon_2^P + d\varepsilon_2^P + \int \alpha dT \\
\varepsilon_3 &= \frac{1}{E}\{\sigma_3 - \upsilon(\sigma_2 + \sigma_1)\} + \varepsilon_3^P + d\varepsilon_3^P + \int \alpha dT
\end{aligned} \tag{2.54}$$

in which ε_1^p, ε_2^p, and ε_3^p are the total plastic strain components at the end of the previous load increment.

The remaining continuum field equations of equilibrium, strain displacement, and strain compatibility are unchanged. The complete set of governing equations is presented in Table 2.3 and are written in terms of rectangular Cartesian coordinates and employ the usual indicial notation in which a repeated Latin index implies summation. This set of equations is augmented by an experimentally determined uniaxial stress-strain relation.

When the problem under consideration is statically determinate, so that stresses can be found from equilibrium conditions alone, the resulting plastic deformation can be determined directly. However, when the problem is statically indeterminate such that the stresses and deformation must be found simultaneously, then the full set of plasticity equations proves to be quite formidable even in the case of simple loadings and geometries.

One numerical procedure which has been used with considerable success is the Method of Successive Substitutions. This method can be applied to any problem for which an elastic solution can be obtained, either in closed form or numerically. A full discussion of this technique, including a number of technologically useful examples, is contained in Mendelson (1968).

The method involves breaking the load path up into a number of small increments. For example, in mechanical analysis of fuel rods, the loads are the coolant pressure and either fuel rod internal gas pressure or a prescribed displacement of the inside surface of the cladding due to thermal expansion of

Table 2.3 Elastic-Plastic Governing Equations
Equilibrium
$$\sigma_{ji,j} + \rho f_i = 0$$ where: σ_{ji} = stress tensor ρ = mass density f_i = components of body force per unit mass
Stress Strain
$$\varepsilon_{ij} = \frac{1+\nu}{E}\sigma_{ij} - \delta_{ij}\left(\frac{\nu}{E}\sigma_{kk} - \alpha dT\right) + \varepsilon_{ij}^{P} + d\varepsilon_{ij}^{P}$$
Compatibility
$$\varepsilon_{ij,kl} + \varepsilon_{kl,ij} - \varepsilon_{ik,jl} - \varepsilon_{jl,ij} = 0$$
Definitions Used in Plasticity
$$\sigma e \triangleq \sqrt{\frac{3}{2} S_{ij} S_{ij}}$$ $$S_{ij} \triangleq \sigma_{ij} - \frac{1}{3}\sigma_{kk}$$ $$d\varepsilon^{P} \triangleq \sqrt{\frac{2}{3} d\varepsilon_{ij}^{P} d\varepsilon_{ij}^{P}}$$
Prandtl-Reuss Flow Rule
$$d\varepsilon_{ij}^{P} = \frac{3}{2}\frac{d\varepsilon^{P}}{\sigma_e} S_{ij}$$

the fuel. These loads all vary during the operating history of the fuel rod. For each new increment of the loading, the solution to all the plasticity equations listed in Table 2-3 is obtained as described below.

First, an initial estimate of the plastic strain increment, $d\varepsilon_{ij}^{p}$, is made. On the basis of this value, the equations of equilibrium, Hooke's law, and strain displacement and compatibility are solved as for any elastic problem. From the stresses so obtained, the deviatoric stresses, S_{ij}, may be calculated. This "pseudo-elastic" solution represents one path in the computational scheme.

Independently, through use of the $d\varepsilon_{ij}^{p}$ values, the increment of effective plastic strain, $d\varepsilon^{p}$, may be calculated. From this result and the stress-strain curve, a value of the effective stress, σ_e, can be obtained.

Finally, a new estimate of the plastic strain increment is obtained from the Prandtl-Reuss rule:

$$d\varepsilon_{ij}^{P} = \frac{3}{2}\frac{d\varepsilon^{P}}{\sigma_e} S_{ij} \tag{2.55}$$

and the entire process is continued until the $d\varepsilon_{ij}^{p}$ converge. A schematic of the iteration scheme is provided in Figure 2.11.

The mechanism by which improved estimates of $d\varepsilon_{ij}^{p}$ are obtained results from the fact that the effective stress obtained from $d\varepsilon^{p}$ and the stress-strain curve will not be equal to the effective stress that would be obtained with the stresses from the elastic solution. The effective stresses will only agree when convergence is obtained.

The question of convergence is one that cannot, in general, be answered a priori. However, convergence can be shown (Mendelson 1968) to be obtained for sufficiently small load increments. Experience has shown that this technique is suitable for both steady-state and transient fuel rod analyses.

2.4.2 Extension to Creep and Hot Pressing

The method of solution described for the time-independent plasticity calculations can also be used for time-dependent creep and hot pressing calculations. In this context, the term creep refers to any time-dependent constant volume permanent deformation, whereas the term hot pressing refers to any time-dependent process which results in a permanent change in volume. Both creep and hot pressing are stress-driven processes and are usually highly dependent on temperature.

The only change required to extend the Method of Successive Substitutions to allow consideration of creep and hot pressing is to re-write the Prandtl-Reuss flow rule, Equation 2.52, as:

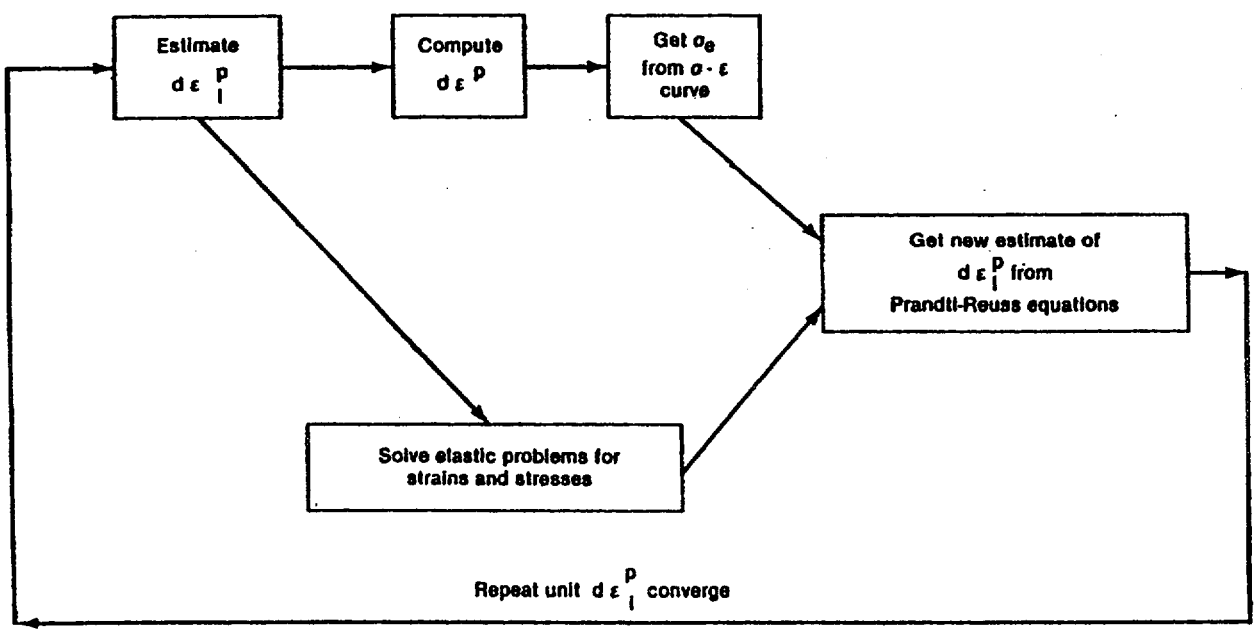

Figure 2.11 Schematic of the Method of Successive Elastic Solutions

$$d\varepsilon_1^c = 1.5\frac{\dot{\varepsilon}^c\ \Delta t}{\sigma_e} S_1 + \frac{\dot{V}^c\ \Delta t}{9}\ \frac{(\sigma_1 + \sigma_2 + \sigma_3)}{\sigma_m}$$

$$d\varepsilon_2^c = 1.5\ \frac{\dot{\varepsilon}^c\ \Delta t}{\sigma_e} S_2 + \frac{\dot{V}^c\ \Delta t}{9}\ \frac{(\sigma_1 + \sigma_2 + \sigma_3)}{\sigma_m} \tag{2.56}$$

$$d\varepsilon_3^c = 1.5\frac{\dot{\varepsilon}^c\ \Delta t}{\sigma_e} S_3 + \frac{\dot{V}^c\ \Delta t}{9}\ \frac{(\sigma_1 + \sigma_2 + \sigma_3)}{\sigma_m}\ .$$

where: σ_m = the mean stress.

The first term on the right hand side of each of these equations calculates the constant volume creep strain, whereas the second term in each equation calculates the permanent change in volume. To use this form of the flow rule, two additional material property correlations must be available. These correlations are shown in the next two sections.

2.4.2.1 Constant Volume Creep

The correlation for constant volume creep strain, ε^c, as a function of stress, time, temperature, and neutron flux, is assumed to be:

$$\varepsilon^c = f(\sigma,\ T,\ t,\ \dot{F}) \tag{2.57}$$

where: σ_e = uniaxial stress, N/m^2
T = temperature, K
t = time, s
F = neutron flux, n/m^2-s

The strain hardening hypothesis (Mendelson 1968) is assumed, which implies that the creep strain correlation can be differentiated and solved for the creep strain rate in the form:

$$\dot{\varepsilon}^c = h(\sigma,\ \varepsilon^c,\ T,\ \dot{F}) \tag{2.58}$$

which is no longer an explicit function of time. This equation is obtained from MATPRO during the creep calculations.

2.4.2.2 Transient Volume Fuel Creep

The correlation between the rate of change of volume and the applied stress is assumed to be:

$$\dot{V}^c = f(\sigma_m,\ T,\ t,\ V_{avail}) \tag{2.59}$$

where: σ_m = mean stress, N/m^2
T = temperature, K
t = time, s
V_{avail} = measure of maximum permanent volume change possible, m^3

The permanent volumetric strain increment, dV^c, is related to the plastic strain increments by the equation:

$$dV^c + d\varepsilon_1^c + d\varepsilon_2^c + d\varepsilon_3^c \ . \tag{2.60}$$

Permanent volumetric strain is considered only in the fuel. The source of the permanent volume change is assumed to be the closing of the cracks in the relocated fuel. The maximum amount of volume available for permanent volume change is thus the amount of volume generated by fuel relocation. The equation for the permanent volume change was generated by comparing calculated and measured length changes for experimental fuel rods irradiated in the Power Burst Facility and the Halden Boiling Water Reactor. The correlation which resulted in the best agreement with measured fuel rod length changes was found to be:

$$\Delta V_n = -V\ [1 - \exp\ (-A\sigma^B \Delta t)] \tag{2.61}$$

where: ΔV_n = rate of volume change at current time step (m^3/s)
A = 1.48×10^{-38}
σ = fuel-cladding interface pressure (N/m^2)
V = relocation volume remaining (m^3)
$= V_o - \sum_{n=1}^{N} \Delta V_n\ \Delta t$
V_o = initial void volume in fuel generated by fuel relocation (m^3)
N = number of current time step
Δt = time step size (s)
B = 4.5.

2.4.2.3 Initial Void Volume and Fuel Relocation

The initial void volume is related to the radial displacement due to fuel relocation by the equation:

$$V_o = \pi[(r_p + U_r)^2 - r_p^2] \tag{2.62}$$

where: r_p = as-fabricated radius of fuel pellets (m)
U_r = radial displacement of outer surface of fuel pellets due to relocation (m)

2.4.3 Rigid Pellet Model (FRACAS-I)

To summarize the mechanical response calculations, the code assumes that stress-induced deformation of the fuel pellets is ignored. The cladding deformation model in FRACAS-I is described in Section 2.4.3.1. Modifications to the MATPRO cladding mechanical properties models are described in Section 2.4.3.2. The fuel deformation model is described in Section 2.4.3.3. If the fuel-cladding gap is closed, the fuel deformation model will apply a driving force to the cladding deformation model. The cladding deformation model, however, never influences the fuel deformation model.

2.4.3.1 Cladding Deformation Model

The cladding deformation model in FRACAS-I is based on the following assumptions:

1. Incremental theory of plasticity
2. Prandtl-Reuss flow rule
3. Isotropic work hardening
4. No low-temperature creep deformation of cladding
5. Thin wall cladding (stress, strain, and temperature uniform through cladding thickness)
6. No axial slippage occurs at fuel-cladding interface when fuel and cladding are in contact
7. Bending strains and stresses in cladding are negligible
8. Axisymmetric loading and deformation of the cladding.

Deformation and stresses in the cladding in the open gap regime are calculated using a model which considers the cladding to be a thin cylindrical shell with specified internal and external pressures and a prescribed uniform temperature.

Calculations for the closed gap regime are made using a model which assumes that the cladding is a thin cylindrical shell with prescribed external pressure and a prescribed radial displacement of its inside surface. The prescribed displacement is obtained from the fuel thermal expansion model. Furthermore, because no slippage is assumed to take place when the fuel and cladding are in contact, the axial expansion of the fuel is transmitted directly to the cladding. Hence, the change in axial strain in the shell is also prescribed.

Two additional models are used to calculate changes in yield stress with work hardening, given a uniaxial stress-strain curve. This stress-strain curve is obtained from MATPRO-11 (Hagrman, Reymann, and Mason 1980). The first model calculates the effective total strain and new effective plastic stress given a value of effective stress and the effective plastic strain at the end of the last loading increment. Depending on the work-hardened value of yield stress, loading can be either elastic or plastic, and unloading is constrained to occur elastically. (Isotropic work hardening is assumed in these calculations.)

The decision as to whether or not the fuel is in contact with the cladding is made by comparing the radial displacement of the fuel with the radial displacement that would occur in the cladding due to the prescribed external (coolant) pressure and the prescribed internal (fission and fill gas) pressure. The decision is expressed by the equation:

$$u_r^{fuel} \geq u_r^{clad} + \delta \tag{2.63}$$

where: δ = as-fabricated fuel-cladding gap size (m)
u_r = radial displacement (m)

If the above equation is satisfied, the fuel is determined to be in contact with the cladding. The loading history enters into this decision by virtue of the permanent plastic cladding strains imposed in the cladding by the cladding loads.

If the fuel and cladding displacements are such that Equation 2.63 is not satisfied, the fuel-cladding gap has closed during the current loading step and the open gap solution is used.

If Equation 2.63 is satisfied, however, the fuel and cladding have come into contact during the current loading increment. At the contact interface, radial continuity requires that:

$$u_r^{clad} = u_r^{fuel} - \delta \tag{2.64}$$

while in the axial direction the assumption is made that no slippage occurs between the fuel and cladding. This state is referred to as PCMI.

Note that only the additional strain which occurs in the fuel after PCMI has occurred is transferred to the cladding. Thus, if $\varepsilon_{z,o}^{clad}$ is the axial strain in the cladding just prior to contact and $\varepsilon_{z,o}^{fuel}$ is the corresponding axial strain in the fuel, then the no-slippage condition in the axial direction becomes:

$$\varepsilon_z^{clad} - \varepsilon_{z,o}^{clad} = \varepsilon_z^{fuel} - \varepsilon_{z,o}^{fuel} \ . \tag{2.65}$$

After u_r^{clad} and ε_z^{clad} have been calculated, a solution is made of the stresses and strains in a thin cylindrical shell with prescribed axial strain, external pressure, and prescribed radial displacement of the inside surface. The solution also gives the interface pressure between the fuel and cladding.

The open gap modeling considers a thin cylindrical shell loaded by both internal and external pressures. Axisymmetric loading and deformation are assumed. Loading is also restricted to being uniform in the axial direction, and no bending is considered. The geometry and coordinates are shown in Figure 2.12. The displacements of the midplane of the shell are u and w in the radial and axial directions, respectively.

For this case, the equilibrium equations are identically satisfied by:

$$\sigma_\theta = \frac{r_i P_i - r_o P_o}{t} \tag{2.66}$$

$$\sigma_z = \frac{\pi r_i^2 P_i - \pi r_o^2 P_o}{\pi(r_o^2 - r_i^2)} \tag{2.67}$$

where: σ_θ = hoop stress (N/m^2)
σ_z = axial stress (N/m^2)
r_i = inside radius of cladding (m)
r_o = outside radius of cladding (m)
P_i = internal pressure of fuel rod (N/m^2)
P_o = coolant pressure (N/m^2)
t = cladding thickness (m)

From membrane shell theory (Wang 1953), the strains are related to the midplane displacements by:

$$\varepsilon_z = \frac{\partial w}{\partial z} \tag{2.68}$$

$$\varepsilon_\theta = \frac{u}{\bar{r}} \tag{2.69}$$

where $\bar{r}$ is the radius of the midplane. Strain across the thickness of the shell is allowed. The radial stress is neglected. The hoop stress, σ_θ, and axial stress, σ_z, are uniform across the cladding thickness.

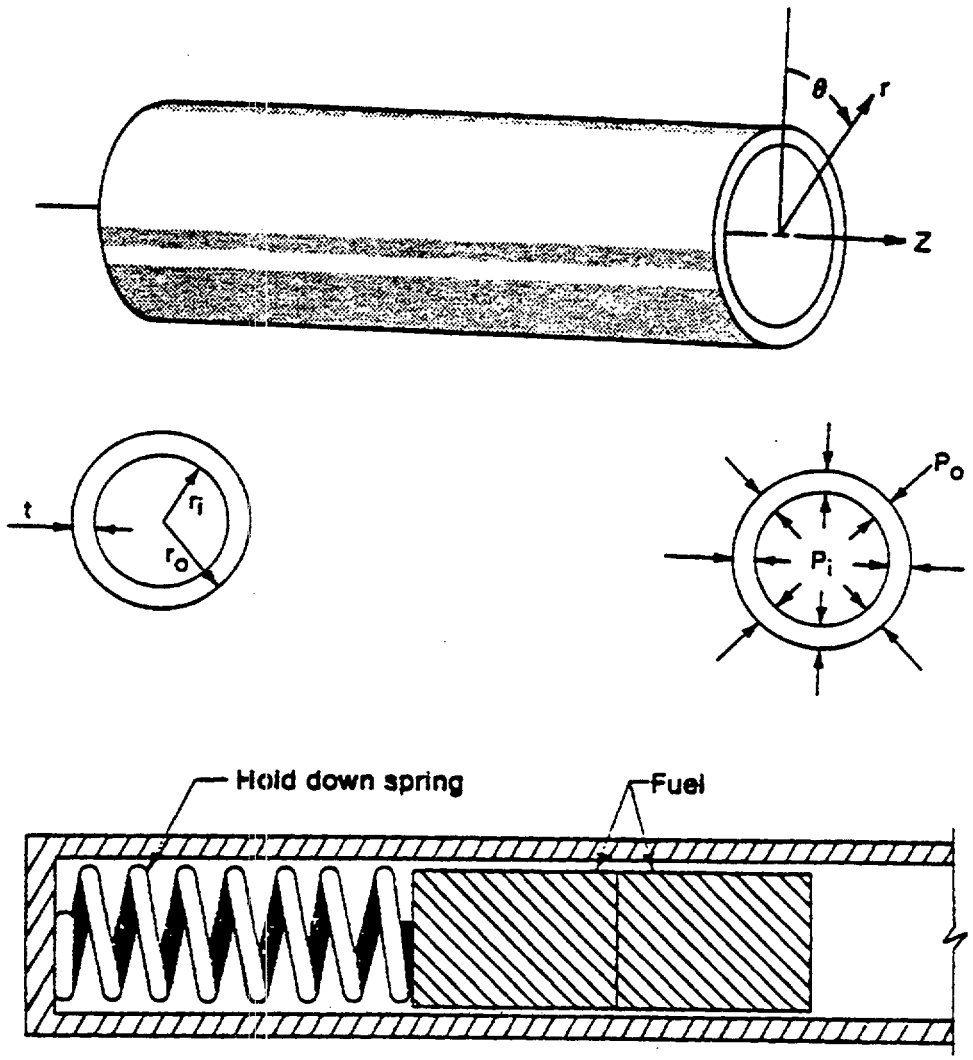

Figure 2.12 Fuel Rod Geometry and Coordinates

The radial strain is due only to the Poisson's effect and is uniform across the cladding thickness. (Normally, radial strains are not considered in the shell analysis, but when plastic deformations are considered, plastic radial strains must be included.)

The stress-strain relations are written in the incremental form:

$$\varepsilon_\theta = \frac{1}{E}\{\sigma_\theta - \upsilon\,\sigma_z\} + \varepsilon_\theta^P + d\varepsilon_\theta^P + \int_{T_o}^{T} \alpha\, dT \tag{2.70}$$

$$\varepsilon_z = \frac{1}{E}\{\sigma_z - \upsilon\,\sigma_\theta\} + \varepsilon_z^P + d\varepsilon_z^P + \int_{T_o}^{T} \alpha\, dT \tag{2.71}$$

$$\varepsilon_r = -\frac{\upsilon}{E}\{\sigma_\theta + \sigma_z\} + \varepsilon_r^P + d\varepsilon_r^P + \int_{T_o}^{T} \alpha \, dT \tag{2.72}$$

where: T_o = strain-free reference temperature (K)
α = coefficient of thermal expansion (K^{-1})
T = current cladding temperature (K)
E = modulus of elasticity (N/m^2)
ν = Poisson's ratio

The terms ε_θ^p, ε_z^p, and ε_r^p are the plastic strains at the end of the last load increment, and $d\varepsilon_\theta^p$, $d\varepsilon_z^p$, and $d\varepsilon_r^p$ are the additional plastic strain increments which occur during the new load increment.

The magnitudes of the additional plastic strain increments are determined by the effective stress and the Prandtl-Reuss flow rule, which are expressed as:

$$\sigma_e = \frac{1}{\sqrt{2}}\left\{(\sigma_\theta - \sigma_z)^2 + (\sigma_z)^2 + (\sigma_\theta)^2\right\}^{1/2} \tag{2.73}$$

$$d\varepsilon_i^P = \frac{3}{2}\frac{d\varepsilon^P}{\sigma_e} S_i \quad \text{for} \quad i = r, \theta, z \tag{2.74}$$

$$S_i = \sigma_i - \frac{1}{3}(\sigma_\theta + \sigma_z) \text{ for } i = r, \theta, z \tag{2.75}$$

The solution of the open gap case proceeds as follows. At the end of the last load increment the plastic strain components, ε_θ^p, ε_z^p, and ε_r^p are known, and also the total effective plastic strain, ε^p, is known.

The loading is now incremented with the prescribed values of P_i, P_o, and T. The new stresses can be determined from Equations 2.66 and 2.67, and a new value of effective stress is obtained from Equation 2.73.

The increment of effective plastic strain, $d\varepsilon^p$, which results from the current increment of loading, can then be determined from the uniaxial stress-strain curve at the new value of σ_e, as shown in Figure 2.13. (The new elastic loading curve depends on the value of ε^p.)

Once $d\varepsilon^p$ is determined, the individual plastic strain components are found from Equation 2.74, and the total strain components are obtained from Equations 2.70 through 2.72.

The displacement of the inside surface of the shell must be determined so that a new fuel-cladding gap width can be calculated. The radial displacement of the inside surface is given by

$$u(r_i) = \bar{r}\,\varepsilon_\theta - \frac{t}{2}\varepsilon_r \tag{2.76}$$

where the first term is the radial displacement of the midplane (from Equation 2.69) and ε_r is the uniform strain across the thickness.

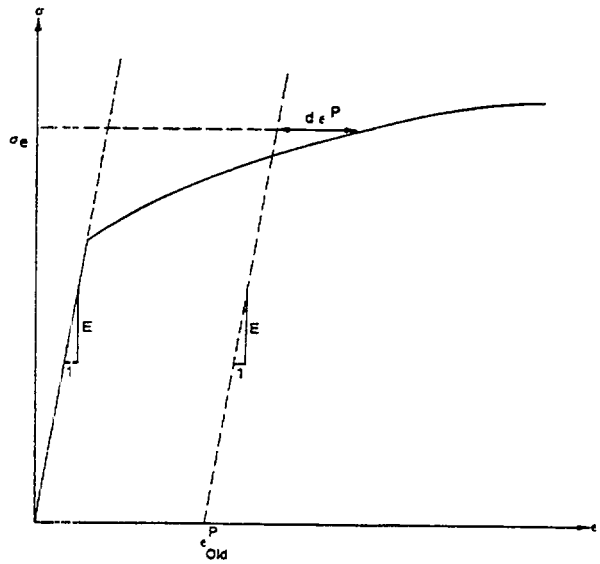

Figure 2.13 Calculation of Effective Stress σ_e from $d\varepsilon^P$

The cladding thickness, t, is computed by the equation

$$t = (1 + \varepsilon_r)\, t_o \tag{2.77}$$

where: t_o = as-fabricated thickness of cladding.

The final step performed is to add the plastic strain increments to the previous strain values, that is,

$$(\varepsilon_\theta^P)_{new} = (\varepsilon_\theta^P)_{old} + d\varepsilon_\theta^P \tag{2.78}$$

$$(\varepsilon_z^P)_{new} = (\varepsilon_z^P)_{old} + d\varepsilon_z^P \tag{2.79}$$

$$(\varepsilon_r^P)_{new} = (\varepsilon_r^P)_{old} + d\varepsilon_r^P \tag{2.80}$$

$$(\varepsilon^P)_{new} = (\varepsilon^P)_{old} + d\varepsilon^P \tag{2.81}$$

Thus, all the stresses and strains can be computed directly because, in this case, the stresses are determinate. In the case of the "fuel-driven" cladding displacement, the stresses depend on the displacement and such a straight-forward solution is not possible.

The closed gap modeling considers the problem of a cylindrical shell for which the radial displacement of the inside surface and axial strain are prescribed. Here the stresses cannot be calculated directly because the pressure at the inside surface is exerted by the fuel instead of the internal gas and must be determined as part of the solution.

As in the open gap modeling, the displacement at the cladding inside surface is given by

$$u(r_i) = u - \frac{t}{2}\,\varepsilon_r \tag{2.82}$$

where u is the radial displacement of the cladding midplane. From Equation 2.70, $u = r\varepsilon_\theta$ and

$$u(r_i) = \bar{r}\,\varepsilon_\theta - \frac{t}{2}\,\varepsilon_r\,. \tag{2.83}$$

Thus, prescribing the displacement of the inside surface of the shell is equivalent to a constraining relation between ε_θ and ε_r. As before, Hooke's Law is taken in the form:

$$\varepsilon_\theta = \frac{1}{E}\,(\sigma_\theta - \upsilon\,\sigma_z) + \varepsilon_\theta^P + d\varepsilon_\theta^P + \int_{T_o}^{T} \alpha dT \tag{2.84}$$

$$\varepsilon_z = \frac{1}{E}\,(\sigma_z - \upsilon\,\sigma_\theta) + \varepsilon_z^P + d\varepsilon_z^P + \int_{T_o}^{T} \alpha dT \tag{2.85}$$

$$\varepsilon_r = -\frac{\upsilon}{E}\,(\sigma_\theta + \sigma_z) + \varepsilon_r^P + d\varepsilon_r^P + \int_{T_o}^{T} \alpha dT \tag{2.86}$$

Use of Equations 2.83 and 2.86 in Equation 2.84 results in a relation between the stresses, σ_θ and σ_z, and the prescribed displacement $u(r_i)$:

$$\begin{aligned} &\frac{u(r_i)}{\bar{r}} + \frac{1}{2}\left(\frac{t}{r}\right)\left\{\varepsilon_r^P + d\varepsilon_r^P + \int_{T_o}^{T} \alpha dT\right\} \\ &\quad - \left\{\varepsilon_\theta^P + d\varepsilon_\theta^P + \int_{T_o}^{T} \alpha dT\right\} = \frac{1}{E}\left[\left(1 + \frac{\upsilon}{2}\,\frac{t}{\bar{r}}\right)\sigma_\theta + \upsilon\left(\frac{1}{2}\,\frac{t}{\bar{r}} - 1\right)\sigma_z\right] \end{aligned} \tag{2.87}$$

Equations 2.85 and 2.87 are now a pair of simultaneous algebraic equations for the stresses σ_θ and σ_z, which may be written as:

$$\begin{bmatrix} A_{11} & A_{12} \\ A_{21} & A_{22} \end{bmatrix} \begin{bmatrix} \sigma_\theta \\ \sigma_z \end{bmatrix} = \begin{bmatrix} B_1 \\ B_2 \end{bmatrix} \tag{2.88}$$

where: $A_{11} = 1 + \frac{\nu}{2}\frac{t}{\bar{r}}$

$$A_{12} = n\left(\frac{1}{2}\frac{t}{\bar{r}} - 1\right)$$

$A_{21} = -\nu$

$A_{22} = 1$

$$B_1 = E\frac{u(r_i)}{\bar{r}} + \frac{E}{2}\frac{t}{\bar{r}}\left\{e_r^P + d\varepsilon_r^P + \int_{T_0}^{T} \alpha dT\right\}$$

$$-E\left\{\varepsilon_\theta^P + d\varepsilon_\theta^P + \int_{T_0}^{T} \alpha dT\right\}$$

$$B_2 = E\left\{\varepsilon_2 - E\,\varepsilon_z^P + d\varepsilon_z^P + \int_{T_0}^{T} \alpha dT\right\}$$

Then the stresses can be written explicitly as:

$$\sigma_\theta = \frac{B_1\,A_{22} - B_2\,A_{12}}{A_{11}\,A_{22} - A_{12}\,A_{21}} \tag{2.89}$$

$$\sigma_z = \frac{B_2\,A_{11} - B_1\,A_{21}}{A_{11}\,A_{22} - A_{12}\,A_{21}} \tag{2.90}$$

These equations relate the stress to $u(r_i)$ and ε_z, which are prescribed, and to $d\varepsilon_\theta^P$, $d\varepsilon_z^P$, and $d\varepsilon_r^P$, which are to be determined. The remaining equations which must be satisfied are:

$$\sigma_e = \frac{1}{\sqrt{2}}\left\{(\sigma_\theta - \sigma_z)^2 + (\sigma_\theta)^2 + (\sigma_z)^2\right\}^{1/2} \tag{2.91}$$

$$d\varepsilon^P = \frac{\sqrt{2}}{3}\left\{(d\varepsilon_r^P - d\varepsilon_\theta^P)^2 + (d\varepsilon_\theta^P - d\varepsilon_z^P)^2 + (d\varepsilon_z^P - d\varepsilon_r^P)^2\right\}^{1/2} \tag{2.92}$$

and the Prandtl-Reuss flow equations (defined in Equation 2.74)

$$d\varepsilon_\theta^P = \frac{3}{2}\frac{d\varepsilon^P}{\sigma_e}\left[\sigma_\theta - \frac{1}{3}(\sigma_\theta + \sigma_z)\right] \tag{2.93}$$

$$d\varepsilon_z^P = \frac{3}{2}\frac{\sigma\varepsilon^P}{\sigma_e}\left[\sigma_z - \frac{1}{3}(\sigma_\theta + \sigma_z)\right] \tag{2.94}$$

$$d\varepsilon_r^P = - d\varepsilon_\theta^P - d\varepsilon_z^P \ . \tag{2.95}$$

The effective stress, σ_e, and the effective plastic strain increment, $d\varepsilon^p$, must be related by the uniaxial stress-strain law. Equations 2.89 through 2.95 must be simultaneously satisfied for each loading increment.

As discussed in Section 2.4.1, a straight-forward numerical solution to these equations can be obtained by means of the Method of Successive Elastic Solutions. By this method, arbitrary values are initially assumed for the increments of plastic strain, and Equations 2.89 through 2.95 are used to obtain improved estimates of the plastic strain components. The steps performed are as follows for each increment of load.

1. Values of $d\varepsilon_\theta^p$, $d\varepsilon_z^p$, and $d\varepsilon_r^p$ are assumed. Then, $d\varepsilon^p$ is calculated from Equation 2.92 and the effective stress is obtained from the stress-strain curve with strain at the value of ε^p.

2. From Hooke's Law, still using the assumed plastic strain increments and the prescribed values of $u(r_i)$ and ε_z, values for the stresses can be obtained from Equations 2.89 and 2.90.

3. New values for $d\varepsilon_\theta^p$, $d\varepsilon_z^p$, and $d\varepsilon_r^p$ are now calculated from the Prandtl-Reuss relations: using σ_e as computed in Step 1 and σ_θ and σ_z as computed in Step 2.

$$d\varepsilon_i^P = \frac{3}{2} \frac{d\varepsilon^P}{\sigma_e} \left[\sigma_i - \frac{1}{3} (\sigma_\theta + \sigma_z) \right] \quad i = r, \theta, z \tag{2.96}$$

4. The old and new values of $d\varepsilon_\theta^p$, $d\varepsilon_z^p$, and $d\varepsilon_r^p$ are compared and the process continues until convergence is obtained.

5. Once convergence has been obtained, the fuel-cladding interfacial pressure is computed from Equation 2.66 as follows:

$$P_{int} = \frac{t\ \sigma_\theta + r_o\ P_o}{r_i} \ . \tag{2.97}$$

When Steps 1 through 5 have been completed, the solution is complete provided that the fuel-cladding interface pressure is not less than the local gas pressure. However, due to unequal amounts of plastic straining in the hoop and axial directions upon unloading, the fuel-cladding interfacial pressure, as obtained in Step 5, is often less than the internal gas pressure, even though the fuel-cladding gap has not opened. When this situation occurs, the frictional "locking" mechanism (which is assumed to constrain the cladding axial deformation to equal the fuel axial deformation) can no longer act. The axial strain and stress adjust themselves so that the fuel-cladding interfacial pressure just equals the gas pressure, at which point the axial strain is again "locked." Thus, upon further unloading, the axial strain and the hoop and axial stresses continually adjust themselves to maintain the fuel-cladding interfacial pressure equal to the gas pressure until the fuel-cladding gap is open. Because the unloading occurs elastically, a solution for this portion of the fuel-cladding interaction problem can be obtained directly as discussed below.

Because the external pressure and the fuel-cladding interfacial pressure are known, the hoop stress is obtained from Equation 2.66 as:

$$\sigma_\theta = \frac{r_i P_{int} - r_o P_o}{t} \tag{2.98}$$

From Equation 2.83, the following expression can be written:

$$\varepsilon_\theta = \frac{u_r^{fuel} - \delta + t/2\ \varepsilon_r}{\bar{r}} \tag{2.99}$$

Substitution of ε_θ and ε_r, as given by Equations 2.84 and 2.86, into Equation 2.99 results in an explicit equation for σ_z:

$$\begin{aligned} \upsilon\ r_i\ \sigma_z = (\bar{r} + \upsilon\ t/2)\ \sigma_\theta + \bar{r}\ E \left(\int \alpha_\theta dT + \varepsilon_\theta^P \right) \\ - \frac{t}{2} E \left(\int \alpha_r dT + \varepsilon_r^P \right) - E\ u\ (r_i) \end{aligned} \tag{2.100}$$

in which σ_z is known from Equation 2.98. With σ_z and σ_θ known, the strains may be computed from Hooke's Law, Equations 2.84 through 2.86. This set of equations is automatically invoked whenever P_{int} is calculated to be less than the local internal gas pressure.

Both the closed and open gap models require the relation of stress to strain, taking into consideration the direction of loading and the previous plastic deformation. A typical stress-strain curve is shown in Figure 2.14. This curve represents the results of a uniaxial stress-strain experiment and may be interpreted (beyond initial yield) as the locus of work-hardened yield stress. The equation of the curve is provided by MATPRO for a wide range of temperatures.

To utilize this information, the usual idealization of the mechanical behavior of metals is made. Thus, linear elastic behavior is assumed until a sharply defined yield stress is reached, after which plastic (irrecoverable) deformation occurs. Unloading from a state of stress beyond the initial yield stress, σ_y^o, is assumed to occur along a straight line having the elastic modulus for its slope. When the (uniaxial) stress is removed completely, a residual plastic strain remains, and this completely determines the subsequent yield stress. That is, when the specimen is loaded again, loading will occur along line BA in Figure 2.15, and no additional plastic deformation will occur until point A is again reached. Point A is the subsequent yield stress. If $\sigma = f(\varepsilon)$ is the equation of the plastic portion of the stress=strain curve (YAC), then for a given value of plastic strain, the subsequent yield stress is found by simultaneously solving the pair of equations:

$$\begin{aligned} \sigma &= f(\varepsilon) \\ \sigma &= E(\varepsilon - \varepsilon^P) \end{aligned} \tag{2.101}$$

which may be written as

$$\sigma = f\left(\frac{\sigma}{E} + \varepsilon^P \right) \tag{2.102}$$

The solution to this nonlinear equation may be found very efficiently by Newton's iteration scheme:

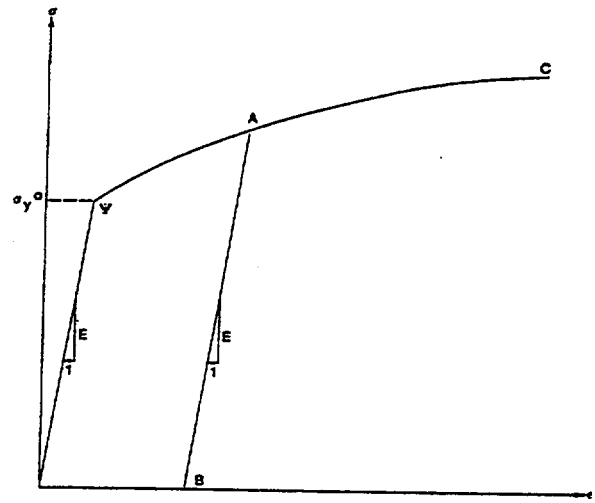

Figure 2.14 True Stress-Strain Curve and Unloading Path

$$\sigma^{(m+1)} = f\left[\frac{\sigma^{(m)}}{E} + \varepsilon^P\right] m = 0, 1, 2, \ldots \tag{2.103}$$

The initial iterate, $\sigma^{(0)}$, is arbitrary and, without loss of generality, is taken as 34.5 MPa. For any monotonically increasing stress-plastic strain relation, the iteration scheme in Equation 2.103 can be proven to converge uniformly and absolutely.

To compute the new value of the total strain, ε, and the increment of plastic strain, $d\varepsilon^p$, the following steps are performed.

1. For the given temperature, the $\sigma = f(\varepsilon)$ relation is obtained from MATPRO.

2. The yield stress, σ_y, for the old ε^p is calculated from Equation 2.103.

3. The value of the increment of plastic strain is calculated from the equations

$$\text{if } \sigma \le \sigma_y,\ \varepsilon = \frac{\sigma}{E} + \varepsilon^P \tag{2.104}$$

$$\varepsilon^P_{new} = \varepsilon^P_{old} \tag{2.105}$$

$$\text{if } \sigma > \sigma_y,\ \varepsilon = f(\sigma) \tag{2.106}$$

$$\varepsilon^P_{new} = \varepsilon - \sigma/E \tag{2.107}$$

$$d\varepsilon^P = \varepsilon^P_{new} - \varepsilon^P_{old}\ . \tag{2.108}$$

To compute the new value of stress, σ, given the temperature, old value of effective plastic strain, and increment of plastic strain, $d\varepsilon^p$, the following steps are performed.

1. For the given temperature, the $\sigma = f(\varepsilon)$ relation is obtained from MATPRO.

2. The yield stress, σ_y, for given ε^p, is calculated from Equation 2.103.

3. Given $d\varepsilon^p$ (see Figure 2.15):

Because $d\varepsilon^p > 0$, the new values of stress and strain must lie on the plastic portion of the stress-strain curve, $\sigma = f(\varepsilon)$. Therefore, σ and ε are obtained by simultaneously solving, as before:

$$\sigma = f(\varepsilon)$$

$$\sigma = E(\varepsilon - \varepsilon^P_{new}) \tag{2.109}$$

2.4.3.2 Modified MATPRO Cladding Mechanical Properties Models

The mechanical properties of fuel rod Zircaloy cladding are known to change with irradiation because of damage induced from the fast neutron fluence. The changes are similar to cold-working the material because dislocation tangles are created that tend to both strengthen and harden the cladding while decreasing the ductility. In addition to the fast fluence effects, the presence of excess hydrogen in the Zircaloy, in the form of hydrides, also impacts the mechanical properties.

An analysis of recent data from mechanical testing of irradiated Zircaloy was conducted as part of the development work for FRAPCON-3 and revised equations for use in MATPRO routines were then generated (Lanning, Beyer, and Painter 1997). The revised MATPRO routines have also been incorporated in FRAPTRAN. Provided in the following is a summary of the revised mechanical property equations.

$$\varepsilon^P_{new} = \varepsilon^P_{old} + d\varepsilon^P \tag{2.110}$$

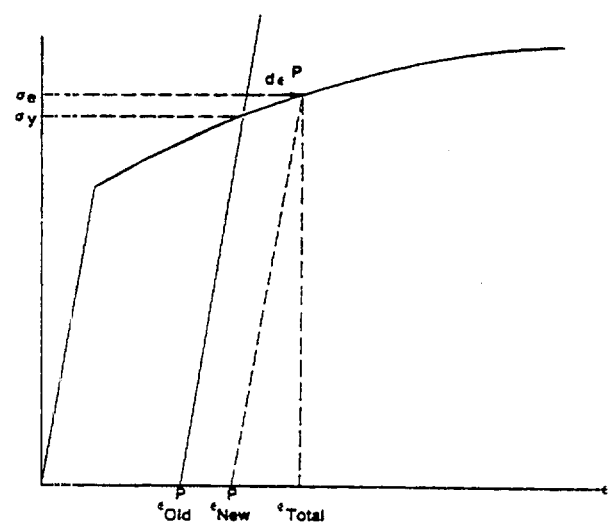

Figure 2.15 Calculation of Effective True Stress for a Given Increment of Plastic Strain

Three MATPRO models have been modified to account for the effects of excess hydrogen from waterside corrosion and high fast neutron fluence levels. Those models are a) the strength coefficient in CKMN, b) the strain hardening exponent in CKMN, and c) the uniform strain in CMLIMT. The MATPRO subroutine CANEAL for annealing the effects of cold work and irradiation damage (dependent on fast neutron fluence) on the strength coefficient and strain hardening exponent has been retained as described in MATPRO 11, Revision 2. There has been one modification to CANEAL so that coldwork (CW) and fast fluence dependence are set equal to zero, i.e., cladding is fully annealed, when cladding temperatures exceed 1255K.

Strength Coefficient, K

To include a hydrogen-dependent term in MATPRO's strength coefficient model, MATPRO's dependence on temperature, cold work, and fast fluence were assumed to be correct. When evaluating data, it was found that the strength coefficient has a strong dependence on hydrogen concentration which can be expressed as:

$$K(h_{ex}) = h_{ex}\cdot[1.288\text{x}10^6 + h_{ex}\cdot(7.546\text{x}10^3 - h_{ex}\cdot 17.84)] \tag{2.111}$$

where: $K(h_{ex})$ = hydrogen contribution to strength coefficient (MPa)
h_{ex} = excess hydrogen concentration, limited to 400 ppm

The complete expression for the strength coefficient is:

$$K = K(T) + K(CW,\Phi) + K(h_{ex}) \tag{2.112}$$

where:
K = strength coefficient (MPa)
$K(T)$ = temperature dependence from MATPRO (MPa)
= $1.17628\text{x}10^9 + T\cdot(4.54859\text{x}10^5 + T\cdot(-3.28185\text{x}10^3 + T\cdot 1.72752))$
$K(CW,\Phi)$ = cold work and fast fluence dependence from MATPRO (MPa)
= $0.546\cdot CW\cdot K(T) + 5.54\text{x}10^{-18}\cdot\Phi$
T = temperature (K)
CW = cold work fraction
Φ = fast neutron fluence ($n/m^2 > 1.0$ MeV)

Strain-Hardening Exponent, n

The MATPRO temperature dependence for the strain-hardening exponent was retained. When evaluating data, it was found that the strain-hardening exponent dependence on hydrogen concentration can be expressed as:

$$n(h_{ex}) = 1.0 + 2.298\text{x}10^{-3}\cdot h_{ex} + 4.138\text{x}10^{-6}\cdot h_{ex}^2 - 1.5\text{x}10^{-8}\cdot h_{ex}^3 \tag{2.113}$$

where: $n(h_{ex})$ = hydrogen dependence of the strain-hardening exponent (unitless)
h_{ex} = excess hydrogen concentration, limited to 400 ppm

The complete expression for the strain-hardening coefficient is:

$$n = n(T)\cdot n(\Phi)\cdot n(h_{ex}) \tag{2.114}$$

where: $n(T)$ = temperature dependence from MATPRO
= $-9.490\times10^{-2} + T\cdot(1.165\times10^{-3} + T\cdot(-1.992\times10^{-6} + T\cdot9.588\times10^{-10}))$
$n(\Phi)$ = fast neutron fluence dependence from MATPRO
= $1.369 + 0.032\times10^{-25}\cdot\Phi$
T = temperature (K)
Φ = fast neutron fluence ($n/m^2 > 1.0$ MeV)

Uniform Strain, ε

The dependence of uniform strain upon hydrogen concentration was determined to be:

$$\varepsilon(h_{ex}) = -(h_{ex}/8.05\times10^5)^{0.5} \tag{2.115}$$

where: $\varepsilon(h_{ex})$ = hydrogen dependence of uniform strain
h_{ex} = excess hydrogen concentration, limited to 400 ppm

The complete expression for uniform strain is:

$$\varepsilon = \varepsilon(T) + \varepsilon(\Phi) + \varepsilon(h_{ex}) \tag{2.116}$$

where: $\varepsilon(T)$ = temperature dependence of uniform strain
= $0.096 - 1.142e\text{-}4\cdot T$
$\varepsilon(\Phi)$ = fast fluence dependence of uniform strain
= $0.01856\exp(-\Phi/10^{25})$
T = temperature (K)
Φ = fast neutron fluence ($n/m^2 > 1.0$ MeV)

Assembled Model

Tensile strength, yield strength, and strain are calculated using the same relationships in MATPRO's CMLIMT subroutine with slight modifications. The true ultimate strength is calculated using:

$$\sigma = K\cdot(\dot{\varepsilon}/10^{-3})^m\cdot\varepsilon_{p+e}^n \tag{2.117}$$

where: σ = true ultimate strength (MPa)
K = strength coefficient (MPa)
$\dot{\varepsilon}$ = strain rate (unitless)
m = strain rate sensitivity constant from MATPRO (unitless)
ε_{p+e} = true strain at maximum load (unitless)
n = strain hardening exponent (unitless)

This is a change in the original MATPRO model in that the true strain at maximum load in the original model was set equal to the strain hardening exponent. Also, the original MATPRO model for true ultimate strength was dependent on true plastic strain only while the above equation is based on true elastic and true plastic strain.

The CMLIMT subroutine equations predicting true yield strength and true strain at yield remain unchanged. True uniform strain is calculated using the revised uniform strain model.

The excess hydrogen concentration factors modifying the strength coefficient (K(hex)), strain-hardening exponent (n(hex)), and uniform strain (Eqs 2.111, 2.113, and 2.115), are based on data collected over the following ranges:

cladding temperature:	560 to 700K
oxide corrosion thickness:	0 to 100 μm
excess hydrogen level:	0 to 400 ppm
strain rate:	10^{-4} to 10^{-5} s^{-1}
fast neutron fluence:	0 to $12x10^{25}$ n/m^2
Zircaloy:	cold work and stress relieved

The fluence and temperature factors [terms] in Eqs 2.112, 2.114, and 2.116 are from MATPRO and are based on data collected over the following ranges:

cladding temperature:	300 to 1700K
strain rate:	10^{-2} to 10^{-5} s^{-1}
fast neutron fluence:	0 to 10^{25} n/m^2
Zircaloy:	cold work and stress relieved

The FRAPTRAN deformation equations have a strain rate dependency that models strain rate effects. In the absence of additional data that span a wider range of strain rate, it is assumed that the strain rate modeling applies over the wider range of transient conditions that FRAPTRAN will be applied to. This assumption is supported by the FRAPTRAN assessment (NUREG/CR-xxxx, Volume 2) where reasonable agreement with the RIA (high strain rate) experimental data was obtained.

2.4.3.3 Fuel Deformation Model

This section describes the models used to calculate fuel deformation in FRACAS-I. Models are used to calculate the fuel stack length change, fuel radial displacement, fuel crack volume, and fuel open porosity.

The fuel deformation model is based on the following assumptions.

1. The sources of fuel deformation are thermal expansion, fuel relocation, and a user input option to specify transient gaseous fuel swelling.

2. No resistance to the fuel deformation occurs.

3. Axial thermal expansion of the fuel stack is equal to thermal expansion of a line projected through the dish shoulder of the fuel pellets. If no disk specifications are input, then axial thermal expansion is based on the fuel centerline.

4. No creep deformation of the fuel occurs.

5. The fuel has isotropic properties.

The length change of the fuel pellet stack is assumed equal to the thermal expansion of the line projected through the shoulders of the fuel pellet dishes, as illustrated in Figure 2.16. The length change is given by:

$$\Delta L_f = \sum_{n=1}^{N} \left[\varepsilon_T(T_{sn}) - \varepsilon_T(T_o)\right] \Delta Z_n \tag{2.118}$$

where: ΔL_f = fuel stack length change (m)
$\varepsilon_T(T)$ = thermal expansion of fuel at temperature T (obtained from MATPRO) (m/m)
T_{sn} = fuel temperature at pellet shoulder at axial node n (K)
T_o = strain free fuel reference temperature (K)
ΔZ_n = fuel stack length associated with axial node n (m)

Fuel radial displacement from thermal expansion is calculated by:

$$U_f = U_T + U_c \tag{2.119}$$

where: U_F = radial displacement of fuel pellet outer surface (m)
U_T = radial displacement of fuel due to thermal expansion (m)

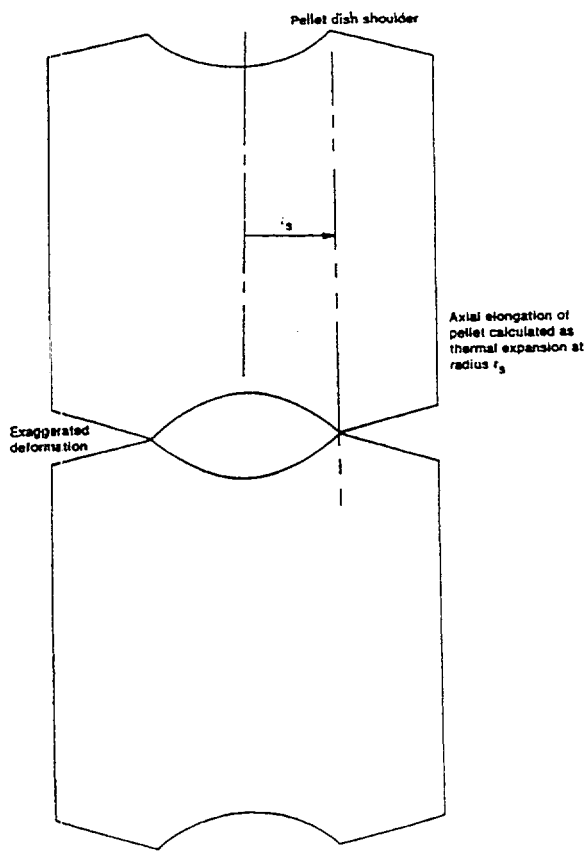

Figure 2.16 Axial Thermal Expansion Using FRACAS-I

$$= \int_0^{r_f} \varepsilon_T[T(r)]dr$$

ε_T = thermal expansion of fuel (m/m)
r_f = as-fabricated fuel pellet outer radius (m)
$T(r)$ = fuel temperature at radial coordinate r (K)
U_c = the additional radial displacement that occurs due to "hourglassing" of the fuel pellets.

The additional radial displacement, U_c, is assumed to occur at the ends of the fuel pellets and affect both both fuel-cladding mechanical interaction and fuel-cladding heat transfer. The same gap is used for both mechanical and thermal calculations.

The additional radial displacement is calculated by the expression:

$$\begin{aligned} U_c &= 0.0025\ r_f & P_I &= 0 \\ U_c &= 0.0025\ r_f\ (1 - P_I / 3.45 \times 10^7) & 0 < P_I &< 3.45 \times 10^7 \\ U_c &= 0 & P_I &\geq 3.45 \times 10^7 \end{aligned} \qquad (2.120)$$

where: P_i = fuel-cladding interfacial pressure, N/m^2.

Once the fuel-cladding gap is closed, the cladding is assumed to follow the fuel dimensional changes from fuel thermal expansion and fuel melting. This assumes that there is little fuel creep or compliance. This may overpredict fuel-cladding mechanical interaction strains for some transients with high fuel centerline temperatures (>2000C) because some of the expansion may result in some fraction of dish filling which would not contribute to fuel-cladding mechanical interaction strains. These assumptions may also lead to the code overpredicting cladding strains for slow transients on the order of minutes that can also be adequately predicted with steady-state fuel performance codes.

Fuel pellet cracking, beginning with the initial ascension to power, promotes an outward relocation (movement) of the pellet fragments that causes additional gap closure. A simplified relocation model is provided in FRAPTRAN that is based on the model used in FRAPCON-3 (Lanning, Beyer, and Painter 1997). The model used in FRAPTRAN is as follows:

if burnup = 0, relocation = 0.3*gap
if burnup > 0, relocation = 0.45*gap

where gap is the as-fabricated radial fuel-cladding gap. Because of the rapid nature of transients, no recovery of the relocation is allowed by FRAPTRAN, whereas FRAPCON-3 does allow some recovery under some conditions. The application of this model to fuel rods with diametral cold gaps of 0.005 inch or less may result in premature gap closure, fuel-cladding mechanical interaction, and under underpredicted fuel temperatures.

If FRAPTRAN is initialized using a FRAPCON-3 file, then relocation is included in the burnup-dependent radial dimensions and the above model is by-passed.

The fuel crack volume is the sum of the volume of the fuel radial cracks. The cracks create space which is occupied by the fuel rod internal gas. Axial cracks are not considered. Closed radial cracks are assumed to exist in the fuel even in the cold state. As the fuel rises in temperature, the cracks open, with the crack width increasing with radius. The width of the radial cracks is the difference between the circumferential change caused by radial displacement and circumferential thermal expansion. The total width is independent of the number of cracks and is calculated by:

$$\Delta c(r) = 2\pi \left(\int_0^r \varepsilon_T [T(r)]\, dr - r\, \varepsilon_T [T(r)] \right) \tag{2.121}$$

where: $\Delta c(r)$ = sum of widths of all radial cracks at radius r.

The first term in the parentheses in Equation 2.121 is the circumference change at cold state radius r due to the radial displacement. The second term is the circumferential change due to circumferential thermal expansion.

The volume of the radial cracks is:

$$V_{CR} = \int_0^{r_f} \Delta c(r)\, dr \tag{2.122}$$

The open porosity of the fuel is empirically correlated with fuel density. The open porosity is multiplied by the fuel volume to determine the volume of gas in the fuel pores that is connected to the fuel-cladding gap. This quantity is used in the calculation of fuel rod internal gas pressure.

Depending on fuel density, one of the following correlations is used to calculate fuel open porosity:

$$\begin{aligned} P &= 16.9297 - 0.232855\,(D-1.25) \\ &\quad - 8.71836 \times 10^{-4}\,(D-1.25)^2 \\ &\quad + 1.52442 \times 10^{-5}\,(D-1.25)^3 && (D < 92.5) \\ P &= 1.20196 \times 10^{-3}\,(95.25-D) && (92.5 \le D \le 95.25) \\ P &= 0 && (D > 95.25) \end{aligned} \tag{2.123}$$

where: P = open porosity of fuel (fraction of theoretical volume)
D = fuel density (percentage of theoretical maximum density).

2.4.4 Cladding Ballooning Model

After the cladding deformation has been calculated by FRACAS-I, a check is made to determine whether or not the cladding ballooning model should be used. The check consists of comparing the cladding effective plastic strain, which is part of the calculated deformation, with the cladding instability strain

given by MATPRO. If the cladding effective plastic strain is greater than the cladding instability strain, the ballooning model is used to calculate the localized, nonuniform staining of the cladding. The cladding instability strain is assumed to be uniform strain; therefore, the ballooning model is used when uniform strain is exceeded.

The ballooning model, BALON2, calculates the extent and shape of the localized large cladding deformation that occurs between the time that the cladding effective strain exceeds the instability strain and the time of cladding rupture. The cladding is assumed to consist of a network of membrane elements subjected to a pressure difference between the inside surface and the outside surface as shown in Figure 2.17. The equations for the model are derived from the thin shell membrane equilibrium equation and geometric constraints. In addition, the model calculates the temperature rise of the cladding due to heat transfer across the fuel-cladding gap. Fuel surface and claddding temperature are assumed to be uniform. The model accounts for the extra cooling the cladding receives as it bulges outwardly.

The details of the BALON2 model are provided by Hagrman (1981).

2.5 Fuel Rod Internal Gas Pressure Response Model

The pressure of the gas in the fuel rod must be known in order to calculate the deformation of the cladding and the transfer of heat across the fuel-cladding gap. The pressure is a function of the temperature, volume, and quantity of gas. Because the temperature is spatially nonuniform, the fuel rod must be divided into several smaller volumes so that the temperature in each small volume can be assumed to be uniform. In particular, the fuel rod is divided into a plenum volume and several fuel-cladding gap and fuel void volumes. The temperature of each volume is given by the temperature model, the size of the volume by the deformation model, and the quantity of gases by the fission gas release model.

The internal gas pressure can be calculated by either a static pressure model (which assumes that all volumes inside the fuel rod equilibrate in pressure instantaneously) or by a transient pressure model which takes into account the viscous flow of the gas in the fuel rod. The transient model is an input option. Unless the fuel-cladding gap is small (<25 μm) or closed, the static and transient models give identical results.

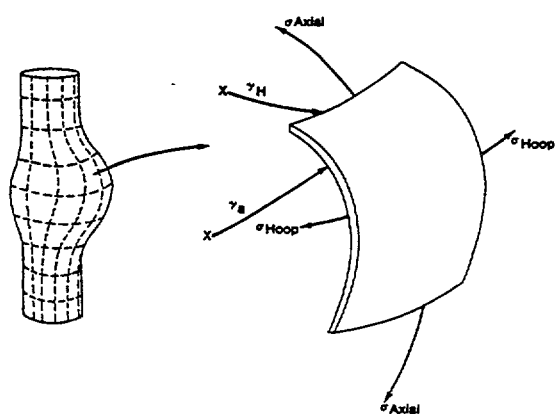

Figure 2.17 Description of the BALON2 Model

The static fuel rod gas pressure model is based on the following assumptions.

1. The gas behaves as a perfect gas.
2. The gas pressure is the same throughout the fuel rod.
3. The gas in the fuel cracks is at the average fuel temperature.

The transient fuel rod gas pressure model is based on the following assumptions.

1. The gas behaves as a perfect gas.
2. The gas flow past the fuel column is a quasi-steady process.
3. The gas flow is compressible and laminar.
4. The gas flow past the fuel column can be analyzed as Poiseuille flow that is, by force balance only).
5. Gas expansion in the plenum and ballooning zone is an isothermal process.
6. The entire fuel-cladding gap can be represented as one volume containing gas at a uniform pressure.
7. The flow distance is equal to the distance from the plenum to the centroid of the fuel-cladding gap at the ballooning node.
8. The minimum cross-sectional area of flow is equivalent to an annulus with inner radius equal to that of the fuel pellet radius and a radial thickness of 25 μm.

2.5.1 Static Fuel Rod Internal Gas Pressure

The static pressure is calculated by the perfect gas law, modified to include volumes at different temperatures, as follows:

$$P_G = \frac{M_G R}{\frac{V_p}{T_p} + \sum_{n=1}^{N} \left[\frac{\pi(r_{cn}^2 - r_{fn}^2)}{T_{Gn}} + \frac{V_{cn}}{T_{aven}} + \frac{V_{Dn}}{T_{Dn}} + \frac{V_{pn}}{T_{aven}} + \frac{V_{rfn}}{T_{fsn}} + \frac{V_{rcn}}{T_{csn}} \right] \Delta Z_n} \tag{2.124}$$

where:
- P_G = internal fuel rod pressure (N/m^2)
- M_g = moles of gas in fuel rod, which is the sum of the moles of fill gas and released fission gases (g-moles)
- R = universal gas constant (N-m/K-g-mole)
- V_p = plenum volume (m^3)
- T_p = temperature of gas in plenum (K)
- n = axial node number
- N = number of axial nodes

r_{cn} = radius of inside surface of cladding at axial node n (m)
r_{fn} = radius of outside surface of fuel at axial node n (m)
T_{Gn} = temperature of gas in gas (fuel-cladding) gap at axial node n (K)
ΔZ_n = fuel rod length associated with axial node n (m)
V_{cn} = fuel crack volume per unit length at axial node n (m^3/m)
T_{cn} = temperature of gas in fuel cracks at axial node n (K)
V_{Dn} = volume of fuel pellet dishes per unit length of fuel stack at axial node n (m^3/m)
T_{Dn} = temperature of gas in fuel dishes at axial node n (K)
V_{pn} = volume of gas in fuel open porosity per unit length at axial node n (m^3/m)
T_{aven} = volumetric average fuel temperature at axial node n (K)
V_{rfn} = volume of gas voids due to fuel surface roughness per unit length at axial node n (m^3/m)
T_{fsn} = temperature of fuel surface (K)
V_{rcn} = volume of gas in voids due to roughness on cladding inside surface per unit length (m^3/m)
T_{csn} = temperature of cladding inside surface (K)

2.5.2 Transient Internal Gas Flow

Transient flow of gas between the plenum and fuel-cladding gap is calculated by the Poiseuille equation for viscous flow along an annulus according to Equation 2.125. Assumptions inherent in Equation 2.125 are ideal gas, laminar flow, and density based on linear average pressure:

where: $\dot{m}$ = mass flow rate (g-moles/s)
μ = gas viscosity at temperature T_A ($N\text{-}s/m^2$)
T_i = gas temperature at node I (K)
T_A = volume-averaged temperature of gas in gas (fuel-cladding) gap (K)
ℓ_I = axial length of node I (m)

$$\dot{m} = \frac{\pi\,(P_p^2 - P_s^2)}{R\mu \sum_{i=I_s}^{I_p} \dfrac{\ell_i T_i Ha}{D_g D_h^3}} \tag{2.125}$$

t_{gi} = fuel-cladding radial gap thickness at node I (m)
I_p = number of top axial node
I_s = number of axial node closest to centroid of gas gap (see Figure 2.18)
Ha = Hagen number (defined below)
P_p = fuel rod plenum gas pressure (N/m^2)
P_s = fuel-cladding gap gas pressure (N/m^2)
R = universal gas constant (N-m/K-g-moles)
D_g = mean diameter of fuel-cladding gap (m)
D_h = hydraulic diameter of fuel-cladding gap = $2t_{gi}$ for a small gap (m)

The Hagen number is calculated by:

$$Ha = 22 + 0.24558/(2t_{gi} - 0.0007874) \tag{2.126}$$

where: t_{gi} is in inches.

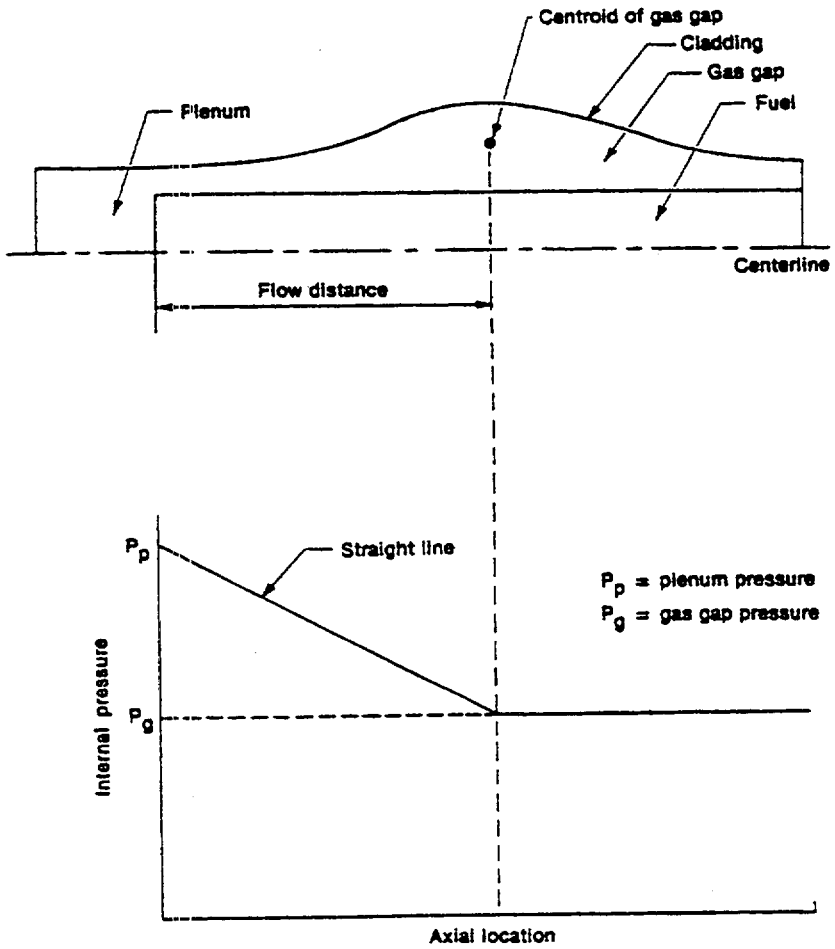

Figure 2.18 Internal Pressure Distribution With the Gas Flow Model

A plot of the relation between Hagen number and gap width given by Equation 2.126 is shown in Figure 2.19. For gaps smaller than 25 μm, the function is cut off at a value of 1177.

To calculate the fuel-cladding gap pressure, a modified form of Equation 2.124 is used. The plenum term is deleted and the moles of gas in the fuel-cladding gap is substituted in place of the moles of gas in the fuel rod.

2.5.3 Fission Gas Production and Release

FRAPTRAN does not have a model to calculate the transient release of fission gases as a function of temperature. The fill gas composition and pressure at the time of the transient, which is dependent on fission gas release prior to the transient, is either manually entered by the user or read from a FRAPCON-3 burnup initialization file.

A user input option is available (MODEL data block) to specify the fission gas release to the fuel-cladding gap and rod plenum during a transient. The user specifies the rod-average fractional fission gas

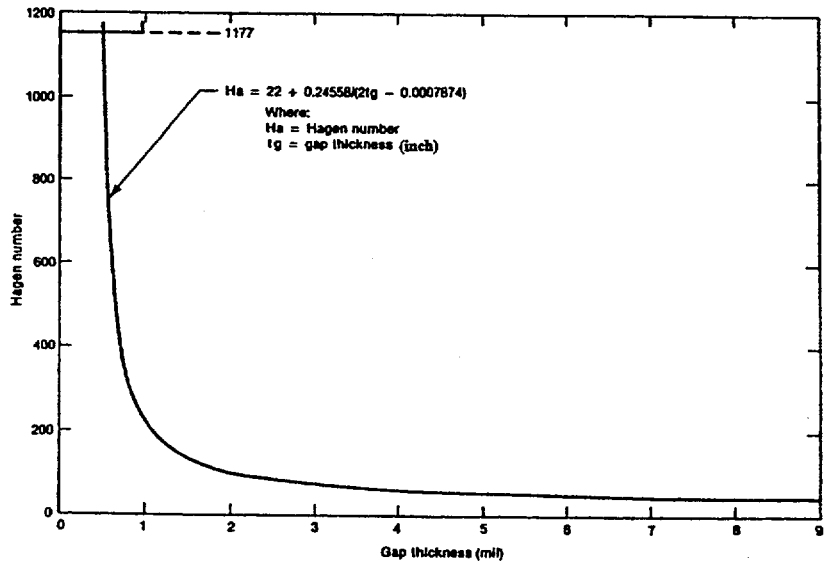

Figure 2.19 Hagen Number Versus Width of Fuel-Cladding Gap

release as a function of time during the transient. Rod-average burnup is used to calculate the rod-average fission gas production which is available to be released. The released fission gas does affect the gas pressure and composition, which in turn impacts the transient thermal and mechanical calculations.

3 USER INFORMATION

In this section, the code structure and computational scheme of FRAPTRAN are outlined and the input and output information are summarized. The link with the FRAPCON-3 code, which can be used to provide initial fuel rod conditions, is also described. Finally, the user's means of controlling computation accuracy and computer running time are outlined. This also includes guidance on using the code.

3.1 Code Structure and Computation Flow

FRAPTRAN is a computer code composed of several subcodes that iteratively calculate the interrelated effects of fuel and cladding temperature, fuel rod plenum temperature, fuel and cladding deformation, and rod internal gas pressure. Each subcode comprises the FORTRAN programming of a major FRAPTRAN model. The name and function of principal subcodes are listed in Table 3.1. Some of the subcodes have the same function, and the user is given the option to select the subcode to be used. Some of the subcodes are not required, and the user is given the option to bypass the use of the subcode, which reduces the computer run time. These options are also noted in Table 3.1. Charts of the overall flow of the computations are shown in Figures 3.1 through 3.3. The input requirements and initialization procedure are shown in Figure 3.1; the temperature, mechanical response, and pressure calculations are shown in Figure 3.2; and the cladding oxidation, local cladding ballooning, and fission gas release calculations are shown in Figure 3.3.

As shown in Figure 3.2, the temperature, mechanical response, and internal gas pressure calculations are performed iteratively so that all significant interactions are taken into account. For example, the deformation of the cladding affects the fuel rod internal gas pressure because the internal volume of the rod is changed. The deformation of the cladding also affects the temperature of the fuel and cladding because the flow of heat from the fuel to the cladding is dependent on the fuel-cladding gap width.

Table 3.1. Name and Function of Principal FRAPTRAN Subcodes

Subcode Name	Function	Selection Option	Bypass Option
HEAT	Compute temperature of fuel and cladding.	no	no
PLNT	Compute temperature of gas in fuel rod plenum. If bypassed, the gas temperature is set equal to the coolant temperature plus 10K.	no	yes
DEFORM	Compute mechanical response of fuel and cladding using FRACAS-I. Stress-induced deformation of the fuel is not modeled.	no	no
GSFLOW	Compute the gas pressure in the fuel rod.	no	no
BALON2	Compute localized ballooning of cladding. If bypassed, uniform cladding straining during ballooning is assumed to occur.	yes	yes
COBILD	Compute oxidation of cladding with best estimate model. If bypassed, no cladding oxidation is assumed to occur.	yes	yes
METWTB	Same function as COBILD, but modeling conforms to requirement of a licensing audit code.	yes	yes

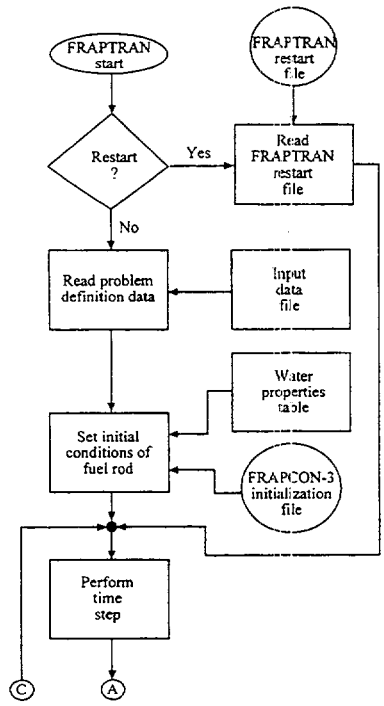

Figure 3.1 Flow Chart of FRAPTRAN (Part 1)

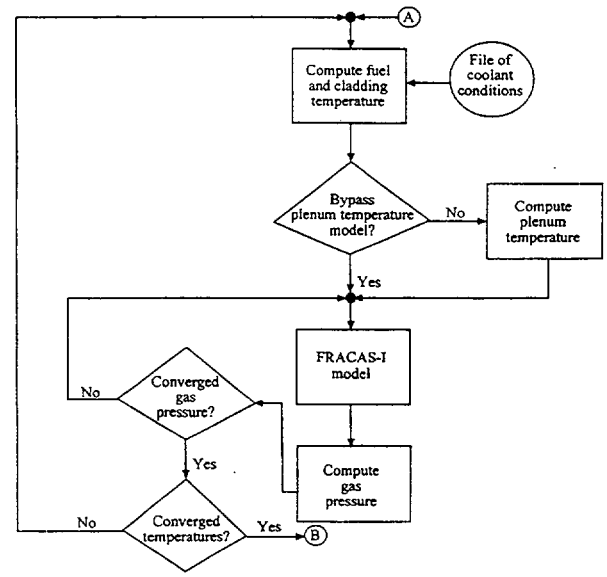

Figure 3.2 Flow Chart of FRAPTRAN (Part 2)

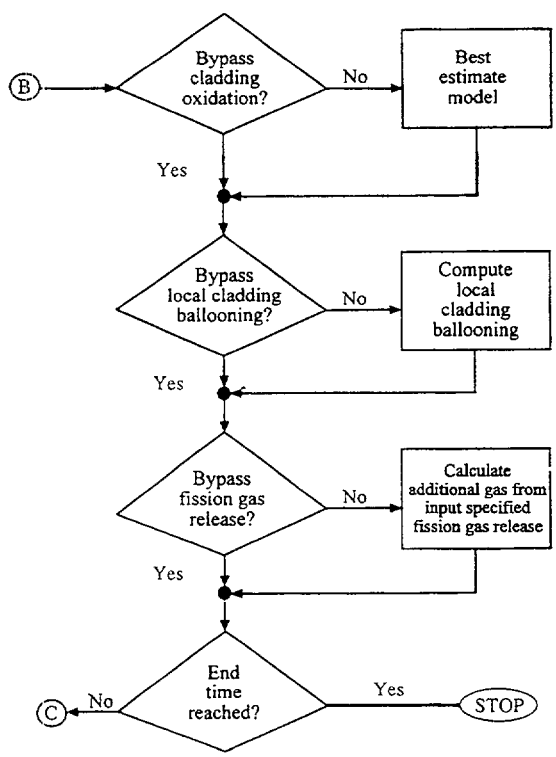

Figure 3.3 Flow Chart of FRAPTRAN (Part 3)

These and all other interactions are taken into account by repeatedly cycling through two nested loops of calculations until convergence is achieved. In the outside loop, the fuel rod temperature and mechanical response are alternately calculated. On the first cycle through this loop, the gap conductance is calculated using the fuel-cladding gap size from the past time step.

Then the fuel rod temperature distribution is calculated. This temperature distribution then feeds into the mechanical response calculations and influences such variables as the fuel and cladding thermal expansions and the cladding stress-strain relation. A new fuel-cladding gap is calculated which is used in the gap conductance calculation on the next cycle of calculations. The calculations are cycled until two successive cycles compute the same temperature distribution within the convergence criteria.

The inner loop of calculations, shown in Figure 3-2, is cycled in a manner similar to that used for the outer loop, but with the internal gas pressure being the variable determined by iteration. The fuel rod mechanical response and gas pressure are alternately determined. The temperature distribution remains the same during the inner loop of calculations. On the first cycle through this loop, the mechanical response is calculated using the past time step gas pressure. Variables that influence the gas pressure solution, such as fuel-cladding gap width and plenum volume, are calculated. Then the gas pressure calculation is made, and an updated cladding internal gas pressure is fed back to the mechanical response calculations. The calculations are cycled until two successive cycles result in the same gas pressure within the convergence criteria.

After the two loops of calculations have converged, cladding oxidation, local cladding ballooning, and fission gas release are calculated. These calculations are performed only once per time step.

3.2 Input Information

The execution of FRAPTRAN must be preceded by the creation of one or more sets of information. The sets of information are listed below:

1. The problem definition data (required)

2. Coolant condition file (optional)

3. Water properties file (optional)

4. FRAPCON-3 initialization file (optional)

5. FRAPTRAN restart file (optional)

The flow charts in Figures 3.1 and 3.2 show the positions in the path of calculations at which these sets of information are input to the code. Each set of information is input through a different FORTRAN logical unit. The FORTRAN logical unit for each set of information and the conditions for omitting a data set are provided in Table 3.2.

The problem definition data consist of data which describe the design of the fuel rod, the power of the fuel rod, and, optionally, the values of burnup dependent variables and the coolant conditions. The design data specify the fuel pellet geometry, fuel density, cladding geometry, and amount and type of fill

Table 3.2 Input Information		
Data Set	**Fortran Logical Unit**	**Conditions for Omitting**
problem definition data	5	FRAPTRAN restart file is read
coolant condition file	4	Cladding surface heat transfer is defined in the problem definition data or the coolant conditions at the bottom of the fuel rod are defined in the problem definition data.
water properties table	15	Cladding surface heat transfer is defined in the problem definition data.
Initialization file from FRAPCON3	22	(a) no previous burnup of fuel rod or, (b) burnup-dependent variables are defined in the problem definition data.

gas. The power data specify the history and spatial distribution of heat generation in the fuel due to fissioning and the decay of radioactive fission products. In particular, the data specify the time history of the rod-average linear heat generation rate (averaged over rod length), the normalized axial power profile (assumed to be invariant during the time span of a FRAPTRAN calculation), and the axially-dependent normalized radial power profile (assumed to be invariant during the time span of a FRAPTRAN calculation). The burnup-dependent data specify the incurred permanent strain of the cladding (from creep) at the time of the calculation, the incurred permanent strain of the fuel (from densification and fission-product induced swelling) at the time of the calculation, and the fill gas pressure and composition. The burnup-dependent data can be omitted and be input instead by reading an initialization file generated by FRAPCON-3. The coolant condition data specify the pressure, mass flux, and enthalpy of the coolant surrounding the fuel rod. As an alternative, the coolant condition data can specify the cladding surface heat transfer coefficient, coolant temperature, and coolant pressure. The coolant condition data may vary with time and elevation. The coolant condition data can be omitted and be input instead through the reading of a coolant condition file.

The coolant condition file consists of data which describe the conditions of the coolant surrounding the fuel rod. The coolant conditions are normally calculated by a thermal-hydraulic systems analysis code such as RELAP4 (Fisher et al. 1978) and the results stored on an output file. The required contents and format of the input tape for FRAPTRAN are provided in Appendix G.

Using the initialization file generated by FRAPCON-3 results in overwriting the initial user-input values for burnup dependent variables with values calculated by FRAPCON-3. A list of the variables written by FRAPCON-3 and read by FRAPTRAN for initializing burnup-dependent variables is provided in Table 3.3. Except for a few variables, the variables are generally a function of axial and radial nodes. This initialization file (FILE22) can be omitted and the burnup dependent data input instead as part of the problem definition data. This latter option, however, requires a manual processing of the burnup dependent variables from a steady-state fuel performance code or other source. Provided in Table 3.3 is information on how the data provided in the initialization file might be entered manually. Note that some data can not be readily entered manually (e.g., cladding strains).

Also provided in Table 3.3 is the formatting used by FRAPCON-3 to write the data to the file. This information could be used to generate a routine in a different fuel performance code to generate a file that could be read by FRAPTRAN.

Table 3.3. Variables Writen by FRAPCON-3 and Read by FRAPTRAN for Burnup Initialization			
For each FRAPCON-3 time step, the following information is written to a file. FRAPTRAN then reads the information at the first time step after the time specified in the FRAPTRAN input file (variable *trest*).			
Data Written/Read (unit)	**Comments**	**Format**[a]	**Input variable (Appendix A) if don't use FRAPCON-3 file**
time (s)		`write (22,10) time`	
number of axial nodes	number of nodes must be matched by FRAPTRAN (variable *naxn*)	`write (22,20) naxn`	
cladding OD oxide layer thickness for each axial node (inch)		`write (22,10) (BOSOxideThick(k),k=1,naxn)`	*odoxid* and *oxideod*
excess hydrogen concentration in cladding for each axial node (ppm)		`write (22,10) (cexh2a(k),k=1,naxn)`	*cexh2a*
cladding peak temperature, to this point in the history, for each axial node (K)		`write (2,10) (CladMaxT(k),k=1,naxn)`	no input option
fuel open porosity for each axial node (fraction)		`write (2,10) (OpenPorosity(k),k=1,naxn)`	*OpenPorosityFraction*
cross-section average fuel burnup for each axial node (MW-s/kg)		`write (2,10) (AxBurnup(k),k=1,naxn)`	derived from *bup* and *AxPowProfile*
radial node numbers for fuel surface, cladding ID, and cladding OD		`write (2,20) nfofs, ncifs, ncofs`	number of radial nodes defined by *nfmesh*
total quantity of gas in fuel rod, initial plus fission gas release (g-moles)		`write (2,10) TotalGasMoles`	defined by *gsms* or by using *gappr0* plus *tgas0*
gas composition (fraction): helium, argon, krypton, xenon, hydrogen, air, moisture		`write (2,10) (GasFraction(j),j=1,7)`	*gfrac*
radius to each radial fuel node (ft)	these are subsequently normalized to the FRAPTRAN radial node structure	`write (2,10) (radfs(l),l=1,nfofs)`	defined when specify *nfmesh* and *FuelPelDiam*

cladding plastic strain in hoop, axial, and radial directions for each axial node		`do ldir=1,3`
		`do k=1,naxn`
		`write (2,10) CldPlasStrnFrapcon(k,ldir)`
		`end do`
		
		`where: ldir=1=hoop, ldir=2=axial, ldir=3=radial`
			no input option

cladding effective plastic strain for each axial node		`do k=1,naxn`
		`write (2,10) EffStrain(k)`
		`end do`
			no input option

Table 3.3. (contd)			
Data Written/Read (unit)	**Comments**	**Format** [a]	**Input variable (Appendix A) if don't use FRAPCON-3 file**
radial temperature profile for each axial node (F)	these are subsequently interpolated to match the FRAPTRAN radial node structure	`write (22,10) (tempfs(l),l=1,ncofs)`	no input option
net permanent fuel deformation from swelling and densification at each axial node (inch)		`write (22,10) (SwellDispl(k),k=1,naxn)`	*radpel*
net permanent cladding deformation from creep and plastic strain (inch)		`write (22,10) (colddec(k),k=1,naxn)`	*eppinp*
permanent fuel relocation displacement (inch)		`write (22,10) (ureloc(k),k=1,naxn)`	no input option
gadolinia content in the fuel (fraction)		`write (22,10) gadolin`	*gadoln*

radial burnup profile (units?)	Interpolated to define burnup profile at FRAPTRAN nodal structure	`do k=1,naxn`
		`do l=1,nfofs`
		`write (22,10) burado(k,l)`
		`end do`
			butemp

relative radial power profile	interpolated to define relative radial power profile at FRAPTRAN nodal structure	`do k=1,naxn`
		`do l=1,nfofs`
		`write (22,10) radpowo(k,l)`
		`end do`
			RadPowProfile

Format statements: 10 format (2x, 30 (e10.4,2x)); for real variables 20 format (2x, 30 (i5,2x)); for integer variables			
(a) Variable names used are those in FRAPTRAN.			

3.3 Output Information

The FRAPTRAN output provides a complete description of the fuel rod response to the user-specified transient. This output includes, for example, the fuel and cladding temperature, internal gas pressure, and cladding deformation histories, all of which may be printed. Quantities such as peak cladding temperature and time and location of cladding failure are readily determined from the code output.

A list of the FRAPTRAN output information written to Unit 6 (see Appendix A) is provided in Table 3.4. An example of the code output is provided in Appendix B.

Another output option is the generation of a file to be used for graphics plotting. This is discussed further in Section 3.5 and Appendix A.

3.4 Nodalization, Accuracy, and Computation Time Considerations

The code user has four means of controlling accuracy and computer running time. These are through input specifications of 1) nodalization, 2) temperature convergence criteria, 3) pressure convergence criteria, and 4) time step size.

Table 3.4. FRAPTRAN Output Information	
1. Fuel rod radial and axial temperature distribution	10. Fuel elastic and permanent strains
2. Fuel diameter, fuel-cladding gap thickness, and cladding outer diameter	11. Amount of produced and released fission gases
3. Length change of fuel stack and cladding	12. Fuel rod void volume
4. Pressure of internal fuel rod gas	13. Cladding oxide thickness
5. Cladding surface heat transfer coefficient	14. Energy generated by cladding oxidation
6. Critical heat flux at fuel rod surface	15. Stored energy in fuel
7. Fuel-cladding gap heat transfer coefficient	16. Amount of melted fuel
8. Cladding plastic strain	17. Plenum gas temperature
9. Radial stress at fuel-cladding interface	18. Coolant conditions

The nodalization input data specify the locations at which variables such as temperature, stress, and strain are to be calculated. Increasing the number of locations provides greater spatial detail at the expense of longer computer run time and larger storage requirements. The nodalization data consist of axial nodalization and radial nodalization.

The axial nodalization data specify the elevations at which the radial distribution of the fuel rod variables are to be calculated. Each of these elevations is defined as an axial node. The axial nodes are considered to be points on the longitudinal axis of the fuel rod. Unequal spacing of the axial nodes is permitted.

The radial nodes lie in planes that pass through the axial nodes and are perpendicular to the fuel rod axis; that is, the centerline of the fuel rod. The first radial node is at the center of the fuel rod. Other radial nodes are placed at the fuel pellet surface and at the cladding inside and outside surfaces. In addition, an arbitrary number of radial nodes can be placed within the fuel and cladding. Unequal spacing of the radial nodes in the fuel is permitted, and the default situation is a spacing that results in equal-area rings of fuel.

An example of the fuel rod nodalization is shown in Figure 3.4. The axial nodes are numbered from bottom to top. The radial nodes are numbered from the fuel rod centerline to the cladding outside surface.

The computer running time is directly proportional to the number of axial nodes but is not as sensitive to the number of radial nodes. If the number of axial nodes is doubled, the computer running time is doubled. If the number of radial nodes is doubled, the running time is increased approximately 15%. In general, about ten axial nodes and, 15 radial nodes in the fuel are recommended for a full-length fuel rod.

Because of the thin-wall cladding mechanical solution, only two cladding nodes (inner surface and outer surface) are used. If cladding ballooning can occur, and an accurate calculation of the ballooning length is desired, a closely spaced axial nodalization is required in the region of anticipated cladding ballooning. In this region, the axial nodes should not be spaced farther apart than a distance equal to ten cladding diameters.

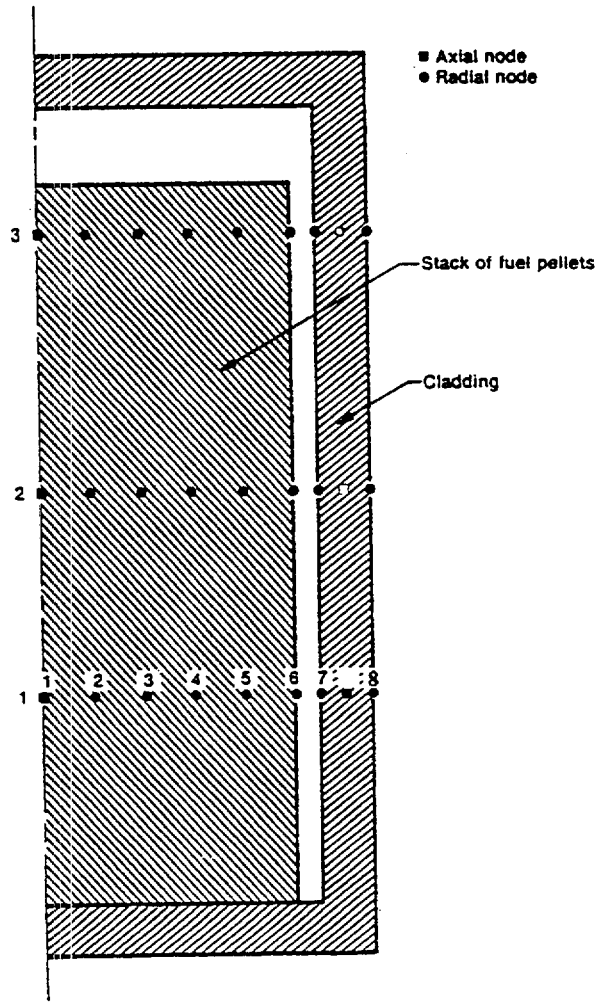

Figure 3.4 Example of Fuel Rod Nodalization

The accuracy of the temperature solution is controlled by the input convergence criterion for the maximum permissible fractional difference[a] in temperature calculated by two successive cycles through the temperature-deformation loop, as shown in Figure 3-2. If the temperature difference between the two successive cycles at any point in the fuel rod is greater than the convergence criteria, another cycle of calculations occurs. The temperature calculations, however, are not repeated at the axial nodes for which the temperature differences at all radial nodes were less than the convergence criterion.

The accuracy of the solution for internal gas pressure is controlled by the input convergence criterion for the maximum permissible fractional difference in the internal fuel rod gas pressure calculated by two successive cycles through the deformation-pressure loop of calculations. If the pressure difference between successive cycles is greater than the convergence criterion, another cycle of calculation occurs.

---

[a]Fractional difference is defined as $(T^n - T^{n-1})/T^{n-1}$, where T^n is the temperature calculated by the n-th cycle through the temperature-deformation loop, and T^{n-1} is the temperature calculated by the previous cycle.

In general, the temperature and pressure convergence criteria should be each be set to equal to 0.001, which results in an implicit solution of the transient. By making the temperature and pressure accuracies large (>1), each loop is cycled through only once, which results in an explicit solution of the transient. This approach may reduce computer running time and precludes convergence problems. If sufficiently small time steps are specified, adequate calculational accuracies can be assured.

The accuracy of the solution for mechanical response is internally fixed and cannot be controlled by the code user. With the FRACAS-I model the fuel and cladding are not in contact, a noniterative solution is made and no check for convergence needs to be made. If the fuel and cladding are in contact, the solution for the cladding permanent strains is iterative, with convergence declared after less than a 0.001 fractional difference in permanent strains between two successive iterations.

Both the accuracy and run time of the overall solution are controlled by the time step sizes. The time steps must be small enough so that detail in the power and coolant condition histories are not truncated. If a jump in the state of the fuel rod is occurring, such as a transition from nucleate boiling to film boiling, a small time step is required to accurately model the transition process. On the other hand, because the run time is roughly proportional to the number of time steps required to perform the analysis, the size of the time step should be made as large as possible. Therefore, the minimal run time solution usually requires different time step sizes for different parts of the problem time span.

3.5 Comments and Guidance on Operating FRAPTRAN

Provided in this section is some guidance on operating FRAPTRAN; i.e., time step sizes for particular transients, limits to operation, etc. Additional information may be found in the assessment report, NUREG/CR-6739, Volume 2. The input files for the assessment cases are provided in Appendix B of NUREG/CR-6739, Volume 2, and provide examples of preparing input files.

The mechanical solution scheme in FRAPTRAN is sensitive to rapid strain rates and may not iteratively converge if the time step size is too large during periods of high strain rate. Reactivity initiated accident (RIA) calculations are an example of when this problem might be encountered. If the strain rate is too high, the code will stop and print the following messages:

> in the prompt window: "COUPLE: cladding plastic strain increment between time steps is too great for iteration procedure, reduce time step by a factor of 5"
>
> in the output file: "COUPLE: cladding plastic strain increment between time steps is too great for iteration procedure, reduce time step by a factor of 5. Execution stopped at time = xxxx"

Experience in running the RIA assessment cases indicates that time steps $\leq 1 \times 10^{-5}$ seconds are needed.

Another case where strain rate may become too high is when elevated cladding temperatures, such as for a LOCA-type transient, result in very low yield strength values, i.e., <6 MPa. However, rather than stopping for this situation, the code goes to a simplified mechanical solution for strain, i.e., ignores elastic strain, and is allowed to continue running. The following message is printed to both the prompt window and the output file:

"The cladding average temperature is greater than 1089K, the temperature at which the cladding strain rate becomes excessive. Calculation continuing by bypassing the iterative solution in COUPLE."

Some general guidelines for selecting time step size are:

- For RIAs, time step should be $\leq 1 \times 10^{-5}$ seconds beginning with the power increase and continued through at least one second.
- For a large break LOCA, a time step size of about 0.1 is recommended during the first few seconds of the transient when the coolant flow changes rapidly with time.
- For a small break LOCA, both the power and coolant conditions change slowly with time, so a time step size ≥ 1 second may be used.
- During a period of possible film boiling at any location along the rod, the time step size should be ≤ 0.2 seconds.
- During a period of possible cladding ballooning, the time step size should be ≤ 0.5 seconds.

In general, if difficulties are encountered in having a specific problem converge, the time step size should generally be decreased.

The input power history and time step size arrays are interpreted differently by the code. The power history array is interpolated along the time history while the time step size is constant until changed. The interpretatations are visually presented in Figure A.2.

In the "model" input block (Table A.7), the user has the option to specify time dependent rod-average fission gas release (*presfgr* and *relfrac* variables) and fuel swelling (*TranSwell* and *FuelGasSwell* variables). These are options are provided primarily to allow the user to simulate the postulated rapid changes in fission gas release and fuel swelling that might occur during an RIA. The rod-average fission gas release (fractional release with the inventory based on the rod-average burnup) affects both the gas composition and rod gas pressure during the calculation. The fuel swelling input is an adder to the fuel radial thermal expansion. Both sets of array input are interpolated between data points.

The input instructions, Appendix A, identify the option to specify a file (FILE66) for graphics data output. This file is designed to be read by a PNNL-developed routine that works with EXCEL™ software. The file name needs to be of the format "stripf.i" where "i" is an alpha-numeric name selected by the user. The EXCEL™ routine and user instructions will be provided along with the FRAPTRAN code to users.

4 REFERENCES

Behling, S. R., et al. *RELAP4/MOD7: A Computer Program to Calculate Thermal and Hydraulic Phenomena in a Nuclear Reactor or Related Systems.* NUREG/CR-1998 (EGG-2089), Idaho National Engineering Laboratory, Idaho Falls, Idaho. 1981.

Berna, G. A., et al. *FRAPCON-3: A Computer Code for the Calculation of Steady-State, Thermal-Mechanical Behavior of Oxide Fuel Rods for High Burnup.* NUREG/CR-6534 (PNNL-11513), Vol. 2, Pacific Northwest National Laboratory, Richland, Washington. 1997.

Cadek F. F., et al. *PWR FLECHT Final Report Supplement.* WCAP-7931. 1972.

Crank, J., and P. Nicolson. "A Practical Method for Numerical Evaluation of Solutions of Partial Differential Equations of the Heat Conduction Type," in *Proceedings, Cambridge Philosophical Society,* 43(1974), pp. 50-64. 1974.

Dittus, F. W., and L.M.K. Boelter. *Heat Transfer in Automobile Radiators of the Tubular Type.* University of California Publications, pg. 443-461. 1930.

Dougall, R. L., and W. W. Rohsenow. *Film Boiling on the Inside of Vertical Tubes with Upward Flow of the Fluid at Low Qualities.* MIT-TR-907-26, Massachusetts Institute of Technology. 1963.

Groeneveld, D. C. *An Investigation of Heat Transfer in the Liquid Deficient Regime.* AECL-3281, Revised. Atomic Energy Canada Limited. 1969.

Hagrman, D. L., G. A. Reymann, and R. E. Mason. *MATPRO-Version 11 (Revision 2): A Handbook of Materials Properties for Use in the Analysis of Light Water Reactor Fuel Rod Behavior.* NUREG/CR-0497 (TREE-1280, Rev. 2), Idaho National Engineering Laboratory, Idaho Falls, Idaho. 1981.

Hagrman, D. L. *Zircaloy Cladding Shape at Failure (BALON2).* EGG-CDAP-5379, EG&G Idaho, Inc., Idaho Falls, Idaho. 1981.

Kreith, F. *Principles of Heat Transfer.* 8th Edition, Scranton: International Text Book Company. 1964.

Lanning, D. D., C. E. Beyer, and C. L. Painter. *FRAPCON-3: Modifications to Fuel Rod Material Properties and Performance Models for High-Burnup Application.* NUREG/CR-6534 (PNNL-11513), Vol. 1, Pacific Northwest National Laboratory, Richland, Washington. 1997.

Lucuta, P. G., H. S. Matzke, and I. J. Hastings. "A Pragmatic Approach to Modeling Thermal Conductivity of Irradiated UO_2 Fuel: Review and Recommendations," *Journal of Nuclear Materials,* Vol. 232, pp. 166-180. 1996.

McAdams, W. H. *Heat Transmission.* 3rd Edition, New York: McGraw-Hill Book Company, Inc. 1954.

McDonough, J. B., W. Milich, and E. C. King. *Partial Film Boiling with Water at 2000 psia in a Round Tube.* MSA Research Corporation, Technical Report 62. 1958.

Mendelson, A. *Plasticity: Theory and Applications*. New York: The MacMillian Company. 1968.

Murphy, G. *Advanced Mechanics of Materials*. New York: McGraw-Hill Book Company, Inc. 1946.

Prandtl, L. "Spannungsverteilung in Plastischen Koerpern," *Proceedings of the First International Conference Applied Mechanics*. 1924.

Scatena, G. J., and G. L. Upham. *Power Generation in a BWR Following Normal Shutdown on Loss-of-Coolant Accident Conditions*. NEDO-10625. 1973.

Siefken, L. J., et al. *FRAP-T6: A Computer Code for the Transient Analysis of Oxide Fuel Rods*. NUREG/CR-2148 (EGG-2104), EG&G Idaho, Inc., Idaho Falls, Idaho. 1981.

Siefken, L. J., et al. *FRAP-T6: A Computer Code for the Transient Analysis of Oxide Fuel Rods*. NUREG/CR-2148 Addendum (EGG-2104 Addendum), EG&G Idaho, Inc., Idaho Falls, Idaho. 1983.

Wagner, R. J. *HEAT-1: A One-Dimensional Time Dependent or Steady-State Heat Conduction Code*. IDO-16887. 1963.

Wang, C. *Applied Elasticity*. New York: McGraw-Hill Book Company, Inc. 1953.

APPENDIX A

INPUT INSTRUCTIONS FOR FRAPTRAN

APPENDIX A

INPUT INSTRUCTIONS FOR FRAPTRAN

Provided in this Appendix are the input instructions for FRAPTRAN. Also included is guidance on using options and/or how data are to be input.

An example input file is provided as Figure A.1; please refer to this figure while reading the following instructions. Lines beginning with * in the first column are comment lines only and are not acted on. The line beginning /* identifies the beginning of the case input, which uses a set of NAMELIST inputs. Only the first data input line, the title card, is formatted.

An input file for FRAPTRAN provides three basic sets of information. First, the input and output units used by FRAPTRAN are defined. The defined, and needed, files are:

- FILE05: principal FRAPTRAN unit for supplying input data
- FILE15: unit for supplying water properties data
- FILE22: unit for supplying FRAPCON-3 initialization input. This is used to initialize burnup dependent parameters. This unit is used in conjunction with input parameters *inp*[a] and *trest* (Table A.3) are used
- FILE06: principal FRAPTRAN unit for output
- FILE66: unit used to collect data for plotting. This file is designed to be used with a PNNL-developed Excel™ plotting program.

Second, a title card is supplied as shown in Table A.1. Third, using NAMELIST input format, the parameters of the problem are entered. The NAMELIST input is read in by FRAPTRAN and a formatted input is created in a file called *formin*. FRAPTRAN then reads this file to get the input data it needs.

Input parameter data are entered in data blocks using NAMELIST format. Tables A.2 through A.9 provide the NAMELIST blocks and the input variables in those blocks. To start a NAMELIST block, state the name of the block beginning with a dollar sign in column 2 of the line; e.g., $*iodata*[b]. Then, on the following lines in column 2 or greater, type the variable names with their value after that; i.e., *temp=1.2*. Alphanumeric variables must be input in quotes. For example, *heat='on'* will set the alphanumeric variable "*heat*" to "*on*". When a block is finished, type $*end* beginning in column 2 in the line after the last piece of data.

To not use an option or a suboption, simply do not input any of the variable contained within. In some cases, there are certain variables to set certain options or suboptions. The "MODEL" and "BOUNDARY" data blocks, in particular, provide the opportunity for the user to specify options and suboptions for modeling and coolant conditions. In the tables defining the data blocks, variables defining

---

[a]For readability and differentiation from the other text in this appendix, input variables and some files are identified in the text using lower case and italics; note, however, that italics are not used in the actual input file.
[b]Namelist input is case sensitive.

options are typically followed by variables defining suboptions, which are in turn followed by the necessary input variables to implement the suboption. The data block flow, thus, is generally as follows:

Option 1
suboption 1a
variable
variable
suboption 1b
variable
variable
Option 2
suboption 2a
variable
etc.

Default of options and suboptions is to be turned off, so the user must actively turn on options and suboptions.

Before specifying the NAMELIST arrays, it is necessary to write "*start*" on the first line after the begin NAMELIST input and before the line $*iodata*. Even if a data block is not used, it must be included in the input file; i.e.,:

$tuning
$end

In the "units" columns of the following tables, the first unit is for SI unit input and the second unit is for British unit input. If only one unit is listed, it applies to either or both input options.

All default values are 0.0 (reals) or 0 (integers) unless specified otherwise in the accompanying tables.

```
************************************************************************
* FrapTran, transient fuel rod analysis code                           *
*----------------------------------------------------------------------*
*                                                                      *
*  CASE DESCRIPTION: Standard Problem #1                               *
*                                                                      *
*  UNIT   FILE DESCRIPTION                                             *
*  ----   ----------------------------------------------               *
*   --    Input:                                                      *
*   15      Water properties data                                     *
*                                                                      *
*   --    Output:                                                     *
*    6      STANDARD PRINTER OUTPUT                                   *
*   66      STRIPF FILE FOR GRAFITI                                   *
*                                                                      *
*   --    Scratch:                                                    *
*    5      SCRATCH INPUT FILE FROM ECHO1                             *
*                                                                      *
* Input: FrapTran INPUT FILE                                           *
*                                                                      *
************************************************************************
*
* GOESINS:
FILE05='nullfile', STATUS='scratch', FORM='FORMATTED',
        CARRIAGE CONTROL='LIST'
FILE15='sth2xt',  STATUS='old', FORM='UNFORMATTED'
*
* GOESOUTS:
FILE06='out.stdprob1',   STATUS='UNKNOWN', CARRIAGE CONTROL='LIST'
FILE66='stripf.stdprob1', STATUS='UNKNOWN', FORM='FORMATTED',
        CARRIAGE CONTROL='LIST'
/***********************************************************************
Standard Problem #1
 $begin
   ProblemStartTime = 0.0,
   ProblemEndTime = 20.0,
 $end
start
 $iodata
  unitout=1, dtpoa(1)=0.5, dtplt=0.25, pow=1,
 $end
 $solution
  dtmaxa(1)=0.001, 0.0, 0.001, 4.9, 0.01, 5.0, 0.01, 20.0, dtss=1.e5
  prsacc=0.001, tmpac1=0.001, maxit=100, noiter=100, epsht1=1.0,
  zelev=0.5,1.5,2.5,3.5,4.25,4.75,5.25,5.75,
        6.25,6.75,7.25,7.75,8.5,9.5,10.5,11.5,
  nfmesh=15,
 $end
 $design
  RodLength=12.0, RodDiameter=0.03517,
  rshd=0.01008, dishd=0.000625, pelh=0.0251, dishv0=0.0000002,
  FuelPelDiam=0.0305, roughf=1.14, frden=0.932457, fotmtl=2.0, tsntrk=1883.0,
  gapthk=3.25e-4, coldw=0.1, roughc=2.16, cldwdc=0.04,fgrns=10.0,
  ncs=22, spl=0.4583, scd=0.0291, swd=0.006333, vplen=0.00038,
  gfrac(1)=1.0, gappr0=2243.0, gsms=0.03,
 $end
 $power
  RodAvePower=11.08,       0.0,     3.695,       0.6,      2.01,       2.3,
           1.413,      8.7,     0.815,       10.0,     1.902,     13.0,
           0.543,      16.3,    0.402,       45.0,
  AxPowProfile=0.56,     0.545,      1.17,    1.6333,      1.46,       2.7,
          1.61,    3.8125,      1.58,       4.9,      1.48,   5.99166,
          1.34,     7.075,      1.15,   8.15833,      0.94,      9.25,
          0.70,      10.3,      0.36,  11.39166,
```

Figure A.1 Example of Input Data File Illustrating Necessary Data Lines

```
RadPowProfile=0.982,  0.00,          0.983,  0.0022875,       0.984,  0.0038125,
        0.985,  0.0053375,    0.988,  0.0068625,       0.991,  0.0083875,
        0.996,  0.0099125,    1.002,  0.0114375,       1.009,  0.0129625,
        1.017,  0.0144875,    1.03,    1.525e-2,
$end
$model
 internal='on',
 metal='on', cathca=1,
 deformation='on',
$end
$boundary
 heat='on'
 press=12, pbh2(1)=2273.0,      0.00,      1561.0,      0.51,
                   1405.0,      1.01,      1198.0,      2.15,
                   1166.0,      2.75,       940.0,      6.95,
                    908.0,      7.55,       856.0,      8.15,
                    686.0,      9.87,       568.0,     11.07,
                    206.0,     15.87,        50.0,     20.07,
 zone=3, htco=12, tem=12,
 htclev(1)=3.0, 9.0, 12.0,
 htca(1,1)=51600.0,    0.00,      166.0,       0.51,
             36.0,     1.01,       28.1,       2.15,
            120.0,     2.75,      100.0,       6.95,
             52.0,     7.55,        5.0,       8.15,
              5.0,     9.87,      160.0,      11.07,
             60.0,    15.87,       50.0,      20.07,

 tblka(1,1)=638.3,     0.0,       601.5,       0.51,
            587.5,     1.01,      743.8,       2.15,
            563.5,     2.75,      537.2,       6.95,
            533.1,     7.55,      553.2,       8.15,
           1333.8,     9.87,      531.0,      11.07,
            384.2,    15.87,      893.2,      20.07,

 htca(1,2)=62300.0,   0.0,       158.0,        0.51,
             36.0,    1.01,      281.0,        2.15,
            116.0,    2.75,      100.0,        6.95,
             52.0,    7.55,        5.0,        8.15,
              5.0,    9.87,      160.0,       11.07,
             60.0,   15.87,       50.0,       20.07,

 tblka(1,2)=638.3,    0.00,      601.5,       0.51,
            587.5,    1.01,      743.8,       2.15,
            563.5,    2.75,      537.2,       6.95,
            533.1,    7.55,      553.2,       8.15,
           1333.8,    9.87,      531.0,      11.07,
            384.2,   15.87,      893.2,      20.07,

 htca(1,3)=39300.0,   0.0,      250.0,       0.51,
             40.0,    1.01,     281.0,       2.15,
            128.0,    2.75,     110.0,       6.95,
             52.0,    7.55,       5.0,       8.15,
              5.0,    9.87,     160.0,      11.07,
             60.0,   15.87,      50.0,      20.07,

 tblka(1,3)=638.3,     0.0,       601.5,       0.51,
            587.5,     1.01,      743.8,       2.15,
            563.5,     2.75,      537.2,       6.95,
            533.1,     7.55,      553.2,       8.15,
           1333.8,     9.87,      531.0,      11.07,
            384.2,     15.87,     893.2,      20.07,
$end
$tuning
$end
```

Figure A.1 (contd)

Table A.1 Title Card (first input data card)		
CARD 1 - Title Card		
Columns	Format	Contents
1-80	A	Title of Problem

Table A.2 Data Block for Specifying Problem Control Input

Problem Control Data Block
$begin

Variable Type	Description/Definition	Units	Defaults/ Limitations
ProblemStartTime[a] (F)	Start time of calculation. If *ncards=0*, leave this variable blank	s	
ProblemEndTime (F)	End time of calculation. If *ncards=0*, leave this variable blank	s	
ncards (I)	If *ncards=1* (default), a new calculation (cold start) is to be performed. This option is required if the run will use burnup initialization data from FRAPCON-3. If *ncards=0*, a previous calculation is to be continued. This requires a REQUEST card for TAPE1 which gives the restart tape number. This data block is the only data block read in. If *ncards=2*, a second transient calculation is performed considering the history effects of a previous transient. The time read on the restart tape is back shifted to zero. This permits analysis of a second transient with initiation at time of zero. The input power and coolant condition histories should assume that a time of zero corresponds with time of transient initiation. The steady state condition of the fuel rod is calculated to determine the fuel rod initial conditions. the input variables that are changed from the first to the second transient are the only required input. In general, the data in the power coolant condition blocks will be different and so needs to be input. The data in the tuning, design and model selection blocks would usually be the same and so these data blocks can be omitted. In the solution control data block, only the time step history would usually be different. So this variable can be input and the other variables in the data block omitted. The radial and axial nodalization can never be changed.		Default = 1

[a]F = real, I = integer, A = alphanumeric

Table A.3 Data Block for Specifying Input and Output Options

Input/Output Data Block
$iodata

Variable (Type)	Description/Definition	Units	Defaults/Limitations
unitin (I)	Option to specify that the input data are in SI units. Enter a value of *unitin=1* for SI input units. If this option is omitted, the input is assumed to be in British units.	*	Default = 0 (British units)
inp (I)	Option to specify the initialization of burnup dependent variables by reading a FRAPCON-3 created file. Enter a value of *inp=1* to turn on. The entire problem must be set up in the input file, with the FRAPCON-3 input just re-setting some burnup dependent variables. FRAPCON-3 data are read from unit 22. FRAPCON-3 writes to a file called 'RESTART.' The user must define unit 22 and file name in the input deck (as is done for the FRAPTRAN output file). The initialization file from FRAPCON-3 is a formatted file. Both *inp* and *trest* must be specified to use a FRAPCON-3 data file.	*	Default = 0 (no FRAPCON-3 initialization)
trest (F)	*trest*=FRAPCON-3 problem time for initialization. For example, a FRAPCON-3 problem time of zero corresponds to no burnup, while a time of 9.46e7 seconds (three years) corresponds to high burnup.	s	Default = 0 (no FRAPCON-3 initializaton)
unitout (I)	Option to specify that the output are to be in SI units even though the input is in British units. Enter a value of *unitout=1* for SI output units. If this suboption is omitted, the output will be in the same units as the input; i.e., will get SI units out if SI units are specified as input.		Default =0 (output same as specified input units)
dtpoa (F)	Specify the interval of problem time between printouts. *dtpoa(1)*=time interval between printout at problem time of *dtpoa(2)* until a new time interval is input. Continue entering data pairs as necessary. If the print interval is constant with time for the entire history, *dtpoa(1)* is the constant print interval and the balance of the *dtpoa* input is omitted.	s	Default = 100s
dtplt (F)	Specify the output of a plot file. *dtplt*=problem time interval between time points in the plot file. If *dtplt=0*, the plot time interval is set to 1/10 of the print time interval. The interval of time between points on the plot file should be set equal to the smallest time step specified in the Solution Control Data Block.	s	Default = 0
res (F)	Option to specify that a restart file is to be created so that the calculations can be continued at some other time. Enter a value of *res=1* to turn on. If this suboption is specified, the contents of file TAPE2 (restart file) must be saved.	*	Default =0 (no restart file)
pow (F)	Option to specify the printout of the fuel rod state at each step of the first power ramp. Enter a value of *pow=1* to turn on. At the initial problem time, the power is increased in 0.05 kW/ft steps from zero power to the power at the initial time.	*	Default = 0

* = non-dimensional.

Table A.4 Data Block for Specifying Control of the Problem			
Solution Control Data Block $solution			
Variable (Type)	**Description/Definition**	**Units**	**Defaults/ Limitations**
dtmaxa (F)	Specify the time step history. *dtmaxa(1)*=time step size at time *dtmaxa(2)*. Continue entering data pairs as necessary. Each time step size is used until a new time step size is input for a later time; this is illustrated in Figure A.2. The recommended time step sizes for various types of problems are given in Table A.10. If the time step size is constant with time for the entire transient history, *dtmaxa(1)* is the constant time step size and the balance of the *dtmaxa* input is omitted. If using FRAPCON-3 initialization of burnup dependent variables, the starting time for a FRAPTRAN calculation [*dtmaxa(2)*] will be still be 0 seconds, even if *trest>0*, because *dtmaxa* is relative to the start of the transient calculation, not the start of the "irradiation." The information in Table A.10 is modified as follows: For a small break LOCA such as the TMI-2 accident, a time step of 10s may be used during the adiabatic heatup period. But during the period of rod quenching for any accident, the time step should be reduced to 0.1 to 0.2s.	s	Required input. A maximum of 20 time step pairs are allowed.
dtss (F)	Option to specify the solution of the fuel rod temperature by the steady state equation instead of the transient equation. For accident analysis, this suboption is normally omitted. *dtss*=time step threshold for steady-state solution. If the time step is equal to or greater than *dtss*, the steady-state equation is used to solve for the fuel rod temperature Otherwise, the transient equation is used.	s	Default = 1×10^5 s
prsacc (F)	Option to specify an implicit solution. *prsacc*=maximum fractional change in internal fuel rod pressure between two successive iterations for convergence. The test is $(p^{r+1} - p^r)/p^r \leq prsacc$, where p^r is the pressure calculated by the rth iteration.	*	The implicit solution is recommended. If cladding ballooning is possible, specify a value of 0.001 for *prsacc*. Whenever film boiling occurs at the cladding surface and fuel rod internal pressure is equal to greater than the coolant pressure, ballooning is possible. If no possibility exists for cladding ballooning, a value of 0.01 may be specified for *prsacc*. Default=0.005.
tmpac1 (F)	For implicit solution, *tmpac1* = maximum fractional change in temperature at any radial node between two successive iterations for convergence.	*	Default=0.005.
soltyp (F)	Option to specify an explicit solution by *soltyp=1*. One iteration per time step is performed and no check is made of accuracy of solution. If *soltyp = 1*, do not input values for *prsacc* or *tmpac1*.	*	Default=0 (implicit solution)
maxit (I)	Maximum number of iterations in the steady state temperature solution.	*	Default=200
noiter (I)	Maximum number of iterations in the transient temperature solution.	*	Default=200

Table A.4 (contd)

Solution Control Data Block $solution			
Variable (Type)	**Description/Definition**	**Units**	**Defaults/ Limitations**
epsht1 (F)	Maximum temperature change between iterations on thermal properties before convergence declared.	K; °F	Default=0.001
naxn (I)	Number of evenly spaced axial nodes, with nodes at mid-point of axial regions; see Figure A-3. *zelev* variable is not used if specify *naxn*. When specifying axial nodalization, neither *naxn* or *zelev* have to match the input axial power profile. (When using FRAPCON-3 initialization, *naxn* must match the number of axial nodes used in the FRAPCON-3 case, with a maximum of 22.)		*naxn* or zelev are required input, maximum value of 25 for *naxn*. Do not enter a value for *naxn* if going to specify axial elevations via *zelev*.
zelev (F)	Option to specify elevation of axial nodes above the bottom of the rod. *naxn* variable is not used if specify *zelev*. The input elevations specify the location of the axial nodes as shown in Figure A-4. Continue entry until all positions are specified.	m; ft	Maximum of 25 values for *zelev*. Do not enter values if using evenly spaced nodalization via *naxn*.
nfmesh (I)	Number of equal-area radial nodes in the fuel. *fmesh* variable is not used if specify *nfmesh*. The first radial node is placed at the fuel center and the last node at the fuel surface.		*nfmesh* or *fmesh* are required input. *nfmesh*≥*2;* normally *nfmesh* ~15; maximum of 25.
fmesh (F)	Option to specify radii of radial nodes in the fuel; always set *fmesh(1)=0*. Continue until the radius of each radial node has been specified. The last input radius must equal the fuel pellet radius and account for any permanent fuel dimensional changes; i.e., fuel swelling and densification (see *gapthk* in DESIGN variables). *nfmesh* variable is not used if specify *fmesh*.	m; ft	Maximum of 25 values for *fmesh*. Do not enter values if using equal-area nodalization via *nfmesh*.
* -= non-dimensional			

Table A.5 Data Block for Specifying the Design of the Fuel Rod			
Design of Fuel Rod Data Block $design			
Variable (Type)	**Definition**	**Units**	**Defaults/ Limitations**
	Variables *pitch, pdrato, rnbnt,* and *totnb* define the option to model the the restraint to the cladding ballooning given by adjacent fuel rods. The instability strain is set equal to the rupture strain, so that the full range of cladding ballooning is modeled by the FRACAS-I subcode. The BALLOON subcode is not used. If option not included, no restraint to rod ballooning is to be modeled. Enter a value of *pitch > 0.* to turn on this option.		
pitch (F)	Center-to-center spacing of fuel rods. Normally, this option is omitted. Enter a value > 0 to turn on.	m; ft	Default=0.
pdrato (F)	Ratio of rod pitch to rod outer diameter. Omit if a 17x17 PWR bundle. Enter a value > 1.0 to change default	non-dimensional	Default =1.32
rnbnt (F)	Ratio of balloonable rods to total rods in bundle; normally, this ratio is 0.92. Control rods and water rods are examples of rods which cannot balloon. Omit if a 17x17 PWR bundle. Enter a value > 0.01 to change default.	non-dimensional	Default=1.0
totnb (F)	Total number of rods in fuel bundle. Omit if a 17x17 bundle. Enter a value > 1.0 to change default.	non-dimensional	Default=289
RodLength (F)	Fuel pellet stack length.	m; ft	Required input. Default=0.0
RodDiameter (F)	Cladding outer diameter. For a zero burnup case, this is the as-fabricated cladding diameter. If a FRAPCON-3 initialization tape is to be read, the as-fabricated cladding diameter is still input, and then *RodDiameter* is re-initialized with the FRAPCON-3 results. If manually inputting burnup-dependent values for variables, *eppinp* should be used to specify the axially varying permanent hoop strain for the cladding resulting from the steady-state irradiation with *RodDiameter* specifying the initial condition. (If no axial variation is assumed, then *RodDiameter* may be used to specify the burnup condition if it accounts for the burnup-induced claddig permanent diameter change (i.e., creepdown) at 300K.)	m; ft	Required input. Default=0.0
rshd (F)	Room temperature (300K) radius of fuel pellet shoulder. Optional input.	m; ft	Default=0.0
dishd (F)	Room temperature (300K) depth of fuel pellet dish. Optional input.	m; ft	Default=0.0
pelh (F)	Room temperature (300K) height of fuel pellet.	m; ft	Required input. Default=0.0
dishv0 (F)	Room temperature (300K) volume of fuel pellet dish. If the pellet is dished at both ends, *dishv0* is the sum of the dish volume at each end of the pellet. Optional input.	m^3; ft^3	Default=0.0

Table A.5 (contd)

Design of Fuel Rod Data Block $design			
Variable (Type)	**Definition**	**Units**	**Defaults/ Limitations**
FuelPelDiam (F)	Fuel pellet diameter. For a zero burnup case, this is the as-fabricated pellet diameter. If a FRAPCON-3 initialization tape is to be read, a value for pellet diameter is still input, and then *FuelPelDiam* is re-initialized with the FRAPCON-3 results. If manually inputting burnup-dependent values for variables, *radpel* should be used to specify the axially varying permanent change in fuel pellet radius resulting from the steady-state irradiation with *pelod* specifying the initial, as-fabricated condition. (If no axial variation is assumed, then *pelod* may be used to specify the burnup condition if it accounts for the burnup-induced fuel permanent radius change (i.e., densification and/or swelling) at 300K.)	m; ft	Required input. Default=0.0
roughf (F)	Arithmetic mean roughness of fuel pellet surface. Optional input.	μm	Default = $1.x10^{-3}$
frden (F)	Fractional theoretical density of fuel pellet.		Required input. Default =0.
OpenPorosityFraction	Option to specify the fuel open porosity fraction. If the default value of 0.0 is used, FRAPTRAN will use an internal correlation of open porosity fraction as a function of density (see Section 2.4.3.3). If a positive, non-zero value is entered for *OpenPorosityFraction*, that value will override the internal calculation of the open porosity fraction.	non-dimensional	Default = 0.
bup (F)	Rod-average burnup of fuel. Optional input. Needed if user a) wants to use non-zero burnup value of fuel relocation, or b) specifies time-dependent fission gas release history in the model data block.	MWs/kg	Default = 0.
frpo2 (F)	Fraction of fuel weight which is PuO_2. Optional input.		Default = 0.
fotmtl (F)	Ratio of fuel oxygen atoms to uranium and plutonium atoms. Optional input	non-dimensional	Default = 2.0
tsntrk (F)	Fuel sintering temperature. Optional input.	K	Default = 1883
fgrns (F)	Fuel grain size. Optional input and not used in FRACAS-I.	μm	Default=10
gadoln (F)	Weight fraction of gadolinia (Gd_2O_3) in fuel pellets. Optional input.		Default=0.0

Table A.5 (contd)

Design of Fuel Rod Data Block $design			
Variable (Type)	**Definition**	**Units**	**Defaults/ Limitations**
gapthk (F)	Radial fuel-cladding gap thickness. For a zero burnup case, this is the as-fabricated radial fuel-cladding gap thickness. If a FRAPCON-3 initialization tape is to be read, a value for radial gap thickness is still input, and then *gapthk* is re-initialized with the FRAPCON-3 results. If manually inputting axially varying burnup-dependent values for cladding and fuel via *eppinp* and *radpel*, the gap thickness is automatically corrected. If no axial variation is assumed or input for a burnup case, then *gapthk* should account for permanent changes in the radial fuel-cladding gap at 300K due to permanent changes in the cladding and fuel dimensions. Values for *gapthk* should be based on no change in the cladding thickness from the as-fabricated condition.	m; ft	Default = 0.0
coldw (F)	Reduction of cross-sectional area of cladding by cold working process (cold work factor for strength). Optional input. *coldw*=$(A_o-A)/A_o$ where A_o = cross-sectional area prior to cold working, and A =cross-sectional area after cold working		Required input. Default = 0.0
roughc (F)	Arithmetic mean roughness of cladding inner surface. Optional input	μm	Default= $1.x10^{-3}$
cfluxa (F)	Axially averaged and time averaged fast neutron flux that cladding was exposed to during lifetime. Fast neutrons are defined to have an energy > 1 MeV. If the fast flux suboption of the "OPTION VARIABLES" option is not input, the axial profile of the fast flux is assumed to be the same as the axial power profile. Optional input.	n/m^2-s	Default = 0.0
tflux (F)	Time span that cladding is exposed to fast neutron flux. *cfluxa*tflux* must equal axially averaged fast neutron fluence received by the cladding. Optional input.	s	Default = 0.0
cldwdc (F)	Cold work factor for ductility; recommended value is 0.04. Optional input.		Default = 0.0
ncs (I)	Number of coils in upper plenum spring. Optional input.		Default = 1
spl (F)	Uncompressed height of upper plenum spring. Optional input.	m; ft	Default=0.0
scd (F)	Uncompressed outer diameter of upper plenum spring coils. Optional input.	m; ft	Default=0.0
swd (F)	Diameter of upper plenum spring wire. Optional input.	m; ft	Default=0.0
vplen (F)	Volume of upper plenum, including volume of upper plenum spring. Optional input. Option to specify geometry of lower plenum of fuel rod. Omit this option if there is no lower plenum.	m^3; ft^3	Default=0.0

Table A.5 (contd)

Design of Fuel Rod Data Block $design			
Variable (Type)	**Definition**	**Units**	**Defaults/ Limitations**
ncolbp (I)	Number of coils in lower plenum spring. Optional input.		Default = 1
splbp (F)	Uncompressed height of lower plenum spring. Optional input.	m; ft	Default = 0.0
coldbp (F)	Uncompressed outer diameter of lower plenum spring coils. Optional input.	m; ft	Default = 0.0
spdbp (F)	Diameter of lower plenum spring wire. Optional input.	m; ft	Default = 0.0
volbp (F)	Volume of lower plenum, including volume of lower plenum spring. Optional input.	m^3; ft^3	Default = 0.0
gfrac(1) (F)	Fraction of gas that is helium. The mole fractions of gas components *gfrac* must sum to 1.0		Default = 1.0
gfrac(2) (F)	Fraction of gas that is argon		Default = 0.0
gfrac(3) (F)	Fraction of gas that is krypton		Default = 0.0
gfrac(4) (F)	Fraction of gas that is xenon		Default = 0.0
gfrac(5) (F)	Fraction of gas that is hydrogen		Default = 0.0
gfrac(6) (F)	Fraction of gas that is air		Default = 0.0
gfrac(7) (F)	Fraction of gas that is water vapor		Default = 0.0
gsms (F)	Quantity of gas in fuel rod; leave blank if *tgas0* is non-zero	g-moles	
gappr0 (F)	As-fabricated fill gas pressure. If *tgas0=0*, the only use of *gappr0* is for guessing gas pressure for initialization and an accurate value, therefore, is not required. If *tgaso>0*, *gappr0* is a term in the calculation of moles of gas in the fuel rod and an accurate value, then, is required.	N/m^2; psia	
tgas0 (F)	As-fabricated fill gas temperature. If *gsms* is nonzero, leave blank.	K; °F	Default=0.0
fluxz (F)	Option to specify the axial profile of the cladding fast neutron flux. *fluxz(1)*=ratio of fast neutron flux to axially-averaged fast neutron flux at elevation *fluxz(2)*. Continue to enter pairs until fully specified. *fluxz(1)*cfluxa*tflux* = fast neutron fluence at elevation *fluxz(2)*	non-dimensional, m; non-dimensional, ft	
radpel (F)	*radpel*(1) = positive deviation from nominal fuel pellet radius (*pelod*/2) at an elevation of *radpel*(2). Enter the radius deviation versus elevation pairs until the deviation has been specified along the entire length of the rod. *radpel* should account for permanent changes in the fuel pellet radius at 300K (i.e., densification, swelling, fuel outward relocation). The code checks for negative gap thickness values resulting from the use of *radpel* and *eppinp*.	m, m; ft, ft	

Table A.5 (contd)

Design of Fuel Rod Data Block $design			
Variable (Type)	**Definition**	**Units**	**Defaults/ Limitations**
eppinp (F)	*eppinp*(1) = initial cladding permanent hoop strain, relative to *RodDiameter* at an elevation of *eppinp*(2). Enter the cladding permanent hoop strain versus elevation pairs until the hoop strain has been specified along the entire length of the rod. *eppinp* should account for permanent changes in the cladding diameter at 300K (i.e., creepdown).	non-dimensional, m; non-dimensional, ft	

Table A.6 Data Block for Specifying the Power History			
Power Data Block $power			
Variable (Type)	**Definition**	**Units**	**Defaults/Limitations**
RodAvePower (F)	Rod-average linear heat generation rate history. **Required input**. Input pairs of linear heat generation rate and time; continue until power history is fully defined. The coding interpolates between input pairs of data to define the "current" rod-average linear heat rate; this is illustrated in Figure A.2.	kW/m, s; kW/ft, s	Maximum of 50 pairs of power-time. If the "DECAY HEAT OPTION" is specified, *RodAvePower* must not include power due to decay heat. Also exclude gamma energy not deposited in the fuel rod.
NumAxProfiles	Number of axial power profiles.		Default values = 1; maximum of 10 axial profiles
ProfileStartTime	Time when each successive axial power profile begins. First profile begins at time zero.	s	Default value = 0.
AxPowProfile (F)	Axial power profile. One profile required. For each profile input pairs of axial power factor (normalized to rod-average) and elevation, beginning from the bottom of the rod; continue until axial power profile is fully defined.	non-dimensional, m; non-dimensional, ft	A maximum of 25 power factor-elevation pairs can be input for each profile. The first profile begins at *AxPowProfile* (1, 1), the second profile at *AxPowProfile* (1, 2), etc. Input should account for any local variations in power due to enrichment variances, central fuel hole, etc., in addition to axial flux profile.
RadPowProfile (F)	Normalized radial power profiles for each axial node. **Required input**. Input pairs of radial power factor and radius for bottom axial node, from fuel centerline to edge, and then continue for each axial node. Not required to have the same number of pairs to define the radial profile as the number of radial fuel nodes; however, each radial power profile must have the same number of pairs for each axial node. No time dependencies for radial profiles.	non-dimensional, m	*NOTE: Fuel radii values must be input in units of meters (m), even if other input is in British units.* User may enter 25 pairs for 25 axial nodes.
butemp (F)	Radial burnup profiles for each axial node. Optional input. Input pairs of burnup value and radius for bottom axial node, from fuel centerline to edge, and then continue for each axial node. Not required to have the same number of pairs to define the burnup profile as the number of radial fuel nodes; however, each radial burnup profile must have the same number of pairs for each axial node.	MWd/MTM, m	Default value is 0.01 MWd/MTM. NOTE: Fuel radii values must be input in units of meters (m), even if other input is in British units. User may enter 25 pairs for 25 axial nodes.
fpowr (F)	Option to apply a multiplying factor to the input power history (*ptha* data). *fpowr* is a multiplicative constant to be applied tothe power history input. *fpowr* is used to scale the input power history (*ptha* array) for power sensitivity studies.		Default=0.0

Table A.6 (contd)

Power Data Block $power			
Variable (Type)	**Definition**	**Units**	**Defaults/Limitations**
powop (F)	Option to calculate the decay heat by the ANS-5.1 formula and add the decay heat to the power specified by the *ptha* array. *powop* is the axially-averaged fuel rod power prior to accident initiation	kW/m; kW/ft	
timop (F)	Time at which the fuel rod power was equal to *powop*	s	
fpdcay (F)	Multiplicative factor applied to power given by the ANS formula; normally, *fpdcay*=1.		Default=1.0
tpowf (F)	Time at which *fpdcay* is fully applied.	s	Default=0.0
CladPower (F)	Option to specify heating of the cladding by gamma radiation. *CladPower* is the ratio of heat generation per unit volume in the cladding to the spatially averaged heat generation per unit volume in the fuel; normally, *CladPower≈0.01*.		Default=0.0

Table A.7 Data Block for Specifying Modeling Options			
Model Selection Data Block $model			
Variable (Type)	**Definition**	**Units**	**Defaults/Limitations**
internal (A)	Option to specify one or more of the rod internal gas models set by the suboptions listed below. Enter a value of *internal='on'* to turn on.		Default = 'off'
PlenumTemp (I)	Suboption to specify calculation of plenum gas temperature. Default is for plenum gas temperature set equal to local bulk coolant temperature plus 10K. Enter a value of *PlenumTemp=1* to turn on the plenum temperature model described in Section 2.3. Both upper and local plenum gas temperatures are calculated using the selected option.		Default = 0; plenum gas temperature set equal to local bulk coolant temperature plus 10K
gasflo (I)	Suboption to model transient flow of gas between fuel rod plenum and cladding ballooning region. Enter a value of *gasflo=1* to turn on. If the suboption is omitted, the internal gas pressure is assumed to be spatially uniform inside the fuel rod. Normally, this suboption is omitted. For a reactivity initiated accident, the suboption must be omitted.		Default = 0 If this suboption is specified, at least three axial nodes are required.
prescri (I)	Suboption to prescribe the fuel rod internal gas pressure history. Enter a value of *prescri=1* to turn on, and then enter values for *gasphs*		Default = 0
gasphs (F)	Specified rod internal gas pressure history; enter pairs of pressure and time until history is specified.	N/m^2, s; psi, s	A maximum of 10 pressure-time pairs are allowed.
presfgr (I)	Suboption to specify fission gas release history as a function of time during the transient. Enter a value of *presfgr=1* to turn on, and then enter values for *relfrac*.		Default = 0
relfrac (F)	Specified fission gas release history as a function of time during the transient; enter pairs of rod-average fission gas release fraction and time until the desired history is specified. Maximum of 25 fission gas release fraction and time pairs.	fraction, s	must also input a value for "bup" in DESIGN data block
metal (A)	Option to specify a model for metal-water reaction (cladding oxidation). Enter a value of *metal='on'* to turn on. If this option is omitted, metal-water reaction is not modeled (variable *modmw=1*). Normally, this option is specified. If the maximum cladding temperature is not expected to exceed 1800K, the CATHCART suboption should be specified. If there is a possibility of complete oxidation of the cladding, the BAKER-JUST suboption should be specified. the CATHCART model is more accurate for cladding temperature less than 1800K, but the BAKER-JUST model is more accurate for cladding temperatures greater than 1800K. For temperatures less than 1800K, the BAKER-JUST model overpredicts the amount of oxidation.		Default = 'off'

Table A.7 (contd)

Model Selection Data Block $model			
Variable (Type)	**Definition**	**Units**	**Defaults/Limitations**
idoxid (I)	Suboption to specify the initial oxide thickness on the inner surface of the cladding; default value is $3x10^{-6}$ m (3 μm). Enter a value of *idoxid>0* to turn on; *idoxid*= number of axial nodes, and then enter values for *oxideid*		
oxideid (F)	Initial oxide thickness on the inner surface of the cladding. Enter values for each axial node specified in data block SOLUTION CONTROL. Continue entry until values are supplied for all axial nodes.	m	Default value is $3x10^{-6}$ m (3 μm); enter values in m even if other input is in British units.
odoxid (I)	Suboption to specify the initial oxide thickness on the outer surface of the cladding; default value is $3x10^{-6}$ m (3 μm). Enter a value of *odoxid>0* to turn on; *odoxid*= number of axial nodes, and then enter values for *oxideod.*		
oxideod (F)	Initial oxide thickness on the outer surface of the cladding Enter values for each axial node specified in data block SOLUTION CONTROL. Continue entry until values are supplied for all axial nodes.	m	Default value is $3x10^{-6}$ m (3 μm); enter values in m even if other input is in British units
cexh2a (F)	Suboption to specify excess hydrogen concentration in cladding. Enter values for each axial node specified in data block SOLUTION CONTROL. Continue entry until values are supplied for all axial nodes.	ppm	Default=0.0
cathca (I)	Suboption to specify the modeling of the metal-water reaction with the COBILD subroutine and the Cathcart correlation of MATPRO. Enter a value of *cathca=1* to turn on. Normally, this suboption is specified. (Variable *modmw=0*)		
baker (I)	Suboption to specify the modeling of the metal-water reaction with the Baker-Just model. Enter a value of *baker=1* to turn on. (Variable *modmw=2*)		
deformation (A)	Option to specify one or more of the suboptions listed below. *deformation='on'* to set. (default is FRACAS-I with none of the suboptions turned on (*modfd=0, modkf=2*)		Default = 'off'
noball (I)	Suboption (*modfd=0, nbalsw=1*) to specify that the BALON subcode is to be bypassed and cladding failure occurs when the effective cladding plastic strain exceeds the instability strain. Enter a value of *noball=1* to turn off the BALON model. In case of slow heatup of cladding (<1 K/s), cladding may balloon into rod-to-rod contact (hoop strain > 40%) without rupturing. In this case, axial propagation of ballooning may occur. To model this phenomenon, the *noball* suboption must be specified in the Model Selection Data Block and the *bundle* option specified in the Design Data Block.		Default = 0

Table A.7 (contd)

Model Selection Data Block $model			
Variable (Type)	**Definition**	**Units**	**Defaults/Limitations**
TranSwell (I)	Option to specify transient fuel swelling history as a function of time during the transient. Enter a value of *TranSwell=1* to turn on, and then enter values for *FuelGasSwell*		Default = 0
FuelGasSwell (F)	Specified fuel swelling history as a function of time during the transient; enter pairs of relative change in fuel radius (i.e., 1.0 = no change in radius due to transient fuel swelling; 1.01 = 1% increase in radius due to transient fuel swelling) and time until the desired history is specified. Maximum of 25 fuel radii and time pairs.	fraction, s	
difgap (F)	Specify the ratio of the fuel-cladding gap thickness at which axial pellet-cladding mechanical interaction (PCMI) begins to the as-fabricated fuel-cladding gap thickness as a function of axial elevation. Continue as necessary to specify the axial profile. If axial and radial PCMI begin at the same time, then *difgap* equals zero and no input data need to be specified. If *difgap(1)* applies along the entire length of the fuel rod, then only the value for *difgap(1)* is input.	non-dimensional, m; non-dimensional, ft	A maximum of 10 pairs of normalized differential gap versus elevation may be input.
hightem (I)	Suboption for high temperature PCMI; enter a value of *hightem=1* to turn on.		Default = 0
heat (A)	Option to specify a central void in the fuel pellets. Enter a value of *heat='on'* to turn on.		Default = 'off'
cenvoi (I)	Suboption to specify that a portion of the fuel pellets have a central void, such as that required to contain a thermocouple to measure the temperature of the center of the fuel. Enter a value of *cenvoi=1* to turn on.		Default = 0
zvoid1 (F)	Distance from bottom of fuel pellet stack to the bottom of the central void.	m; ft	
zvoid2 (F)	Distance from bottom of fuel stack to the top of the central void.	m; ft	
rvoid (F)	Radius of central void. The radial nodalization as specified in the Solution Control Data Block is automatically adjusted to put the second radial node at the surface of the central void.	m; ft	Default = 0.
inst (A)	If *inst='instrument'*, the central void is assumed to contain an instrument instead of the fuel rod gas. If no instrument in the central void, leave this input blank.		Default = 'off'

Table A.8 Data Block for Specifying Fuel Rod Boundary Conditions			
Boundary Condition Data Block $boundary			
Variable (Type)	**Description/Definition**	**Units**	**Defaults/Limitations**
coolant (A)	Option to specify pressure, mass flux, and enthalpy of coolant. Enter a value of *coolant='on'* to turn on.		Default = 'off'
geomet (I)	Suboption to specify geometry of coolant channel cooling fuel rod. Enter a value of *geomet=1* to turn on, and then enter values for *dhe*, *dhy*, and *achn*		Default = 0
dhe (F)	Heated equivalent diameter of flow channel (4*flow area/heated perimeter). The terms in the calculation of *dhe* are defined in Table A.11.	m; ft	
dhy (F)	Hydraulic diameter of flow channel (4*flow area/wetted perimeter)	m; ft	
achn (F)	Flow cross-sectional area	m^2; ft^2	
tape1 (I)	Suboption to specify that coolant conditions are input on file. Enter a value of *tape1=1* to turn on. The *lower plenum enth*, *pressure*, and *mass flux* suboptions are omitted. The file is read by Fortran logical unit 4 and must contain data in the format given in Appendix G. The *tape input* suboption (option Number 3 of Table A.12) is recommended. Specification of this suboption requires a calculation of the transient fuel rod coolant conditions by a code such as RELAP5. If these calculations cannot be performed, option Number 1of Table A.12 may be used and the coolant enthalpy calculated by FRAPTRAN. The FRAPTRAN calculation of enthalpy is satisfactory for operational transients. But for large and small break LOCAs and RIAs, difficulties in the numerical solution occur. If option Number 1 is specified, the time step should not exceed 0.05s.		Default = 0
nvol1 (I)	Number of coolant zones stacked on top of each other and surrounding fuel rod. The coolant conditions are assumed uniform within each zone.		
nchn (I)	Number of coolant channels in contact with the fuel rod. If coolant conditions are azimuthally uniform, as is normally the case, only one coolant channel borders the fuel rod and the input for *nchn* is omitted.		
lowpl (I)	Suboption to specify the enthalpy history of coolant at bottom of fuel rod (inlet enthalpy). Enter a value of *lowpl>0* to turn on; *lowpl=* number of enthalpy/time pairs. If this suboption is specified, then tables of inlet enthalpy (maximum of 50 enthalpy-time pairs), coolant pressure (maximum of 50 pairs), and mass flux (maximum of 100 pairs) must be input.		Default = 0

Table A.8 (contd)

Boundary Condition Data Block $boundary			
Variable (Type)	**Description/Definition**	**Units**	**Defaults/Limitations**
hinta (F)	Inlet enthalpy and time data pairs. Continue until the inlet enthalpy history is defined for the time range of the problem. (*lowpl* data pairs)	J/kg, s; BTU/lb_m, s	
upppl (I)	Suboption to specify the enthalpy history of coolant at the top of the fuel rod(exit enthalpy). Enter a value of *upppl>0* to turn on; *upppl*=number of enthalpy/time pairs If this suboption is specified, then tables of exit plenum enthalpy (maximum of 50 enthalpy-time pairs), coolant pressure (maximum of 50 pairs), and mass flux (maximum of 100 pairs) must be input		Default = 0
hupta (F)	Exit enthalpy and time data pairs. Continue until the exit enthalpy history is defined for the time range of the problem. (*upppl* data pairs)	J/kg, s; BTU/lb_m, s	
pressu (I)	Suboption to specify the coolant pressure history. Enter a value of *pressu>0* to turn on; *pressu* = number of pressure/time pairs. (Maximum of 50)		Default = 0
pbhl (F)	Coolant pressure and time data pairs. Continue until the coolant pressure history is defined for the time range of the problem. (*pressu* data pairs)	N/m^2, s; psia, s	
massfl (I)	Suboption to specify the coolant mass flux history. Enter a value of *massfl>0* to turn on; *massfl*= number of flux/time pairs. (Maximum for 50)		Default = 0
gbh (F)	Coolant mass flux and time data pairs. Continue as necessary until the mass flux history is defined for the time range of the problem (*massfl* data pairs).	kg/m^2s, s; lb_m/ft^2hr, s	
coreav (I)	Suboption to specify the core average coolant enthalpy history. Enter a value of *coreav>0* to turn on; *coreav* = number of enthalpy/time pairs. The coolant is assumed to have the input enthalpy at all elevations of the fuel rod. This option is normally omitted.		Default = 0
hbh(1) (F)	Core average coolant enthalpy and time data pairs. Continue as necessary until the core average coolant enthalpy history is defined for the time range of the problem. (*coreav* data pairs)	J/kg, s; BTU/lb_m, s	
chf (I)	Suboption to select the critical heat flux (CHF) correlation to be used. Enter a value of *chf=1* to turn on. The correlations are described in Appendix D. If this suboption is omitted, the W-3 correlation is used.		Default = 0

Table A.8 (contd)

Boundary Condition Data Block $boundary			
Variable (Type)	**Description/Definition**	**Units**	**Defaults/Limitations**
jchf (A)	Indicator of CHF correlation to be used. For a PWR, the LOFT or CE-1 correlation is recommended. For a BWR, the GE correlation is recommended. *jchf='b'* selects the B&W-2 correlation. For coolant pressure less than 1300 psia, however, the modified Barnett correlation is used. *jchf='g'* selects the General Electric correlation. *jchf='s'* selects the Savannah River correlation. *jchf='w'* selects a combination of the W-3 Hsu-Beckner and modified Zuber correlations. If the coolant is subcooled, only the W-3 correlation is used. For low coolant flow (<10,000 lb_m/ft^2hr), only the modified Zuber correlation is used. For high coolant flow (>20,000 lb_m/ft^2hr), the modified Zuber correlation is not used. *jchf='c'* selects the Combustion Engineering correlation. *jchf='l'* selects the LOFT correlation. *jchf='r'* selects the RELAP4 MOD7 correlation. *jchf='m'* selects the MacBeth correlation		
filmbo (I)	Suboption to select the film boiling heat transfer correlation to be used. Enter a value of *filmbo=1* to turn on. The correlations are described in Appendix D. If this suboption is omitted, a combination of the Tong-Young and Condie-Bengston heat transfer correlations is used. The Groeneveld correlation is recommended. If the TAPE INPUT suboption is specified, however, it is recommended that the film boiling correlation be the same as that used in the calculations which produced the coolant condition tape.		Default = 0

Table A.8 (contd)

Boundary Condition Data Block $boundary			
Variable (Type)	**Description/Definition**	**Units**	**Defaults/Limitations**
jfb (A)	*jfb* is the indicator of the film boiling correlation to be used *jfb='cl'* selects the cluster geometry form of the Groeneveld correlation. For coolant pressures <500 psia, however, the Dougall-Rohsenow correlation is used. *jfb='an'* selects the open annulus form of the Groeneveld correlation *jfb='do'* selects the Dougall-Rohsenow correlation *jfb='co'* selects the Condie-Bengston correlation *jfb='to'* selects a combination of the Tong-Young and Condie-Bengston correlations. The Tong-Young correlation calculates the transition component and Condie-Bengston the stable component of the film boiling heat transfer coefficient.		
coldwa (I)	Suboption to modify the critical heat flux for cold wall effect. Enter a value of *coldwa=1* to turn on. Normally, this suboption is omitted.		Default = 0
axpow (I)	Suboption to modify the critical heat flux for effect of axially varying power. Enter a value of *axpow=1* to turn on. If flow reversal occurs, the suboption is automatically turned off. If the W-3 critical heat flux correlation is used, this suboption should be omitted.		Default = 0
bowing (I)	Suboption to modify the critical heat flux as calculated according to the *chf* correlation suboption for fuel rod bowing effect. Enter a value of *bowing>0* to turn on; *bowing*= number of axial nodes for bowing. Normally, this suboption is omitted.		Default = 0
ffch (F)	User-supplied multiplier in equation for CHF reduction due to bowing. Equation is described in Section 3 of Appendix D.		
bowthr (F)	Maximum fractional amount of bowing that can occur without any effect on CHF. If even a small amount of bowing affects CHF, set *bowthr=0*. If effect does not occur until rod bows into contact with an adjacent rod, set *bowthr=1*.		

Table A.8 (contd)

Boundary Condition Data Block $boundary			
Variable (Type)	**Description/Definition**	**Units**	**Defaults/Limitations**
ExtentOfBow (F)	Axial array of ratio of deflection due to bowing to maximum possible deflection. The maximum possible deflection is equal to fuel rod spacing minus fuel rod diameter. Enter a value for every axial node.		
spefbz (I)	Suboption to prescribe film boiling over part of fuel rod. Enter a value of *spefbz>0* to turn on; *spefbz*=number of axial nodes for which film boiling is prescribed. For each axial node at which film boiling is prescribed, the number of the axial node and the start and end time of film boiling are specified. This suboption allows film boiling to be prescribed over a portion of the fuel rod. A card must be input for each axial node at which film boiling is prescribed. The suboption name is placed on the first card and then omitted on the cards which specify film boiling at other axial nodes.		Default = 0
nodchf(i) (I)	Axial node at which film boiling is prescribed		
tschf(i) (F)	Start time of film boiling at axial node *nodchf(i)*	s	
techf(i) (F)	End time of film boiling at axial node *nodchf(i)*. Continue on separate cards for each axial node with prescribed film boiling. Because of the high cladding temperature attained during the period of prescribed film boiling, film boiling will usually continue after the prescribed period.	s	
reflood (A)	Option to calculate cladding surface heat transfer coefficient during reactor core reflooding according to the generalized FLECHT correlation. Enter a value of *reflood='on'* to turn on. If this option is specified, the following options must be specified: *time, inlet temperature, reflood rate*, and *pressure*.		Default = 'off'
geometry (I)	Suboption to specify geometry parameters. Enter a value of *geometry=1* to turn on. If this suboption is omitted, the geometry parameters are set by the *geometry* suboption of the *coolant condition* option.		Default = 0
hydiam (F)	Hydraulic diameter of coolant flow channel (4*flow area/wetted perimeter)	m; ft	
flxsec (F)	Cross-sectional area of flow channel	m^2; ft^2	

Table A.8 (contd)

Boundary Condition Data Block $boundary			
Variable (Type)	**Description/Definition**	**Units**	**Defaults/Limitations**
nbundl (I)	Leave blank if wish to use the 15x15 FLECHT correlation. If the FLECHT-SEASET correlation is to be used, input *nbundl = 15* for a 15x15 rod bundle, *nbundl = 17* for a 17x17 rod bundle, and so forth. The FLECHT-SEASET correlation is developed from a larger data base than the 15x15 FLECHT.		
time (I)	Suboption to specify start time of reactor core reflooding. Enter a value of *time=1* to turn on.		
emptm (F)	Time at which reactor core is empty of coolant and adiabatic heatup begins	s	
refdtm (F)	Time at which flooding of reactor core begins *(emptm<rfdtm)*.	s	
radiat (I)	Suboption to specify the radiation heat transfer at the cladding surface during reflood; normally, this option is omitted. Enter a value of *radiat=1* to turn on.		Default = 0
hrad (F)	Radiation heat transfer coefficient. If *hrad<0.*, the radiation heat transfer coefficient is calculated and the input value of *hrad* is ignored.	W/m^2K; BTU/ft^2hrF	
zad (F)	adiabatic heat-up parameter for FLECHT-SEASET		
zs (F)	adiabatic heat-up parameter for FLECHT-SEASET		
fltgap (F)	gap multiplier		
ruptur (I)	Suboption to specify the rupture plane as the line of demarcation between the FLECHT and steam cooling models. Enter a value of *ruptur=1* to turn on. This is the normal suboption. If no cladding rupture has occurred, cooling is calculated according to the FLECHT correlation along the entire length of the fuel rod. If the cladding has ruptured and the flooding rate is >0.4 in./s, the FLECHT correlation is only applied from the bottom of the fuel rod to the elevation of cladding rupture. Above the rupture elevation, cooling is calculated according to the steam cooling model.		Default = 0
liquid (I)	Suboption to specify the collapsed liquid level as the line of demarcation instead of the rupture plane. Enter a value of *liquid=1* to turn on. If this option is specified, the *rupture plane* option is omitted.		Default = 0
inlet (I)	Suboption to specify the inlet temperature of flooding water as a function of time. Enter a value of *inlet>0* to turn on; *inlet*= number of temperature/time pairs.		Default = 0

Table A.8 (contd)

Boundary Condition Data Block $boundary			
Variable (Type)	**Description/Definition**	**Units**	**Defaults/Limitations**
temptm(i) (F)	Inlet temperature of flooding water and time data pairs. The maximum allowed temperature must be at least 16°F cooler than the saturation temperature. Time is specified from the beginning of reflood; *temptm(2)* must equal 0. Continue as necessary to specify reflood history; a maximum of 20 pairs may be entered.	K, s; °F, s	
reflo (I)	Suboption to specify reflood rate as a function of time. Enter a value of *reflo>0* to turn on; *reflo*= number of rate/time pairs.		Default = 0
fldrat (F)	Reflood rate and time data pairs. Time is specifed from the beginning of reflood and *fldrat(2)* must equal 0. Continue as necessary to specify reflood history; a maximum of 100 pairs may be entered.	m/s, s; in./s, s	The minimum allowable reflood rate is 0.4 in./s and the maximum allowable reflood rate is 10 in./s.
pressure (I)	Suboption to specify reactor vessel pressure as a function of time. Enter a value of *pressure>0* to set; *pressure*= number of pressure/time pairs.		Default = 0
prestm (F)	Reactor vessel pressure and time data pairs. Time is specified from the beginning of reflood and *prestm(2)* must equal 0. Continue as necessary to specify reflood history; a maximum of 20 pairs may be entered.	N/m^2, s; psia, s	The maximum allowed pressure is 90 psia.
collaps (I)	Suboption to specify the fraction of flooding water carried out of the core. Enter a value of *collaps>0* to turn on; *collaps*= number of liquid level/time pairs. If this suboption is not specified, the carryover fraction is calculated by a correlation. If this suboption is specified, the collapsed liquid level history must be input. The carryover fraction is then calculated by the equation $f=(R-(Z_2-Z_1)/\Delta T)/R$ where f=carryover fraction, R=reflood rate, Z_1 and Z_2=collapsed liquid level at start and end of time step, respectively, and ΔT=time step, If the FLECHT-SEASET correlation is specified (REFLOOD/GEOMETRY suboption), the field variable specifies the quench elevation history instead of the collapsed liquid level. Alternatively, this suboption may be omitted and the code will calculate the quench elevation history.		Default = 0

Table A.8 (contd)

Boundary Condition Data Block $boundary			
Variable (Type)	**Description/Definition**	**Units**	**Defaults/Limitations**
hlqcl (F)	Collapsed liquid level and time data pairs. Time is specified from the beginning of reflood and *hlqcl(2)* must equal 0. Continue as necessary to specify reflood history. A maximum of 100 pairs may be entered.	m, s; ft, s	
frapt4 (I)	Suboption to specify the FRAP-T4 FLECHT correlation instead of the generalized FLECHT correlation. Enter a value of *frapt4=1* to turn on. Normally, this suboption is omitted.		Default = 0
radiation (A)	Suboption to model heat transfer by radiation from cladding surface to surrounding flow shroud. Enter a value of *radiation='on'* to turn on. If a fuel rod is not surrounded by a flow shroud, omit this option.		Default = 'off'
geom (I)	Suboption to specify the inner radius of the flow shroud. Enter a value of *geom=1* to turn on.		Default = 0
rshrd (F)	Inner radius of flow shroud	m; ft	
temp (I)	Suboption to specify temperature history of flow shroud. Enter a value of *temp>0* to turn on; *temp*=number of temerature/time pairs.		Default = 0
ts (F)	Flow shroud temperature and time data pairs. Continue as necessary to specify flow shroud temperature history.	K, s; °F, s	
heat (A)	Option to specify the heat transfer coefficient at the cladding outer surface. Enter a value of *heat='on'* to turn on. If this option is specified, the COOLANT CONDITION option and all of its suboptions are omitted.		Default = 'off'
tape 2 (I)	Suboption to specify that the heat transfer coefficients, coolant temperature, and pressure are input on tape. Enter a value of *tape2=1* to specify. All of the other suboptions are omitted. The tape is read by Fortran logical unit 4 and must contain data in the format given in Appendix G.		
nvol2 (I)	Number of heat transfer coefficient zones stacked on top of each other. The heat transfer coefficient, coolant temperature, and pressure are assumed uniform within each zone.		Default = 0
fltgap2 (F)	gap multiplier		
press (I)	Suboption to specify coolant pressure. Enter a value of *press>0* to turn on; *press*= number of pressure/time pairs.		Default = 0
pbh2(i) (F)	Coolant pressure and time data pairs. Continue as necessary to specify coolant pressure history.	N/m^2, s; psia, s	

Table A.8 (contd)

Boundary Condition Data Block $boundary			
Variable (Type)	**Description/Definition**	**Units**	**Defaults/Limitations**
zone (I)	Suboption to specify the top elevation of heat transfer coefficient zone 1. Enter a value of *zone>0* to turn on; *zone*= number of heat transfer coefficient zones. The maximum number of heat transfer coefficient zones is 10. The maximum number of pairs of heat transfer coefficient versus time data, or temperature versus time data, is 25.		Default = 0
htclev (F)	Array of top elevations of heat transfer coefficient zones.	m, ft	
htco (I)	Suboption to specify heat transfer coefficient history for zones. Enter a value of *htco>0* to turn on; *htco*=number of heat transfer coefficient/time pairs.		Default = 0
htca (F)	Heat transfer coefficient and time data pairs for zones. Continue as necessary to specify heat transfer coefficient history for zones. Specify history for first zone before continuing for subsequent zones.	W/m^2K, s; BTU/ft^2hrF, s	
tem (I)	Suboption to specify coolant temperature history for zone 1. Enter a value of *tem>0* to turn on; *tem*=number of temperature/time pairs.		Default = 0
tblka (F)	Coolant temperature and time data pairs. Continue as necessary to specify coolant temperature history for zones; specify history for first zone before continuing for subsequent zones. The input temperature must be the coolant sink temperature. For subcooled or super-heated forced convection heat transfer, the actual coolant temperature is input. But for boiling heat transfer, the coolant saturation temperature is input.	K, s; °F, s	

Table A.9 Data Block for Specifying Tuning Parameters			
Numerical Tuning Data Block $tuning			
Variable	**Description/Definition**	**Units**	**Limitations**
fhgap (F)	Array of multiplication factors for gap conductance at axial nodes. For this option the number of axial nodes (*naxn*) must be ≤20. Continue input as necessary.		
ffcon (F)	Additive term for fuel thermal conductivity.	W/mK	
fhfb1 (F)	Multiplicative factor for transition flow film boiling heat transfer coefficient		
fhfb2 (F)	Multiplicative factor for stable flow film boiling heat transfer coefficient		
fhfb3 (F)	Multiplicative factor for pool film boiling heat transfer coefficient		
fhfb4 (F)	Multiplicative factor for free convection heat transfer coefficient		
naxhtc (I)	Axial node at which surface heat transfer is to be modified to account for ballooning of neighboring fuel rods		
tshtc (F)	Time at which modification is to start.	s	
fhtc (F)	Array of multiplicative factors and time data pairs for cladding surface heat transfer coefficients.	Non-dimensional, s	
fchf (F)	Multiplicative factor for critical heat flux correlation		

Table A.10 Recommended Time Step Sizes for Various Transients		
Transient/Accident	**Period of Transient/Accident**	**Time Step, s**
Steady-state equilibration		>40
Large Break Loss of Coolant	Blowdown	0.2
	Reflood	0.5
Small Break Loss of Coolant	Prior to Scram	0.2
	~Adiabatic Heatup	2.0
	Quenching	0.5
Reactivity Initiated Accident	During Power Pulse	1.0e-5
Anticipated Transient with Scram	all	0.2

Table A.11 Definition of Coolant Channel Geometry Terms
Case 1: Fuel rod in middle of cluster of fuel rods
$A_f = S^2 - \pi d_r^2/4$
$P_h = \pi d_r$
$P_w = \pi d_r$
Case 2: Single fuel rod surrounded by unheated flow shroud
$A_f = \pi d_s^2/4 - \pi d_r^2/4$
$P_h = \pi d_r$
$P_w = \pi d_s + \pi d_r$
Definitions:
A_f = flow area of coolant channel
S = fuel rod spacing (pitch)
d_r = fuel rod outer diameter
d_s = shroud inner diameter
P_h = heater perimeter
P_w = wetted perimeter

Table A.12 Summary of Coolant Condition Input Options

Option Number	Option Name	Suboption Names	Input	Data Input
1	Coolant Condition	Geometry Lower Plenum Enthalpy Pressure Mass Flux	data file	D_e, D_h, A, $h_{in}(t)$, G(t), P(t)
2	Coolant Condition	Geometry Lower Plenum Enthalpy Core Average Enthalpy Pressure Mass Flux	data file	D_e, D_h, A, $h_{in}(t)$, h(t), G(t), P(t)
3	Coolant Condition	Geometry file input	input file	D_e, D_h, A, h(z,t), G(z,t), P(z,t)
4	Heat Transfer Coefficient	Pressure Zone Heat Transfer Coefficient Temperature	data file	P(t), $h_c(z,t)$, T(z,t)
5	Heat Transfer Coefficient	file input	input file	P(z,t), $h_c(z,t)$, T(z,t)

Symbol Definition: D_e = equivalent heat diameter of flow channel; D_h = hydraulic diameter; A = flow area; h = enthalpy; h_{in} = inlet enthalpy; G = mass flux; P = pressure; h_c = heat transfer coefficient; T= temperature; z = elevation; t = time

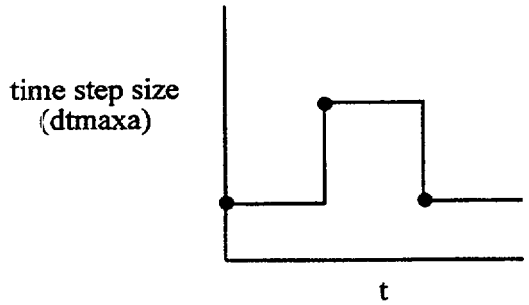

a) Illustration of how "dtmaxa" array is interpreted by FRAPTRAN - circles indicate input time step history

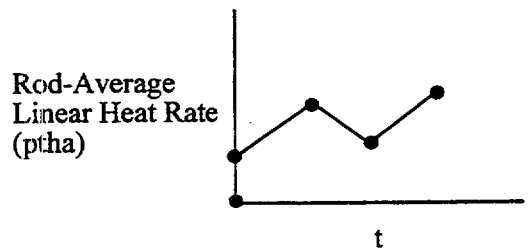

b) Illustration of how "ptha" array is interpreted by FRAPTRAN - circles indicate input rod-average linear heat rate history

Figure A.2 Illustration of How Time Step Size and Power History are Interpreted by FRAPTRAN

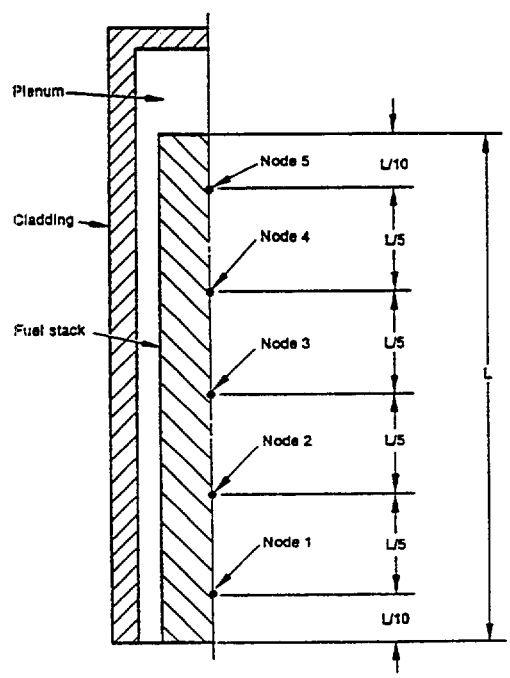

Figure A.3 Illustration of Node Location for Five Evenly Spaced Axial Nodes

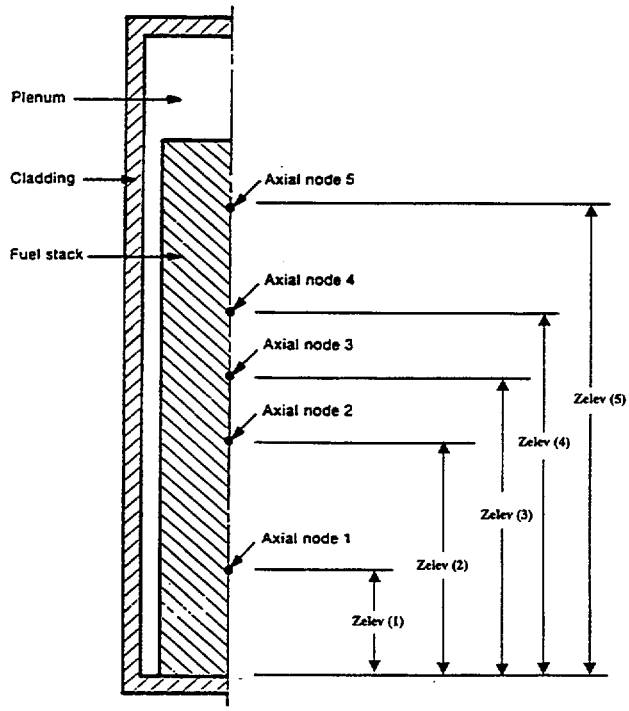

Figure A.4 Illustration of Node Location for Five Unevenly Spaced Axial Nodes

APPENDIX B

EXAMPLE PROBLEM

APPENDIX B

EXAMPLE PROBLEM

Provided in this appendix is an example of the output resulting from a FRAPTRAN run. The example problem is the same presented in Table A.1 to illustrate a FRAPTRAN input file. Portions of the output file from running this case are provided as Figure B.1.

This example problem was developed for FRAP-T5 and FRAP-T6 to analyze the behavior of the hot fuel rod in a pressurized-water reactor after a loss-of-coolant accident. This case assumes a beginning-of-life rod so that FRAPCON-3 initialization of burnup-dependent variables is not used. The power history during the case simulates a scram from operating conditions, with a concurrent decrease in coolant pressure. The basic design parameters of the assumed fuel rod are provided in Table B.1.

Table B.1. Basic Fuel Rod Design Parameters for Example Problem

Design Parameter	SI Units	British Units
Cladding OD	0.0107 m	0.03517 ft
Fuel-Cladding Gap Thickness	9.91e-5 m	3.25e-4 ft
Fuel Pelled OD	0.0093 m	0.0305 m
Fuel Pellet Density	93.2 %TD	93.2 %TD
Fuel Column Length	3.66 m	12 ft
Fill Gas Pressure	15.5 MPa	2243 psia
Fill Gas Composition	100% He	100% He

Provided in Figure B.1 is a listing of the beginning of the output file generated by running the input file provided in Figure A.1. The output file is formatted to fit a continuous paper printer with 14-inch wide paper. In Figure B.1, the file is printed in an 8-pt Courier New font so that the output will fit on an 8½x11 paper in landscape orientation. Comments describing the output file have been inserted into the output in a 12-point Arial font, with the comments within brackets, so that they can be distinguished from the FRAPTRAN-generated output.

This problem was used as part of the assessment of the FRAPTRAN code. A description of the problem and the calculated results may be found in NUREG/CR-6739, Vol. 2, *FRAPTRAN: Integral Assessment.*

```
FFFFFFFFFF  RRRRRRRRR      AAAA     PPPPPPPPP   TTTTTTTTTT  RRRRRRRRR     AAAA      NNN     NN
FFFFFFFFFF  RRRRRRRRRR    AAAAAA    PPPPPPPPPP  TTTTTTTTTT  RRRRRRRRRR   AAAAAA     NNN     NN
FF          RR      RR   AA    AA   PP      PP      TT      RR      RR   AA    AA   NNNN    NN
FF          RR      RR  AA      AA  PP      PP      TT      RR      RR  AA      AA  NN NN   NN
FFFFFFFFFF  RRRRRRRRRR  AAAAAAAAAA  PPPPPPPPPP      TT      RRRRRRRRRR  AAAAAAAAAA  NN  NN  NN
FFFFFFFFFF  RRRRRRRRR   AAAAAAAAAA  PPPPPPPPP       TT      RRRRRRRRR   AAAAAAAAAA  NN   NN NN
FF          RR   RR     AA      AA  PP              TT      RR   RR     AA      AA  NN    NNNN
FF          RR    RR    AA      AA  PP              TT      RR    RR    AA      AA  NN     NNN
FF          RR     RR   AA      AA  PP              TT      RR     RR   AA      AA  NN     NNN
FF          RR      RR  AA      AA  PP              TT      RR      RR  AA      AA  NN     NNN
```

```
                        run on: Wed Jun 20, 2001  time: 13:55:27
FrapTran, transient fuel rod analysis code
   current date: Wed Jun 20, 2001  time: 13:55:27
   unit:  55  input file: formin
```

[Repeat back of some of the input file]

```
*********************************************************************
* FrapTran, transient fuel rod analysis code                        *
*-------------------------------------------------------------------*
*                                                                   *
*  CASE DESCRIPTION: Standard Problem #1                            *
*                                                                   *
*  UNIT   FILE DESCRIPTION                                          *
*  ----   ---------------------------------------------             *
*   --    Input:                                                    *
*   15      Water properties data                                   *
*                                                                   *
*   --    Output:                                                   *
*    6      STANDARD PRINTER OUTPUT                                 *
*   66      STRIPF FILE FOR GRAFITI                                 *
*                                                                   *
*   --    Scratch:                                                  *
*    5      SCRATCH INPUT FILE FROM ECHO1                           *
*                                                                   *
* Input: FrapTran INPUT FILE                                        *
*                                                                   *
*********************************************************************
*
* GOESINS:
FILE05='nullfile', STATUS='scratch', FORM='FORMATTED',
        CARRIAGE CONTROL='LIST'
# fortran unit  5 opened
#    file name: nullfile
#    status   : scratch           form     : FORMATTED
#    access   : SEQUENTIAL        carriage : LIST
FILE15='sth2xt',  STATUS='old', FORM='UNFORMATTED'
# fortran unit 15 opened
#    file name: sth2xt
```

Figure B.1 Example of FRAPTRAN Output File

```
#    status   : old              form     : UNFORMATTED
#    access   : SEQUENTIAL       carriage : NONE
*
* GOESOUTS:
FILE06='std.prob1.out',   STATUS='UNKNOWN', CARRIAGE CONTROL='LIST'
# fortran unit  6 opened
#    file name: std.prob1.out
#    status   : UNKNOWN          form     : FORMATTED
#    access   : SEQUENTIAL       carriage : LIST
FILE66='stripf.stdprb1', STATUS='UNKNOWN', FORM='FORMATTED',
        CARRIAGE CONTROL='LIST'
# fortran unit 66 opened
#    file name: stripf.stdprb1
#    status   : UNKNOWN          form     : FORMATTED
#    access   : SEQUENTIAL       carriage : LIST
/*********************************************************************
# end of file processing
FrapTran Version May 1a  2001;  Fuel Rod Analysis Program - Transient; Pacific Northwest National Laboratory


*** start time = 0.00000E+00 s   , end time = 0.20000E+02 s  ***
```

[Listing of the formatted input file generated from the Namelist input file.]

```
*** FrapTran execution started. this run begins from scratch. input cards to be read. ***
                1         2         3         4         5         6         7         8
        12345678901234567890123456789012345678901234567890123456789012345678901234567890

        /iodata block
        input
        end
        output
                            si
                            pr                  .5000E+00 .0000E+00
                            pl                  .2500E+00
                            po
        end
        end block
        /solution control data block
        property tables
                            fu                    100     .6233E+02 .5840E+04
                            cl                     50     .6233E+02 .4040E+04
        end
        time control
                            ti                  .1000E+00 .0000E+00 .1000E-02 .4900E+01
                                                .1000E-01 .5000E+01 .1000E-01 .2000E+02
        end
        convergence
                            im                  .1000E-02 .1000E-02
                            te                    100       100     .1000E+01
        end
```

Figure B.1 (contd)

```
nodalization
                    ax                  .5000E+00 .1500E+01 .2500E+01 .3500E+01
                                        .4250E+01 .4750E+01 .5250E+01 .5750E+01
                                        .6250E+01 .6750E+01 .7250E+01 .7750E+01
                                        .8500E+01 .9500E+01 .1050E+02 .1150E+02
                    fu                     11
                    cl                      2
end
end block
/design
bu                                                  .2890E+03
fu                  .1200E+02 .3517E-01
pe                  .1008E-01 .6250E-03 .2510E-01 .2000E-06 .3050E-01 .1140E+01
                    .9325E+00 .0000E+00 .0000E+00 .2000E+01 .1883E+04 .1000E+02
                    .0000E+00 .0000E+00
cl                  .3250E-03 .1000E+00 .2160E+01 .0000E+00 .0000E+00 .4000E-01
up                     22     .4583E+00 .2910E-01 .6333E-02 .3800E-03
ga                  .1000E+01 .0000E+00 .0000E+00 .0000E+00 .0000E+00 .0000E+00
                    .0000E+00 .3000E-01 .2243E+04
end
end block
/power specification
po                  .1108E+02 .0000E+00 .3695E+01 .6000E+00 .2010E+01 .2300E+01
                    .1413E+01 .8700E+01 .8150E+00 .1000E+02 .1902E+01 .1300E+02
                    .5430E+00 .1630E+02 .4020E+00 .4500E+02
ax                  .5600E+00 .5450E+00 .1170E+01 .1633E+01 .1460E+01 .2700E+01
                    .1610E+01 .3812E+01 .1580E+01 .4900E+01 .1480E+01 .5992E+01
        1         2         3         4         5         6         7         8
12345678901234567890123456789012345678901234567890123456789012345678901234567890
        1         2         3         4         5         6         7         8
12345678901234567890123456789012345678901234567890123456789012345678901234567890

                    .1340E+01 .7075E+01 .1150E+01 .8158E+01 .9400E+00 .9250E+01
                    .7000E+00 .1030E+02 .3600E+00 .1139E+02
ra                  .9820E+00 .0000E+00 .9830E+00 .2288E-02 .9840E+00 .3812E-02
                    .9850E+00 .5338E-02 .9880E+00 .6862E-02 .9910E+00 .8388E-02
                    .9960E+00 .9912E-02 .1002E+01 .1144E-01 .1009E+01 .1296E-01
                    .1017E+01 .1449E-01 .1030E+01 .1525E-01

end block
/model
internal
metal-water reaction
                    ca
deformation
end block
/boundary
heat transfer coef
                    pre                 .2273E+04 .0000E+00
                                        .1561E+04 .5100E+00
```

Figure B.1 (contd)

```
                                .1405E+04 .1010E+01
                                .1198E+04 .2150E+01
                                .1166E+04 .2750E+01
                                .9400E+03 .6950E+01
                                .9080E+03 .7550E+01
                                .8560E+03 .8150E+01
                                .6860E+03 .9870E+01
                                .5680E+03 .1107E+02
                                .2060E+03 .1587E+02
                                .5000E+02 .2007E+02
                    zo          .3000E+01
                    hea         .5160E+05 .0000E+00
                                .1660E+03 .5100E+00
                                .3600E+02 .1010E+01
                                .2810E+02 .2150E+01
                                .1200E+03 .2750E+01
                                .1000E+03 .6950E+01
                                .5200E+02 .7550E+01
                                .5000E+01 .8150E+01
                                .5000E+01 .9870E+01
                                .1600E+03 .1107E+02
                                .6000E+02 .1587E+02
                                .5000E+02 .2007E+02
                    tem         .6383E+03 .0000E+00
                                .6015E+03 .5100E+00
                                .5875E+03 .1010E+01
                                .7438E+03 .2150E+01
                                .5635E+03 .2750E+01
                                .5372E+03 .6950E+01
                                .5331E+03 .7550E+01
                                .5532E+03 .8150E+01
                                .1334E+04 .9870E+01
         1         2         3         4         5         6         7         8
12345678901234567890123456789012345678901234567890123456789012345678901234567890
         1         2         3         4         5         6         7         8
12345678901234567890123456789012345678901234567890123456789012345678901234567890

                                .5310E+03 .1107E+02
                                .3842E+03 .1587E+02
                                .8932E+03 .2007E+02
                    zo          .9000E+01
                    hea         .6230E+05 .0000E+00
                                .1580E+03 .5100E+00
                                .3600E+02 .1010E+01
                                .2810E+03 .2150E+01
                                .1160E+03 .2750E+01
                                .1000E+03 .6950E+01
                                .5200E+02 .7550E+01
                                .5000E+01 .8150E+01
                                .5000E+01 .9870E+01
                                .1600E+03 .1107E+02
```

Figure B.1 (contd)

```
                                        .6000E+02 .1587E+02
                                        .5000E+02 .2007E+02
                        tem             .6383E+03 .0000E+00
                                        .6015E+03 .5100E+00
                                        .5875E+03 .1010E+01
                                        .7438E+03 .2150E+01
                                        .5635E+03 .2750E+01
                                        .5372E+03 .6950E+01
                                        .5331E+03 .7550E+01
                                        .5532E+03 .8150E+01
                                        .1334E+04 .9870E+01
                                        .5310E+03 .1107E+02
                                        .3842E+03 .1587E+02
                                        .8932E+03 .2007E+02
                        zo              .1200E+02
                        hea             .3930E+05 .0000E+00
                                        .2500E+03 .5100E+00
                                        .4000E+02 .1010E+01
                                        .2810E+03 .2150E+01
                                        .1280E+03 .2750E+01
                                        .1100E+03 .6950E+01
                                        .5200E+02 .7550E+01
                                        .5000E+01 .8150E+01
                                        .5000E+01 .9870E+01
                                        .1600E+03 .1107E+02
                                        .6000E+02 .1587E+02
                                        .5000E+02 .2007E+02
                        tem             .6383E+03 .0000E+00
                                        .6015E+03 .5100E+00
                                        .5875E+03 .1010E+01
                                        .7438E+03 .2150E+01
                                        .5635E+03 .2750E+01
                                        .5372E+03 .6950E+01
                                        .5331E+03 .7550E+01
                                        .5532E+03 .8150E+01
                                        .1334E+04 .9870E+01
                1         2         3         4         5         6         7         8
        12345678901234567890123456789012345678901234567890123456789012345678901234567890
                1         2         3         4         5         6         7         8
        12345678901234567890123456789012345678901234567890123456789012345678901234567890

                                        .5310E+03 .1107E+02
                                        .3842E+03 .1587E+02
                                        .8932E+03 .2007E+02
        end block
        /tuning
        end block
                1         2         3         4         5         6         7         8
        12345678901234567890123456789012345678901234567890123456789012345678901234567890
    156 input cards
```

Figure B.1 (contd)

[Descriptive summary of the input.]
[Summary of input/output control.]

```
                                    input/output option selection block

        input options selected
            British units

        output options selected
            output in SI units

            print interval is constant at     0.5000 seconds
            plot output file requested
            power ramp print out requested

input/output block input completed
```

[Summary of solution control input.]

```
                                    solution control definition input block
        time control options selected

             time dependent time step
               no. of pairs      time          time          time          time          time
                              increment                   increment                   increment
                    4            (s)           (s)           (s)           (s)           (s)
                              0.1000E+00    0.0000E+00    0.1000E-02    0.4900E+01    0.1000E-01    0.5000E+01

                              0.1000E-01    0.2000E+02
        convergence control options selected
           implicit calculations selected with
             a minimum fractional difference in rod pressure of    0.1000E-02
             a minimum fractional difference in temperature of     0.1000E-02
            maximum number of iterations for steady state solution is  100
            maximum number of iterations on material properties is     100
            convergence criteria for temperature subcode is    0.1000E+01(F)
        nodalization options selected
            specified axial nodes

                 node       elevation   node       elevation   node       elevation
                              (ft)                   (ft)                   (ft)
                   1       0.5000E+00     2       0.1500E+01     3       0.2500E+01
                   4       0.3500E+01     5       0.4250E+01     6       0.4750E+01
                   7       0.5250E+01     8       0.5750E+01     9       0.6250E+01
                  10       0.6750E+01    11       0.7250E+01    12       0.7750E+01
                  13       0.8500E+01    14       0.9500E+01    15       0.1050E+02
                  16       0.1150E+02
```

Figure B.1 (contd)

```
     11 equal area radial nodes in fuel selected
      2 evenly spaced radial nodes in cladding selected

solution control block input completed
```

[Summary of fuel rod design input.]

```
                                        design of fuel rod input block

bundle data
     pitch                                          =     0.0000(ft)
     pitch to diameter ratio                        =     1.3200
     ratio of balloonable to cells to total cells =     1.0000
     total number of cells in a bundle              =       289.

fuel rod data
     fuel stack cold length            =    12.0000(ft)
     rod fabrication temperature       =     80.3(F)
     cold fuel rod outer diameter      = 0.35170E-01(ft)

pellet data
     cold state radius to pellet shoulder   = 0.10080E-01(ft)
     cold state pellet dish depth           = 0.62500E-03(ft)
     cold state pellet height               = 0.25100E-01(ft)
     cold state pellet dish volume          = 0.20000E-06(ft**3)
     pellet outer diameter                  = 0.30500E-01(ft)
     pellet surface roughness               = 0.11400E+01(microns)
     pellet fraction of theoretical density =   0.932500
     fuel burnup                            =     0.0000E+00(MWs/kg)
     puo2 weight fraction                   =     0.0000
     fuel open porosity fraction            =     0.0000
     fuel sintering temperature             =     1883.0(K)
     fuel grain size                        =    10.0000(microns)
     weight fraction of Gd2O3               =     0.0000
     ratio of fuel oxygen atoms to uranium and plutonium atoms =     2.0000

cladding data
     axially and time averaged fast flux for lifetime =   0.0000E+00(nt/m**2-s)
     time span of fast flux exposure =     0.0000E+00(s)
     gas gap radial thickness        =     0.32500E-03(ft)
     strength cold work              =     0.1000
     ductility cold work             =     0.0400
     inner surface roughness         =     2.1600(microns)
     cladding thickness              =     0.20100E-02(ft)

upper plenum data
     number of coils in spring  =   22
     uncompressed spring height =   0.4583E+00(ft)
     uncompressed coil diameter =   0.2910E-01(ft)
     spring wire diameter       =   0.6333E-02(ft)
     total plenum volume        =   0.3800E-03(ft**3)
```

Figure B.1 (contd)

```
gas composition data
     fraction of helium          =   0.1000E+01
     fraction of argon           =   0.0000E+00
     fraction of krypton         =   0.0000E+00
     fraction of xenon           =   0.0000E+00
     fraction of hydrogen        =   0.0000E+00
     fraction of air             =   0.0000E+00
     fraction of water vapor     =   0.0000E+00
     amount of gas in rod    =    0.3000E-01(g-moles)
     cold state gas pressure estimate =   0.2243E+04(psia)

design of fuel rod block input completed
```

[Summary of power history input.]

power input block

power time history

no.of pairs	linear power (kW/ft)	time (sec)	linear power (kW/ft)	time (sec)	linear power (kW/ft)	time (sec)	linear power (kW/ft)	time (sec)
8	1.1080E+01	0.0000E+00	3.6950E+00	6.0000E-01	2.0100E+00	2.3000E+00	1.4130E+00	8.7000E+00
	8.1500E-01	1.0000E+01	1.9020E+00	1.3000E+01	5.4300E-01	1.6300E+01	4.0200E-01	4.5000E+01

axial power profile number 1

no. of pairs	axial power ratio	axial distance (ft)	axial power ratio	axial distance (ft)	axial power ratio	axial distance (ft)	axial power ratio	axial distance (ft)
11	5.6000E-01	5.4500E-01	1.1700E+00	1.6330E+00	1.4600E+00	2.7000E+00	1.6100E+00	3.8120E+00
	1.5800E+00	4.9000E+00	1.4800E+00	5.9920E+00	1.3400E+00	7.0750E+00	1.1500E+00	8.1580E+00
	9.4000E-01	9.2500E+00	7.0000E-01	1.0300E+01	3.6000E-01	1.1390E+01		

Relative radial power profiles in fuel for each axial node

```
   0.9820    0.9820    0.9820    0.9820    0.9820    0.9820    0.9820    0.9820    0.9820    0.9820    0.9820    0.9820    0.9820
0.9820    0.9820    0.9820
   0.9830    0.9830    0.9830    0.9830    0.9830    0.9830    0.9830    0.9830    0.9830    0.9830    0.9830    0.9830    0.9830
0.9830    0.9830    0.9830
   0.9840    0.9840    0.9840    0.9840    0.9840    0.9840    0.9840    0.9840    0.9840    0.9840    0.9840    0.9840    0.9840
0.9840    0.9840    0.9840
   0.9850    0.9850    0.9850    0.9850    0.9850    0.9850    0.9850    0.9850    0.9850    0.9850    0.9850    0.9850    0.9850
0.9850    0.9850    0.9850
   0.9880    0.9880    0.9880    0.9880    0.9880    0.9880    0.9880    0.9880    0.9880    0.9880    0.9880    0.9880    0.9880
0.9880    0.9880    0.9880
   0.9910    0.9910    0.9910    0.9910    0.9910    0.9910    0.9910    0.9910    0.9910    0.9910    0.9910    0.9910    0.9910
0.9910    0.9910    0.9910
   0.9960    0.9960    0.9960    0.9960    0.9960    0.9960    0.9960    0.9960    0.9960    0.9960    0.9960    0.9960    0.9960
0.9960    0.9960    0.9960
   1.0020    1.0020    1.0020    1.0020    1.0020    1.0020    1.0020    1.0020    1.0020    1.0020    1.0020    1.0020    1.0020
1.0020    1.0020    1.0020
```

Figure B.1 (contd)

```
   1.0090    1.0090    1.0090    1.0090    1.0090    1.0090    1.0090    1.0090    1.0090    1.0090    1.0090    1.0090    1.0090
1.0090    1.0090    1.0090
   1.0170    1.0170    1.0170    1.0170    1.0170    1.0170    1.0170    1.0170    1.0170    1.0170    1.0170    1.0170    1.0170
1.0170    1.0170    1.0170
   1.0300    1.0300    1.0300    1.0300    1.0300    1.0300    1.0300    1.0300    1.0300    1.0300    1.0300    1.0300    1.0300
1.0300    1.0300    1.0300

power definition block input completed
```

[Summary of model selection input.]

```
                                        model selection input block

deformation options selected
    Fracas-1 with 0.25 percent of the fuel radius for relocation


internal gas pressure model with
     gas temperature set at coolant temperature + 10

Metal Water Reaction Model
     Initial values of cladding inside surface oxide thickness (m)
       0.30E-05  0.30E-05  0.30E-05  0.30E-05  0.30E-05  0.30E-05  0.30E-05  0.30E-05  0.30E-05  0.30E-05
       0.30E-05  0.30E-05  0.30E-05  0.30E-05  0.30E-05  0.30E-05
     Initial values of cladding outside surface oxide thickness (m)
       0.30E-05  0.30E-05  0.30E-05  0.30E-05  0.30E-05  0.30E-05  0.30E-05  0.30E-05  0.30E-05  0.30E-05
       0.30E-05  0.30E-05  0.30E-05  0.30E-05  0.30E-05  0.30E-05
     Initial values of cladding excess H2 (ppm)
       0.00E+00  0.00E+00  0.00E+00  0.00E+00  0.00E+00  0.00E+00  0.00E+00  0.00E+00  0.00E+00  0.00E+00
       0.00E+00  0.00E+00  0.00E+00  0.00E+00  0.00E+00
     Initial values of cladding excess H2 (ppm)
       0.00E+00
     metal water reaction modeled using Cathcart model


model selection block input completed
```

[Summary of boundary condition (coolant history) input.]

```
                                boundary condition input block
heat transfer coefficient specification input
     heat transfer coefficient history for zone   1 with top boundary elevation of  0.300000E+01(ft)
     no. of pairs        htc          time          htc          time          htc          time
                   (btu/hr-ft**2-F) (s)       (btu/hr-ft**2-F) (s)       (btu/hr-ft**2-F) (s)
          12       5.1600E+04   0.0000E+00   1.6600E+02   5.1000E-01   3.6000E+01   1.0100E+00
                   2.8100E+01   2.1500E+00   1.2000E+02   2.7500E+00   1.0000E+02   6.9500E+00
                   5.2000E+01   7.5500E+00   5.0000E+00   8.1500E+00   5.0000E+00   9.8700E+00
                   1.6000E+02   1.1070E+01   6.0000E+01   1.5870E+01   5.0000E+01   2.0070E+01
```

Figure B.1 (contd)

heat transfer coefficient history for zone 2 with top boundary elevation of 0.900000E+01(ft)

no. of pairs	htc (btu/hr-ft**2-F)	time (s)	htc (btu/hr-ft**2-F)	time (s)	htc (btu/hr-ft**2-F)	time (s)
12	6.2300E+04	0.0000E+00	1.5800E+02	5.1000E-01	3.6000E+01	1.0100E+00
	2.8100E+02	2.1500E+00	1.1600E+02	2.7500E+00	1.0000E+02	6.9500E+00
	5.2000E+01	7.5500E+00	5.0000E+00	8.1500E+00	5.0000E+00	9.8700E+00
	1.6000E+02	1.1070E+01	6.0000E+01	1.5870E+01	5.0000E+01	2.0070E+01

heat transfer coefficient history for zone 3 with top boundary elevation of 0.120000E+02(ft)

no. of pairs	htc (btu/hr-ft**2-F)	time (s)	htc (btu/hr-ft**2-F)	time (s)	htc (btu/hr-ft**2-F)	time (s)
12	3.9300E+04	0.0000E+00	2.5000E+02	5.1000E-01	4.0000E+01	1.0100E+00
	2.8100E+02	2.1500E+00	1.2800E+02	2.7500E+00	1.1000E+02	6.9500E+00
	5.2000E+01	7.5500E+00	5.0000E+00	8.1500E+00	5.0000E+00	9.8700E+00
	1.6000E+02	1.1070E+01	6.0000E+01	1.5870E+01	5.0000E+01	2.0070E+01

bulk temperature history for zone 1 with top boundary elevation of 0.300000E+01(ft)

no. of pairs	temperature (F)	time (s)	temperature (F)	time (s)	temperature (F)	time (s)
12	6.3830E+02	0.0000E+00	6.0150E+02	5.1000E-01	5.8750E+02	1.0100E+00
	7.4380E+02	2.1500E+00	5.6350E+02	2.7500E+00	5.3720E+02	6.9500E+00
	5.3310E+02	7.5500E+00	5.5320E+02	8.1500E+00	1.3340E+03	9.8700E+00
	5.3100E+02	1.1070E+01	3.8420E+02	1.5870E+01	8.9320E+02	2.0070E+01

bulk temperature history for zone 2 with top boundary elevation of 0.900000E+01(ft)

no. of pairs	temperature (F)	time (s)	temperature (F)	time (s)	temperature (F)	time (s)
12	6.3830E+02	0.0000E+00	6.0150E+02	5.1000E-01	5.8750E+02	1.0100E+00
	7.4380E+02	2.1500E+00	5.6350E+02	2.7500E+00	5.3720E+02	6.9500E+00
	5.3310E+02	7.5500E+00	5.5320E+02	8.1500E+00	1.3340E+03	9.8700E+00
	5.3100E+02	1.1070E+01	3.8420E+02	1.5870E+01	8.9320E+02	2.0070E+01

bulk temperature history for zone 3 with top boundary elevation of 0.120000E+02(ft)

no. of pairs	temperature (F)	time (s)	temperature (F)	time (s)	temperature (F)	time (s)
12	6.3830E+02	0.0000E+00	6.0150E+02	5.1000E-01	5.8750E+02	1.0100E+00
	7.4380E+02	2.1500E+00	5.6350E+02	2.7500E+00	5.3720E+02	6.9500E+00
	5.3310E+02	7.5500E+00	5.5320E+02	8.1500E+00	1.3340E+03	9.8700E+00
	5.3100E+02	1.1070E+01	3.8420E+02	1.5870E+01	8.9320E+02	2.0070E+01

average core pressure history is:

no. of pairs	pressure (psia)	time (s)	pressure (psia)	time (s)	pressure (psia)	time (s)
12	2.2730E+03	0.0000E+00	1.5610E+03	5.1000E-01	1.4050E+03	1.0100E+00
	1.1980E+03	2.1500E+00	1.1660E+03	2.7500E+00	9.4000E+02	6.9500E+00
	9.0800E+02	7.5500E+00	8.5600E+02	8.1500E+00	6.8600E+02	9.8700E+00
	5.6800E+02	1.1070E+01	2.0600E+02	1.5870E+01	5.0000E+01	2.0070E+01

boundary condition block input completed

Figure B.1 (contd)

[Summary of tuning factor input.]

```
                                                factor selection block
 gap conductance multiplication factors not input
 fuel thermal conductivity addition factor not input
 transition film boiling multiplication factor not input
 stable flow film boiling htc multiplication factor not input
 pool film boiling  htc multiplication factor not input
 heat transfer multiplier and time history not input

 numerical tuning block input completed
```

[Other input and initialization summary information.]

```
                                                      default summary


          input/output defaults


          time control defaults


          deformation model defaults


                cladding fast flux axial flux profile is the same as the axial power profile

 end of default summary

                                                   input common block definitions


fuel melting temperature =  5144.0 F                 3113.2 K
fuel heat of fusion =   7.5150E+04 btu/ft**3     2.8000E+09 j/m**3
clad melting temperature =  3317.0 F                 2098.2 K
clad heat of fusion =   3.9611E+04 btu/ft**3     1.4759E+09 j/m**3


 nfmesh, nmesh =           11          13
 nfmesh, nmesh =           11          13
 input common block definition complete


 input variables have been placed in common

                                              ***** input processing completed *****


 ***  total number of words in restart data block =   3827 ***
```

Figure B.1 (contd)

[Start of calculational output: zero time, first power step when approaching initial power of 11.08 kW/ft.]

```
FrapTran Version May 1a  2001;  Fuel Rod Analysis Program - Transient; Pacific Northwest National Laboratory
Standard Problem #1

Conditions at time = 0.000000E+00 sec      (0.000000E+00 hours)
```

[Rod-average conditions.]

```
time step = 0.100000E+00 sec    number of temperature-deformation-pressure loop iterations  =    2
number of deformation-pressure loop iterations =    1
average fuel rod power (kW/m)                    3.281E-05
volume averaged fuel temperature (K)             610.0
energy generated by metal-water reaction(kW)     0.0000E+00

fuel stack axial extension (mm)                  1.138E+01
cladding axial extension (mm)                    4.317E+00

plenum gas temperature (K)                       615.5
plenum gas pressure (n/m**2)                     0.8896E+07
gas flow rate from plenum (gm-moles/sec)         0.0000E+00

fraction of molten fuel in fuel rod              0.0000

total free gas volume (mm)**3                    0.171834E+05
 plenum volume fraction                          0.510150
 crack volume fraction                           0.000000
 gap volume fraction                             0.311374
 open porosity volume fraction                   0.000000
 dish volume fraction                            0.157571
 central void volume fraction                    0.000000
 fuel surface roughness volume fraction          0.007171
 cladding surface roughness volume fraction      0.013734

current fission gas release fraction             0.0000
current fill gas composition                     1.000 He, 0.000 Ar, 0.000 Kr, 0.000 Xe, 0.000 H2, 0.000 air, 0.000 H2O
current moles of gas in rod                      0.300000E-01

current transient fuel swelling factor =    1.000000
```

[Axial node specific conditions.]

time(sec) = 0.000000E+00

axial node number	1	2	3	4	5	6
elevation (m)	0.152	0.457	0.762	1.067	1.295	1.448
local fuel rod power (kW/m)	1.754E-05	3.594E-05	4.612E-05	5.144E-05	5.243E-05	5.197E-05
radially ave. fuel enthalpy (jou/kg)	0.8442E+05	0.8442E+05	0.8442E+05	0.8442E+05	0.8442E+05	0.8442E+05
energy in fuel per unit length (kW-s)	0.5855E+02	0.5855E+02	0.5855E+02	0.5855E+02	0.5855E+02	0.5855E+02
energy in cladding per unit length (kW-s)	0.1220E+02	0.1220E+02	0.1220E+02	0.1220E+02	0.1220E+02	0.1220E+02

Figure B.1 (contd)

energy input after steady state (kW-s/m)	0.0000E+00	0.0000E+00	0.0000E+00	0.0000E+00	0.0000E+00	0.0000E+00
energy output after steady state (kW-s/m)	0.0000E+00	0.0000E+00	0.0000E+00	0.0000E+00	0.0000E+00	0.0000E+00
coolant bulk temperature(K)	610.0	610.0	610.0	610.0	610.0	610.0
coolant quality	0.000E+00	0.000E+00	0.000E+00	0.000E+00	0.000E+00	0.000E+00
coolant pressure (n/m**2)	1.567E+07	1.567E+07	1.567E+07	1.567E+07	1.567E+07	1.567E+07
coolant mass flux (kg/sec-m2	0.000E+00	0.000E+00	0.000E+00	0.000E+00	0.000E+00	0.000E+00
surface heat flux (watt/m**2)	5.199E-01	1.065E+00	1.367E+00	1.524E+00	1.554E+00	1.540E+00
critical heat flux (watt/m**2)	0.000E+00	0.000E+00	0.000E+00	0.000E+00	0.000E+00	0.000E+00
critical heat flux / surface heat flux	0.000E+00	0.000E+00	0.000E+00	0.000E+00	0.000E+00	0.000E+00
surface heat transfer coef. (watt/m**2-K)	2.930E+05	2.930E+05	2.930E+05	3.538E+05	3.538E+05	3.538E+05
heat transfer mode	1	1	1	1	1	1
gap heat transfer coef. (watt/m**2-K)	2.790E+03	2.790E+03	2.790E+03	2.790E+03	2.790E+03	2.790E+03
thermal radial gas gap (mm)	4.924E-02	4.924E-02	4.924E-02	4.924E-02	4.924E-02	4.924E-02
structural radial gas gap (mm)	4.924E-02	4.924E-02	4.924E-02	4.924E-02	4.924E-02	4.924E-02
gap gas pressure (n/m**2)	8.896E+06	8.896E+06	8.896E+06	8.896E+06	8.896E+06	8.896E+06
interface pressure, struct. gap(n/m**2)	0.000E+00	0.000E+00	0.000E+00	0.000E+00	0.000E+00	0.000E+00
displacement of fuel outer surface (mm)	5.580E-02	5.580E-02	5.580E-02	5.580E-02	5.580E-02	5.580E-02
displacement of clad inner surface (mm)	5.974E-03	5.974E-03	5.974E-03	5.974E-03	5.974E-03	5.974E-03
displacement of clad outer surface (mm)	7.607E-03	7.607E-03	7.607E-03	7.607E-03	7.607E-03	7.607E-03
cladding hoop strain (midplane)	1.344E-03	1.344E-03	1.344E-03	1.344E-03	1.344E-03	1.344E-03
cladding permanent hoop strain	0.000E+00	0.000E+00	0.000E+00	0.000E+00	0.000E+00	0.000E+00
cladding permanent axial strain	0.000E+00	0.000E+00	0.000E+00	0.000E+00	0.000E+00	0.000E+00
cladding hoop stress (n/m**2)	-6.958E+07	-6.958E+07	-6.958E+07	-6.958E+07	-6.958E+07	-6.958E+07
cladding axial stress (n/m**2)	-4.099E+07	-4.099E+07	-4.099E+07	-4.099E+07	-4.099E+07	-4.099E+07
effective cladding stress (n/m**2)	6.057E+07	6.057E+07	6.057E+07	6.057E+07	6.057E+07	6.057E+07
cladding yield stress (n/m**2)	2.541E+08	2.541E+08	2.541E+08	2.541E+08	2.541E+08	2.541E+08
cladding effective plastic strain	0.000E+00	0.000E+00	0.000E+00	0.000E+00	0.000E+00	0.000E+00
cladding instability strain	5.000E-01	5.000E-01	5.000E-01	5.000E-01	5.000E-01	5.000E-01
oxide temperature drop (K)	7.765E-07	1.591E-06	2.041E-06	2.277E-06	2.320E-06	2.300E-06
oxide thickness,clad outer surface(mm)	3.000E-03	3.000E-03	3.000E-03	3.000E-03	3.000E-03	3.000E-03
oxygen stabilized alpha thickness(mm)	0.000E+00	0.000E+00	0.000E+00	0.000E+00	0.000E+00	0.000E+00
oxide depth, clad inner surface(mm)	3.000E-03	3.000E-03	3.000E-03	3.000E-03	3.000E-03	3.000E-03
metal-water reaction energy (kW/m)	0.000E+00	0.000E+00	0.000E+00	0.000E+00	0.000E+00	0.000E+00
excess hydrogen (ppm)	0.000E+00	0.000E+00	0.000E+00	0.000E+00	0.000E+00	0.000E+00

temperatures by radial mesh points using axial power profile number 1

no.	mesh radius (mm)	temperatures (K)					
1	0.000E+00	610.0	610.0	610.0	610.0	610.0	610.0
2	1.470E+00	610.0	610.0	610.0	610.0	610.0	610.0
3	2.079E+00	610.0	610.0	610.0	610.0	610.0	610.0
4	2.546E+00	610.0	610.0	610.0	610.0	610.0	610.0
5	2.940E+00	610.0	610.0	610.0	610.0	610.0	610.0
6	3.287E+00	610.0	610.0	610.0	610.0	610.0	610.0
7	3.600E+00	610.0	610.0	610.0	610.0	610.0	610.0
8	3.889E+00	610.0	610.0	610.0	610.0	610.0	610.0
9	4.157E+00	610.0	610.0	610.0	610.0	610.0	610.0

Figure B.1 (contd)

10	4.410E+00	610.0	610.0	610.0	610.0	610.0	610.0
11**	4.648E+00	610.0	610.0	610.0	610.0	610.0	610.0
12	4.747E+00	610.0	610.0	610.0	610.0	610.0	610.0
13	5.360E+00	610.0	610.0	610.0	610.0	610.0	610.0

time(sec) = 0.000000E+00

axial node number	7	8	9	10	11	12
elevation (m)	1.600	1.753	1.905	2.057	2.210	2.362
local fuel rod power (kW/m)	5.079E-05	4.928E-05	4.746E-05	4.534E-05	4.296E-05	4.008E-05
radially ave. fuel enthalpy (jou/kg)	0.8442E+05	0.8442E+05	0.8442E+05	0.8442E+05	0.8442E+05	0.8442E+05
energy in fuel per unit length (kW-s)	0.5855E+02	0.5855E+02	0.5855E+02	0.5855E+02	0.5855E+02	0.5855E+02
energy in cladding per unit length (kW-s)	0.1220E+02	0.1220E+02	0.1220E+02	0.1220E+02	0.1220E+02	0.1220E+02
energy input after steady state (kW-s/m)	0.0000E+00	0.0000E+00	0.0000E+00	0.0000E+00	0.0000E+00	0.0000E+00
energy output after steady state (kW-s/m)	0.0000E+00	0.0000E+00	0.0000E+00	0.0000E+00	0.0000E+00	0.0000E+00
coolant bulk temperature(K)	610.0	610.0	610.0	610.0	610.0	610.0
coolant quality	0.000E+00	0.000E+00	0.000E+00	0.000E+00	0.000E+00	0.000E+00
coolant pressure (n/m**2)	1.567E+07	1.567E+07	1.567E+07	1.567E+07	1.567E+07	1.567E+07
coolant mass flux (kg/sec-m2	0.000E+00	0.000E+00	0.000E+00	0.000E+00	0.000E+00	0.000E+00
surface heat flux (watt/m**2)	1.505E+00	1.461E+00	1.407E+00	1.344E+00	1.273E+00	1.188E+00
critical heat flux (watt/m**2)	0.000E+00	0.000E+00	0.000E+00	0.000E+00	0.000E+00	0.000E+00
critical heat flux / surface heat flux	0.000E+00	0.000E+00	0.000E+00	0.000E+00	0.000E+00	0.000E+00
surface heat transfer coef. (watt/m**2-K)	3.538E+05	3.538E+05	3.538E+05	3.538E+05	3.538E+05	3.538E+05
heat transfer mode	1	1	1	1	1	1
gap heat transfer coef. (watt/m**2-K)	2.790E+03	2.790E+03	2.790E+03	2.790E+03	2.790E+03	2.790E+03
thermal radial gas gap (mm)	4.924E-02	4.924E-02	4.924E-02	4.924E-02	4.924E-02	4.924E-02
structural radial gas gap (mm)	4.924E-02	4.924E-02	4.924E-02	4.924E-02	4.924E-02	4.924E-02
gap gas pressure (n/m**2)	8.896E+06	8.896E+06	8.896E+06	8.896E+06	8.896E+06	8.896E+06
interface pressure, struct. gap(n/m**2)	0.000E+00	0.000E+00	0.000E+00	0.000E+00	0.000E+00	0.000E+00
displacement of fuel outer surface (mm)	5.580E-02	5.580E-02	5.580E-02	5.580E-02	5.580E-02	5.580E-02
displacement of clad inner surface (mm)	5.974E-03	5.974E-03	5.974E-03	5.974E-03	5.974E-03	5.974E-03
displacement of clad outer surface (mm)	7.607E-03	7.607E-03	7.607E-03	7.607E-03	7.607E-03	7.607E-03
cladding hoop strain (midplane)	1.344E-03	1.344E-03	1.344E-03	1.344E-03	1.344E-03	1.344E-03
cladding permanent hoop strain	0.000E+00	0.000E+00	0.000E+00	0.000E+00	0.000E+00	0.000E+00
cladding permanent axial strain	0.000E+00	0.000E+00	0.000E+00	0.000E+00	0.000E+00	0.000E+00
cladding hoop stress (n/m**2)	-6.958E+07	-6.958E+07	-6.958E+07	-6.958E+07	-6.958E+07	-6.958E+07
cladding axial stress (n/m**2)	-4.099E+07	-4.099E+07	-4.099E+07	-4.099E+07	-4.099E+07	-4.099E+07
effective cladding stress (n/m**2)	6.057E+07	6.057E+07	6.057E+07	6.057E+07	6.057E+07	6.057E+07
cladding yield stress (n/m**2)	2.541E+08	2.541E+08	2.541E+08	2.541E+08	2.541E+08	2.541E+08
cladding effective plastic strain	0.000E+00	0.000E+00	0.000E+00	0.000E+00	0.000E+00	0.000E+00
cladding instability strain	5.000E-01	5.000E-01	5.000E-01	5.000E-01	5.000E-01	5.000E-01
oxide temperature drop (K)	2.248E-06	2.181E-06	2.101E-06	2.007E-06	1.901E-06	1.774E-06
oxide thickness,clad outer surface(mm)	3.000E-03	3.000E-03	3.000E-03	3.000E-03	3.000E-03	3.000E-03
oxygen stabilized alpha thickness(mm)	0.000E+00	0.000E+00	0.000E+00	0.000E+00	0.000E+00	0.000E+00
oxide depth, clad inner surface(mm)	3.000E-03	3.000E-03	3.000E-03	3.000E-03	3.000E-03	3.000E-03
metal-water reaction energy (kW/m)	0.000E+00	0.000E+00	0.000E+00	0.000E+00	0.000E+00	0.000E+00
excess hydrogen (ppm)	0.000E+00	0.000E+00	0.000E+00	0.000E+00	0.000E+00	0.000E+00

Figure B.1 (contd)

temperatures by radial mesh points using axial power profile number 1

no.	mesh radius (mm)	temperatures (K)					
1	0.000E+00	610.0	610.0	610.0	610.0	610.0	610.0
2	1.470E+00	610.0	610.0	610.0	610.0	610.0	610.0
3	2.079E+00	610.0	610.0	610.0	610.0	610.0	610.0
4	2.546E+00	610.0	610.0	610.0	610.0	610.0	610.0
5	2.940E+00	610.0	610.0	610.0	610.0	610.0	610.0
6	3.287E+00	610.0	610.0	610.0	610.0	610.0	610.0
7	3.600E+00	610.0	610.0	610.0	610.0	610.0	610.0
8	3.889E+00	610.0	610.0	610.0	610.0	610.0	610.0
9	4.157E+00	610.0	610.0	610.0	610.0	610.0	610.0
10	4.410E+00	610.0	610.0	610.0	610.0	610.0	610.0
11**	4.648E+00	610.0	610.0	610.0	610.0	610.0	610.0
12	4.747E+00	610.0	610.0	610.0	610.0	610.0	610.0
13	5.360E+00	610.0	610.0	610.0	610.0	610.0	610.0

time(sec) = 0.000000E+00

axial node number	13	14	15	16
elevation (m)	2.591	2.896	3.200	3.505
local fuel rod power (kW/m)	3.557E-05	2.897E-05	2.092E-05	1.069E-05
radially ave. fuel enthalpy (jou/kg)	0.8442E+05	0.8442E+05	0.8442E+05	0.8442E+05
energy in fuel per unit length (kW-s)	0.5855E+02	0.5855E+02	0.5855E+02	0.5855E+02
energy in cladding per unit length (kW-s)	0.1220E+02	0.1220E+02	0.1220E+02	0.1220E+02
energy input after steady state (kW-s/m)	0.0000E+00	0.0000E+00	0.0000E+00	0.0000E+00
energy output after steady state (kW-s/m)	0.0000E+00	0.0000E+00	0.0000E+00	0.0000E+00
coolant bulk temperature(K)	610.0	610.0	610.0	610.0
coolant quality	0.000E+00	0.000E+00	0.000E+00	0.000E+00
coolant pressure (n/m**2)	1.567E+07	1.567E+07	1.567E+07	1.567E+07
coolant mass flux (kg/sec-m2	0.000E+00	0.000E+00	0.000E+00	0.000E+00
surface heat flux (watt/m**2)	1.054E+00	8.584E-01	6.199E-01	3.167E-01
critical heat flux (watt/m**2)	0.000E+00	0.000E+00	0.000E+00	0.000E+00
critical heat flux / surface heat flux	0.000E+00	0.000E+00	0.000E+00	0.000E+00
surface heat transfer coef. (watt/m**2-K)	3.538E+05	2.232E+05	2.232E+05	2.232E+05
heat transfer mode	1	1	1	1
gap heat transfer coef. (watt/m**2-K)	2.790E+03	2.790E+03	2.790E+03	2.790E+03
thermal radial gas gap (mm)	4.924E-02	4.924E-02	4.924E-02	4.924E-02
structural radial gas gap (mm)	4.924E-02	4.924E-02	4.924E-02	4.924E-02
gap gas pressure (n/m**2)	8.896E+06	8.896E+06	8.896E+06	8.896E+06
interface pressure, struct. gap(n/m**2)	0.000E+00	0.000E+00	0.000E+00	0.000E+00
displacement of fuel outer surface (mm)	5.580E-02	5.580E-02	5.580E-02	5.580E-02
displacement of clad inner surface (mm)	5.974E-03	5.974E-03	5.974E-03	5.974E-03
displacement of clad outer surface (mm)	7.607E-03	7.607E-03	7.607E-03	7.607E-03
cladding hoop strain (midplane)	1.344E-03	1.344E-03	1.344E-03	1.344E-03
cladding permanent hoop strain	0.000E+00	0.000E+00	0.000E+00	0.000E+00
cladding permanent axial strain	0.000E+00	0.000E+00	0.000E+00	0.000E+00

Figure B.1 (contd)

cladding hoop stress (n/m**2)	-6.958E+07	-6.958E+07	-6.958E+07	-6.958E+07
cladding axial stress (n/m**2)	-4.099E+07	-4.099E+07	-4.099E+07	-4.099E+07
effective cladding stress (n/m**2)	6.057E+07	6.057E+07	6.057E+07	6.057E+07
cladding yield stress (n/m**2)	2.541E+08	2.541E+08	2.541E+08	2.541E+08
cladding effective plastic strain	0.000E+00	0.000E+00	0.000E+00	0.000E+00
cladding instability strain	5.000E-01	5.000E-01	5.000E-01	5.000E-01
oxide temperature drop (K)	1.574E-06	1.282E-06	9.258E-07	4.729E-07
oxide thickness,clad outer surface(mm)	3.000E-03	3.000E-03	3.000E-03	3.000E-03
oxygen stabilized alpha thickness(mm)	0.000E+00	0.000E+00	0.000E+00	0.000E+00
oxide depth, clad inner surface(mm)	3.000E-03	3.000E-03	3.000E-03	3.000E-03
metal-water reaction energy (kW/m)	0.000E+00	0.000E+00	0.000E+00	0.000E+00
excess hydrogen (ppm)	0.000E+00	0.000E+00	0.000E+00	0.000E+00

temperatures by radial mesh points using axial power profile number 1

no.	mesh radius (mm)	temperatures (K)			
1	0.000E+00	610.0	610.0	610.0	610.0
2	1.470E+00	610.0	610.0	610.0	610.0
3	2.079E+00	610.0	610.0	610.0	610.0
4	2.546E+00	610.0	610.0	610.0	610.0
5	2.940E+00	610.0	610.0	610.0	610.0
6	3.287E+00	610.0	610.0	610.0	610.0
7	3.600E+00	610.0	610.0	610.0	610.0
8	3.889E+00	610.0	610.0	610.0	610.0
9	4.157E+00	610.0	610.0	610.0	610.0
10	4.410E+00	610.0	610.0	610.0	610.0
11**	4.648E+00	610.0	610.0	610.0	610.0
12	4.747E+00	610.0	610.0	610.0	610.0
13	5.360E+00	610.0	610.0	610.0	610.0

[Second power step on ascension to stated initial power.]

```
 FrapTran Version May 1a  2001;  Fuel Rod Analysis Program - Transient; Pacific Northwest National Laboratory
 Standard Problem #1

Conditions at time = 0.000000E+00 sec      (0.000000E+00 hours)

time step = 0.100000E+00 sec    number of temperature-deformation-pressure loop iterations  =    2
number of deformation-pressure loop iterations =    1
average fuel rod power (kW/m)                 3.281E-01
volume averaged fuel temperature (K)          615.9
energy generated by metal-water reaction(kW)  0.0000E+00

fuel stack axial extension (mm)               1.162E+01
cladding axial extension (mm)                 4.332E+00

plenum gas temperature (K)                    615.5
plenum gas pressure (n/m**2)                  0.8940E+07
gas flow rate from plenum (gm-moles/sec)      0.0000E+00
```

Figure B.1 (contd)

fraction of molten fuel in fuel rod	0.0000
total free gas volume (mm)**3	0.171476E+05
plenum volume fraction	0.510334
crack volume fraction	0.000307
gap volume fraction	0.310593
open porosity volume fraction	0.000000
dish volume fraction	0.157816
central void volume fraction	0.000000
fuel surface roughness volume fraction	0.007187
cladding surface roughness volume fraction	0.013763
current fission gas release fraction	0.0000
current fill gas composition	1.000 He, 0.000 Ar, 0.000 Kr, 0.000 Xe, 0.000 H2, 0.000 air, 0.000 H2O
current moles of gas in rod	0.300000E-01
current transient fuel swelling factor =	1.000000

time(sec) = 0.000000E+00

axial node number	1	2	3	4	5	6
elevation (m)	0.152	0.457	0.762	1.067	1.295	1.448
local fuel rod power (kW/m)	1.755E-01	3.594E-01	4.612E-01	5.145E-01	5.243E-01	5.198E-01
radially ave. fuel enthalpy (jou/kg)	0.8526E+05	0.8614E+05	0.8663E+05	0.8688E+05	0.8693E+05	0.8691E+05
energy in fuel per unit length (kW-s)	0.5913E+02	0.5974E+02	0.6008E+02	0.6026E+02	0.6029E+02	0.6027E+02
energy in cladding per unit length (kW-s)	0.1220E+02	0.1221E+02	0.1221E+02	0.1221E+02	0.1221E+02	0.1221E+02
energy input after steady state (kW-s/m)	0.0000E+00	0.0000E+00	0.0000E+00	0.0000E+00	0.0000E+00	0.0000E+00
energy output after steady state (kW-s/m)	0.0000E+00	0.0000E+00	0.0000E+00	0.0000E+00	0.0000E+00	0.0000E+00
coolant bulk temperature(K)	610.0	610.0	610.0	610.0	610.0	610.0
coolant quality	0.000E+00	0.000E+00	0.000E+00	0.000E+00	0.000E+00	0.000E+00
coolant pressure (n/m**2)	1.567E+07	1.567E+07	1.567E+07	1.567E+07	1.567E+07	1.567E+07
coolant mass flux (kg/sec-m2	0.000E+00	0.000E+00	0.000E+00	0.000E+00	0.000E+00	0.000E+00
surface heat flux (watt/m**2)	5.203E+03	1.066E+04	1.368E+04	1.525E+04	1.555E+04	1.541E+04
critical heat flux (watt/m**2)	0.000E+00	0.000E+00	0.000E+00	0.000E+00	0.000E+00	0.000E+00
critical heat flux / surface heat flux	0.000E+00	0.000E+00	0.000E+00	0.000E+00	0.000E+00	0.000E+00
surface heat transfer coef. (watt/m**2-K)	2.930E+05	2.930E+05	2.930E+05	3.538E+05	3.538E+05	3.538E+05
heat transfer mode	1	1	1	1	1	1
gap heat transfer coef. (watt/m**2-K)	5.074E+03	5.092E+03	5.106E+03	5.114E+03	5.116E+03	5.116E+03
thermal radial gas gap (mm)	4.918E-02	4.901E-02	4.892E-02	4.887E-02	4.887E-02	4.887E-02
structural radial gas gap (mm)	4.918E-02	4.901E-02	4.892E-02	4.887E-02	4.887E-02	4.887E-02
gap gas pressure (n/m**2)	8.940E+06	8.940E+06	8.940E+06	8.940E+06	8.940E+06	8.940E+06
interface pressure, struct. gap(n/m**2)	0.000E+00	0.000E+00	0.000E+00	0.000E+00	0.000E+00	0.000E+00
displacement of fuel outer surface (mm)	5.596E-02	5.612E-02	5.622E-02	5.626E-02	5.627E-02	5.627E-02
displacement of clad inner surface (mm)	6.073E-03	6.076E-03	6.079E-03	6.079E-03	6.080E-03	6.079E-03
displacement of clad outer surface (mm)	7.699E-03	7.703E-03	7.705E-03	7.706E-03	7.706E-03	7.706E-03
cladding hoop strain (midplane)	1.363E-03	1.363E-03	1.364E-03	1.364E-03	1.364E-03	1.364E-03
cladding permanent hoop strain	0.000E+00	0.000E+00	0.000E+00	0.000E+00	0.000E+00	0.000E+00

Figure B.1 (contd)

cladding permanent axial strain	0.000E+00	0.000E+00	0.000E+00	0.000E+00	0.000E+00	0.000E+00
cladding hoop stress (n/m**2)	-6.793E+07	-6.793E+07	-6.793E+07	-6.793E+07	-6.793E+07	-6.793E+07
cladding axial stress (n/m**2)	-4.013E+07	-4.013E+07	-4.013E+07	-4.013E+07	-4.013E+07	-4.013E+07
effective cladding stress (n/m**2)	5.915E+07	5.915E+07	5.915E+07	5.915E+07	5.915E+07	5.915E+07
cladding yield stress (n/m**2)	2.540E+08	2.540E+08	2.540E+08	2.540E+08	2.540E+08	2.540E+08
cladding effective plastic strain	0.000E+00	0.000E+00	0.000E+00	0.000E+00	0.000E+00	0.000E+00
cladding instability strain	5.000E-01	5.000E-01	5.000E-01	5.000E-01	5.000E-01	5.000E-01
oxide temperature drop (K)	7.770E-03	1.592E-02	2.042E-02	2.278E-02	2.322E-02	2.302E-02
oxide thickness,clad outer surface(mm)	3.000E-03	3.000E-03	3.000E-03	3.000E-03	3.000E-03	3.000E-03
oxygen stabilized alpha thickness(mm)	0.000E+00	0.000E+00	0.000E+00	0.000E+00	0.000E+00	0.000E+00
oxide depth, clad inner surface(mm)	3.000E-03	3.000E-03	3.000E-03	3.000E-03	3.000E-03	3.000E-03
metal-water reaction energy (kW/m)	0.000E+00	0.000E+00	0.000E+00	0.000E+00	0.000E+00	0.000E+00
excess hydrogen (ppm)	0.000E+00	0.000E+00	0.000E+00	0.000E+00	0.000E+00	0.000E+00

temperatures by radial mesh points using axial power profile number 1

no.	mesh radius (mm)	temperatures (K)					
1	0.000E+00	614.4	619.0	621.6	622.9	623.1	623.0
2	1.470E+00	614.1	618.3	620.7	621.9	622.2	622.1
3	2.079E+00	613.8	617.8	620.0	621.1	621.3	621.2
4	2.546E+00	613.5	617.2	619.2	620.3	620.5	620.4
5	2.940E+00	613.2	616.5	618.4	619.4	619.6	619.5
6	3.287E+00	612.9	615.9	617.6	618.5	618.6	618.6
7	3.600E+00	612.6	615.3	616.8	617.6	617.7	617.6
8	3.889E+00	612.3	614.6	616.0	616.6	616.8	616.7
9	4.157E+00	611.9	614.0	615.1	615.7	615.8	615.8
10	4.410E+00	611.6	613.3	614.3	614.8	614.9	614.8
11**	4.648E+00	611.3	612.7	613.5	613.8	613.9	613.9
12	4.747E+00	610.2	610.4	610.6	610.6	610.6	610.6
13	5.360E+00	610.0	610.0	610.1	610.0	610.1	610.0

time(sec) = 0.000000E+00

axial node number	7	8	9	10	11	12
elevation (m)	1.600	1.753	1.905	2.057	2.210	2.362
local fuel rod power (kW/m)	5.079E-01	4.929E-01	4.747E-01	4.535E-01	4.296E-01	4.008E-01
radially ave. fuel enthalpy (jou/kg)	0.8685E+05	0.8678E+05	0.8669E+05	0.8659E+05	0.8648E+05	0.8634E+05
energy in fuel per unit length (kW-s)	0.6023E+02	0.6018E+02	0.6012E+02	0.6005E+02	0.5997E+02	0.5988E+02
energy in cladding per unit length (kW-s)	0.1221E+02	0.1221E+02	0.1221E+02	0.1221E+02	0.1221E+02	0.1221E+02
energy input after steady state (kW-s/m)	0.0000E+00	0.0000E+00	0.0000E+00	0.0000E+00	0.0000E+00	0.0000E+00
energy output after steady state (kW-s/m)	0.0000E+00	0.0000E+00	0.0000E+00	0.0000E+00	0.0000E+00	0.0000E+00
coolant bulk temperature(K)	610.0	610.0	610.0	610.0	610.0	610.0
coolant quality	0.000E+00	0.000E+00	0.000E+00	0.000E+00	0.000E+00	0.000E+00
coolant pressure (n/m**2)	1.567E+07	1.567E+07	1.567E+07	1.567E+07	1.567E+07	1.567E+07
coolant mass flux (kg/sec-m2	0.000E+00	0.000E+00	0.000E+00	0.000E+00	0.000E+00	0.000E+00
surface heat flux (watt/m**2)	1.506E+04	1.461E+04	1.407E+04	1.345E+04	1.274E+04	1.188E+04
critical heat flux (watt/m**2)	0.000E+00	0.000E+00	0.000E+00	0.000E+00	0.000E+00	0.000E+00
critical heat flux / surface heat flux	0.000E+00	0.000E+00	0.000E+00	0.000E+00	0.000E+00	0.000E+00

Figure B.1 (contd)

surface heat transfer coef. (watt/m**2-K)	3.538E+05	3.538E+05	3.538E+05	3.538E+05	3.538E+05	3.538E+05
heat transfer mode	1	1	1	1	1	1
gap heat transfer coef. (watt/m**2-K)	5.115E+03	5.113E+03	5.111E+03	5.109E+03	5.106E+03	5.103E+03
thermal radial gas gap (mm)	4.888E-02	4.889E-02	4.891E-02	4.893E-02	4.895E-02	4.898E-02
structural radial gas gap (mm)	4.888E-02	4.889E-02	4.891E-02	4.893E-02	4.895E-02	4.898E-02
gap gas pressure (n/m**2)	8.940E+06	8.940E+06	8.940E+06	8.940E+06	8.940E+06	8.940E+06
interface pressure, struct. gap(n/m**2)	0.000E+00	0.000E+00	0.000E+00	0.000E+00	0.000E+00	0.000E+00
displacement of fuel outer surface (mm)	5.626E-02	5.624E-02	5.623E-02	5.621E-02	5.619E-02	5.616E-02
displacement of clad inner surface (mm)	6.079E-03	6.079E-03	6.079E-03	6.078E-03	6.078E-03	6.077E-03
displacement of clad outer surface (mm)	7.706E-03	7.706E-03	7.705E-03	7.705E-03	7.704E-03	7.704E-03
cladding hoop strain (midplane)	1.364E-03	1.364E-03	1.364E-03	1.364E-03	1.364E-03	1.363E-03
cladding permanent hoop strain	0.000E+00	0.000E+00	0.000E+00	0.000E+00	0.000E+00	0.000E+00
cladding permanent axial strain	0.000E+00	0.000E+00	0.000E+00	0.000E+00	0.000E+00	0.000E+00
cladding hoop stress (n/m**2)	-6.793E+07	-6.793E+07	-6.793E+07	-6.793E+07	-6.793E+07	-6.793E+07
cladding axial stress (n/m**2)	-4.013E+07	-4.013E+07	-4.013E+07	-4.013E+07	-4.013E+07	-4.013E+07
effective cladding stress (n/m**2)	5.915E+07	5.915E+07	5.915E+07	5.915E+07	5.915E+07	5.915E+07
cladding yield stress (n/m**2)	2.540E+08	2.540E+08	2.540E+08	2.540E+08	2.540E+08	2.540E+08
cladding effective plastic strain	0.000E+00	0.000E+00	0.000E+00	0.000E+00	0.000E+00	0.000E+00
cladding instability strain	5.000E-01	5.000E-01	5.000E-01	5.000E-01	5.000E-01	5.000E-01
oxide temperature drop (K)	2.249E-02	2.183E-02	2.102E-02	2.008E-02	1.902E-02	1.775E-02
oxide thickness,clad outer surface(mm)	3.000E-03	3.000E-03	3.000E-03	3.000E-03	3.000E-03	3.000E-03
oxygen stabilized alpha thickness(mm)	0.000E+00	0.000E+00	0.000E+00	0.000E+00	0.000E+00	0.000E+00
oxide depth, clad inner surface(mm)	3.000E-03	3.000E-03	3.000E-03	3.000E-03	3.000E-03	3.000E-03
metal-water reaction energy (kW/m)	0.000E+00	0.000E+00	0.000E+00	0.000E+00	0.000E+00	0.000E+00
excess hydrogen (ppm)	0.000E+00	0.000E+00	0.000E+00	0.000E+00	0.000E+00	0.000E+00

temperatures by radial mesh points using axial power profile number 1

no.	mesh radius (mm)	temperatures (K)					
1	0.000E+00	622.7	622.4	621.9	621.4	620.8	620.0
2	1.470E+00	621.8	621.4	621.0	620.5	620.0	619.3
3	2.079E+00	621.0	620.7	620.3	619.8	619.3	618.7
4	2.546E+00	620.1	619.8	619.5	619.0	618.6	618.0
5	2.940E+00	619.3	619.0	618.6	618.3	617.8	617.3
6	3.287E+00	618.4	618.1	617.8	617.5	617.1	616.6
7	3.600E+00	617.5	617.2	617.0	616.7	616.3	615.9
8	3.889E+00	616.5	616.4	616.1	615.8	615.5	615.2
9	4.157E+00	615.6	615.5	615.3	615.0	614.8	614.4
10	4.410E+00	614.7	614.6	614.4	614.2	614.0	613.7
11**	4.648E+00	613.8	613.7	613.5	613.4	613.2	613.0
12	4.747E+00	610.6	610.6	610.6	610.5	610.5	610.5
13	5.360E+00	610.0	610.0	610.0	610.0	610.0	610.0

time(sec) = 0.000000E+00

axial node number	13	14	15	16
elevation (m)	2.591	2.896	3.200	3.505

Figure B.1 (contd)

local fuel rod power (kW/m)	3.558E-01	2.897E-01	2.092E-01	1.069E-01
radially ave. fuel enthalpy (jou/kg)	0.8612E+05	0.8581E+05	0.8542E+05	0.8493E+05
energy in fuel per unit length (kW-s)	0.5973E+02	0.5951E+02	0.5924E+02	0.5890E+02
energy in cladding per unit length (kW-s)	0.1221E+02	0.1221E+02	0.1221E+02	0.1220E+02
energy input after steady state (kW-s/m)	0.0000E+00	0.0000E+00	0.0000E+00	0.0000E+00
energy output after steady state (kW-s/m)	0.0000E+00	0.0000E+00	0.0000E+00	0.0000E+00
coolant bulk temperature(K)	610.0	610.0	610.0	610.0
coolant quality	0.000E+00	0.000E+00	0.000E+00	0.000E+00
coolant pressure (n/m**2)	1.567E+07	1.567E+07	1.567E+07	1.567E+07
coolant mass flux (kg/sec-m2	0.000E+00	0.000E+00	0.000E+00	0.000E+00
surface heat flux (watt/m**2)	1.055E+04	8.589E+03	6.203E+03	3.169E+03
critical heat flux (watt/m**2)	0.000E+00	0.000E+00	0.000E+00	0.000E+00
critical heat flux / surface heat flux	0.000E+00	0.000E+00	0.000E+00	0.000E+00
surface heat transfer coef. (watt/m**2-K)	3.538E+05	2.232E+05	2.232E+05	2.232E+05
heat transfer mode	1	1	1	1
gap heat transfer coef. (watt/m**2-K)	5.098E+03	5.091E+03	5.082E+03	5.070E+03
thermal radial gas gap (mm)	4.902E-02	4.907E-02	4.915E-02	4.924E-02
structural radial gas gap (mm)	4.902E-02	4.907E-02	4.915E-02	4.924E-02
gap gas pressure (n/m**2)	8.940E+06	8.940E+06	8.940E+06	8.940E+06
interface pressure, struct. gap(n/m**2)	0.000E+00	0.000E+00	0.000E+00	0.000E+00
displacement of fuel outer surface (mm)	5.612E-02	5.606E-02	5.599E-02	5.590E-02
displacement of clad inner surface (mm)	6.076E-03	6.075E-03	6.074E-03	6.071E-03
displacement of clad outer surface (mm)	7.703E-03	7.702E-03	7.700E-03	7.697E-03
cladding hoop strain (midplane)	1.363E-03	1.363E-03	1.363E-03	1.362E-03
cladding permanent hoop strain	0.000E+00	0.000E+00	0.000E+00	0.000E+00
cladding permanent axial strain	0.000E+00	0.000E+00	0.000E+00	0.000E+00
cladding hoop stress (n/m**2)	-6.793E+07	-6.793E+07	-6.793E+07	-6.793E+07
cladding axial stress (n/m**2)	-4.013E+07	-4.013E+07	-4.013E+07	-4.013E+07
effective cladding stress (n/m**2)	5.915E+07	5.915E+07	5.915E+07	5.915E+07
cladding yield stress (n/m**2)	2.540E+08	2.540E+08	2.540E+08	2.540E+08
cladding effective plastic strain	0.000E+00	0.000E+00	0.000E+00	0.000E+00
cladding instability strain	5.000E-01	5.000E-01	5.000E-01	5.000E-01
oxide temperature drop (K)	1.575E-02	1.283E-02	9.264E-03	4.732E-03
oxide thickness,clad outer surface(mm)	3.000E-03	3.000E-03	3.000E-03	3.000E-03
oxygen stabilized alpha thickness(mm)	0.000E+00	0.000E+00	0.000E+00	0.000E+00
oxide depth, clad inner surface(mm)	3.000E-03	3.000E-03	3.000E-03	3.000E-03
metal-water reaction energy (kW/m)	0.000E+00	0.000E+00	0.000E+00	0.000E+00
excess hydrogen (ppm)	0.000E+00	0.000E+00	0.000E+00	0.000E+00

temperatures by radial mesh points using axial power profile number 1

no.	mesh radius (mm)	temperatures (K)			
1	0.000E+00	618.9	617.3	615.2	612.7
2	1.470E+00	618.2	616.7	614.8	612.5
3	2.079E+00	617.7	616.3	614.5	612.3
4	2.546E+00	617.1	615.8	614.2	612.1

Figure B.1 (contd)

5	2.940E+00	616.5	615.3	613.8	611.9
6	3.287E+00	615.9	614.8	613.4	611.8
7	3.600E+00	615.2	614.3	613.1	611.6
8	3.889E+00	614.6	613.7	612.7	611.4
9	4.157E+00	613.9	613.2	612.3	611.2
10	4.410E+00	613.3	612.7	611.9	611.0
11**	4.648E+00	612.7	612.2	611.6	610.8
12	4.747E+00	610.4	610.4	610.3	610.1
13	5.360E+00	610.0	610.0	610.0	610.0

Figure B.1 (contd)

APPENDIX C

CALCULATION OF CLADDING SURFACE TEMPERATURE

APPENDIX C

CALCULATION OF CLADDING SURFACE TEMPERATURE

The numerical solution of the heat conduction equation (15) requires solving a set of tridiagonal equations. This set of equations is shown as follows:

$$\begin{vmatrix} b_1 & c_1 & 0 & 0 & & \\ a_2 & b_2 & c_2 & 0 & & 0 \\ 0 & a_3 & b_3 & c_3 & & \\ . & . & . & . & & . \\ . & . & . & . & & . \\ & 0's & a_{n-1} & b_{n-1} & & c_{n-1} \\ & & & a_n & & b_n \end{vmatrix} \begin{vmatrix} T_1^{m+1} \\ T_2^{m+1} \\ T_3^{m+1} \\ . \\ . \\ T_{n-1}^{m+1} \\ T_n^{m+1} \end{vmatrix} = \begin{vmatrix} d_1 \\ d_2 \\ d_3 \\ . \\ . \\ d_{n-1} \\ d_n \end{vmatrix} \qquad \text{(C.1)}$$

where a_n, b_n, c_n, and d_n are terms of the heat conduction equation in finite difference form at the n-th mesh point and

where: T_n^{m+1} = temperature at n-th mesh point at time step m+1
n = number of mesh point at outer surface.

The mesh point temperatures are solved by the Gaussian elimination method.

$$T_n^{m+1} = (d_n - a_n F_{n-1})/(b_n - a_n E_{n-1})$$

$$T_j^{m+1} = -E_j T_{j+1}^{m+1} + F_j \text{ for } j = n-1, n-2, \ldots 2, 1$$

$$\left.\begin{aligned} E_1 &= c_1/b_1 \text{ and } F_1 = d_a/b_1 \\ E_j &= c_j/(b_j - a_j E_{j-1}) \\ F_j &= (d_j - a_j F_{j-1})/(b_j - a_j E_{j-1}) \end{aligned}\right\} \text{for } j = 2, 3 \ldots n-1 \qquad \text{(C.2)}$$

The coefficients a_n, b_n, and d_n in the first equation of Equation C.2 are derived from the energy balance equation for the half mesh interval bordering the outside surface. The continuous form of the energy balance equation for this half mesh interval is

$$\rho C_p \, \Delta V \, \frac{\partial T}{\partial t} = -A_{n-1/2} \, K \left. \frac{\partial T}{\partial r} \right|_{r \, = \, r_n \, - \, \Delta r/2} - \theta \, A_n + q \Delta V \tag{C.3}$$

where all the terms in Equation C.3 are defined below.

The finite difference form of Equation C.3 is

$$\underbrace{\frac{-0.5 \, A_{n-1/2} \, K}{\Delta r}}_{a_n} T_{n-1}^{m+1} + \left(\underbrace{\frac{\rho C_p \Delta V}{\Delta t} + \frac{0.5 A_{n-1/2} \, K}{\Delta r}}_{b_n} T_n^{m+1} \right)$$

$$= \underbrace{\frac{\rho C_p \, \Delta V}{\Delta r} T_n^m \quad \frac{-0.5 \, A_{n-1/2} \, K}{\Delta r} (T_n^m - T_{n-1}^m) - 0.5 A_n (\theta^m + \theta^{m+1}) + q^{m+1/2} \Delta V}_{d_n} \tag{C.4}$$

The complete expressions for the coefficients a_n, b_n, and d_n are then

$$a_n = \frac{-0.5 A_{n-1/2} \, K}{\Delta r}$$

$$b_n = \left(\frac{\rho C_p \, \Delta V}{\Delta t} + \frac{0.5 A_{n-1/2} \, K}{\Delta r} \right)$$

$$d_n = \frac{\rho C_p \, \Delta V}{\Delta t} T_n^m \; \frac{0.5 A_{n-1/2} \, K}{\Delta r} (T_n^m - T_{n-1}^m)$$

$$-0.5 A_n \, (\theta^{m+1} + \theta^m) + \rho^{m+1/2} \, \Delta V$$

$$\begin{aligned} A_{n-1/2} &= 2\pi \, (r_n - \Delta r/2) \\ A_n &= 2\pi r_n \\ V &= \pi \, (r_n \Delta r - \Delta r^2/4) \end{aligned} \tag{C.5}$$

where K = thermal conductivity of material in half mesh interval bordering the surface
C_p = specific heat of material in half mesh interval bordering the surface
ρ = density of material in half mesh interveral bordering the surface
r_n = radius to outside surface
Δr = width of mesh interval bordering outside surface
Δt = time step

θ^m = surface heat flux at m-th time step
T_n^m = surface temperature at m-th time step
$q^{m-1/2}$ = heat generation rate in half mesh interval bordering outside surface (heat generation caused by cladding oxidation).

Because the coefficients a_n, b_n, d_n, E_{n-1}, and F_{n-1} in Equation C.2 do not contain temperature, the first equation of Equation C.2 can be writen as

$$A_1 \; T_n^{m+1} + B_1 = \theta^{m+1} \tag{C.6}$$

where

$$A_1 = -(b_n - a_n E_{n-1})0.5A_n$$

$$B_1 = -\left[\frac{0.5\,\theta^m A_n + a_n F_{n-1} \dfrac{-\rho C_p}{\Delta t} \Delta V \, T_n^m - a_n (T_n^m - T_{n-1}^m) - q^{m-1/2} \Delta V}{0.5A_n}\right] \tag{C.7}$$

As shown in Equation C.2, the coefficients E_{n-1} and F_{n-1} are evaluated by forward reduction of Equation C.1. So Equation C.6 contains only T_n^{m+1} and θ^{m+1} as unknown quantities.

Empirically derived heat transfer correlations are available from which the surface heat flux due to convection can be calculated in terms of surface temperature, geometric parameters and flow conditions. Also, the equation for radiation heat transfer from a surface to surrounding water is known. Thus, the total surface heat flux can be expressed by the equation

$$\theta^{m+1} = f_i\,(C, G, T_n^{m+1}) + \sigma F_A F_E \left[(T_n^{m+1})^4 - T_w^4)\right] \tag{C.8}$$

where θ^{m+1} = surface heat flux at time step m+1
f_1 = function specifying rate at which heat is transferred from surface by convention heat transfer during heat transfer mode i. (These functions are defined in Table D.1 of Appendix D)
i = number identification of convective heat transfer mode (nucleate boiling, film boiling, etc.)
C = set of parameters describing coolant conditions
G = set of parameters describing geometry
σ = Stefan-Boltzmann constant
F_A = configuration factor for radiation heat transfer
F_E = emissivity factor for radiation heat transfer
T_W = bulk temperature of water surrounding fuel rod surface.

Equations C.6 and C.8 are two independent equations with unknowns T_n^{m+1} and Q^{m+1}. Simultaneous solution of the two equations yields the new surface temperature T_n^{m+1}.

APPENDIX D

HEAT TRANSFER CORRELATIONS AND COOLANT MODELS

APPENDIX D

HEAT TRANSFER CORRELATIONS AND COOLANT MODELS

The cladding-coolant heat transfer correlations used in FRAPTRAN are described in this appendix. The heat transfer correlations supply one of the equations required for calculation of the fuel rod surface temperature, as discussed in Section 2.2.1. Also described are the optional coolant enthalpy model and the calculation of coolant void fraction.

D.1 Heat Transfer and Critical Heat Flux Correlations

Most of the heat transfer and critical heat flux correlations in FRAPTRAN were taken from the RELAP4[D.1] code. In some cases, more than one correlation is available for a given heat transfer mode. In these cases, the particular correlation to be used is specified by the input data. The available correlations for each heat transfer mode except for reflood heat transfer are described in Table D.1 at the end of this appendix. The symbols used in Table D.1 are defined in Table D.2.

The following critical heat flux correlations are available:

1. B&W-2[D.2]
2. Local Barnett[D.3]
3. Modified Barnett[D.4]
4. General Electric[D.5]
5. Savannah River[D.6]
6. W-3[D.1]
7. Hsu and Beckner[D.1]
8. LOFT[D.7]
9. Modified Zuber[D.8]
10. Combustion Engineering (CE)-1.[D.9]

The correlations are described in Table D.3.

The B&W-2 correlation is restricted to coolant pressures greater than 1500 psia. If the coolant pressure is less than 1300 psia, the B&W-2 correlation is replaced with the Barnett correlation. A combination of the two correlations is used for intermediate pressures.

If the LOFT correlation is selected and the coolant conditions fall outside of its valid range, the B&W-2 or its appropriate low pressure substitute is used.

D.2 Reflood Heat Transfer

The generalized FLECHT[D.10, D.11] correlation is used to calculate the heat transfer coefficient at the cladding surface during the reflood phase of a LOCA. The heat transfer coefficient is a function of flooding rate, cladding temperature at the start of flooding, fuel rod power at the start of flooding,

flooding water temperature, vessel pressure, elevation, and time. The ranges of these variables for which the FLECHT correlation is applicable are shown in Table D.6. The FLECHT correlation divides the reflood heat transfer into four time periods and has a different heat transfer correlation for each period. Using the definitions shown in Table D.7, the four regimes are described below.

D.2.1 Period of Radiation Only

Only heat transfer due to radiation is modeled during $0 > t \geq t_1$, with the heat transfer coefficient being calculated by the expression

$$h = h_o + \Delta h \, [1 - \exp(-0.0025 \, t^2)] \tag{D.1}$$

where

$$t_1 = 274 \exp(-0.0034 \, T_{init}) \exp(-0.465 \, V_{in}) \exp(-1.25 \, Q'_{max}) / (1 + 50.** \{-0.2(P - 30)\})$$

$$h_o = \begin{cases} 3.67 \, Q'_{max} \, (1 - \exp\{-(T_{init} - 700)/435\}) \, F, & \text{if } T_{init} > 700°F \\ 0, & \text{if } T_{init} \leq 700°F \end{cases}$$

$$F = F_2 + (1 - F_2)/(1 + 50 ** (Z - 7))$$

$$F_2 = 0.3 + 0.7/(1 + 50 ** (2 - V_{in}))$$
$$\Delta h = 0.0397 \, Q'_{max} \, (T_{init} - 100) \tag{D.2}$$

D.2.2 Period I

During Period I, the flow develops from the radiation dominated prereflood condition to single phase steam flow, to dispersed flow, and finally to unstable film boiling. If the flooding rate is less than 3 in./s however, unstable film boiling does not develop. The heat transfer coefficient during this period changes from a low value due to radiation to a relatively high value due to unstable film boiling (high flooding rates) or dispersed flow (low flooding rates). The time range of Period I is

$$t_1 < t \tag{D.3}$$

and

$$t_q < t_{q2} \tag{D.4}$$

where the variables in the expression for time range are defined as

$$t_q = \frac{t - t_1}{t_{q6} - t_1} \tag{D.5}$$

where

$$\begin{aligned}
t_{q6} = {} & 98.39 \left[\exp(-0.0107\ \Delta T_{sub}) \{1 - \exp(0.667\ V_{in})\}\right. \\
& \{1 + 0.5 \exp(-0.000037p^3) + 1.3 \exp(-0.111\ V_{in}^2) \\
& + 17.3 \exp(-0.000037p^3) \exp(-0.49\ V_{in}^2)\} (1.207\ Q'^{1.5}_{maxtq} - 0.667) \\
& \left. + \{(3.28/V_{in})^{1.1} - 2.8 \exp(-V_{in})\} \{1 + 0.5 \exp(-0.000037p^3)\}\right] \\
& (1 + 0.0000588T_{init} - 1.05 \exp(-0.0025\ T_{init})) \\
& (1 + 0.5/\{1 + 50 ** (2 - 0.667\ V_{in})\}) \left[1 + 0.32/\{1 + 50 ** (5 - 0.1\ p)\}\right] \\
t_{q2} = {} & 0.62\ ((1 - \exp(-0.192\ Z)) - 0.115\ Z \exp(-0.0368Z^2))
\end{aligned} \tag{D.6}$$

The heat transfer coefficient during Period I is calculated using the correlation

$$\begin{aligned}
h = {} & h_1 \left[1 - \exp(-10(X_2 - X)/X_2)\right] + \left[h_{12} - h_1 \{1 - \exp(-10(X_2 - X)/X_2)\}\right] \\
& \left[1 - \exp(-X) - 0.9\ X \exp(-X^2)\right] \left[1 - 2.21 \exp(-0.4\ V_{in}) u \exp(-u)\right. \\
& \exp\{-(0.588\ Z_{in} - 3.824)^2\} / \\
& \left.(1 + 100 ** \{10\ (t_q/t_{q2} - 9\})\right]
\end{aligned} \tag{D.7}$$

where

$$\begin{aligned}
h_1 = {} & 3.67\ Q'_{max} (1 - \exp\{-(T_{init} - 700)/435\}) \\
& + \Delta h\ (1 - \exp(-0.0025\ t_1^2)),\ \text{if } T_{init} > 700°F \\
= {} & \Delta h\ (1 - \exp(0.0025\ t_1^2)),\ \text{if } T_{init} \le 700°F \\
X_2 = {} & 17.6 \left[1 + 4.37 \exp(-0.0166\ \Delta T_{sub})\right] \left[1 - \exp\{-(0.00075\right. \\
& \left. + 0.0000272\ (V_{in} - 8)^2)\ f_6\}\right] t_{q2}\ f_1 \\
h_{12} = {} & 2.644 + 1.092\ Q'_{max} + \left[35.7 + (22 - 0.00303\ Z^{4.1})\right. \\
& \left.(1 - \exp(-0.0383\ P) - 0.034\ P \exp(-0.0011\ P^2))\right] \left[1 - \exp(-0.2\ V_{in})\right] \\
& + 8 \left[1 - \exp(-2\ V_{in})\right] \left[1 - \exp(-B/25)\right]
\end{aligned}$$

$$X = 17.6 \left[1 + 4.37 \exp(-0.0166\ \Delta T_{sub})\right] \left[1 - \exp\left\{-(0.0075 + 0.0000272\ (V_{in} - 8)^2)\ f_6\right\}\right] t_q \left(\frac{t - t_1}{t_{q2}(t_{q6} - t_1)}\right) ** f_2$$

$$u = 9 \left[f_1 t_q / ((t_{q2} ** (1 + f_2 f_3))\right]^2$$

$$f_1 = 0.436 + 0.455\ f_5$$

$$f_2 = 0.564 - 0.455\ f_5 \qquad \text{(D.8)}$$

$$f_3 = 2.8 - 4.8 \exp(0.688 - 1.67\ V_{in})$$

$$f_4 = 1 - \exp\left\{-(0.026\ P + 1.041\ V_{in} + 10.28 \exp(-3.01\ Q'_{max}) - 0.651)\right\}$$

$$f_5 = Q'_{max} + (1.24 - Q'_{max}) / \left\{1 + 50 ** (5 - 2\ V_{in})\right\}$$

$$f_6 = 0.5 \left[T_{init} - 1000 + \left\{T_{init}^2 - 2000\ T_{init} + 1.0001(10^6)\right\}^{1/2}\right] + 350$$

D.2.3 Period II

During this period, the flow pattern has fully developed to a quasi-steady state of either unstable film boiling (high flooding rate) or dispersed flow (low flooding rate), and the heat transfer coefficient reaches a plateau with a rather slow increase. The time range of Period II is

$$t_{q2} < t_q < t_{q3} \qquad \text{(D.9)}$$

where the new variable in the expression for time range is defined as

$$t_{q3} = 1.55\ ((1. - \exp(-0.205\ Z)) - 0.154\ Z \exp(-0.0421\ Z^2)) + 0.26 \exp(-2.77\ (10^{-6})\ T_{init}^2) \qquad \text{(D.10)}$$

The heat transfer coefficient during Period II is computed by the equation

$$h = h_2 + b_1\left[y^2 + b_2(y^2 - b_3\ y^3) + b_4\ y^2 \exp(-6.38\ y)\right] + 60 \exp\left[-2.77\text{x}10^{-6}\ T_{init}^2\right] (y/y_3) \exp\left[-2.25\ (y/y_3)^2\right] \qquad \text{(D.11)}$$

where

$$h_2 = h_{12}\left[(1 - \exp(-X_2)) - 0.9\, X_2 \exp(-X_2^2)\right]$$

$$b_1 = \left[682 - 650\left\{1 - \exp(4 - Z)\right\}\right]\left[1 - \exp\left\{-0.95\,(1 - 0.0488\, Z)\, V_{in}\right\}\right]$$

$$\left[1 - \exp\left\{-0.0238\, \Delta T_{sub}\right\}\right]\left[0.696 + 0.304 \exp(-B/25)\right]$$

$$\left[1 + 0.2\,(1 - f_4)\right]\left[1 + \exp(-0.8503\, Z^2 + 1.0986123\, Z + 2.3025851)\right]$$

$$y = t_q - t_{q2} \tag{D.12}$$

$$D_2 = 0.4\, Z\, [1 - \exp\left\{-2\,(Z - 3.5)\right\}]\left[1.33\,(1 - \exp(-0.0227\, P)) - 1\right]$$

$$-2.9\left[1 - \exp(-V_{in}/2.5)\right]\left[1 - \exp(-B/25)\right]$$

$$b_3 = 2.55\,(Z - 3.7)^2 \exp(3.7 - Z)$$

$$b_4 = 87.5\, V_{in} \exp(-V_{in}^2) \exp(-0.036\, \Delta T_{sub})$$

$$\text{if } Z < 4,\ b_3 = b_2 = 0$$

D.2.4 Period III

During this period, the flow pattern changes to stable film boiling and the heat transfer coefficient increases rapidly as the quench front approaches. The time range of Period III is

$$t_{q3} < t_q \tag{D.13}$$

where t_q is the time of quenching. The heat transfer coefficient during Period III is calculated by the expression

where

$$h = h_3 + C\,(t_q - t_{q3}) \tag{D.14}$$

$$h_3 = h_2 + b_1\left[y_3^2 + b_2(y_3^2 - b_3\, y_3^3) + b_4\, y_3^2 \exp(-6.38\, y_3)\right]$$

$$C = 420\left[1 - \exp(-0.00625\, b_1)\right] f_4 \tag{D.15}$$

$$y_3 = t_{q3} - t_{q2}$$

D.2.5 Modification for Low Flooding Rates

The heat transfer coefficients for Periods I, II, and III given above are based on the original FLECHT tests. Later tests performed at low flooding rates showed that a modification was necessary to best match the data. This modification is accomplished by multiplying the heat transfer coefficients for Periods I, II, and III by a factor f where

$$f = f_7 \, f_8 \tag{D.16}$$

where

$$\begin{aligned} f_7 &= 0.978 + 0.022/\left[1 + 30 ** \left\{t_{q2} - t_q\right\}(t_{q6} - t_1)\right] \\ f_8 &= f_a + (1 - f_a)/\left[1 + 50 ** (Z - 7)\right] \\ f_a &= f_b + (1 - f_b)/\left[1 + 50 ** (2 - V_{in})\right] \\ f_b &= 0.3 + 0.7\left[1 - \exp(-1.5t_q)\right] \end{aligned} \tag{D.17}$$

D.2.6 Modification for Variable Flooding Rates and Variable Rod Length

The variable t in the FLECHT heat transfer correlation is the time after the start of flooding as adjusted for variable flooding rate. The adjustment of time is made according to the equation

$$t = t_A + (0.214\,Z - 0.386)\left[\frac{\int_0^{t_A} V_{in}(t)dt}{V_{in}(t_A)} - t_A\right] \tag{D.18}$$

where t = adjusted time (s)
t_A = actual time since start of flooding (s)
Z = equivalent FLECHT elevation (ft)
$V_{in}(t)$ = flooding rate at time t (in./s).

The integral-of-power method[D.12] is used to calculate the elevation in the FLECHT facility that is equivalent to a given elevation in a nuclear reactor. By using the equivalent FLECHT elevation in the FLECHT correlation, the heat transfer coefficient at the given elevation in the nuclear reactor is calculated. The equation used to calculate the equivalent FLECHT elevation is

$$\int_0^{Z_1} P_F(Z)dZ = \frac{F_F}{F_L}\int_0^{Z_2} P_L(Z)\,dZ \tag{D.19}$$

where $P_F(Z)$ = normalized power of FLECHT rod at elevation Z
$P_L(Z)$ = normalized power of nuclear rod at elevation Z
F_F = axial power peaking factor for FLECHT rod = 1.66
F_L = axial power peaking factor for nuclear rod (specified by code input)
Z_2 = elevation on nuclear fuel rods
Z_1 = elevation on FLECHT rods that is equivalent to elevation Z_2 on nuclear fuel rods.

The procedure for solving for the equivalent FLECHT elevation Z_1 that corresponds with the nuclear reactor elevation Z_2 is

1. Store in computer memory a table of the integral of normalized FLECHT power versus elevation.

2. Numerically integrate the normalized power of the nuclear rod from elevation zero to elevation Z_2.

3. By interpolation in the table of Step 1, find the FLECHT elevation that has the same integral of power as the nuclear reactor at elevation Z_2.

D.3 Influence of Rod Bowing Upon Critical Heat Flux

The calculation of critical heat flux reduction due to fuel rod bowing is a user option in FRAPTRAN. If this option is used, both critical heat flux and fuel rod power are calculated according to the amount of fuel rod bowing. The reductions are calculated by empirical correlations. The correlations for critical heat flux reduction are

$$\begin{aligned} \Delta f_{CHF}(Z) &= F_{BCHF}\,(W(Z) - W_{Thr})/(1 - W_{Thr}) \\ \Delta f_{CHF}(Z) &= 0 \text{ if } W(Z) \le W_{Thr} \\ q_{CHFR}(Z) &= (1 - \Delta f_{CHF}(Z)\; q_{CHF}(Z)) \end{aligned} \tag{D.20}$$

where $\Delta f(Z)$ = fractional decrease in critical heat flux due to fuel rod bowing at elevation Z
q_{CHFR} = reduced critical heat flux
q_{CHF} = critical heat flux in absence of fuel rod bowing
$W(Z)$ = amount of fuel rod bowing (fraction of bowing required to contact adjacent fuel rod, 0 = no bowing, 1 = maximum possible bowing)
W_{Thr} = maximum amount of bowing which can occur without an effect on CHF (fraction of maximum bowing possible) (this quantity is specified by user input).
F_{BCHF} = multiplication factor specified by user input.

The reduction in fuel rod power due to bowing is calculated by the equation

$$\begin{aligned} P_r &= \left[1 + 0.01\,(0.94W(Z) - 2.84\,W(Z)^2)\right]P \\ P_r &= P \qquad\qquad (\text{for } W(Z) \le 0.3) \end{aligned} \tag{D.21}$$

where P_r = power reduced to account for fuel rod bowing
P = power in absence of fuel rod bowing.

D.4 Void Fraction

The void fraction of the coolant is calculated by the equation

$$\alpha = XV_g \,/\, \left[(1-X)V_f\gamma + XV_g\right] \tag{D.22}$$

where α = void fraction
X = coolant quality
V_f = specific volume of saturated liquid
V_g = specific volume of saturated gas
γ = slip velocity ratio.

The slip velocity ratio for void fraction calculations is always assumed to be 1.0 (homogeneous flow).

D.5 Coolant Enthalpy Model

The coolant enthalpy is calculated by a one-dimensional transient fluid flow model.[D.13] The model is given as input information the coolant enthalpy and mass flux at the bottom of the fuel rods and the elevation averaged coolant pressure. The input information can vary with time. The model also receives the FRAPTRAN calculated cladding surface heat flux. The heat flux can vary with time and elevation. The coolant enthalpy model then calculates the coolant enthalpy, which varies with time and elevation.

The model includes an energy conservation equation and a mass conservation equation. The coolant pressure is assumed to be spatially uniform and to change slowly with time so that the spatial and transient pressure terms are omitted from the energy equation. Thus, sonic effects are ignored. The model assumes homogeneous two-phase flow and a flow channel with a constant cross-sectional area.

The energy and mass conservation equations are

$$\rho\frac{\partial H}{\partial t} + G\frac{\partial H}{\partial z} = \frac{1}{L}(\phi + rq) \tag{D.23}$$

$$\frac{\partial \rho}{\partial t} + \frac{\partial G}{\partial z} = 0 \tag{D.24}$$

where ρ = coolant density (kg/m^3)
G = coolant mass flux (kg/m^2•s)
H = coolant enthalpy (J/kg)
$\frac{1}{L}(\phi+rq)$ = volumetric heat addition to coolant (J/m^3•s)
L = flow area per unit transfer surface are per unit axial length (m)
ϕ = surface heat flux (J/m^2•s)

q = heat generation rate/area (J/m^2-s)
r = fraction of heat generated directly in the coolant by neutrons and gamma rays
t = time (s)
z = axial elevation (m).

Assuming constant pressure, coolant conditions are considered a function of enthalpy only so that

$$\rho = \rho\ (H) \text{ and } \frac{\partial \rho}{\partial t} = \frac{\partial H}{\partial t}\left(\frac{d\rho}{dH}\right) \tag{D.25}$$

where density is evaluated at a reference pressure. By combining Equations D.23, D.24, and D.25, a relation can be established between the axial mass flux distribution and axial enthalpy distribution.

$$\frac{\partial G}{\partial z} = -\frac{\partial \rho}{\partial t} = -\frac{\partial H}{\partial t}\left(\frac{d\rho}{dH}\right) = -\frac{1}{\rho}\left(\frac{d\rho}{dH}\right)\left[\frac{1}{L}(\phi + rq) - G\frac{\partial H}{\partial z}\right] \tag{D.26}$$

The numerical solution for the local coolant enthalpy is given by the finite difference form of Equation D.25 with forward difference in time and averaged between spatial nodes. The equation is

$$H_j^{\ell+1} = H_{j-1}^{\ell} - (H_{j-1}^{\ell+1}) - H_j^{\ell}\left[\frac{1 - \alpha_{j-1/2}^{\ell}}{1 + \alpha_{j-1/2}^{\ell}}\right] + \frac{2\Delta t^{\ell+1} Q_{j-1/2}^{\ell}}{\rho_{j-1/2}^{\ell}\,(1 + \alpha_{j-1/2}^{\ell})} \tag{D.27}$$

where $\alpha_{j-1/2}^{\ell} = \dfrac{G_{j-1/2}^{\ell+1}\Delta t^{\ell}}{\rho_{j-1/2}^{\ell}\,\Delta z_j}$

$$\rho_{j-1/2}^{\ell} = \frac{1}{2}\,(\rho_j^{\ell} + \rho_{j-1}^{\ell})$$

$$G_{j-1/2}^{\ell+1} = \frac{1}{2}\,(G_j^{\ell+1} + G_{j-1}^{\ell+1})$$

$$Q_{j-1/2}^{\ell} = \frac{1}{2L}\left[\phi_j^{\ell} + \phi_{j-1}^{\ell}\right] + \frac{1}{2L}\left[(rq)_j^{\ell} + (rq)_{j-1}^{\ell}\right]$$

j = FRAPTRAN axial node number (see Figure D.1)
ℓ = time step number
$Z_j = Z_j - Z_{j-1}$
$\Delta t^{\ell} = t^{\ell} - t^{\ell-1}$

The numerical solution for the mass flux at the midpoint between axial nodes j and j-1 at the new time step is given by the finite difference form of Equation D.26. The equation is

$$G_j^{\ell+1} = G_{j-1}^{\ell+1}\left[\frac{2 + A_{j-1/2}}{2 - A_{j-1/2}}\right] + \frac{2\left(\dfrac{1}{\rho_{j-1/2}^{\ell}}\dfrac{d\rho}{dH_{j-1/2}}\,Q_{j-1/2}^{\ell}\,\Delta z_j\right)}{(A_{j-1/2} - 2)} \tag{D.28}$$

where $A_{j-½} = \Delta H \frac{1}{\rho^{\ell}_{j-½}} \frac{d\rho}{dH_{j-½}}$

$$\frac{d\rho}{dH_{j-½}} = \frac{\rho^{\ell}_j - \rho^{\ell}_{j-1}}{H^{\ell}_j - H^{\ell}_{j-1}}$$

$$\Delta H = H^{\ell}_j - H^{\ell}_{j-1}$$

$G_j^{\ell+1}$ is calculated using Equation D.28 before $H_j^{\ell+1}$ is calculated with Equation D.27. After the coolant enthalpy at the new time step has been calculated, the coolant density at the new time step is determined from the equation of state for water.

In summary, coolant inlet enthalpy and mass flux are input to define conditions at node zero. The mass fluxes for the remaining nodes are calculated from Equation D.28 using values for heat flux, enthalpy and density calculated in the previous time step or iteration. The enthalpy is then updated using Equation D.27, and a corresponding density is calculated from the fluid property relationships. Using the fluid conditions in the heat transfer correlations, a new heat flux is calculated, and the process is repeated.

If the time step is less than the minimum time for a drop of coolant to pass between any two axial nodes, the solution scheme is stable. This criterion is given by the equation

$$\Delta t^{\ell} \leq \left[\Delta z_j / v^{\ell}_{j+½}\right]_{min} \tag{D.29}$$

where $V_{j-½}$ = velocity of coolant at midpoint between axial nodes j and j + 1 (m/s)

The coolant quality and temperature are computed by the following equations:

Case 1. $H_i(z) \leq H_F(P)$

$$X_i(z) = 0.0 \tag{D.30}$$

$$T_i(z) = \theta(h_i(z), P)$$

Case 2.

$$H_F(P) \leq H_i(z) \leq H_G(P)$$
$$X_i(z) = (H_i(z) - H_F(P))/(H_G(P) - H_F(P)) \tag{D.31}$$
$$T_i(z) = T_s(P)$$

Case 3.

$$H_i(z) \geq H_G(P)$$
$$X_i(z) = 1.0 \tag{D.32}$$
$$T_i(z) = \theta(H_i(z), P)$$

where $H_i(z)$ = enthalpy (J/kg) of coolant in flow channel i at distance z from flow inlet
X_i = quality of coolant in flow channel i at distance z from flow inlet
$T_i(z)$ = temperature of coolant in flow channel I at distance z from flow inlet (K)
$H_F(P)$ = enthalpy (J/kg) of saturated liquid at coolant pressure P (N/m^2)
$H_G(P)$ = enthalpy (J/kg) of saturated gas at coolant pressure P
$T_s(P)$ = saturation temperature (K) at coolant pressure P
$\theta(H,p)$ = function specifying temperature (K) of coolant as a function of enthalpy and pressure.

The functions H_F, H_G, $\theta(h,P)$, and T_S are supplied by the water properties package.

D.6 References

D.1 S. R. Behling, et al., *RELAP4/MOD7: A Computer Program to Calculate Thermal and Hydraulic Phenomena in a Nuclear Reactor or Related System*, NUREG/CR-1998, EGG-2089 (1981).

D.2 J. S. Gellerstedt, et al., "Correlation of Critical Heat Flux in a Bundle Cooled by Pressurized Water," *Two-Phase Flow and Heat Transfer in Rod Bundles*, Symposium presented at the Winter Annual Meeting of the American Society of Mechanical Engineers, Los Angeles, California, (November 1969) pp. 63-71.

D.3 P. G. Barnett, *A Correlation of Burnout Data for Uniformly Heated Annuli and Its Use for Predicting Burnout in Uniformly Heated Rod Bundles*, AEEW-R463 (1966).

D4. E. D. Hughes, *A Correlation of Rod Bundle Critical Heat Flux for Water in the Pressure Range 150 to 725 psia*, IN-1412 (July 1970).

D.5 B. C. Slifer and J. E. Hench, *Loss-of-Coolant Accident and Emergency Core Cooling Models for General Electric Boiling Water Reactors*, NEDO-10329 (April 1971).

D.6 D. H. Knoebel, et al., *Forced Convection Subcooled Critical Heat Flux, D_2O, and H_2O Coolant with Aluminum and Stainless Steel Heaters*, DP-1306 (February 1973).

D.7 S. A. Eide and R. G. Gottula, *Evaluation and Results of LOFT Steady State Departure from Nucleate Boiling Tests*, TREE-NUREG-1043 (April 1977).

D.8 R. A. Smith and P. Griffith, "A Simple Model for Estimating Time to CHF in a PWR LOCA," *Transactions of American Society of Mechanical Engineers*, Paper No. 76-HT-9 (1976).

D.9 CENPD-162-P-1 Supplement 1-A, *C-E Critical Heat Flux for CE Fuel Assemblies with Standard Spacer Grids*, February 1977.

D.10 F. F. Cadek, et al., *PWR FLECHT Final Report Supplement*, WCAP-7931 (October 1972).

D.11 J. C. Lin, *Reflood Heat Transfer and Carryover Rate Fraction Correlations for LOFT Evaluation Model Calculations*, LTR-20-96, EG&G Idaho (March 1979).

D.12 F. M. Bordelon, et al., *LOCTA IV Program: Loss-of-Coolant Transient Analysis*, WCAP-8305 (June 1974).

D.13 J. E. Meyer and J. S. Williams, Jr., *A Momentum Integral Model for the Treatment of Transient Fluid Flow*. WAPD-BT-25.

D.14 F. W. Dittus and L.M.K. Boelter, *Heat Transfer in Automobile Radiators of the Tubular Type*, University of California Publications, 2 (1930) pp. 443-461.

D.15 J. Chen, "A Correlation of Boiling Heat Transfer to Saturated Fluids in Convective Flow," *Process Design Development, 5* (1966) pp. 322-327.

D.16 J. B. McDonough, W. Milich, E. C. King, *Partial Film Boiling with Water at 2000 Psia in a Round Tube*, MSA Research Corporation, Technical Report 62 (1958).

D.17 D. C. Groeneveld, *An Investigation of Heat Transfer in the Liquid Deficient Regime*, AECL-3281 (Rev.) (December 1978; Revised August 1979).

D.18 R. L. Dougall and W. M. Rohsenow, *Film Boiling on the Inside of Vertical Tubes with Upward Flow of the Fluid at Low Qualities*, MIT-TR-9079-26 (1963).

D.19 Y. Y. Hsu and W. D. Beckner, "A Correlation for the Onset of Transient CHF," Cited in L. S. Tong and G. L. Bennett, "PNRC Water Reactor Safety Research Program," *Nulear Safety, 18* (January/February 1977).

D.20 M. L. Pomeranz, "Film Boiling on a Horizontal Tube in Increased Gravity Fields," *Journal of Heat Transfer, 86*, (1974) pp. 213-219.

D.21 L. S. Tong, *Boiling Crisis and Critical Heat Flux*, TID-25887 (August 1972).

Table D.1 Heat Transfer Correlations

Mode 1: Subcooled Liquid Forced Convection: Dittus-Boelter[D.14]

$$h = 0.023 \frac{k}{D_e} Pr^{0.4} Re^{0.8}$$

so that

$$q = h (T_w - T_f)$$

Mode 2: Saturated Nucleate Boiling: Chen[D.15]

$$h = h_{mic} + h_{mac}$$

where $h_{mac} = 0.023 \frac{k_f}{D_e} Pr_f^{0.4} Re_f^{0.8} F$

$$h_{mic} = 0.00122 \frac{k_f^{0.79} C_{pf}^{0.45} \rho_f^{0.49} g_c'^{0.25}}{\sigma^{0.5} \mu_f^{0.29} h_{fg}^{0.24} \rho_g^{0.24}} \Delta P^{0.75} S$$

F = Reynolds number factor (see Table D.4)

S = Suppression factor (see Table D.5)

so that

$$q = (h_{mic} + h_{mac}) \Delta T_{sat}$$

Subcooled Nucleate Boiling: Modified Chen[D.15]

The modified Chen correlation is obtained by setting F = 1, such that

$$q = h_{mic} \Delta T_{sat} + h_{mac} (T_w - T_f)$$

Mode 4: High Flow Transition Boiling: Modified Tong-Young[D.1]

$$q_{total} = q_{TB} + q_{FB}$$

where q_{TB} = transition boiling (TB) heat flux = $q_{CHF} \phi_{TB}$ (Btu/ft^2-hr)
q_{CHF} = heat flux at departure from nucleate boiling (Btu/ft^2-hr)
ϕ_{TB} = exponential decay term = e^{-f}
q_{FB} = film boiling (FB) heat flux (Btu/ft^2-hr)

Table D.1 (contd)

$$f = \frac{0.001\ X_e^{2/3}}{\dfrac{q_{total}}{Gh_{fg}}\ \dfrac{\pi D_r}{A}}\ \frac{\Delta T_{sat}^{(1\ +\ 0.0016\Delta T_{sat})}}{100}$$

X_e = equilibrium quality

Mode 4: Optional High Flow Transition Boiling: McDonough, Milich, and King[D.16]

$$q = q_{CHF} - C(P)\ (T_w - T_{w,CHF})$$

Pressure, psi	C(P)
2,000	979.2
1,200	1,180.8
800	1,501.2

where $T_{w,CHF} = T_{sat} + 0.072\ \exp\ (-P/1260)(q_{CHF})^{0.5}$

Mode 5: High Flow Film Boiling: Condie-Bengston III[D.1]

$$q_{total} = q_{TB} + q_{FB}$$

where $q_{FB} = h\ \Delta T_{sat}$

$$h = \frac{k_g^{0.4376} Pr_w^{2.3070} Re_g [0.6004 + 0.2456\ \ln(1 + X_e)]}{D_e^{0.7842} (1 + X_e)^{2.59028}}$$

and where the subscript w indicates evaluation at the wall temperature.

Mode 5: Optional High Flow Film Boiling: Groeneveld[D.17]

$$h = a\ \frac{k_g}{D_e}\ Pr_w^c \left\{ Re_g \left[X + \frac{\rho_g}{\rho_f}\ (1-X) \right] \right\}^b$$

$$\left[1.0 - 0.1\ (1-X)^{0.4}\ \left(\frac{\rho_f}{\rho_g} - 1\right)^{0.4} \right]^d$$

Table D.1 (contd)

Coefficient	Groeneveld Equation (5.9) (cluster geometry)	Groeneveld Equation (5.7) (annular geometry)
a	0.00327	0.052
b	0.901	0.688
c	1.32	1.26
d	-1.50	-1.06

Mode 5: Optional High Flow Film Boiling: Dougall and Rohsenow [D.18]

$$h = 0.023 \frac{k_g}{D_e} Pr_g^{0.4} \left\{ Re_g \left[X + \frac{\rho_g}{\rho_f} (1-X) \right] \right\}^{0.8}$$

Mode 6: Low Flow Conditions

High Void Fraction Free Convection and Radiation

$$q_{total} = q_{liquid} + q_{vapor}$$

where $q_{vapor} = h\ (T_w - T_v)\alpha$

$$h = h_c + h_r$$

$$h_c = 0.4 \frac{k}{D_e} (Gr\ Pr)^{0.2}$$

$$Gr = (D_e/2)^3\ g'_c\ \beta\ (T_w - T_f)\ (\rho/\mu)^2$$

Properties are evaluated at T_{film}, where

$$T_{film} = \frac{(T_w + T_f)}{2}$$

Low Void Fraction: Modified Hsu [D.19] and Bromley-Pomeranz[D.20]

$$q_{total} = q_{liquid} + q_{vapor}$$

where $q_{liquid} = h\Delta t_{sat}\ (0.96-\alpha)$

$$h = h_{TB} + h_{FB}$$

$$h_{TB} = A \exp\ (-B\Delta T_{sat})$$

$$A = 2.71828 \frac{q_{CHF} - q_{vapor}}{\Delta T_{Hsu}} - (0.96 - \alpha)\ h_{FB}\big|_{\Delta T_{Hsu}}$$

Table D.1 (contd)

$\Delta T_{Hsu} = 1/B$

log-log interpolation with pressure where

$B = 0.0076,\ P = 60$ psia
$B = 0.0082,\ P = 90$ psia

$$h_{FB} = h_{Bromley-Pomerang} = 0.62 \frac{D_e^{0.172}}{\lambda_c} \frac{k_g^3 \rho_g \left(e_f - e_g\right) h_{fg}\ g^{0.25}}{D_e\ \mu_g\ \Delta T_{sat}}$$

$$\lambda_c = 2\pi \frac{g_c\ \sigma^{0.5}}{g\ (\rho_f - \rho_g)}$$

Mode 8: Superheated Vapor Forced Convection: Dittus and Boelter[D.14]

$$h = 0.023 \frac{k}{D_e} Pr^{0.4}\ Re^{0.8}$$

Mode 9: Low Pressure Flow Film Boiling: Dougall and Rohsenow[D.18]

$$h = 0.023 \frac{Kg}{D_e} Pr_g^{0.4} \left\{ Re_g \left[X + \frac{\rho_g}{\rho_f}(1 - X) \right] \right\}^{0.8}$$

Table D.2 Symbol Definitions for Tables D.1 and D.3

where

h	=	heat transfer coefficient, Btu/ft^2•hr•°F
h_r	=	radiation heat transfer coefficient
k	=	thermal conductivity, Btu/ft•hr•°F
D_e	=	equivalent diameter based on wetted perimeter, ft
D_{HY}	=	$D_r (D_r + D_{HE})^{0.5} - D_R$, ft
D_{HE}	=	heated equivalent diameter, ft
D_r	=	fuel rod diameter, ft
Pr	=	Prandtl number, $\frac{c_p \mu}{k}$
Re	=	Reynolds number, $\frac{GD_e}{\mu}$
G	=	mass flux (lbm/ft^2•hr)
μ	=	viscosity, lb$_m$/ft•hr
C_p	=	specific heat, Btu/lb$_m$•°F
H	=	enthalpy (Btu/lb)
H_{fg}	=	latent heat of vaporization (Btu/lb$_m$)
T_{sat}	=	saturation temperature, °F
T_w	=	wall temperature, °F
ΔT_{sat}	=	T_W-T_{sat}, °F
T_f	=	coolant temperature, °F
q	=	heat flux, Btu/ft^2•hr
P	=	pressure, psia
ΔP	=	difference between saturation pressures at T_W and T_{sat}, lb$_f$/ft^2
Xe	=	equilibrium quality
α	=	void fraction
n	=	X_A/X_E
ρ	=	density, lb$_m$/ft^3
L	=	channel length, in.
g	=	local acceleration due to gravity, ft/s^2
g_c	=	gravitational constant, 32.2 ft-lb$_m$/lb$_f$•s^2
g'_c	=	$3600^2 g_c$
σ	=	surface tension, lb$_f$/ft
Q	=	volumetric flow rate, ft^3/s
A	=	flow area, ft^2
β	=	coefficient of thermal expansion, $\frac{1}{°F}$
S	=	ratio of velocity of vapor phase to velocity of liquid phase (slip ratio)
		and subscripts
CHF	=	critical heat flux
total	=	total heat flux
f	=	saturated liquid conditions
g	=	saturated vapor conditions
v	=	superheated vapor conditions
E	=	equilibrium
w	=	wall
A	=	actual

Table D.3 Critical Heat Flux Correlations

1. Babcock & Wilcox Company, B&W-2[D.2]

$$q_{CHF} = \frac{1.15509 - 0.40703(12De)}{12.71 \times (3.0545G')^{A}} \left[(0.3702\times10^{8})\ (0.59137G')^{B} - 0.15208XH_{fg}G\right] \Big/ F_{APk}$$

where $A = 0.71186 + (2.0729\times10^{-4})\ (P-2000)$
$B = 0.834 + (6.8479\times10^{-4}\ (P-2000)$

and where $G' = \dfrac{G}{10^{6}}$

H_{fg} = heat of vaporization
F_{APk} = axial power profile factor for the B&W-2 correlation at elevation station k.

The axial power profile factor is calculated by

$$F_{APk} = \left\{ 1.02\ S_1 + \sum_{i=2}^{k} \left[\left\{ q_i - (dq/dZ)_i \right\} \exp\left(C_1(Z_i - Z_k) \right) - \left\{ q_{i-1} - (dq/dZ)_i \right\} \exp\left(C_1(Z_{i-1} - Z_k) \right) \right] \right\} \Big/ C_2 q_k$$

where q_i = surface heat flux at axial node I (Btu/ft^2•hr)
Z_i = elevation of axial node i (ft)
$(dq/dZ)_i = (q_i - q_{i-1})/C_1(Z_i - Z_{i-1})$
$C_1 = 2.988(1-X)^{7.82}/(G/10^{6})^{0.457}$
$C_2 = -C_1 Z_K$
$S_1 = q_i\ [\exp(C_1(Z_1 - Z_K)) - \exp(C_2)]$.

The correlation was developed from data on rod bundles in water over the parametric ranges given by:

Equivalent diameter	0.2 to 0.5 in.
Length	72 in.
Pressure	2,000 to 2,400 psia
Mass flux	0.75×10^{6} to 4.0×10^{6} lb/ft^2•hr
Burnout quality	-0.03 to 0.20

Table D.3 (contd)

2. **Local Barnett**[D.3]

$$q_{CHF} = 10^6 \left[\frac{A + B(H_{fg}X)}{C}\right]$$

where $A = 69.40\ D_{HE}^{\ 0.751} G'^{0.226} \left[1.0 - 0.672\ \exp(-6.090 D_{HY}\ G')\right]$

$B = -0.250\ D_{HE}^{\ 1.000}\ G'^{1.000}$

$C = 165.9\ D_{HY}^{\ 1.246} G'^{0.329}$

The parametric range of the data is as follows:

Equivalent diameter	0.0215 in. < D_{HE} < 0.316 0.01058 in. < D_{HY} < 0.0729167
Length	24 to 108 in.
Pressure	1,000 psia
Mass flux	0.14×10^6 to 6.20×10^6 $lb_m/ft^2 \bullet hr$
Inlet subcooling	0 to 412 Btu/lb_m

3. **Modified Barnett**[D.4]

$$q_{CHF} = 10^6 \left[\frac{A + B(H_f - H_{in})}{C + L}\right]$$

where $A = 73.71\ D_{HE}^{0.052} G'^{0.663} \left(1.0 - 0.315\ \exp(-11.34 D_{HY}\ G')\right) \dfrac{888.6}{h_{fg}}$

$B = 0.104\ D_{HE}^{1.445} G'^{0.691}$

$C = 45.44\ D_{HY}^{\ 0.0817} G'^{0.5866}$

H_{in} =local coolant enthalpy

Data were from rod bundles containing water and were over parametric ranges given by:

Rod diameter	0.395 to 0.543 in.
Length	32.9 to 174.8 in.
Pressure	150 to 725 psia
Mass Flux	0.03×10^6 to 1.7×10^6 $lb_m/ft^2 \bullet hr$
Inlet subcooling	6 to 373 Btu/lb_m

Table D.3 (contd)

4. **General Electric Company**[D.5]

$$q_{CHF} = 10^6 \ (0.8 - X)$$

for

$$G \geq 0.5x10^6 \ lb_m/ft^2 \bullet hr$$

and

$$q_{CHF} = 10^6 \ (0.84 - x)$$

for

$$G < 0.5x10^6 \ lb_m/ft^2 \bullet hr$$

5. **Savannah River**[D.6]

$$Q_{CHF} = 188{,}000 \ (1.0 + 0.0515V) \ (1.0 + 0.069 \ T_{SUB})$$

where V = fluid velocity, ft/s

T_{SUB} = fluid saturation temperature minus fluid temperature, °F

6. **Westinghouse Company, W-3**[D.1]

$$q_{CHF} = 1.x10^6 \Big[2.022 - 4.302x10^{-4}P$$

$$+ \ (0.1722 - 9.84x10^{-5}P \ \exp((18.177 - 4.129x10^{-3}P)X)\Big]$$

$$\Big[1.157 - 0.869X\Big] (0.1484 + X(-1.596 + 0.1729 \ ABS(X))) \ G' + 1.037\Big]$$

$$\Big[0.8258 + 7.94x10^{-4}(H_f - H_{IN})\Big]\Big[0.2664 + 0.8357 \ \exp(-3.151(12D_{HE}))\Big] \ F_{CW}/F_{APk}$$

where H_f = enthalpy of saturated liquid (Btu/lb_m)
H_{IN} = enthalpy of coolant at bottom of fuel rods (inlet enthalpy) (Btu/lb_m)
F_{CW} = cold wall factor
F_{APk} = axial power profile factor at elevation station k
G' = $G/10^6$.

Table D.3 (contd)

The W-3 correlation is valid in the following parametric ranges:

Equivalent diameter	0.016667 to 0.058333 ft
Length	10-144 in.
Pressure	1000-2400 psia
Mass flux	1×10^6 $lb_m/ft^2 \bullet hr$
Exit quality	≤ 0.15

The cold wall factor is calculated by the equation [D.21]

$$F_{CW} = 1. - (1.-D_E/D_{HE}) \Big[13.76 - 1.372 \exp(1.78X) - 4.732(G/10^6)^{-0.0535} - 0.0619(P/1000)^{0.14} - 8.509(12D_{HE})^{0.107} \Big]$$

The axial power profile factor is calculated by the equation

$$F_{APk} = \left\{ S_1 + \sum_{i=2}^{K} \left[\left\{ q_i - (dp/dZ)_i \right\} \exp(C_1(Z_i - Z_k)) - \left\{ q_{i-1} - (dq/dZ)_i \right\} \exp(C_1(Z_{i-1} - Z_k)) \right] \right\} / C_2 q_k$$

where
F_{APk} = axial power profile factor axial node k
q_i = surface heat flux at axial node i
Z_i = elevation of axial node i (ft)
$(dq/dZ)_i = (q_i - q_{q-1})/C_1(Z_i - Z_{i-1})$
$C_1 = 1.8(1-X)^{4.31}/[(G/10^6)^{0.478}]$
$C_2 = -C_1 Z_k$
$S_1 = q_1 [\exp(C_1(Z_1 - Z_k)) - \exp(C_2)]$.

7. **High Flow Saturation DNB Correlation: Hsu and Beckner[D.19]**

If α (void fraction) <0.96:

$$\frac{q_{CHF} - q_{dry}}{q'_{w-3}} = [1.76\ (0.96 - \alpha)]^{0.5}$$

Table D.3 (contd)

where q_{dry} = Heat flux to vapor as calculated by Dittus-Boelter correlation for Re >2000
q_{dry} = Maximum of heat fluxes calculated by Rohsenow-Choi and Free Convection + Radiation correlations for Re ≤2000
q'W-3 = W-3 CHF correlation evaluated at 0.0 quality (X=0) and zero subcooling ($h_f - h_{in} = 0$).

If the void fraction ≥0.96 then dryout occurs.

8. **LOFT Correlation**[D.7]

For the range $2000 \le P \le 2400$; $0.4\times10^6 \le G < 2.5\times10^6$; $-0.30 \le X \le 0.2$

$$q_{CHF} = 1.31569\times10^6 - 3.79605\times10^2\,P + 8.32015\times10^{-2}\,G$$
$$+ 1.08312\times10^{-2}\,PX - 1.01982\,GX$$

For the range $1000 \le P \le 2000$; $0.4\times10^6 \le G \le 2.0\times10^6$; $-0.05 \le X \le 0.50$

$$q_{CHF} = 1.880919\times10^6 - 850.58P - 1.099GX$$
$$+ 0.13P^2 - 1.186207\times10^6\,X^2$$

9. **Modified Zuber Correlation**[D.8] (used when G < 200,000)

$$q_{CHF} = (0.96-\alpha)\,(0.130)\,(H_{fg})\,(\rho_g)^{0.5}\,[\sigma g_c\,g\,(\rho_f-\rho_g)]^{0.25}\,(\rho_f/(\rho_f+\rho_g))^{0.5}$$

10. **CE-1 Correlation**[D.9]

$$\frac{q_{CHF}}{10^6} = \frac{b_1\left(\frac{d}{d_m}\right)^{b_2}\left[(b_3 + b_4P)\left(\frac{G}{10^6}\right)^{(b_5 + b_6P)} - \left(\frac{G}{10^6}\right)(X)\,(H_{fg})\right]}{F_{APk}\left(\frac{G}{10^6}\right)^{\left(b_7P + b_8\frac{G}{10^6}\right)}}$$

where q_{CHF} = critical heat flux, Btu/hr•ft^2
P = pressure, psia
$\frac{d}{d_m}$ = 1.0
G = local mass velocity at CHF location, lb$_m$/hr•ft^2
X = local coolant quality at CHF location, decimal fraction
H_{fg} = latent heat of vaporization, Btu/lb$_m$
b_1 = 2.8922×10^{-3}

Table D.3 (contd)

b_2 = -0.50749
b_3 = 405.32
b_4 = -9.9290×10^{-2}
b_5 = -0.67757
b_6 = 6.8235×10^{-4}
b_7 = 3.1240×10^{-4}
b_8 = -8.3245×10^{-2}
F_{APk} = axial power profile factor at elevation station k, the factor is calculated the same as is shown for the W-3 correlation.

The CE-1 correlation is valid in the following parametric ranges:

Pressure	1785 to 2415 psia
Local coolant quality	-0.16 to 0.20
Local mass velocity	0.87×10^6 to 3.21×10^6 $lb_m/hr \cdot ft^2$
Inlet temperature	382 to 644 °F
Subchannel wetted equivalent diameter	0.3588 to 0.5447 in.
Subchannel heated equivalent diameter	0.4713 to 0.7837 in.
Heated length	84 to 150 in.

Table D.4 Chen's Reynolds Number Factor, F

Chen's Reynolds Number Factor is calculated by interpolating F as a function of λ, where λ is defined as:

$$\lambda = \left(\frac{X_e}{1 - X_e}\right)^{0.9} \left(\frac{\rho_f}{\rho_f}\right)^{0.5} \left(\frac{\mu_g}{\mu_F}\right)^{0.1}$$

λ	F
0.1	1.07
0.2	1.21
0.3	1.42
0.4	1.63
0.6	2.02
1.0	2.75
2.0	4.30
3.0	5.60
4.0	6.75
6.0	9.10
10.0	12.10
20.0	22.00
50.0	44.70
100.0	76.00
400.0	200.00

Table D.5 The Chen Suppression Factor, S

$(Re_f)F^{1.25}$	S
10^3	1.000
10^4	0.893
$2x10^4$	0.793
$3x10^4$	0.703
$4x10^4$	0.629
$6x10^4$	0.513
10^5	0.375
$2x10^5$	0.213
$3x10^5$	0.142
$4x10^5$	0.115
$6x10^5$	0.093
10^6	0.083
10^8	0.000

Table D.6 Range of applicability of generalized FLECHT correlation

Variable	Applicable range of variable
Flooding rate (in./s)	0.4 - 10
Reactor vessel pressure (psia)	15 - 90
Inlet coolant subcooling (°F)	16 - 189
Initial cladding temperature (°F)	300 - 2200
Peak fuel rod power (kW/ft)	0.51 - 1.4
Flow blockage (%)	0 - 75
Equivalent elevation in FLECHT facility (ft)	2 - 10

Table D.7. Variable and symbol definitions in FLECHT correlation

Variables

V_{in} = flooding rate (in./s)
T_{init} = peak cladding temperature at start of flooding (°F)
Q'_{max} = fuel rod power at axial peak at start of flooding (kW/ft)
P = reactor vessel pressure (psia)
Z = equivalent FLECHT elevation (ft)
T_{sub} = flood water subcooling at inlet (°F)
t = time after start of flooding as adjusted for variable flooding rate (s)
h = heat transfer coefficient (Btu/hr•ft^2•°F)
Q_{maxtq} = radial power shape factor
= 1.0 for a nuclear rod
= 1.1 for electrical rod with radially uniform power
B = flow blockage (%) (B always set equal to zero)

Symbols

a**b = a^b

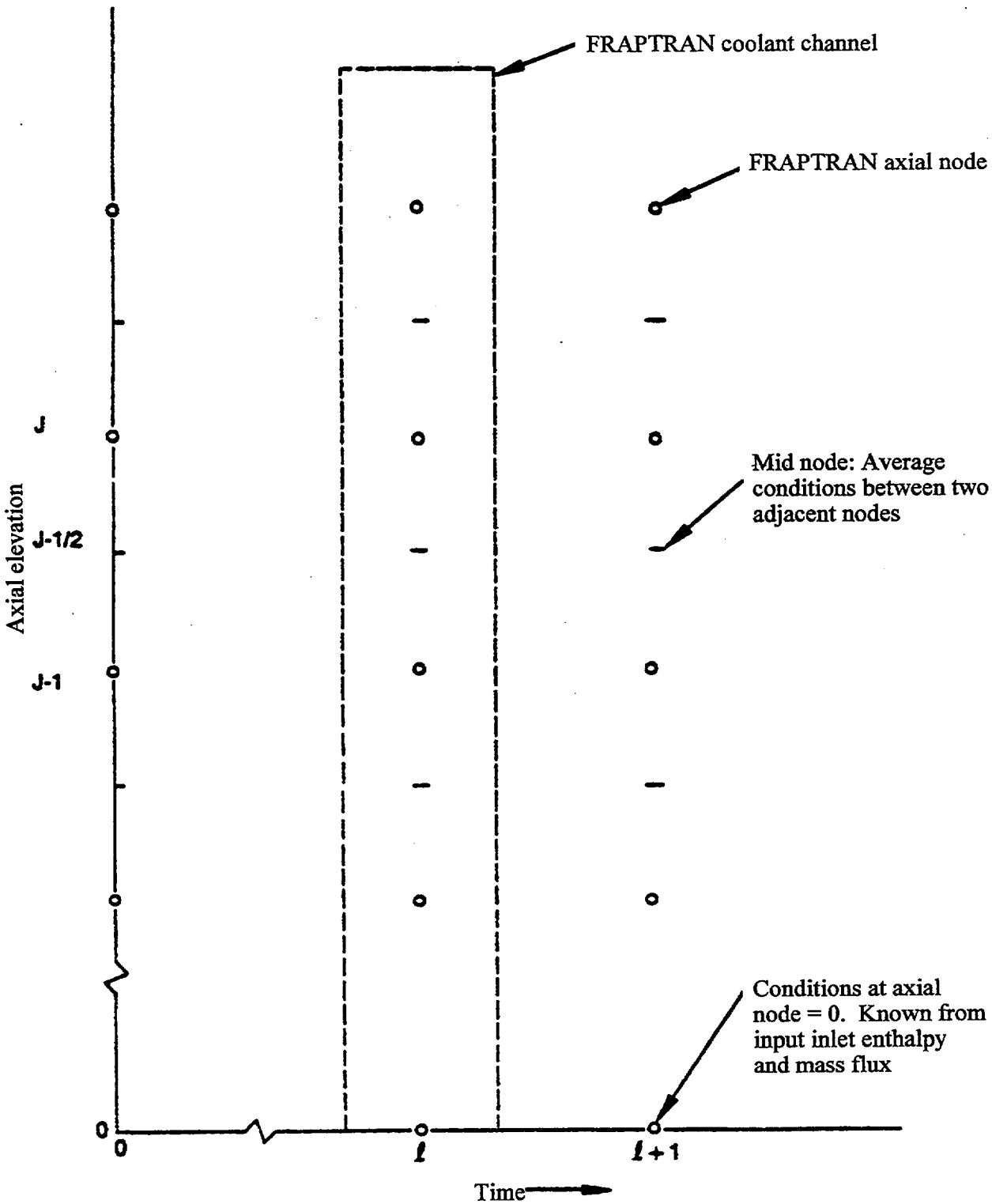

Figure D.1 Description of Geometry Terms in Coolant Enthalpy Model

APPENDIX E

NUMERICAL SOLUTION OF THE PLENUM ENERGY EQUATIONS

APPENDIX E

NUMERICAL SOLUTION OF THE PLENUM ENERGY EQUATIONS

The Crank-Nicolson finite difference form of the six energy equations presented in Section 2.3 is

Plenum Gas:

$$\rho_g V_g C_g \frac{\left(T_g^{m+1} - T_g^m\right)}{} = \frac{A_{ep} h_{ep}}{2}\left(T_{ep}^m - T_g^m - T_g^{m+1} + T_{ip}^{m+1}\right)$$

$$+ \frac{A_{cl} h_{cl}}{2}\left(T_{cli}^m - T_g^m + T_{cli}^{m+1} - T_g^{m+1}\right) \qquad \text{(E.1)}$$

$$+ \frac{A_{ss} h_s}{2}\left(T_{ss}^m - T_g^m + T_{ss}^{m+1} - T_g^{m+1}\right)$$

Spring Center Node:

$$\rho_s V_{sc} C_s \frac{\left(T_{sc}^{m+1} - T_{sc}^m\right)}{\tau} = \bar{q}''' V_{sc} + \frac{A_{sc} K_s}{2\, R_{ss}}\left(T_{ss}^m - T_{sc}^m + T_{ss}^{m+1} - T_{sc}^{m+1}\right) \qquad \text{(E.2)}$$

Spring Surface Node:

$$\rho_s V_{ss} C_s \frac{\left(T_{sc}^{m+1} - T_{sc}^m\right)}{\tau} = \bar{q}''' V_{ss} + \frac{A_{sc} K_s}{2\, R_{ss}}\left(T_{sc}^m - T_{ss}^m + T_{sc}^{m+1} - T_{ss}^{m+1}\right)$$

$$+ A_{ss} \frac{\left(h_{rads} + h_{conc}\right)}{2}\left(T_{cli}^m - T_{ss}^m + T_{cli}^{m+1} - T_{ss}^{m+1}\right) \qquad \text{(E.3)}$$

$$+ A_{ss} \frac{h_s}{2}\left(T_g^m - T_{ss}^m + T_g^{m+1} - T_{ss}^m\right)$$

Cladding Interior Node:

$$\rho_{cli} V_{cli} C_{cl} \frac{\left(T_{cli}^{m+1} - T_{cli}^{m}\right)}{\tau} = \bar{q}''' V_{cli} + \frac{\left(A_{cl} h_{radc} + A_{ss} h_{conc}\right)}{2}$$

$$\left(T_{ss}^{m} - T_{cli}^{m} + T_{ss}^{m+1} - T_{cli}^{m+1}\right) + \frac{A_{cl} h_{cl}}{2} \left(T_{g}^{m} - T_{cli}^{m} + T_{g}^{m+1} - T_{cli}^{m+1}\right) \tag{E.4}$$

$$+ \frac{A_{cl} K_{cl}}{2.\Delta r/2} \left(t_{clc}^{m} - T_{cli}^{m} + T_{clc}^{m+1} - T_{cli}^{m+1}\right)$$

Cladding Center Node:

$$\rho_{cl} C_{cl} V_{clc} \frac{\left(T_{clc}^{m+1} - T_{clc}^{m}\right)}{\tau} = \bar{q}''' V_{clc} + \frac{A_{cl} K_{cl}}{2.\Delta r/2} \left(T_{cli}^{m} - T_{clc}^{m} + T_{cli}^{m+1} - T_{clc}^{m+1}\right)$$

$$+ \frac{A_{cl} K_{cl}}{2.\Delta r/2} \left(T_{clo}^{m} - T_{clc}^{m} + T_{clo}^{m+1} - T_{clc}^{m+1}\right) \tag{E.5}$$

Cladding Exterior Node:

$$T_{clo}^{m+1} = T_{cool}^{m+1} \tag{E.6}$$

The superscripts m and m+1 represent the values of quantities at the old (m) and new (m+1) time. The steady-state finite difference equations are obtained by setting the left side of Equations (E.1) through (E.5) to zero and by dropping the superscripts m and m+1. Equations (E.1) through (E.5) can be written in the following simplified form by combining constant coefficients and known temperatures (T_j^m):

Plenum Gas:

$$A_1 T_g^{m+1} + B_1 T_{cli}^{m+1} + C_1 T_{ss}^{m+1} = I_1 \tag{E.7}$$

Spring Center Node:

$$C_2 T_{ss}^{m+1} + D_2 T_{sc}^{m+1} = I_2 \tag{E.8}$$

Spring Surface Node:

$$A_3 T_g^{m+1} + B_3 T_{cli}^{m+1} + C_3 T_{ss}^{m+1} + D_3 T_{sc}^{m+1} = I_3 \tag{E.9}$$

Combining Equations (E.8) and (E.9):

$$A_3 T_g^{m+1} + B_3 T_{cli}^{m+1} + \bar{C}_3 T_{sc}^{m+1} = \bar{I}_3 \tag{E.10}$$

where

$$\bar{C}_3 = C_3 - \frac{D_3}{D_2} C_2$$

$$\bar{I}_3 = I_3 - \frac{D_3}{D_2} I_2$$

Cladding Interior Node:

$$A_4 T_g^{m+1} + B_4 T_{cli}^{m+1} + C_4 T_{ss}^{m+1} + E_4 T_{clc}^{m+1} = I_4 \tag{E.11}$$

Cladding Center Node:

$$B_5 T_{cli}^{m+1} + E_5 T_{clc}^{m+1} + F_3 T_{clo}^{m+1} = I_5 \tag{E.13}$$

Equations (E.7) through (E.12) represent a set of six equations having six unknowns.

In the above equations, all material properties and heat transfer coefficients (except convection to the coolant) are shown as constants. For the transient case, the temperature-dependent material properties and heat transfer coefficients are evaluated at the average of the temperatures (TBAR) at the start and end times of each time step. For the steady-state calculation, TBAR represents an estimate of the true steady state temperature. Therefore, it is required that the steady state and transient solutions to Equations (E.7) through (E.12) be iterated to convergence on TBAR.

APPENDIX F

DESCRIPTION OF SUBROUTINES

APPENDIX F

DESCRIPTION OF SUBROUTINES

The hierarchy of the subroutines in FRAPTRAN is shown in Tables F.1 through F.10. The function of each subroutine is also provided in the tables. The top of the hierarchy is shown in Table F.1. FRAPTRAN is the program name of the code. Subroutine FRAP is the primary subroutine called by FRAPTRAN. The subroutines called by subroutine FRAP are shown in Table F.2. Four major subroutines are called by subroutine FRAP.

1. CARDIN, which reads and processes the input cards by calling the subroutines shown in Tables F.3 and F.4;

2. INITIA, which initializes the variables for a cold startup by calling the subroutines shown in Table F.5;

3. COMPUT, which calculates the fuel rod response by calling the subroutines shown in Tables F.6 through F.9; and

4. STORE6, which stores and displays the calculated fuel rod response by calling the subroutines shown in Table F.10.

TABLE F.1 First Level of Subroutine Calls

FRAPTRAN	
IOFILES	read input data in NAMELIST format, rewrite in formatted format for routines called by CARDIN
ECHO1	echo out input data to output file
FRAP	main driver routine for performing transient analysis (Table F.2)

TABLE F.2 Subroutine Calls from Subroutine FRAP	
FRAP	
STH2XI	read in the water properties table and store it in an array
START0	if cold startup, initialize variables
CARDIN	read and process input data (Table F.3)
INITIA	initialize variables (Table F.4)
CRANK6	march the solution to the end time by repetitively taking a time step and cycling through the solution scheme
SETUP6	initialize variables
COMPUT	calculate values of variables at an advanced time (Table F.6)
STORE6	equate start of time step variables to end of time step variables (Table F.10)

TABLE F.3 Subroutine Calls from Subroutine CARDIN	
CARDIN	
IZEROT	zero integer array
CININP	set default values
ALIAS	interpret alphanumeric input
IOINP	read/input/output data
NUMINP	read solution control data
DALINP	read model tuning data
POWINP	read power data
INTINP	read fuel rod design data
MODINP	read model selection data
BCDINP	read boundary condition data
UNTINP	convert units
DEFINP	set default values
COMINP	calculates and loads common block variables (Table F.4)

TABLE F.4 Subroutine Calls from Subroutine COMINP	
COMINP	
IZEROT	zero integer array
RLPST1	if active T-H code link, define radial nodalization according to information in the FRAPC common block
FC2PTR	calculate pointers to array storage for fuel deformation model
FR2PTR	calculate amount of storage for fuel deformation model
PHYPRP	MATPRO routine to calculate temperature independent thermal properties
THMPRP	make calls to MATPRO routines CTHCON, CCP, and FCP and generate thermal property tables
GRAFINI	initialize CSWF graphics file
STH2XI	read water properties table and store it in an array

TABLE F.5 Subroutine Calls from Subroutine INITIA	
INITIA	
STARTI	calculate pointers to array storage for 2-D heat conduction model
ZEROUT	set A1 array to zero
POWRMP	calculate power increment for power ramp
PORCOR	calculate open porosity of cladding
PLENV	calculate plenum volume
GAPPRS	calculate moles of gas in fuel rod
RESTFS	read values of burnup dependent variables from a file written by FRAPCON-3; re-initialize variables
CELMOD	MATPRO routine for cladding elastic modulus
CSHEAR	MATPRO routine for shear modulus of cladding
ZRDWR	

TABLE F.6 Subroutine Calls from Subroutine COMPUT	
COMPUT	
TIMSTP	calculate size of time step
ARYMDI	initialize arrays for 2-D heat conduction model
POWER	calculate power peaking factor for the FLECHT correlation
PHYPRP	MATPRO routine to reset values of temperature independent thermal properties
TZSET	reset start of time step variables for 2-D heat conduction model
RLPST2	if active T-H code link, equate FRAPTRAN temperature arrays to the temperature arrays passed to FRAPTRAN
HEAT	if no active T-H code link, calculate fuel and cladding temperature (Table F.7)
PLNT	calculate plenum gas temperature, PLNT calls simultaneous equation solver SIMQ and MATPRO routines CCP, CTHCON, GTHCON, and GVISCO
THETAV	calculate azimuthal average of 2-D heat conduction variables
DEFORM	FRACAS-I rigid fuel deformation model to calculate cladding deformation (Table F.9)
VSWELL	calculate volume generated by local cladding ballooning and average gas gap temperature
GSFLOW	GAPPRS - calculate pressure of gas in fuel rod; use MATPRO routine GVISCO
HONR	use method of Newton to calculate gas pressure for next iteration
COBILD	calculate oxidation of cladding with Cathcart model, if selected
CANEAL	MATPRO routine to calculate annealing of cladding
BALON2	calculate local ballooning of the cladding using subroutines SIMQ and GCONR2; and MATPRO routines CANEAL, CANISO, CCP, CKMN, CMLIMT, CSTRNI, FCP, FTHCON, and CTHCON
CANISO	MATPRO routine to calculate coefficients of cladding anisotropy
CESIOD	MATPRO routine to calculate available quantity of cesium and iodine
FAR1	calculates flow area reduction; uses subroutines BALON2, FTHCON, and GCONR2
	BALON2 calculate local ballooning of the cladding using subroutines SIMQ and GCONR2; and MATPRO routines CANEAL, CANISO, CCP, CKMN, CMLIMT, CSTRNI, FCP, FTHCON, and CTHCON

TABLE F.7 Subroutine Calls from Subroutine HEAT	
HEAT	
COOL	calculate or read coolant conditions; subroutines called are FABEND, PRNTC, PRNTMP, STH2X2, TRANSH, and ZEROUT
ASET	if 2-D heat conduction modeled, spool vectors of 2-D arrays into 1-D arrays; subroutines IDXGN1 and IDXGN2 are called
POWER	calculate heat generation in fuel
QCON	if 2-D heat conduction modeled, calculate azimuthal heat conduction; subroutine IDXGN1 and MATPRO routines FCP, FTHCON, and CTHCON are called
METWTB	calculate cladding oxidation using Baker-Just model, if selected
CHITOX	if cladding failure, calculate oxidation on inside surface of cladding
SURFBC	if steady-state heat conduction, calculate coefficients A and B
HTRC	if steady-state heat conduction, calculate cladding surface temperature, heat flux, and heat transfer coefficient; use MATPRO routine GVISCO
GAPHTC	calculate gap conductance; MATPRO routines GTHCON, CMHARD, CTHCON, FTHCON, and EMSSF2 are called
HT1SST	if steady-state heat conduction, calculate fuel and cladding temperature; subroutines BDCOND, KMOD, MADATA, FTBMOV, and POWRAZ are called
HT1TDP	if transient heat conduction, calculate fuel and cladding temperatures (Table F.8)
ASTOR	if 2-D heat conduction is modeled, spool 1-D arrays into vectors of a 2-D array; subroutines IDXGN1 and IDXGN2 are called
ZOTCON	MATPRO routine for thermal conductivity of zirconium dioxide

TABLE F.8 Subroutine Calls from Subroutine HT1TDP	
HT1TDP	
BDCOND	set coefficients in boundary condition equation
MADATA	calculate thermal properties of each mesh point
POWRAZ	if 2-D heat conduction, calculate azimuthal power factor
REFLOOD	if reflooding of reactor core is specified, calculate cladding surface temperature, heat flux, and heat transfer coefficient; subroutines ZEROUT, STH2X2, STH2X3, CRFZQH, POWING, WCORR, HCALF, TAILND, DBINVS, and ENRISE are called
HTRC	if REFLOOD is not called, calculate cladding surface temperature, heat flux, and heat transfer coefficient; subroutines PCHF (critical heat flux correlations), QDOT (heat transfer correlations), ROOT1, STH2X2, STH2X3, VOID, ZOEMIS, and FABEND are called
CCPMOD	if alpha to beta phase transition in cladding occurs, integrate cladding specific heat with temperature; subroutines CCPINT and CCP are called
ZOTCON	MATPRO routine for thermal conductivity of zirconium dioxide

TABLE F.9 Subroutine Calls from Subroutine DEFORM	
DEFORM	
CTHEXP	calculate cladding thermal expansion
FTHEXP	calculate fuel thermal expansion
CKMN	calculate the equation of state coefficients for the cladding
CMLIMT	calculate the mechanical limits of the cladding
STRESS	calculate cladding effective stress at instability strain; MATPRO routines CELMOD and CSTRES are used
REPACK	calculate fuel relocation
FCMI	calculate stress and strain in cladding
CLADF	calculate cladding stress and strain assuming no pellet-cladding mechanical interaction; subroutine STRAIN is called and MATPRO routines CELMOD, CSHEAR, CTHEXP, CSTRNI, CSTRES, and CSTRAN are used in CLADF and STRAIN
CLOSE	if pellet-cladding mechanical interaction started this time step, calculate stress and strains just prior to interaction; subroutine GAPT is called
COUPLE	calculate cladding stress and strain under condition of pellet-cladding mechanical interaction; subroutines STRESS and STRAIN are called and MATPRO routines CELMOD, CSHEAR, CTHEXP, CSTRES, and CSTRAN are used
REPACK	calculate fuel-cladding interfacial pressure outside region of fuel relocation

TABLE F.10 Subroutine Calls from Subroutine STORE6	
STORE6	
TZSET	if 2-D heat conduction, equate start of time step temperature arrays to end of time step arrays; subroutines IDXGN1 and IDXGN2 are called
GRAFOUT	write a frame of data to the graphics package
RLPST3	if active T-H link, put FRAPTRAN output into arrays in the FRAPC common block for use by the T-H code; subroutine GAPHTC is called
PRNTOT	write time step results to output file; subroutines ENERGY and PRINTM are called and MATPRO routine FENTHL is used
PRNTAZ	if 2-D heat conduction, write azimuthal temperature distribution to output file; subroutine ASET is called

Table F.11 MATPRO Routines Used by FRAPTRAN		
Routine	**Description**	**Coding Relative to MATPRO 11, Rev. 2[a]**
Subroutines		
CANEAL	cladding annealing, change in effective fluence and effective cold work during a time step	matches MATPRO 11, Rev. 2 except for a 1982 INEL modification to explicitly set coldwork to zero if cladding temperature exceeds 1255K or the time step size is too large. This modification is discussed in NUREG/CR-6150.
CANISO	cladding coefficients of anisotropy for relating effective stress to stress components and relating effective strain to strain components	MATPRO 11, Rev. 2
CESIOD	amount of cesium and iodine isotopes available to gap	MATPRO 11, Rev. 2
CKMN	calculates parameters for the cladding equation of state as a function of temperature, fluence, hydrogen, and cold work	see Section 2.4.3.2
CMHARD	cladding Meyer hardness as a function of temperature	MATPRO 11, Rev. 2
CMLIMT	limits of cladding mechanical deformation	see Section 2.4.3.2
COBILD	Cathcart model for cladding oxidation	MATPRO 11, Rev. 2
CSTRAN	cladding strain as a function of true stress and strain rate	SCDAP MATPRO, see Section F.1
CSTRES	cladding effective stress as a function of true strain	SCDAP MATPRO, see Section F.1
CSTRNI	cladding strain	SCDAP MATPRO, see Section F.1
CTHCON	cladding thermal conductivity	MATPRO 11, Rev. 2
CTHEXP	cladding thermal expansion; anisotropic for axial and circumferential	matches coding used in FRAPCON-3; see Section F.2
FTHCON	fuel thermal conductivity	see Section 2.2.4
FTHEXP	fuel thermal expansion	MATPRO 11, Rev. 2
PHYPRP	fuel and cladding melting points, heats of fusion, and cladding alpha-beta transition temperature	MATPRO 11, Rev. 2
ZOEMIS	cladding surface emissivity as a function of temperature and oxide thickness	MATPRO 11, Rev. 2
Functions		
CCP	cladding specific heat	MATPRO 11, Rev. 2
CELMOD	Young's modulus for cladding	MATPRO 11, Rev. 2
CSHEAR	cladding shear modulus	MATPRO 11, Rev. 2
FCP	fuel specific heat	MATPRO 11, Rev. 2
FENTHL	fuel enthalpy relative to zero degrees absolute	MATPRO 11, Rev. 2
FEMISS	fuel emissivity	MATPRO 11, Rev. 2
GTHCON	gas thermal conductivity	MATPRO 11, Rev. 2
GVISCO	gas viscosity	MATPRO 11, Rev. 2
ZOTCON	zirconium dioxide thermal conductivity	MATPRO 11, Rev. 2

(a) All routines have had coding deleted that was related to uncertainty analysis used in FRAP-T6.

F.1 True Stress and Strain

The MATPRO routines CSTRAN, CSTRES, and CSTRNI used in FRAPTRAN match those used in the SCDAP version of FRAPTRAN (Hohorst 1990). All input strain or stress components are assumed to be true strain or stress. True strain equals the change in length divided by the length at the instant of change integrated from the original to the final length. True stress equals the force per unit cross-sectional area determined at the instant of measurement of the force.

The basic equation used to relate stress and plastic strain is:

$$\sigma = K\varepsilon^n(\dot{\varepsilon}/10^{-3})^m$$

where: σ = true effective stress
ε = true effective plastic strain (unitless)
$\dot{\varepsilon}$ = rate of change of true effective plastic strain (1/s)
K,n,m = parameters which describe the metallurgical state of the cladding

The basis equation is used in CSTRES to calculate the effective stress. Solving the basic equation for strain is done CSTRAN.

The strain returned by CSTRNI is obtained from the time integral of the strain-dependent factors in the basic equation assuming stress is constant during the time interval; the integral is:

$$\varepsilon_f = [(\frac{n}{m}+1)10^{-3}(\frac{\sigma}{K})^{1/m}\Delta t + \varepsilon_i^{(n/m+1)}]^{\frac{m}{n+m}}$$

where: ε_f = true effective strain at the end of a time interval (unitless)
ε_i = true effective strain at the start of a time interval (unitless)
Δt = duration of the time interval (s)

F.2 Cladding Thermal Expansion

The MATPRO-11, Revision 2, expression for cladding thermal expansion was derived from single-crystal data and texture coefficients were required to translate the single-crystal data to the projected circumferential and axial expansion coefficients for Zircaloy cladding. The thermal expansion functions used for FRAPTRAN (and FRAPCON-3) are derived from circumferential and axial thermal expansion data from typically produced Zircaloy tubing. The expressions are:

$$[\frac{\Delta L}{L_o}]_{(C,A)} = C_{(C,A)} - K_{(C,A)}(T-273)$$

where: $\left[\frac{\Delta L}{L_o}\right]_{C,A}$ = thermal expansion strain (293K datum) in m/m
T = temperature (K)
$C_{C,A}$ = coefficient for circumferential (C) or axial (A) thermal expansion (m/m)
$K_{C,A}$ = coefficient for circumferential (C) or axial (A) thermal expansion (m/m-K)

The values of C and K are different in the circumferential and axial directions, and are also temperature dependent; see Table F.12 for the values. In the transition region between 1073 and 1273K, the thermal expansion strain is found by interpolation within tabulated values; these values are provided in Table F.13.

Table F.12. Parameters Used in Zircaloy Thermal Expansion Correlations

Constant (unit)	Value for Circumferential Expansion	Value for Axial Expansion
C (m/m) for T<1073K	-2.373×10^{-4}	-2.0506×10^{-5}
C (m/m) for T>1273K	-6.800×10^{-3}	-8.300×10^{-3}
K (m/m-K) for T<1073K	$+6.721 \times 10^{-6}$	$+4.441 \times 10^{-6}$
K (m/m-K) for T>1273K	$+9.700 \times 10^{-6}$	$+9.700 \times 10^{-6}$

Table F.13 Zircaloy Cladding Thermal Expansion Strains in Transition Range (1073<T<1273K)

Temperature, K	Circumferential Strain, m/m	Axial Strain, m/m
1073	0.00514	0.00353
1093	0.00525	0.00350
1113	0.00528	0.00341
1133	0.00522	0.00321
1153	0.00508	0.00280
1173	0.00470	0.00200
1193	0.00410	0.00130
1213	0.00313	0.00130
1233	0.00292	0.00110
1253	0.00286	0.00120
1273	0.00290	0.00140

The applicable ranges for this model are:

temperature: 300 to 2100K
burnup: 0 to 70 GWd/MTU
uncertainty: ±10% relative (estimated), one sigma standard error

The data used to derive these correlations were obtained from the following references.

F.3 References

Hohorst, J. K. 1990. *SCDAP/RELAP5/MOD2 Code Manual, Volume 4: MATPRO - A Library of Materials Properties for Light-Water-Reactor Accident Analysis.* NUREG/CR-5273 (EGG-2555), Volume 4, EG&G Idaho, Inc., Idaho Falls, Idaho.

Kearns, J. J. 1965. *Thermal Expansion and Preferred Orientation in Zircaloy*, WAPD-TM-472, Westinghouse Advanced Products Division (Bettis Laboratory), West Mifflin, Pennsylvania.

Lustman, B. B., and F. Kerze. 1955. *The Metallurgy of Zirconium*, McGraw-Hill Book Company, New York, New York.

Mehan, R. L., and F. W. Weisinger. 1961. *Mechanical Properties of Zircaloy-2*, KAPL-2110, Knowles Atomic Power Laboratory, Schenectady, New York.

Scott, D. B. 1965. *Mechanical Properties of Zircaloy-2 and -4*, WCAP-3269-41, Westinghouse Electric Corporation Atomic Power Division, Pittsburgh, Pennyslvania.

APPENDIX G

INPUT OPTION FOR DATA FILE WITH TRANSIENT COOLANT CONDITIONS

APPENDIX G

INPUT OPTION FOR DATA FILE WITH TRANSIENT COOLANT CONDITIONS

An input option for FRAPTRAN provides for the code to read transient coolant conditions directly from a data file. Described in this appendix is the form of the data set required by FRAPTRAN.

G.1 COOLANT CONDITION OPTION

If the *coolant* option and *tape1* suboption are specified in the BOUNDARY input data block, a data set specifying the transient coolant conditions must be stored on file. The data set will be accessed by FORTRAN logical Unit 4.

The coolant condition data set must be created as follows:

```
        ITHYMX=NCHN-1
        IF(ITHYMX.LE.0)GO TO 40
        WRITE(LU)NCHN
        DO 20 I=1,NCHN
20      WRITE(LU)NROD,ICON,ANGLE
40      CONTINUE
        DO 100 N=1,NTSTEP
        WRITE(LU)T(N)
        WRITE(LU)PLP(N),HLP(N),TBLP(N)
        DO 80 M=1,NZONE
        WRITE(LU)ZB(M),ZT(M),P(M,N),H(M,N),TB(M,N)G(M,N)
        IF(ITHYMX.LE.0)GO TO 80
        DO 60 I=1,ITHYMX
C       BYPASS WRITE FOR ICON=1 OF NROD=1.
60      WRITE(LU)NROD,ICON,HFAC,TFAC,GFAC
80      CONTINUE
100     WRITE(LU)PUP(N),HUP(N),TBUP(N)
```

where: LU = FORTRAN logical unit

NCHN = total number of rod to coolant channel connections. For example, given the coolant geometry shown in Figure G.1, NCHN=3. NCHN is specified in the input data under the TAPE INPUT suboption of the COOLANT CONDITION option.

NROD = fuel rod number

ICON = number of a coolant channel bordering fuel rod number NROD. The first coolant channel must border the azimuthal coordinate of 0°, the last coolant channel must border the upper bound aximuthal angle (180° for one-fold symmetry). The coolant channels are renumbered for each fuel rod. If the total number of rods equals three, for example, the coolant channel number one appears three times.

ANGLE = upper bound azimuthal position of point on cladding surface of fuel rod number NROD which borders coolant channel number ICON (degrees). For example, given the coolant geometry shown in Figure E.1, ICON=1, ANGLE=45°, ICON=2, ANGLE=135°, ICON=3, and ANGLE=180°.

T(N) = time of N-th time point(s) [T(N+1) > T(N)]

PLP(N) = pressure of coolant in lower plenum at time T(N) (psia)

HLP(N) = enthalpy of coolant in lower plenum at time T(N) (Btu/lbm)

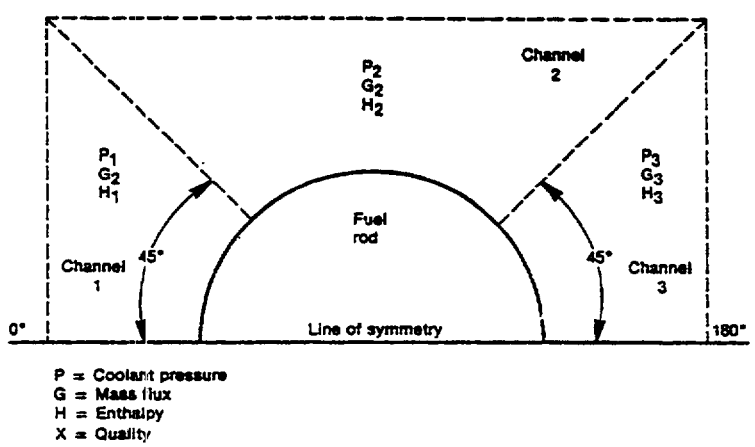

Figure G.1 Example geometry for input of coolant channel data.

TBLP(N) = bulk temperature of coolant in lower plenum at time T(N) (°F)

NZONE = number of different elevation spacings (vertical zones) at which thermal-hydraulic code has calculated coolant conditions

ZB(M) = elevation of bottom of M-th elevation spacing (ft)

ZT(M) = elevation of top of M-th elevation spacing (ft)

[ZB(M+1) must equal ZT(M)]

P(M,N) = coolant pressure between zone bounded by ZB(M) and ZT(M) (psia)

H(M,N) = coolant enthalpy (Btu/lbm). If NCHN > 1, H(M,N) is equal to the coolant enthalpy in coolant channel 1 of rod number 1

TB(M,N) = coolant temperature (°F). If NCHN > 1, TB(M,N) is equal to the coolant temperature in coolant channel 1 of rod number 1

G(M,N) = mass flux (lbm/ft^2-hr). If NCHN > 1, G(M,N) is equal to the mass flux in coolant channel 1 of rod number 1

HFAC = ratio of enthalpy of coolant channel number ICON of fuel rod number NROD to the enthalpy of coolant channel number 1 of fuel rod number 1

TFAC = same as HFAC, but for coolant temperature

GFAC = same as HFAC, but for mass flow

PUP(N) = pressure in upper plenum (psia)

HUP(N) = enthalpy in upper plenum (Btu/lbm)

TBUP(N) = temperature in upper plenum (°F).

G.2 Heat Transfer Coefficient Option

If the *heat* option and *tape2* suboption are specified in the BOUNDARY input data block, the data set prescribing the fuel rod cooling must be created as follows:

```
      DO 100 N = 1,NTSTEP
      WRITE(LU)T(N)
      DO 50 M = 1,NZONE
50    WRITE(LU)ZB(M),ZT(M),HTC(M,N)TB(M,N)P(M,N)
100   CONTINUE
```

where: HTC(M,N) = eat transfer coefficient in region of M-th elevation spacing at N-th time point (Btu/hr-ft^2-F).

The coolant temperature in the coolant condition data set must be such that

Q(M,N) = HTC(M,N) (TCLAD - TB(M,N))

where Q(M,N) = surface heat flux (Btu/ft^2-hr)

TCLAD = cladding surface temperature (°F)

HTC(M,N) = heat transfer coefficient (Btu/ft^2-F-hr)

TB(M,N) = coolant temperature for forced convection mode of heat transfer and saturation temperature for boiling modes of heat transfer (°F).

The data set will be accessed by FORTRAN logical unit 4. The control statement for FORTRAN unit 4 must specify the location of the data set.

NRC FORM 335 (2-89) NRCM 1102, 3201, 3202

U.S. NUCLEAR REGULATORY COMMISSION

BIBLIOGRAPHIC DATA SHEET

(See instructions on the reverse)

1. REPORT NUMBER (Assigned by NRC, Add Vol., Supp., Rev., and Addendum Numbers, if any.)

NUREG/CR-6739, Vol. 1
PNNL-13576

2. TITLE AND SUBTITLE

FRAPTRAN: A Computer Code for the Transient Analysis of Oxide Fuel Rods

3. DATE REPORT PUBLISHED

MONTH	YEAR
August	2001

4. FIN OR GRANT NUMBER

W6200

5. AUTHOR(S)

M.E. Cummingham, C.E. Beyer, P.G. Medvedev, PNNL
G.A. Berna, GABC

6. TYPE OF REPORT

Technical

7. PERIOD COVERED *(Inclusive Dates)*

1998 - 2001

8. PERFORMING ORGANIZATION - NAME AND ADDRESS *(If NRC, provide Division, Office or Region, U.S. Nuclear Regulatory Commission, and mailing address; if contractor, provide name and mailing address.)*

Pacific Northwest National Laboratory
Richland, WA 99352

Subcontractor:
G.A. Berning Consulting
2060 Sequoia Drive
Idaho Falls, ID 83404

9. SPONSORING ORGANIZATION - NAME AND ADDRESS *(If NRC, type "Same as above"; if contractor, provide NRC Division, Office or Region, U.S. Nuclear Regulatory Commission, and mailing address.)*

Division of Systems Analysis and Regulatory Effectiveness
Office of Nuclear Regulatory Research
U.S. Nuclear Regulatory Commission
Washington, DC 20555-0001

10. SUPPLEMENTARY NOTES

H. Scott, NRC Project Manager

11. ABSTRACT *(200 words or less)*

The Fuel Rod Analysis Program Transient (FRAPTRAN) is a FORTRAN language computer code that calculates the transient performance of light-water reactor fuel rods during reactor power and coolant transients for hypothetical accidents such as loss-of-coolant accidents, anticipated transients without scram, and reactivity-initiated accidents. FRAPTRAN calculates the temperature and deformation history of a fuel rod given time-dependent fuel rod power and coolant boundary conditions. The phenomena modeled by FRAPTRAN include: a) heat conduction, b) heat transfer from cladding to coolant, c) cladding oxidation, d) fuel rod gas pressure, and e) elastic and plastic cladding deformation. Transient fission gas release is not mechanistically modeled. Modifications to develop FRAPTRAN from the FRAP-T6 computer code include model updates to improve performance predictions for high burnup fuel; additions to account for data and knowledge gained since FRAP-T6 was released in 1983; and general coding improvements to address known errors, ensure coding consistency, improve usability, and to delete coding and models that are no longer needed. An independent peer review of FRAPTRAN was conducted. Volume 1 (this report) constitutes the code description document and includes the input instructions. A companion document (Volume 2) provides the results of the assessment of the integral code predictions to measured data for various performance parameters.

12. KEY WORDS/DESCRIPTORS *(List words or phrases that will assist researchers in locating the report.)*

Computer Code, Code Description, Model Description, time-dependent heat conduction, Fuel Rod Performance, Cladding Oxidation, Cladding Deformation, High Brunup, Pellet Centerline Temperature

13. AVAILABILITY STATEMENT

unlimited

14. SECURITY CLASSIFICATION

(This Page)
unclassified

(This Report)
unclassified

15. NUMBER OF PAGES

16. PRICE

This form was electronically produced by Elite Federal Forms, Inc.

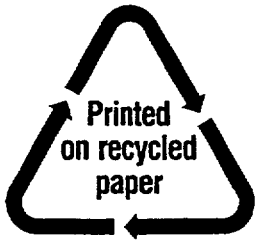

Federal Recycling Program

UNITED STATES
NUCLEAR REGULATORY COMMISSION
WASHINGTON, DC 20555-0001

OFFICIAL BUSINESS
PENALTY FOR PRIVATE USE, $300